Integrating fossils, morphology and molecules to understand the diversification of egerniine skinks

By

Kailah Marie Thorn

Thesis Submitted to Flinders University for the degree of

Doctor of Philosophy

College of Science and Engineering

4th June 2020

CONTENTS

LIST OF FIGURES

LIST OF TABLES

SUMMARY

Squamate reptiles (lizards and snakes) are uncommon in the published Australasian fossil record, despite being a component of most fossil Cenozoic collections. This thesis aimed to address the underrepresentation, of one particular group of lizards, the 'social skinks' of the subfamily Egerniinae (formerly the '*Egernia* group'). The Egerniinae represent Australasia's largest extant scincid lizards, including the iconic Blue-tongued Lizard, Spiny-tailed Skinks, and Shinglebacks. Various degrees of sociality occur across the group, ranging from long-term monogamous bonds to family living. Their presence in palaeoecological projects has thus far not been extensively recorded due to a lack of known species-level osteological apomorphic traits. Mapping when and where these apomorphies occur across their phylogenetic history in combination with a molecular dataset allows us to trace the evolution of phenotypes, species and clades.

The oldest confirmed scincid fossil in Australia *Proegernia mikebulli,* is described from a near-complete reconstructed mandible, maxilla, premaxilla, pterygoid, and referred vertebra and proximal femur. A tip-dated total-evidence phylogeny inclusive of this new taxon and middle Miocene *Egernia* and "*Tiliqua*" from Riversleigh, produced an estimated age of 50 Ma for the subfamily Egerniinae.

The oldest fossil taxa recognised as a tentative member of "*Tiliqua"* and *Egernia* are described from the middle Miocene of Riversleigh World Heritage area in north-western Queensland. Our tip-dated tree combining these extinct taxa with molecular and morphological data suggests that the modern Australian egerniine radiation dates to the end of the Eocene (34.1 Ma). Both fossils are within the Australian crown clade Egerniinae: *Egernia gillespieae* sp. nov. is placed within the extant genus *Egernia*, while *"Tiliqua" pusilla* likely sits basal to the divergence of the clade inclusive of *Tiliqua* and *Cyclodomorphus*. The fossils thus provide direct evidence that the Australian radiation of the Egerniinae was well underway by the mid-Miocene.

Australasia is home to the world's largest scincid lizards, with multiple taxa regularly exceeding 1 kg in body mass and 30 cm in snout-vent length. We reinvestigated two Australian Plio-Pleistocene giants: *Aethesia frangens* Hutchinson and Scanlon, 2009 and *Tiliqua laticephala* Čerňanský and Hutchinson, 2013 from the Wellington Caves in New South Wales. New material from an excavation of Cathedral Cave, and a combing of museum collections in eastern Australia, links the two previously known taxa into one: *Tiliqua frangens* (Hutchinson and Scanlon, 2009). This is the world's largest known scincid lizard with an estimated 2.38 kg body mass and a snout-vent length approaching 60 cm, an armoured giant that might have been an

ecological analogue of land tortoises. The disappearance of this animal from the fossil record at the same time as many of Australia's giant marsupials and birds demonstrates that scincids also lost their largest representatives during the late Pleistocene 'megafauna' extinctions.

This body of work encompasses three significant contributions to our knowledge of Australian herpetofauna and its fossil record: Australasia's iconic Blue-tongued lizards have existed since at least the middle-Miocene; and reached phenotypic extremes beyond that of any other lizard, before succumbing to the late Pleistocene 'megafauna' extinction event. This work has expanded our knowledge of Australia's past biodiversity beyond mammals, birds, and the largest monitor lizards—to include our presently most-speciose lizard clade, the Scincidae. By incorporating all of these newly described fossil taxa into tip-dated phylogenetic trees we now have the means to accurately date the appearance and phenotypic plasticity of extant egerniines and shed light on their susceptibility to the looming anthropogenic extinction crisis.

DECLARATION

I certify that this thesis does not incorporate without acknowledgment any material previously submitted for a degree or diploma in any university; and that to the best of my knowledge and belief it does not contain any material previously published or written by another person except where due reference is made in the text.

Signed...  .....

Date..25/10/2019.....

ACKNOWLEDGEMENTS

This thesis would not have been possible without a large number of people, pets, and a series of fortunate events. While there are many more than I will list below, these are the people without whom this work could not have been done.

First and foremost, my amazing team of supervisors. Many people thought that four is too many, but each of you contribute to this thesis in your own way and have all helped shape the scientist I am today. Gav & Trev have put up with my reptile obsession in good humour and provided me with some amazing field work experiences. I promised Gav I would find a megafauna skink when I started this PhD, I should have put money on it. Mike somehow managed to turn this palaeontologist to the dark side, I now really enjoy using systematics to answer my biggest questions. Thank you for being so patient with me trying to get my head around everything, from Bayes Theorem to editing xml files. Without Mark this project would not have been possible, his enthusiasm for, and encyclopaedic knowledge of, all things Scincidae is inspiring. Thank you for the numerous hours spent nerding out about tiny skink skull elements, taxonomy, nomenclature, and palaeontology in your office.

I am indebted to Paul Stokes for teaching me how to operate the stacking camera facility at the SAM, thanks for taking a flash or two to the eyeballs. Issy Douvartzidis spent numerous Tuesday mornings contributing to the Micro-CT scan database from which all my scans came from. Thank you both for all your time and patience showing me how to mount, scan and photograph my fossil specimens. Thank you to Mike Gemmell, Linda, James and all my other co-workers at the SAM Discovery Centre, and Public Programs. I learnt so much working with each of you, from Mike the walking encyclopaedia to Meg's amazing enthusiasm and organisation skills in outreach. Professor Flint is also a top bloke, thank you for having me hang around as Professor Anning for a while and showing me how to tell my science stories. Michael Mills is alright too.

Museums all over Australia have contributed to this project and my knowledge of Australian Palaeontology as a whole. Thanks to Tim, Ben Superior, Ben Francischelli, James, Douglas, Hazel, Eric, David, and Steve for looking after me on my many visits to Melbourne. Special thanks to Jane Melville, Christy Hipsley and Till Ramm for getting me over to Melbourne again to work with the McEacherns Cave material. Jacqui Nguyen and Matt McCurry were brilliant hosts in Sydney, without your help, *Tiliqua frangens* may have sat alone in that draw for decades to come. Cheers Scott Hocknull for being just as enthused about fossil squamates as I am, and for helping me put

together Queensland's big skink story, your knowledge of all the sites, timeframes and taxa in your collection represent real life goals.

Thank you to all of Flinders Palaeontology. I feel as though an appendix to list all your names would almost be appropriate. Thank you for putting up with my crazy enthusiasm for Flinders University Palaeontology Society, all the events you helped put together, run, and attend in great numbers! FUPS is the best form of procrastination I could have ever hoped for, cheers Sam Arman, Aidan Couzens, Matt McDowell, Amy Tschirn, Nathan Phillips, Sue Double, Ellen Shute, Alice Clement, Phoebe McInerney, Nimue Gibbs, Cassy Petho, Parker Rydon, Teagan Cross, Clare Oakey and Ava Jarldorn. From the lab, without repeating from above, I'll focus on the students who have been through this hell-hole with me and helped me reach the other end: Warren, for sharing my love of TOOL and not showering on field work. Brian Choo, someday I will show you my favourite ZooTycoon 2 zoo. Nathan Brown, cheers for doing a heap of the pit digging at Pinpa for those strat sections. Sue and Elen, extra acknowledgements for the both of you for your BEER'N'BONES editing skills, early morning lab conversations and pun-induced cringes and giggle fits. Ben King for putting up with my noob systematics questions, and Jacob Blokland for bouncing TNT, MrBayes and BEAST frustrations off. Massive thanks to Carey Burke, for teaching me the ways of the camp cook and how hard preparators work behind the scenes to collect the data that most of us take for granted. Aaron Camens, Grant Gully and Diana Fusco stopped my mind from turning to cheese in the last 12 months by challenging me with board games nights. By the time this is submitted I can win back the right to be the green player from Camens. Inanimate objects that also helped include the palaeo beer fridge, and the small bush that stopped the complete erosion of the 'Fish Lens' at Billeroo Creek (RIP). There were multiple dogs that provided me with emotional support throughout this thesis that deserve acknowledgement: Peppa, Diesel, Possum, Snowy, Harry, and Pedro the Science Dawg.

The people who were most helpful in this endeavour know who they are. Lisa, thanks for letting me look through your Bone Gulch fossils, I suppose stegosaurs aren't all bad. Diana, let the records show that I officially submitted my thesis first. Cheers for the numerous beers, fossils and games nights. Thanks for being the other half of all the FUPS hard work, and my work wifey for all these years.

The last, but not the least: Pete, thanks for putting up with my numerous absences for field trips, the late nights, poverty, and my stress-head nature over the duration of this project. I couldn't have done it without you.

CHAPTER 1: INTRODUCTION

1.1 Summary of contribution

This introductory chapter is intended to provide sufficient background context for this thesis. I have included a brief context of the study group, and their importance. I have provided an introduction to the methods used in this investigation, why they were chosen and their current use in the fields of palaeontology and systematics. There are important gaps that need filling in our knowledge of the origins of the Egerniinae; and many of the methods used herein are rarely combined and tested with such recent fossil taxa. I have attempted to fill these gaps using the novel combination of methods in the subsequent chapters.

The original contribution to knowledge generated by this thesis is the description of three important new species of fossil egerniine lizards that together complete the aims of this thesis by:

- Timing the earliest arrival of scincids to Australia by coding Australia's oldest scincid into the complete egerniine morphological data matrix, retrieving *Proegernia* as a new stem taxon, and demonstrating that the Egerniinae is the oldest endemic Australian scincid radiation
- Deciphering the divergence timing and rates of evolution across different branches of the phylogeny of Egerniinae, using tip-dated, total-evidence phylogenetic methods focusing on the division between *Egernia* and *Tiliqua*
- Exploring shape and size diversity in Australia's fossil blue-tongued lizards using continuous morphological characters, and standardised major axis regressions of a living relative

Each of the following primary chapters of this thesis focus on a time period, taxonomic group, or major questions generated in the writing of this literature review, while all being written as separate bodies of publishable work.

Chapter 2 is an investigation of the origins of Australian egerniines. The Namba Formation preserving Australia's oldest scincid remains lacks other sub-familial groups, while providing enough Egerniine material to include the fossils within a morphological character matrix for dating the age of a stem Egerniine clade, *Proegernia*. This chapter involved two field trips to the Namba Formation in central South Australia, in 2017 and 2018.

Chapter 3 describes *Egernia gillespieae*, a 15 million-year-old near-complete skull of an *Egernia* that is contemporaneous with *Tiliqua pusilla*. The two fossils become calibrations for the

split of *Tiliqua* and *Egernia*, and sit approximately in the middle of the newly-estimated evolutionary timescale of the Egerniinae. This work was presented at the 77th meeting of the Society of Vertebrate Palaeontology in Calgary, Canada in 2017, and published in *Journal of Vertebrate Paleontology* in May 2019.

Chapter 4 highlights the extreme morphological possibilities within *Tiliqua*, and describes the giant, spiked, Pleistocene shingleback *Tiliqua frangens*. This taxon, despite its immense size, unusual features, and appearance in multiple fossil sites, nearly went unnoticed by palaeontologists for 150 years. This taxon represents a new species of Australian Pleistocene megafauna, is the world's largest known scincid, and is one of the most bizarre terrestrial lizards globally. This body of work was presented at the Australian Society of Herpetologists meeting in Queensland in December, 2018, and in part in the Romer Prize session at the Society of Vertebrate Palaeontology Meeting in Brisbane, 2019.

Each chapter is the result of collaborations with multiple palaeontologists and herpetologists from Flinders University, the South Australian Museum and other institutions spanning all of the eastern states of Australia. Where collaborators have had a significant impact on the final body of work they have been added as authors and their contributions noted before each chapter. Other contributions are acknowledged separately in each chapter and the beginning of this thesis.

1.2 The role of fossils in our understanding of evolution

Palaeontologists use the fossil record to decipher the evolution of species and their lineages through 'deep time', whether this be across thousands, millions or hundreds of millions of years of Earth history. The transition of form and function occurs across these time frames and includes large-scale morphological changes that are preserved in the fossil record. Palaeontological inferences are honed with neontological data derived from extant taxa, including molecular phylogenies and phenotypic traits such as osteology, life history, diet and habitat preferences. Genetic and phenotypic changes detectable over these much shorter timeframes provide a perspective on extant relationships and ecological drivers. Neontological systematics without morphological data and well-justified fossil calibrations often produce inaccurate timescales of evolution, and morphological data without molecular input is heavily impacted by convergent evolution (Lee and Palci, 2015). Both fields are strengthened with input from the other, and together they create a more robust record of the evolution of life on earth. In this this thesis I combine new osteological evidence from fossils with the morphological and genetic data from neontological

studies to decipher the evolutionary history and origins of a group of Australasian lizards, the Egerniinae.

1.3 Australian reptile diversity

Australian reptiles provide a unique model system to explore evolutionary patterns, with representatives of all of the major extant non-avian reptile clades—crocodiles, turtles, snakes and lizards—diversifying across a largely isolated continent. Australian reptiles are morphologically diverse, despite the region containing only limited lineage diversity (e.g. one 'family' from each of the major lizard lineages; the Scincomorpha, Gekkota, Iguania and Anguimorpha (Milewski, 1981; Pianka, 1986; Wilson and Swan, 2017). The number of recognised Australian reptile species has been increasing at a staggering rate (Uetz, 2010) since the rise of molecular-informed taxonomy and although slowing now, counts rose from 633 in 2001, to 869 in 2007 (Chapman, 2009) to most recently 1082 (Uetz et al., 2019). Skinks are the most speciose of all Australian terrestrial vertebrate families, with 458 species identified so far (Uetz et al., 2019). This thesis aims to build on the published record of Australia's past skink fauna, and help decipher the processes responsible for their present taxonomic richness.

1.4 Australian skinks

The cosmopolitan clade Scincidae Gray, 1825 is dispersed across most of the Earth's terrestrial biomes, excluding boreal and polar regions. Australian skinks were previously recognised within the subfamily Lygosominae Mittleman, 1952, based on morphology (Greer, 1979) and mtDNA (Honda et al., 2000). Within the Lygosominae (*sensu lato* Greer, 1979) are major groups named after prominent included genera: *Lygosoma*, *Sphenomorphus*, *Eugongylus* and *Mabuya*, the last three containing Australian taxa (see Figure 1.1). The non-monophyly of the *Mabuya* group was clarified using mtDNA, splitting into the *Mabuya* group (*sensu stricto*) and the *Egernia* group (Honda et al., 1999). Hedges (2014) took these informally named 'groups' and advocated for family-level definitions of each clade. The current consensus (Uetz et al., 2019) is that these clades are recognised as subfamilies: Lygosominae Mittleman, 1952, Sphenomorphinae Welch, 1982, Eugongylinae Welch, 1982, Mabuyinae Mittleman, 1952 and Egerniinae Welch, 1982. The Lygosominae *sensu stricto* encompasses south eastern Asian taxa such as *Lygosoma* spp. and *Lamprolepis* spp. The Sphenomorphinae, which includes numerous speciose Australian and Asian genera, is the most basal group within what was previously the Lygosominae (*s.l.*; Skinner et al., 2011), and are the only Australian skinks to still retain the plesiomorphic scincid character of an open Meckel's Groove (Greer, 1979). The Eugongylinae are the radiation of skinks reaching New Caledonia and New Zealand (Chapple et al., 2009), and include the speciose Australian genera

Carlia and *Emoia*. The Mabuyinae are the scincid subfamily inclusive of south-eastern Asian genera such as *Dasia* and *Eutropis,* and are the nearest living relatives to extant egerniines (Lambert et al., 2015). The Egerniinae—the 'social skinks'—of Australia, New Guinea and the Solomon Islands are the focus of this project, and will be examined in detail in the following sections. The clade encompassing New Guinean crocodile skinks of the genus *Tribolonotus* lacks strong morphological support for placement in any of the scincid subfamilies. Molecular evidence suggests a relationship whereby *Tribolonotus* is the first branch within the Egerniinae (Hutchinson, 1981; Reeder, 2003). *Tribolonotus* is believed to have diverged from its nearest living relatives as recently as the Early Eocene (54 MYA), the Egerniinae have otherwise currently poorly resolved divergence times from the remainder of the Scincidae (Skinner et al., 2011).

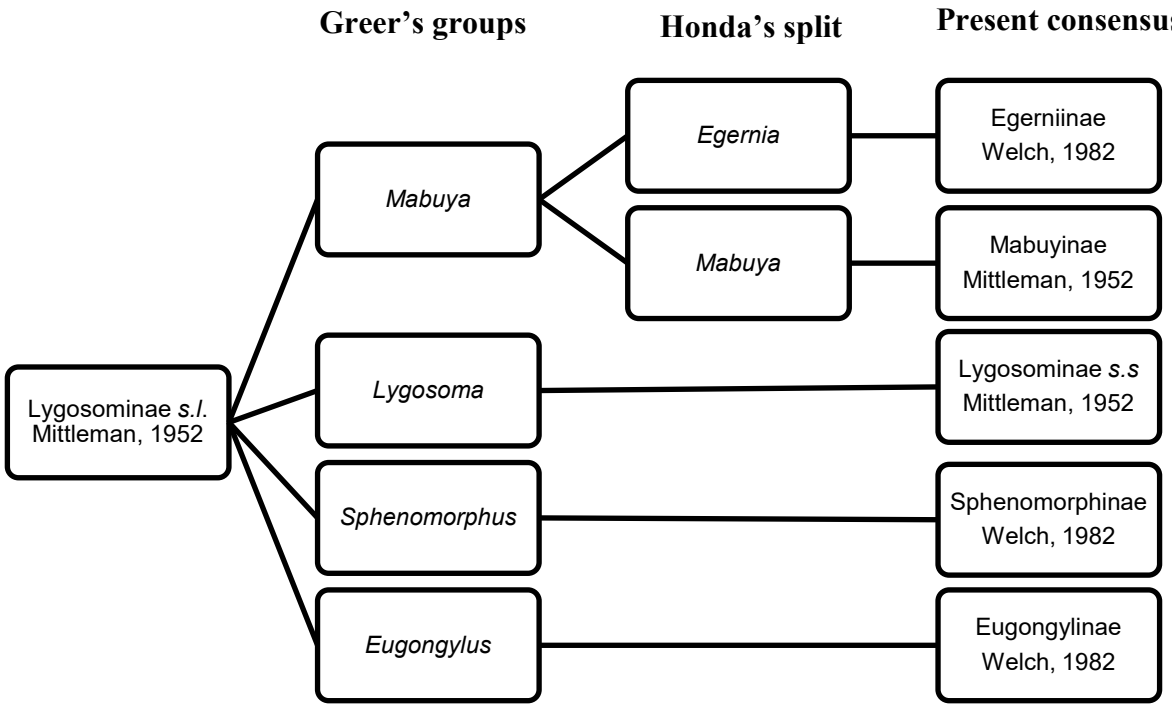

Figure 1.1: The changing taxonomy of Australasian scincid clades (Mittleman, 1952; Greer, 1979; Welch, 1982; Honda et al., 1999; Honda et al., 2000).

1.5 The Egerniinae

This morphologically diverse group of scincids includes: New Guinean Crocodile Skinks (*Tribolonotus*), Monkey-tailed Skinks of the Solomon Islands (*Corucia*), Blue-tongued Skinks (*Tiliqua*), giant Land Mullets (*Bellatorias*), and the Spiny-tailed Skinks (*Egernia*) of Australia (Table 1.1; Greer, 1970; Hedges, 2014). These animals—due to their large size, social groups, and omnivorous diet—are popular in the international pet trade, and are common study species for animal behaviour, physiology, and ecology (Wineski and Gans, 1984; Gans et al., 1985; Brown, 1991; Dubas and Bull, 1991; Bull and Pamula, 1996; Klingenböck et al., 2000; Chapple, 2003; O'Connor and Shine, 2003; Chapple and Keogh, 2005; While et al., 2009; Schofield et al., 2012; Nyakatura et al., 2014).

Table 1.1: The genera within the subfamily Egerniinae, with the number of species in each genus and common names used for the clade or majority of species within it.

Genus	Species	Common names
Tribolonotus	10	Crocodile Skinks
Corucia	1	Solomon Islands' Monkey-tailed Skink
Lissolepis	2	Mourning Skinks
Liopholis	12	Desert, Rock, and Mountain Skinks
Bellatorias	3	Land Mullet, Major's Skink
Egernia	17	Crevice, Spiny-tailed, and Tree Skinks
Tiliqua	7	Blue-tongued Skinks, Shingleback
Cyclodomorphus	9	Pink-tongued skinks

1.5.20 Ecology

1.5.20.1 Reproduction and life history

Life history strategies within the Egerniinae are characterised by their viviparity, large offspring size, delayed maturity, large body size, and life spans usually greater than five years (Chapple, 2003). Large scale phylogenetic analyses for all of Squamata confirm that oviparity is the basal condition for reptiles, and live-birth has evolved multiple times, including once at the beginning of the Egerniine radiation (King and Lee, 2015). Monogamy, parental care, and family structures recorded within this group are uncommon behavioural traits in lizards (Bull, 2000; Gardner et al., 2002), leading this subfamily to be referred to as the 'social skinks' (Uetz et al., 2019). The ancestral condition in squamates was non-social and this complex sociality evolved independently across multiple lineages (O'Connor and Shine, 2003). Unlike birds—which most likely had a social ancestor—squamates are better model organisms for studying the origin and evolution of this behaviour (Chapple, 2003; O'Connor and Shine, 2003). Varying degrees of sociality in the Egerniinae have unknown temporal origins due to the lack of a robustly dated phylogeny.

1.5.20.2 Diet and feeding strategy

The Egerniinae exhibit most of the dietary specialisations found within Squamata. Most egerniines are insectivores, but the subfamily also includes snail-crushing durophages (*Cyclodomorphus gerrardii*), omnivores (*Tiliqua scincoides*, *Egernia* spp. and *Bellatorias*), and

herbivores (*Corucia*, *Tiliqua rugosa* and some large *Egernia* spp.). At least three major dietary transitions have occurred within this radiation (Estes and Williams, 1984; Brown, 1991; Dubas and Bull, 1991; Chapple, 2003; Hagen et al., 2012). Brown (1991) concludes that the degree of herbivory in the genus *Egernia* (*s.l.*) correlates with body size, herbivory only being typical of adults of the larger species. The pygmy bluetongue, *Tiliqua adelaidensis* is the smallest and most insectivorous *Tiliqua* (Bull et al., 2007), the genus that includes large (>1kg) durophages and herbivores. Body size and diet may be linked across the Egerniinae but as yet this has not been mapped across the full family tree.

1.5.21 Distribution

The Egerniinae are widespread across Sahul, the continent comprising New Guinea, Australia and Tasmania, occurring in all major biomes, and extending into the tropics of the Solomon Islands (Figure 1.2). *Tribolonotus* spp. and the monotypic *Corucia zebrata* are endemic to the Bismarck Archipelago and the Solomon Islands. All other egerniine genera occur on mainland Australia. *Lissolepis* is presently restricted to the southern corners of the continent, *L. coventryi* to the southeast and *L. luctuosa* to the southwest. *Bellatorias major* (the 'land mullet') and *Bellatorias frerei* (Major's skink) are mostly confined to the eastern tropics (and subtropics) of northern New South Wales and Queensland, extending into New Guinea (Klingenböck et al., 2000). Critically endangered *Bellatorias obiri*, the Arnhem Land Gorges skink (circled in Figure 1.2), is known only from a small number of individuals from Kakadu National Park in the Northern Territory (Gillespie et al., 2018).

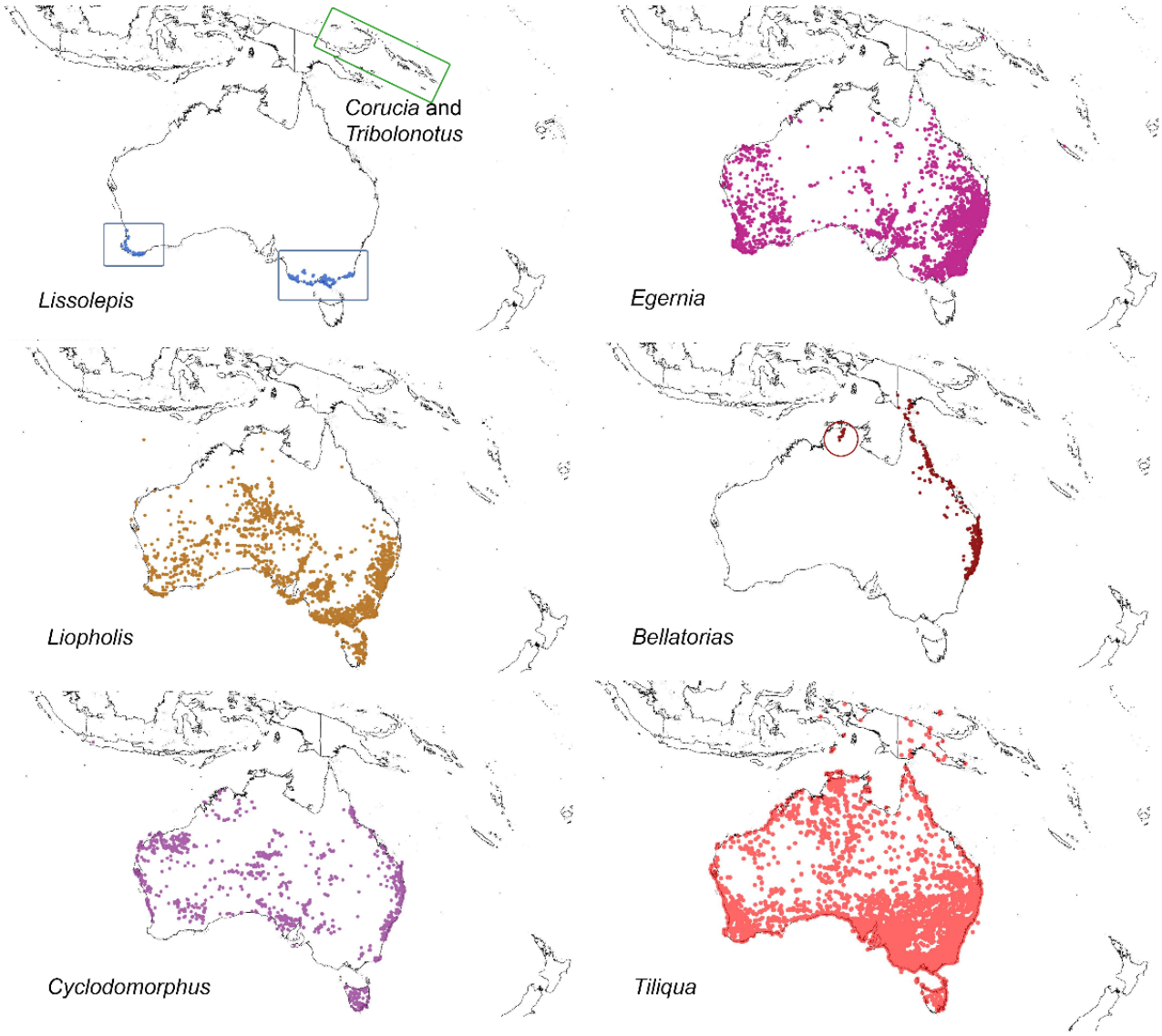

Figure 1.2: Distribution of the genera of Egerniinae across Australia and New Guinea together representing the continent of Sahul. Maps generated in Atlas of Living Australia (2019) spatial portal.

The more widespread genera are also the only representatives of the subfamily in the arid zone of Australia. *Liopholis* are primarily concentrated below the Tropic of Capricorn but inhabit all zones from sandy inland deserts (*Liopholis striata* and *L. inornata* Wilson and Swan, 2017), to mountain ranges (*Liopholis montana*; Clemann et al., 2018). *Egernia* cover similar biomes but also extend further north. Many species are morphologically suited to niche habitats within their ranges with little external variation leading to cryptic species complexes. The species diversity within these complexes is still being established. *Egernia depressa* was recently revealed to encompass *E. eos*, *E. cygnitos*, *E. epsisolus* and *E. depressa* by Doughty et al. (2011), and *E. stokesii* may be the next cryptic species complex identified (M. Gardner pers. comm. 2019). The 'Pink-tongued Skinks' (*Cyclodomorphus*) are widespread and fill multiple habitat niches. *Cyclodomorphus gerrardii* has longer limbs and digits with claws used for a semi-arboreal climbing ability, while *C. melanops* are

elongate in shape with reduced limbs accommodating side-winding locomotion in sandy and leafy substrates.

The most widespread genus in the Egerniinae is *Tiliqua*. Covering all of Australia and extending into New Guinea and Indonesia with *Tiliqua gigas*, this clade inhabits all biomes other than the highest montane zones. Many species have overlapping ranges, so more than one species are found at many survey sites; common sympatric pairs include *T. scincoides* and *T. rugosa*, *T. rugosa* and *T. occipitalis*, and *T. nigrolutea* and *T. scincoides* (Wilson and Swan, 2017).

1.5.22 Phenotypic diversity

Egerniines exemplify the diversification of body shape in Squamata exploring sleek stretched bodies with tiny limbs (*Cyclodomorphus michaeli*) to short, spiny forms with long thin appendages and digits (*Egernia depressa*, Wilson and Swan, 2017). Snout-vent lengths range from 70 mm long insectivores, to a 350 mm long, prehensile-tailed folivore (*Corucia zebrata*, Gardner et al. 2008, Hagen et al. 2012). Keeled and spiny scales are homoplasious within *Egernia*, present in both the *E. cunninghami* clade and *E. stokesii* clade (Gardner et al., 2008). However, rugose osteoderm-filled scales are typical of only extant *Tiliqua rugosa*, arguably the most uniquely shaped Australian squamate with 'armour plating', a stumpy tail, and a vegetarian diet. These phenotypes are not unique to the Australian biome. The fossil record provides evidence of other bony plated medium-sized lizards in a sister group to scincids, the paramacellodids (Evans, 2003). The extant Cordylidae of southern Africa also have traits in common with egerniines such as *T. rugosa*; viviparity and armoured keeled scales, yet they coexist with armour plated chelonians, a niche *Tiliqua rugosa* has been argued to fill in Australia (Milewski, 1981).

1.5.23 Phylogeny

Australasian egerniines were originally divided into the genera *Corucia* Gray, 1856, *Tiliqua* Gray, 1825 and *Egernia* Gray, 1838 (Greer, 1979; Gardner et al., 2008). The relationships within and between these clades have been reworked by multiple authors; Greer (1970) used morphology to deduce that *Corucia* and *Egernia* are closely related, *Tiliqua* their sister clade. Horton (1972) hypothesised a Pliocene origin for *Egernia* branching from the Asian *Mabuya,* with an ancestor similar to *E. major* (*Bellatorias major*). *Corucia* and *Tiliqua* were thought to be older again than *Mabuya*, their morphology depicting the ideal 'ancestor of the skinks' as described by Smith (1937). The genus *Egernia* quickly expanded with multiple new species named in the late 20th century. Immunodistance analyses in Hutchinson (1981) demonstrated that *Egernia* and *Tiliqua* are more closely related to one another than *Tiliqua* is to *Corucia*. Conversely, mitochondrial genes

determine that *Corucia* and *Tiliqua* form a cluster (MP bootstrap value 77%), with *Egernia* an outlier (Honda et al., 1999).

HORTON HYPOTHESIS: This image has been removed due to copyright restriction

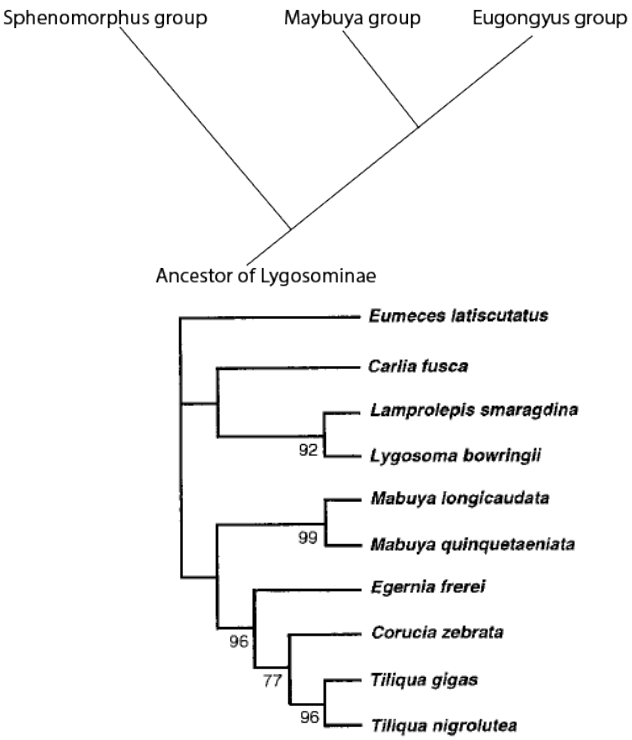

Figure 1.3: Examples of early egerniine phylogenetic hypotheses. Left: Speciation patterns within *Egernia* hypothesised by Horton (1972), dotted lines indicate uncertainty in the relationships. Right top: Greer's original hypothesis for the origins and relationships between Australian scincids, Egerniinae within the 'Mabuya group'. Lower right: The result of a maximum parsimony analyses of two mitochondrial genes across lygosomine scincids, conducted by Honda et al. (1999).

Within *Egernia* there are notable groupings of morphologically and ecologically similar species: the *E. whitii*, *E. major*, *E. luctuosa*, *E. cunninghami*, *E. striolata,* and *E. kingii* groups (Storr, 1978; Gardner et al., 2008). These prompted a more detailed molecular analysis to determine any phylogenetic significance. The composition of *Egernia* Gray, 1838 has now been further split into *Bellatorias* Wells and Wellington, 1984, *Liopholis* Fitzinger, 1843, *Lissolepis* Peters, 1872 and *Egernia* Gray, 1838, based on the robust clades determined by Gardner et al. (2008), see Figure 1.4.

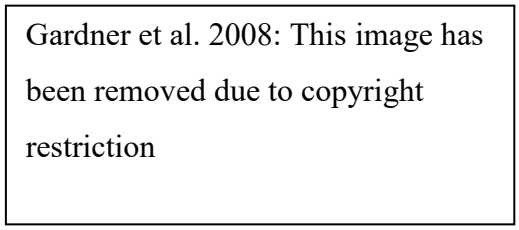

Figure 1.4: Bayesian tree produced by Gardner et al. (2008) showing the relationships retrieved with the Egerniinae from analyses of both mitochondrial RNA and nuclear DNA data. The authors revived the three genera: *Liopholis* Fitzinger, 1843, *Lissolepis* Peters, 1872 and *Bellatorias* Wells and Wellington, 1984 to reflect the diversity within the genus formally encompassed by *Egernia*.

The strict consensus topology resolved by Gardner et al. (2008) provided the current generic divisions of *Egernia,* but the branching order of these divisions remain unclear (Figure 1.4). Important questions relating to the origins of major morphological characters used for taxonomic purposes remain unanswered. For example: within the genus *Egernia* (*sensu lato*) Storr hypothesised a taxonomic divide of the smooth-scaled versus spiny-tailed species. Gardner's molecular evidence suggests that the spiny tails evolved at least twice, once in *E. cunninghami,* and at least once across *E. depressa/stokesii/hosmeri* (possibly twice but support for the node separating these taxa is not strong). The relationships noted in Figure 1.4 have not yet been chronologically calibrated by any fossils and so the timing and possible causes of these branching events are unknown.

Large molecular mega-trees exploring all of Squamata have included egerniine taxa (Pyron et al., 2013; Hedges et al., 2015; Wright et al., 2015b; Tonini et al., 2016; Zheng and Wiens, 2016). These trees produced varying divergence times for the origins of Australian egerniines, from 16.4–52.37 million years (Title and Rabosky, 2016). Many of these are calibrated with non-Australian, pre-Cenozoic scincomorphan fossils (Hedges et al., 2015; Wright et al., 2015b); or node calibrations were provided only as minimum ages for the family Scincidae (Zheng and Wiens, 2016). Mega-phylogenies often have poor fine-scale resolution, with examples of inaccurate branching in small clades: crown Australian Egerniinae recovered inclusive of *Corucia,* while *Bellatorias* is pushed out to the stem (Zheng and Wiens, 2016). Inaccuracy near the terminal branches of these trees demonstrates the need for focused investigations of smaller groups like the Egerniinae.

Before this investigation, none of the few known fossil specimens attributed to the Egerniinae have been incorporated into phylogenetic investigations beyond rough node calibrations

(Skinner et al., 2011), and the fossils themselves have not been described with phylogenetic context. Molecular branch lengths in Gardner et al. (2008) indicate deep divergences between *Egernia* and *Tiliqua*/*Cyclodomorphus*. These genera are presently cosmopolitan in their climate and habitat distribution so the timing and drivers of this divergence cannot be unravelled without fossil calibrations from within both *Egernia* and *Tiliqua*. The age of the Australian radiation of egerniines is best determined using the oldest possible crown fossils for calibration, and more fossils increase the chances of finding new and unusual apomorphies and body forms. Sites with suitable calibration material include late Oligocene sites in central South Australia, the mid-Miocene of Riversleigh in northern Queensland.

1.5.24 Cranial osteology

A skeleton is conservative enough in its broader shape and development to potentially reflect the phylogenetic affinities of species even after extensive change by adaptation (Hildebrand and Goslow, 2001). Most importantly, the skeleton is the easiest structure to preserve and store, and to fossilize, allowing ready comparison of present and past organisms and the changes that occurred between them. Cranial osteology affords especially numerous characters to track the origins of squamates and their divergence from their nearest living relative *Sphenodon*, by revealing variations in shape through time using the fossil record and comparative methods (Estes et al., 1988; Evans and Jones, 2010; Gauthier et al., 2012; Reeder et al., 2015; Simões et al., 2017). Outside of broader scale phylogenetic comparisons, the skeleton can also be used to differentiate between scincid species using palatal, braincase, or tooth morphology (Greer, 1979; Shea, 1990; Kosma, 2003).

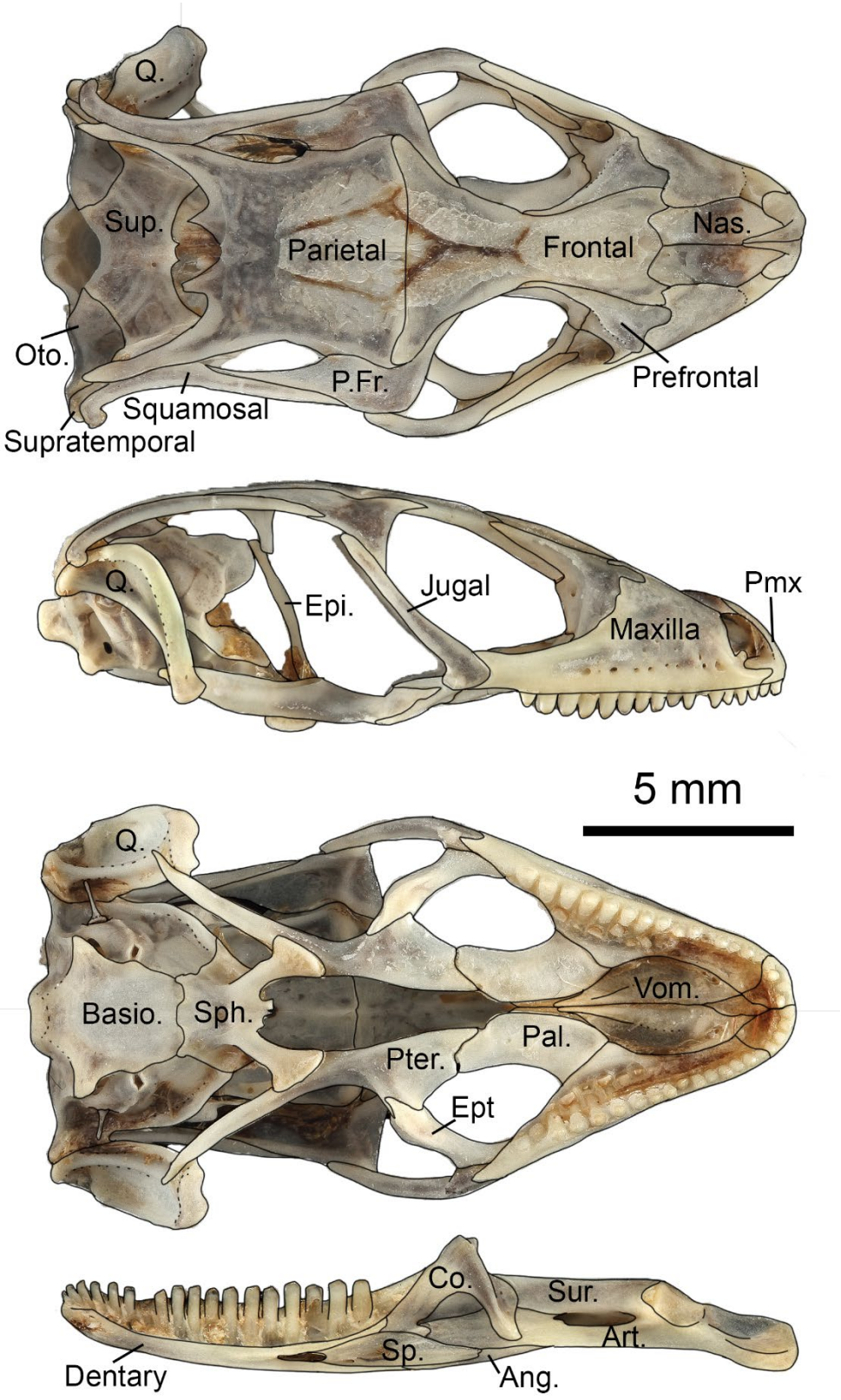

Figure 1.5: *Egernia napoleonis* (WAM R44673) skull and mandible identifying constituent elements. Abbreviations: Art., articular; Ang., angular; Basio., basioccipital; Co., coronoid; Epi., epipterygoid; Ept., ectopterygoid; Nas., nasal; Oto., otoccipital; Pal., palatine; P.Fr., postfrontal; Pmx, premaxilla; Pter., pterygoid; Q., quadrate; Sp., splenial; Sph., sphenoid; and Sur., surangular.

Egerniines have previously been differentiated from other Australian skinks using the following cranial osteological characters in combination (see Figure 1.5): (I) Frontals fused in

adults, a derived trait found in all Australian scincids. (II) Medially separated palatal rami of palatines (but contacting in *Tiliqua* and *Cyclodomorphus*). (III) Vomers paired, elongate, and projecting posteriorly between the palatines and partially dividing the choanal passages. (IV) Meckelian groove closed, overgrown, with a larger splenial notch than seen in members of the Eugongylinae (Hollenshead et al., 2011). Greer (1979) previously included the character: eight or fewer premaxillary teeth, with the exception of the 'primitive' state of nine (5/4 or 4/5) in *Lissolepis*. This character is inconsistent, for example *Egernia cunninghami* NMV D7815 has ten premaxillary teeth (5/5).

Egerniinae are diverse in their dietary adaptations, varying from folivorous herbivores to durophagous omnivores, correlated with much variation in jaw and tooth morphology. Ties may exist between diet and tooth crown morphotypes or coronoid shape (Estes and Williams, 1984; Kosma, 2003). The folivorous *Corucia* has a serrated dentition of laterally compressed, triangular crowns, while *Cyclodomorphus gerrardii* is equipped with a singular notably enlarged rounded crown near the posterior of each tooth row for crushing snail shells. The coronoid bone, a key site of muscle attachment on the mandible, exhibits a high level of shape variation across the group at both generic and species level, conspicuously so in the *Tiliqua* and *Cyclodomorphus* clade (Shea, 1990). The mandible is one of the most common fossil lizard elements to be recovered from Australian deposits, making it possible to trace evolutionary changes in structure and potentially inferred diet through time.

At the genus level, osteological keys have been proposed for the genera *Egernia*, *Bellatorias*, *Lissolepis* and *Liopholis* using dentaries, distinguishing genera by the shape of the splenial notch, position of the inferior alveolar foramen and tooth shape (Hollenshead *et al*. 2011). Shape analyses have been applied to the small species complex of *Egernia depressa, E. cygnitos and E. epsisolus* by Hollenshead (2011), which not only identified species-distinguishing characters, but also that preferred refuge habitats and ontogeny correlate with subtle shape variation in the skull. Further exploration of overall skull shape and morphological characters that can separate the genera and species of the Egerniinae are required to interpret incomplete fossil specimens. Specimens characterised by their morphology within the context of all of the Egerniinae can then provide temporal context to the appearance or alteration of osteological traits through the fossil record.

1.6 Australian squamate fossil record

Squamates are arguably one of the least likely terrestrial vertebrate groups to have skeletons preserved in articulation or association, given their skulls are composed of numerous unfused

elements, unlike those of e.g. mammals that are completely fused. Squamates are rarely the focus of taphonomic research, the few existing studies often focusing on Mesozoic European assemblages (Lyman, 1994; Evans, 2003; Richter and Wuttke, 2012; Smith and Wuttke, 2012). These mesic lake-bed assemblages are markedly different to most Australian Cenozoic depositional environments, which are predominantly fluvial, or predator-accumulated. Where Australian lizard fossils are recovered, mandibles (or usually only the dentary) are the most often retrieved element of the skeleton due to their robust structure and the tooth-search-image biases of palaeontologists (Kosma, 2003).

Despite the high prevalence of lizards in modern Australian ecosystems, they are often poorly represented in fossil deposits, and when they are recorded, they are often only identified to family and occasionally genus level (see Williams, 1980; Reed and Bourne, 2000; Reed and Bourne, 2009). The infrequency of lizard bone identification is intensified for the smaller species; poor excavation methodology such as coarse sieve apertures leading to reduced recovery rates relative to larger forms (Baynes et al., 2019). When specimens are identified, the number of individuals of each species are rarely quantified, even within detailed ecological analyses (e.g. McDowell and Medlin, 2009). The disparity between taxonomic levels of mammalian and reptilian identifications most likely stems from a lack of published works available to differentiate even the extant reptile species using mandibular morphology, and the lack of comparative skeletons in museum collections (Archer, 1978; Bell and Mead, 2014). Cryptic diversity is typical of extant scincids. Species diagnosed by molecular data are often barely morphologically distinguishable by external features such as scale counts or colour, with osteological apomorphies not yet explored and potentially non-existent, offering new challenges when it comes to describing the palaeodiversity of Australia's herpetofauna.

Sites that have previously preserved abundant squamate bones are cave pitfall (Smith, 1976; Archer, 1978; Smith, 1982; Hutchinson, 1992; Reed and Bourne, 2000; Prideaux et al., 2007; Reed and Bourne, 2009) and owl pellet accumulations (McDowell and Medlin, 2009), or low-energy fluvial (Price and Sobbe, 2005) and lake-side deposits (Rich, 1991). The recovery of fossil egerniine scincids at many of these sites results from systematic excavation and screening of sediments, rather than opportunistic fossicking of surface deposits. Differential recovery introduces biases in the number of small vertebrate remains recovered from these fossil deposits, with longer and larger shapes more likely to be retained by the sieve (Baynes et al., 2019).

As a majority of the fossil lizard specimens recovered are dentaries, most identifications are based around features such as tooth number, shape and mode of replacement, positions of foramina,

muscle scars, the symphysis, sutures, and the overall bone shape (Hollenshead et al., 2011). Post-crania are not often used for identification of lizards beyond family, as the distinguishing features of limb bones are few and usually pertain more to locomotion than phylogenetic relationships (Lécuru, 1969). Limb elements often do not preserve diagnostic features well, as demonstrated by Hocknull (2000) ascribing an Eocene femur with some uncertainty to Scincomorpha.

1.7 Fossil record of the Egerniinae

Australian fossil scincids are underrepresented relative to their extant species diversity, but the Egerniinae are the most likely to be preserved due to their large body size and robustness. Larger bodies of work encompassing fossil egerniines to genus or species level are detailed in Table 1.2 below. *Tiliqua* spp. are the most often recorded fossil scincid in Australia; this is due primarily to their size and enlarged tooth crowns. The least expected egerniines to be recorded by body size are *Lissolepis*, *Liopholis,* and small *Egernia* spp. However, these taxa are common in cave deposits due to their mesic distribution, accumulating predators (i.e. raptors; Andrews, 1990) and their saxicolous (rocky-crevice-dwelling) life habits. The more mesic, southern environments that tend to overlap with major cavernous karst regions, are also more heavily sampled by palaeontologists due to their proximity to major population centres and less extreme field conditions. North of the temperate and Mediterranean climatic zone in Australia, the number of fossil sites capable of preserving scincid fossils drops, to a few west of the Great Dividing Range in Queensland, the Riversleigh World Heritage Fossil Area, and archaeological accumulations in northern Western Australia. Extreme arid environments currently supporting a high taxonomic diversity of Australian skinks (Chapple et al., 2004; Rabosky et al., 2007) are less likely to preserve skeletal remains in articulation due to increased exposure and weathering.

Table 1.2: List of published fossil Australian egerniines identified beyond ‘Squamata indet.' Key to the sites and referenced material below table, a map showing the locations of these sites is in Figure 6.

Period	MYA	Epoch	*Lissolepis*	*Liopholis*	*Bellatorias*	*Egernia*	*Tiliqua*	*Cyclodomorphus*	Scincidae indet.
Neogene	0.01	Holocene	1	1–2		1–2	1–5		
	1.8	Pleistocene	1	1–4		1, 4, 13	1–6, 13	5–6, 13	
	5	Pliocene				8	5, 7–9	5, 9	
	23	Miocene			10	10	10		
Paleogene	34	Oligocene				11			
	56	Eocene							12

1 Devils Lair, WA: Hollenshead et al. (2011)

2 Naracoorte Caves World Heritage Area, SA: Smith (1976) and Reed and Bourne (2009)

3 Thylacoleo Caves, Nullarbor Plain, WA: Prideaux et al. (2007)

4 Kelly Hill Caves, Kangaroo Island, SA: Smith (1982)

5 Wellington Caves, NSW: Hutchinson and Scanlon (2009) and Čerňanský and Hutchinson (2013)

6 Darling Downs, and Cement Mills, Qld: Price and Sobbe (2005) and Bartholomai (1977)

7 Corra-Lynn Cave, Curramulka, SA: Pledge (1992)

8 Bluff Downs, Qld: Mackness and Hutchinson (2000)

9 Chinchilla Sand, Qld: Hutchinson and Mackness (2002)

10 Riversleigh World Heritage Area, Qld: Hutchinson (1992) and Shea and Hutchinson (1992)

11 Etadunna and Namba Formations, SA: Vickers-Rich and Rich (1991)

12 Rundle Formation, Qld: Hocknull (2000)

13 Mt Etna, Rockhampton Qld: (Hocknull, 2005)

Figure 1.6: Map of Australian fossil sites with published egerniine taxa. Numbers correspond to those detailed in Table 1.2 with references. The Etadunna Formation is the circle above the 11, the Namba Formation is below.

1.8 Aims

The preceding review of the literature on the Egerniinae highlights some major gaps in Australian palaeontology: Australian herpetofauna are underrepresented in palaeontological literature; the origin of Australia's social skinks is unknown. We don't know how long skinks have been in Australia, and we may never find the direct evidence because fossil deposits of appropriate ages for terrestrial environments are missing. We do not know what drove the expansion of Australian scincid diversity, or how and when the Egerniinae developed large body sizes and morphological variation.

In this thesis I aim to:

- Establish, for the first time, an apomorphy-based osteological characterisation of members of the Egerniinae that can then be applied to extinct and extant taxa.
- Using these characteristics, expand the known fossil diversity of egerniines in the Australian record and infer the phylogenetic affinities and palaeobiology of these extinct taxa;
- Using these newly characterised extinct taxa and phylogenetic methodologies, provide hypotheses of relationship of the social skinks (Egerniinae) and how these have changed through time, from their origins in Australia to the divergence of major clades such as *Tiliqua*.

- Highlight the morphological extremes in body size and skull shapes of Australia's blue-tongued lizards of the genus *Tiliqua*.
- Estimate the timing of the arrival of egerniines to Australia and decipher if they arrived as egerniines or became egerniines

To achieve these aims the following objectives must be met:

- Assess museum fossil collections across Australia for Egerniinae specimens that would assist in characterising extinct egerniines.
- Taxonomically describe fossils identified as egerniines from the late Oligocene Namba Formation of South Australia, mid-Miocene of Riversleigh in Queensland, and the Pleistocene of eastern Australia.
- Make palaeobiological inferences about the most complete fossil taxa.

Achieving these objectives required multiple imaging methods to be applied including:

- Micro-computed tomography scans of extant and extinct lizard skulls, mandibles, and isolated bones to elucidate and measure osteological phenotypic characters.
- Scanning electron microphotography of tooth crowns of some of the smallest taxa to distinguish both species and genus level apomorphies in the dentition of the most basally-positioned Australian Egerniines.
- Traditional microscopy and direct observation of replicate specimens to increase sample size and assess variability between individuals and populations.

The implications of this body of work extend beyond the immediate taxonomic changes introduced in each chapter to include the following:

- The integration of molecular data with continuous and discrete morphological characters, with well-dated and morphologically characterised fossil tips in both recent and deep geological time – a first for fossil lizards
- A major revision of, and increase in, the number of osteological characters for the Egerniinae. These characters can be expanded and modified to include other scincid groups.
- The first detailed description of the largest Australasian skink and its extinction coincident with Late Pleistocene extinctions.

1.9 Methods

1.9.20 Institutional abbreviations

Table 1.3: List of institutional abbreviations for collection numbers, equipment used and research collaborators involved with this thesis.

Abbreviation	Institution
AM	Australian Museum, Sydney
FUR	Flinders University Reference, Adelaide
NMV	Museums Victoria, Melbourne
QM	Queensland Museum, Brisbane
SAMA	South Australian Museum, Adelaide SAMA R: Herpetology collection SAMA P: Palaeontology collection
WAM	Western Australian Museum, Perth

1.9.21 Nomenclature

Cranial anatomical nomenclature of squamates in this thesis is based on Evans (2008). Post-cranial anatomy follows that of Russell and Bauer (2008). Tooth crown features and dentition terminology follows Richter (1994) and Kosma (2003). Muscles, muscle groups, and attachment sites have been interpreted based on those mapped for *Tiliqua rugosa* by Wineski and Gans (1984). Figure captions contain the full names for all abbreviated labelled features.

1.9.22 Morphological data collection

Both skeletonised reference specimens and Micro-Computed Tomography (Micro-CT) of ethanol-preserved 'wet' specimens of egerniines were used for this project. Most of the specimens required for this investigation were sourced from the Herpetology Collection of the South Australian Museum, with a small number from the Western Australian Museum and Queensland Museum Herpetology collections. A list of all specimens used in this thesis is in Appendix 1.

1.9.22.1 Micro CT scanning

Micro-Computed Tomography of preserved extant species and fossil specimens was conducted at Adelaide Microscopy using a Skyscan-1076. Most of the scanning hours contributing to the South Australian Herpetology digital library used in this thesis were conducted by Issy Douvartzidis. Resulting files were reconstructed in NRecon (Bruker software accompanying scanner). Scanning resolution was chosen based on specimen size, between 8.5µ and 17µ. The

corresponding voxel size was entered when opening the Micro-CT data in Avizo Light (v 9.0) to maintain true scale.

Some limitations of this method are due to the lower available kV of the in-vivo Skyscan machine. Fossils had to have a majority of their adhering matrix removed prior to scanning and osteoderms on wet specimens were segmented out in order to leave the skull and mandibular features visible.

1.9.22.2 Dry skeletons

Dry skeletons of extant species within the Egerniinae were sourced from the existing South Australian Museum Herpetology collection and through preparation of a small number of frozen or field-collected carcasses at Flinders University (see Appendix 1).

Specimens collected as articulated or associated skeletons found while conducting palaeontological field work were identified to species based on external soft tissues using keys in Wilson and Swan (2017) and Cogger (2018). Information noted with the collection of these specimens included location, collection date, cause of death (if known, i.e. raptor prey, road kill, pit-fall deaths), gender, and measurements of snout-vent length, head length and width. Maceration in warm water softened the integumental tissues so that skin could be removed. Maceration of a number of specimens generated completely disarticulated skulls for comparison with fossils (FUR071, 191, 130, 176 and 168). Specimens for disarticulation were chosen to represent ontogenetic stages from neonate through to adult of *Tiliqua scincoides*. When possible, complete specimens sourced from other Flinders University research projects (euthanized by the Lizard Ecology, Genetics and Sociality group under their associated ethics permits) were photographed and weighed prior to flensing.

1.9.23 Fossil material

1.9.23.1 Collection of material

The fossil material referred to in this thesis has originated from three major palaeontological sites: the UNSW led research programme on the Riversleigh Fossil World Heritage Area of north-western Queensland; Flinders University Palaeontology excavations in Cathedral Cave in Wellington, New South Wales and the Namba Formation from Frome Downs Station in central South Australia. Each of these fossil sites sample different time periods, palaeoenvironments and taphonomic processes. This material is not examined exclusively: extensive searches of museum palaeontology collections in Adelaide, Brisbane, Sydney and Melbourne maximise the samples of each newly described species and map their distributions spatio-temporally across Sahul.

Associate Professor Trevor Worthy and Dr Aaron Camens' first trip to Lake Pinpa in 2007 unearthed a few small scincid fragments (SAMA P43057–43058). A return trip in 2016 relocated the 'Fish Lens' at Billeroo Creek Site 2. The lens material was collected in bulk and screened in the lab. Screening of this sediment led to a significant increase in the recovery of scincid material. Two further trips to Lake Pinpa in 2017 and 2018 increased the sample of Oligocene fauna. On both occasions, more of 'Fish Lens' at Billeroo Creek (BC2) and Site 12 at Lake Pinpa (LP12) was excavated, unearthing enough material to describe a new species, contributing to the new stem taxon of *Proegernia* in Chapter 2 of this thesis.

Material from Riversleigh World Heritage Area (see Archer et al., 2006) was sent to Dr Mark Hutchinson in the mid-1990's after a summary of the scincid material was published in Hutchinson (1992). Further examination of the *Egernia* sp. cf. *striolata* material from this collection resulted in discussions that became the third chapter of this thesis.

A major excavation of Cathedral Cave at Wellington in New South Wales (see Dawson and Augee, 1997), by Diana Fusco and Prof Gavin Prideaux, began in 2016. The first element identified as scincid was discovered on site by Dr Elen Shute, a single complete frontal of *Tiliqua laticephala*. This element was immediately brought to my attention on the team's return to Flinders University and directed sorting efforts to other material collected from that excavation, resulting in abundant material of this unique taxon, forming the basis of Chapter 4.

1.9.24 Phylogenetic methods

Systematics is now usually informed by phylogenetic analyses of phenotypic or genetic characters to hypothesise genealogical relationships, associated taxonomic groupings and ancestors. These groupings are then visualised in the form of a branching diagram, often called a phylogeny, cladogram, or 'tree'. The first simple tree recognising a branching order of related taxa was drawn by Charles Darwin to illustrate his theory of evolution (Darwin, 1859). Tree theory developed into a rigorous scientific method with the advent of cladistics by Willi Hennig in the mid-20th century, the methods and applications of this field advancing at a rapid pace ever since (Wiley et al., 1991; Hamilton, 2013). At least for analyses involving morphological traits, two methods are currently commonly used: parsimony and Bayesian Inference. Parsimony results in a phylogenetic hypothesis that possesses the fewest number of evolutionary steps (e.g. character-state changes). Bayesian analyses combine maximum likelihood models for each character state change along every branch, and models of evolutionary diversification, with prior knowledge (i.e. maximum and minimum node and tip ages, amounts of rate variation) in order to produce a tree with branches reflecting the highest posterior probability.

1.9.24.1 Morphology and/or molecular data?

Morphological and molecular data complement each other's strengths in a combined analysis. Molecular data are easily accessible online through Genbank or cheap efficient next-gen sequencing, providing giant data matrices of thousands or millions of characters for each taxon. Morphological data collection allows for the integration of fossil taxa, providing dated nodes and/or tips, and ancestral (crown) or extinct (stem) lineages, with intermediate phenotypic forms (Wiens, 2004; Lee et al., 2014).

Morphological character selection and coding methodology is a contentious subject in systematics: phenotypic characters are often not easily divided into discrete character states (Simões et al., 2017). Character selection or elimination is often not detailed thereby invalidating the scientific process of repeatability (Poe and Wiens, 2000). A way to limit biases associated with this process is to replace discretised character states with continuous measurement data (Goloboff et al., 2006; Simões et al., 2017), thereby removing vague definitions such as: small, medium, or large; narrow or wide; and deep or shallow. Measurements can be precise if labelled diagrams or clear instructions are provided, which map out standardised points to measure from. Continuous characters are not without biases; taxon characterisation based on measuring only one specimen cannot adequately capture or characterise ontogenetic, dimorphic or population variation. Where possible, adult specimens are chosen from a population of known morphological variability, and these individuals represent no extreme morphological differences from the modal shape and size of other adults.

Morphological and morphometric variation can be captured using micro-computed tomography scans (Micro-CT), a Scanning Electron Microscope (SEM), conventional microscopy, or with digital callipers and dry skeletal specimens. Each method has various benefits and level of resolution. Dry skeletons can be coded and measured without removing the specimen from a collection, particularly useful for holotypes. Micro-CT is a non-destructive method for viewing skulls within ethanol-preserved specimens or fragile fossils encased in matrix. SEMs and conventional microscopy provide high resolution images of the smallest details, such as tooth crown striae, sutures or muscle scarring.

1.9.24.2 Maximum Parsimony

The first true cladistics analyses were performed according to what is essentially 'Occam's razor' applied to systematics: the simplest answer is often the correct one. Maximum Parsimony (MP) is a method of analysing morphological or molecular characters in order to create the shortest possible tree with the least number of state changes along all branches (see Edwards and Cavalli-

Sforza, 1963; Camin and Sokal, 1965; Hennig, 1966). With increasingly larger datasets, it becomes impossible to evaluate every possible tree topology, and so heuristic tree search methods were developed to search for the 'best' trees (Page, 1993). It is common for more than one shortest tree to result from a single character matrix, in which case multiple equally parsimonious, or 'best', trees need to be combined to find a consensus tree. The support for individual clades can be statistically tested via bootstrapping (Felsenstein, 1985), or Bremer support (Bremer, 1988).

Large data matrices have driven the rise in required computational power for analytical programs for parsimony analyses. The standard computer program for most systematists in recent decades was PAUP* (Swofford, 2003), capable of running most datasets of a reasonable size. TNT (Goloboff et al., 2006; Goloboff and Catalano, 2016), a new program with increased analysis speeds for large data sets, and the ability to handle continuous morphological and morphometric data, is quickly replacing PAUP*. There are still some things that PAUP* can do and TNT cannot, e.g. rapid filtering of trees and characters, and (limited) likelihood analyses.

Parsimony analyses remains a standard inference method for morphological phylogenetic trees. However, the role they play now is diminishing as character evolution might be too complex to be explained by simple parsimony, which essentially assumes that all potential homologies are equal expressions of true relatedness, and that homoplasies are *ad hoc* coincidences or the result of less-accurate phylogenetic reconstructions (Kluge and Grant, 2006). Biology and the process of evolution is not always simple, we have large suites of phenotypic homoplasies so the parsimony assumption is not always ideal. The main assumption of parsimony is that all characters are weighted equally and are all equally phylogenetically informative. Parsimony provides a topology without associated probability statistics, so measures of support (bootstrap, Bremer) can be difficult to interpret mathematically. Fossil phenotypes demonstrate that the number of character transitions are highly variable and with the added complications of reversals the shortest tree may not be the best.

1.9.24.3 Bayesian analyses

Bayesian analyses in phylogenetics are based on Bayes Theorem; the probability of an event is calculated using prior knowledge of the subject, and likelihood based on previously collated data. When applied, it results in a tree and associated branch lengths that is a product of prior knowledge (i.e. diversification and clock priors) and likelihood (how well a tree fits the character and stratigraphic data). The advantages of using Bayesian analyses include the potential incorporation of multiple different data forms (i.e. discrete/meristic/continuous morphological, molecular, biogeographical, and behavioural) and associated models and the ability to calculate the probability

of different hypotheses, e.g. alternative trees or ancestral states. Diversification and clock priors are models that estimate the rate at which characters states change across the tree. While exploring the topology of the tree, Bayesian analyses can co-estimate parameters such as the rate of evolution, branch lengths, and divergence dates. These analyses could involve infinite number of possible solutions, which is why Markov-Chain Monte Carlo (MCMC) random walk methods are used to sample the vast realm of probable trees and parameters (see Yang and Rannala, 1997). The 'Monte Carlo' element is named for the casino-style odds that enough of the posterior probability space is sampled to give an accurate probability that the correct answer has been found (Felsenstein, 2004). Given enough sampling effort (e.g. multiple chains running for longer periods of time i.e. Metropolis-Coupled MCMC or MC3), this method can provide a very representative sample of the possible tree space.

Choosing priors suitable for each analysis is based on the primary aims of the investigation and the sources of data available. Clock priors without fossils help us time divergences (molecular clock models and node age priors). With fossils, relaxed clock priors provide a means of examining differing rates of change on individual branches (e.g. uncorrelated relaxed clock) or rates of change through different time periods (epoch relaxed clock; Lee and Palci, 2015). Models of speciation and extinction rates work with the data and clock models to inform rates of evolution and branching patterns across a tree. Simple Yule (pure birth process; Yule, 1924), Birth–Death (Raup et al., 1973; Yang and Rannala, 1997) models, Fossilised Birth–Death (Heath et al., 2014), and Sampled-Ancestor (Gavryushkina et al., 2014) models increase in complexity, derived from the increasing accuracy of the model to known biological processes involving rates of speciation, extinction and fossilisation.

The programs available for Bayesian analyses have diversified for different uses, employing alternate models, data types and outputs. One of the most commonly used programs is MrBayes (Ronquist et al., 2012b), which allows for discrete morphological and molecular data, and node and tip calibrations producing majority rule consensus trees using heated MC3 chains. BEAST - Bayesian Evolutionary Analyses Sampling Trees (Drummond et al., 2012) was developed with BEAUti, a guided user interface for biologists to construct complex xml scripts with inputs such as a chosen birth-death model, clock, and discrete morphological and molecular data. BEAST has many added advantages in that when dropping BEAUti in favour of rewriting the input text file (.xml) other models and data types can be incorporated. Continuous data (measurements or biogeography), can be analysed under a Brownian Evolution model (Lemey et al., 2010), and clocks can be calibrated with stratigraphic ranges (rather than averaged fossil ages) with fossils as 'tips' rather than nodes. Output log files can be examined in Tracer (Rambaut et al., 2018) to test that the

analyses have explored the possible parameter space sufficiently, and combined results of multiple runs produce a larger sample size of possibilities; TreeAnnotator calculates consensus trees from these Bayesian samples. BEAST2 branched from the BEAST to allow users to develop their own modules, and includes many new models and features. In this context, the sampled ancestor time-trees (Gavryushkina et al., 2014) in BEAST2 are relevant, but the latter cannot yet handle continuous morphological data.

1.9.25 The importance of fossil data

Previous analyses of morphology-only data sets have produced both similar and alternative topologies to the molecular and combined morph+molecular results for squamates. Squamata often breaks into two clades, Iguania (pleurodont and acrodont clades) and Scleroglossa (all other lizards and snakes) in most morphology-only informed trees (Lee, 1998; Conrad, 2008; Gauthier et al., 2012). Recent molecular evidence nests Iguania within Scleroglossa or 'Unidentata', with Dibamidae and Gekkota as the earliest-branching clades (Vidal and Hedges, 2009; Wiens et al., 2012; Pyron et al., 2013; Tonini et al., 2016; Burbrink et al., 2019). Combined studies confirm hidden morphological support for the relationships found in molecular analyses (Reeder et al., 2015). Convergence on limb-loss and body elongation seems to be a major factor influencing the topology of the morphology-only analyses, with snakes grouping with elongate amphisbaenians and scincomorphs. Convergence is often pervasive in morphological data sets, stressing the importance of a molecular backbone to re-optimise morphological characters across well-supported clades (Lee and Palci, 2015).

Including fossil taxa in phylogenetic analyses informs the timing of the origins of major clades (see Laurin, 2012), highlights the existence of stem groups, and introduces new morphological possibilities (e.g. dinosaurs) not seen in extant taxa (Edgecombe, 2010). Fossil taxa are often used as node age constraints in molecular analyses, including many for Australian squamates (Lee et al., 2009a; Oliver and Sanders, 2009; Skinner et al., 2011). Node constraints provide minimum estimates of clade ages based on the presence of a fossil taxon that is presumed to be from that clade (Lee and Palci, 2015). Node calibrations are typically inflexible in the positioning of fossil taxa. If the fossil is fragmentary, it may preserve only plesiomorphic characters representing multiple clades, the node calibration then drawing those clades crownward. Tip-dating is a method usually paired with a combination of both molecular and morphological data, resulting in a 'total-evidence' approach to fossil placement and time calibrations (Ronquist et al., 2012a). The benefits of Bayesian analyses inclusive of tip-dating are that fossils calibrate the rate of morphological change across the tree (see Chapter 3), and fossils can be retrieved as stem lineages

divergent of extant crown groups (see Chapter 4). With new analytical programs, full potential stratigraphic ranges can be provided rather than mean or median dates for tip calibrations.

1.10 References

Andrews, P. 1990. Owls, caves and fossils. The Natural History Museum, London, 230 pp.

Archer, M. 1978. Quaternary vertebrate faunas from the Texas Caves of southeastern Queensland. Memoirs of the Queensland Museum 19:61–109.

Archer, M., D. A. Arena, M. Bassarova, R. M. D. Beck, K. Black, W. E. Boles, P. Brewer, B. N. Cooke, K. Crosby, A. Gillespie, H. Godthelp, S. J. Hand, B. P. Kear, J. Louys, A. Morrell, J. Muirhead, K. K. Roberts, J. D. Scanlon, K. J. Travouillon, and S. Wroe. 2006. Current status of species-level representation in faunas from selected fossil localities in the Riversleigh World Heritage Area, northwestern Queensland. Alcheringa: An Australasian Journal of Palaeontology 30:1–17.

Atlas of Living Australia. 2019. Mapping and Analyses Spatial Portal;Commonwealth Scientific and Industrial Research Organisation.

Bartholomai, A. 1977. The fossil vertebrate fauna from Pleistocene deposits at Cement Mills, Gore, Queensland. Memoirs of the Queensland Museum 18:41–51.

Baynes, A., C. Piper, and K. M. Thorn. 2019. An experimental investigation of differential recovery of native rodent remains from Australian palaeontological and archaeological deposits. Records of the Western Australian Museum 34:1–30.

Bell, C. J., and J. I. Mead. 2014. Not enough skeletons in the closet: Collections-based anatomical research in an age of conservation conscience. The Anatomical Record 297:344–348.

Bremer, K. 1988. The limits of amino acid sequence data in angiosperm phylogenetic reconstruction. Evolution 42:795–803.

Brown, G. 1991. Ecological feeding analysis of south-eastern Australian scincids (Reptilia, Lacertilia). Australian Journal of Zoology 39:9–29.

Bull, C. M. 2000. Monogamy in lizards. Behavioural Processes 51:7–20.

Bull, C. M., and Y. Pamula. 1996. Sexually dimorphic head sizes and reproductive success in the sleepy lizard *Tiliqua rugosa*. Journal of Zoology 240:511–521.

Bull, M., M. Hutchinson, and A. Fenner. 2007. Omnivorous diet of the endangered Pygmy Bluetongue Lizard, *Tiliqua adelaidensis*. Amphibia-Reptilia 28:560–565.

Burbrink, F. T., F. G. Grazziotin, R. A. Pyron, D. Cundall, S. Donnellan, F. Irish, J. S. Keogh, F. Kraus, R. W. Murphy, B. Noonan, C. J. Raxworthy, S. Ruane, A. R. Lemmon, E. M. Lemmon, and H. Zaher. 2019. Interrogating genomic-scale data for Squamata (lizards, snakes, and amphisbaenians) shows no support for key traditional morphological relationships. Systematic biology.

Camin, J. H., and R. R. Sokal. 1965. A method for deducing branching sequences in phylogeny. Evolution 19:311–326.

Čerňanský, A., and M. N. Hutchinson. 2013. A new large fossil species of *Tiliqua* (Squamata: Scincidae) from the Pliocene of the Wellington Caves (New South Wales, Australia). Alcheringa: An Australasian Journal of Palaeontology 37:131–136.

Chapman, A. D. 2009. Numbers of living species in Australia and the world. Australian Biological Resources Study, Toowoomba, Australia.

Chapple, D. G. 2003. Ecology, life-history, and behavior in the Australian scincid genus *Egernia*, with comments on the evolution of complex sociality in lizards. Herpetological Monographs 17:145–180.

Chapple, D. G., and J. S. Keogh. 2005. Complex mating system and dispersal patterns in a social lizard, Egernia whitii. Molecular Ecology 14:1215–1227.

Chapple, D. G., J. S. Keogh, and M. N. Hutchinson. 2004. Molecular phylogeography and systematics of the arid-zone members fo the *Egernia whitii* (Lacertilia: Scincidae) species group. Molecular Phylogenetics and Evolution 33:549–561.
Chapple, D. G., P. A. Ritchie, and C. H. Daugherty. 2009. Origin, diversification, and systematics of the New Zealand skink fauna (Reptilia: Scincidae). Molecular Phylogenetics and Evolution 52:470–487.
Clemann, N., M. Hutchinson, P. Robertson, D. C. Chapple, G. Gillespie, J. Melville, and D. Michael. 2018. *Liopholis montana*; pp. e.T109478522A109478529 The IUCN Red List of Threatened Species.
Cogger, H. G. 2018. Reptiles & Amphibians of Australia. Updated 7th Edition. CSIRO Publishing, Clayton South, Victoria, Australia.
Conrad, J. L. 2008. Phylogeny and systematics of Squamata (Reptilia) based on morphology. Bulletin of the American Museum of Natural History:1–182.
Darwin, C. 1859. The origin of species by means of natural selection or the preservations of favoured races in the struggle for life. 1st Edition. John Murray, London, 502 pp.
Dawson, L., and M. Augee. 1997. The late Quaternary sediments and fossil vertebrate fauna from Cathedral Cave, Wellington Caves, New South Wales. Proceedings-Linnean Society of New South Wales 117:51–78.
Doughty, P., L. Kealley, and S. C. Donnellan. 2011. Revision of the Pygmy Spiny-tailed Skinks (*Egernia depressa* species-group) from Western Australia, with descriptions of three new species. Records of the Western Australian Museum 26:115–137.
Drummond, A. J., M. A. Suchard, D. Xie, and A. Rambaut. 2012. Bayesian phylogenetics with BEAUti and the BEAST 1.7. Molecular biology and evolution 29:1969–1973.
Dubas, G., and C. Bull. 1991. Diet choice and food availability in the omnivorous lizard, *Trachydosaurus rugosus*. Wildlife Research 18:147–155.
Edgecombe, G. D. 2010. Palaeomorphology: fossils and the inference of cladistic relationships. Acta Zoologica 91:72-80.
Edwards, A. W. F., and L. L. Cavalli-Sforza. 1963. The reconstruction of evolution. Annals of Human Genetics 27:105–106.
Estes, R., and E. E. Williams. 1984. Ontogenetic variation in the molariform teeth of lizards. Journal of Vertebrate Paleontology 4:96–107.
Estes, R., K. De Queiroz, and J. Gauthier. 1988. Phylogenetic relationships of the lizard families. Stanford Univ Press, Stanford, CA, Stanford, California, 648 pp.
Evans, S. E. 2003. At the feet of the dinosaurs: the early history and radiation of lizards. Biological Reviews 78:513–551.
Evans, S. E. 2008. The skull of lizards and Tuatara; pp. 1–343 in C. Gans, A. S. Gaunt, and K. Adler (eds.), Biology of the Reptilia 20, Morphology H The skull of Lepidosauria. Society for the Study of Amphibians and Reptiles, Ithaca, NY.
Evans, S. E., and M. E. Jones. 2010. The origin, early history and diversification of lepidosauromorph reptiles; pp. 27–44, New aspects of Mesozoic biodiversity. Springer Berlin Heidelberg.
Felsenstein, J. 1985. Confidence limits on phylogenies: An approach using the bootstrap. Evolution 39:783–791.
Felsenstein, J. 2004. Inferring Phylogenies. Sinauer Associates, Sunderland, Massachusetts.
Gans, C., F. De Vree, and D. Carrier. 1985. Usage pattern of the complex masticatory muscles in the Shingleback lizard, *Trachydosaurus rugosus*: a model for muscle placement. The American Journal of Anatomy 173:219–240.
Gardner, M. G., C. M. Bull, and S. J. B. Cooper. 2002. High levels of genetic monogamy in the group-living Australian lizard Egernia stokesii. Molecular Ecology 11:1787–1794.
Gardner, M. G., A. F. Hugall, S. C. Donnellan, M. N. Hutchinson, and R. Foster. 2008. Molecular systematics of social skinks: phylogeny and taxonomy of the *Egernia* group (Reptilia: Scincidae). Zoological Journal of the Linnean Society 154:781–794.

Gauthier, J. A., M. Kearney, J. A. Maisano, O. Rieppel, and A. D. B. Behlke. 2012. Assembling the Squamate Tree of Life: Perspectives from the Phenotype and the Fossil Record. Bulletin of the Peabody Museum of Natural History 53:3–308.
Gavryushkina, A., D. Welch, T. Stadler, and A. J. Drummond. 2014. Bayesian inference of sampled ancestor trees for epidemiology and fossil calibration. PLOS Computational Biology 10:e1003919.
Gillespie, G., J. Woinarski, P. McDonald, H. Cogger, and A. Fenner. 2018. *Bellatorias obiri*; pp. e.T47155317A47155335 The IUCN Red List of Threatened Species.
Goloboff, P. A., and S. A. Catalano. 2016. TNT version 1.5, including a full implementation of phylogenetic morphometrics. Cladistics 32:221–238.
Goloboff, P. A., C. I. Mattoni, and A. S. Quinteros. 2006. Continuous characters analyzed as such. Cladistics 22:589–601.
Greer, A. E. 1970. A subfamilial classification of scincid lizards. Bulletin of the Museum of Comparative Zoology at Harvard College 139:151–183.
Greer, A. E. 1979. A phylogenetic subdivision of Australian skinks. Records of the Australian Museum 32:339–371.
Hagen, I. J., S. C. Donnellan, and C. M. Bull. 2012. Phylogeography of the prehensile-tailed skink *Corucia zebrata* on the Solomon Archipelago. Ecology and evolution 2:1220–1234.
Hamilton, A. 2013. The evolution of phylogenetic systematics. University of California Press, Oakland, California, 320 pp.
Heath, T. A., J. P. Huelsenbeck, and T. Stadler. 2014. The fossilized birth–death process for coherent calibration of divergence-time estimates. Proceedings of the National Academy of Sciences 111:E2957–E2966.
Hedges, S. B. 2014. The high-level classification of skinks (Reptilia, Squamata, Scincomorpha). Zootaxa 3765:317–338.
Hedges, S. B., J. Marin, M. Suleski, M. Paymer, and S. Kumar. 2015. Tree of life reveals clock-like speciation and diversification. Molecular biology and evolution 32:835–845.
Hennig, W. 1966. Phylogenetic systematics. University of Illinois Press, Chicago, USA, 263 pp.
Hildebrand, M., and G. E. Goslow. 2001. Analysis of vertebrate structure. 5th Edition. Wiley, New York, 635 pp.
Hocknull, S. A. 2000. Remains of an Eocene skink from Queensland. Alcheringa: An Australasian Journal of Palaeontology 24:63–64.
Hocknull, S. A. 2005. Ecological succession during the late Cainozoic of central eastern Queensland: extinction of a diverse rainforest community. Memoirs of the Queensland Museum 51:39–122.
Hollenshead, M. G. 2011. Geometric morphometric analysis of cranial variation in the *Egernia depressa* (Reptilia: Squamata: Scincidae) species complex. Records of the Western Australian Museum 26:138–153.
Hollenshead, M. G., J. I. Mead, and S. L. Swift. 2011. Late Pleistocene *Egernia* group skinks (Squamata: Scincidae) from Devils Lair, Western Australia. Alcheringa: An Australasian Journal of Palaeontology 35:31–51.
Honda, M., H. Ota, M. Kobayashi, and T. Hikida. 1999. Phylogenetic relationships of Australian skinks of the *Mabuya* group (Reptilia: Scincidae) inferred from mitochondrial DNA sequences. Genes and Genetics Systems 74:135–139.
Honda, M., H. Ota, M. Kobayashi, J. Nabhitabhata, H.-S. Yong, and T. Hikida. 2000. Phylogenetic relationships, character evolution, and biogeography of the subfamily Lygosominae (Reptilia: Scincidae) inferred from mitochondrial DNA sequences. Molecular Phylogenetics and Evolution 15:452–461.
Horton, D. R. 1972. Evolution in the genus *Egernia* (Lacertilia:Scincidae). Journal of Herpetology 6:101–109.

Hutchinson, M. N. 1981: The systematic relationships of the genera *Egernia* and *Tiliqua* (Lacertilia: Scincidae). A review and immunological reassessment. Proceedings of the Melbourne Herpetological Symposium, 1981.
Hutchinson, M. N. 1992. Origins of the Australian scincid lizards: a preliminary report on the skinks of Riversleigh. The Beagle, Records of the Northern Territory Museum of Arts and Sciences 9:61–70.
Hutchinson, M. N., and B. S. Mackness. 2002. Fossil lizards from the Pliocene Chinchilla Local Fauna, Queensland. Records of the South Australian Museum 35:169–184.
Hutchinson, M. N., and J. D. Scanlon. 2009. New and unusual Plio-Pleistocene lizard (Reptilia: Scincidae) from Wellington Caves, New South Wales, Australia. Journal of Herpetology 43:139–147.
King, B., and M. S. Y. Lee. 2015. Ancestral state reconstruction, rate heterogeneity, and the evolution of reptile viviparity. Systematic biology 64:532–544.
Klingenböck, A., K. Osterwalder, and R. Shine. 2000. Habitat use and thermal biology of the "Land mullet" *Egernia major*, a large Scincid lizard from remnant rain forest in southeastern Australia. Copeia 2000:931–939.
Kluge, A. G., and T. Grant. 2006. From conviction to anti-superfluity: old and new justifications of parsimony in phylogenetic inference. Cladistics 22:276–288.
Kosma, R. 2003. The dentitions of recent and fossil scincomorphan lizards (Lacertilia, Squamata) - Systematics, Functional Morphology, Palecology. Department of Geosciences and Geography, University Hannover, Hanover, Germany, 231 pp.
Lambert, S. M., T. W. Reeder, and J. J. Wiens. 2015. When do species-tree and concatenated estimates disagree? An empirical analysis with higher-level scincid lizard phylogeny. Molecular Phylogenetics and Evolution 82:146–155.
Laurin, M. 2012. Recent progress in paleontological methods for dating the Tree of Life. Frontiers in Genetics 3.
Lécuru, S. 1969: Étude morphologique de l'humérus des lacertiliens. Annales des Sciences Naturelles, Zoologie (12), 1969.
Lee, M. S. Y. 1998. Convergent evolution and character correlation in burrowing reptiles: towards a resolution of squamate relationships. Biological Journal of the Linnean Society 65:369–453.
Lee, M. S. Y., and A. Palci. 2015. Morphological phylogenetics in the genomic age. Current Biology 25:R922–R929.
Lee, M. S. Y., P. M. Oliver, and M. N. Hutchinson. 2009a. Phylogenetic uncertainty and molecular clock calibrations: A case study of legless lizards (Pygopodidae, Gekkota). Molecular Phylogenetics and Evolution 50:661–666.
Lee, M. S. Y., A. Cau, D. Naish, and G. J. Dyke. 2014. Morphological Clocks in Paleontology, and a Mid-Cretaceous Origin of Crown Aves. Systematic biology 63:442–449.
Lemey, P., A. Rambaut, J. J. Welch, and M. A. Suchard. 2010. Phylogeography takes a relaxed random walk in continuous space and time. Molecular biology and evolution 27:1877–1885.
Lyman, R. L. 1994. Vertebrate Taphonomy. Cambridge University Press, Cambridge, 555 pp.
Mackness, B. S., and M. N. Hutchinson. 2000. Fossil lizards from the Early Pliocene Bluff Downs Local Fauna. Transactions of the Royal Society of South Australia 124:17–30.
McDowell, M. C., and G. C. Medlin. 2009. The effects of drought on prey selection of the barn owl (*Tyto alba*) in the Strzelecki Regional Reserve, north-eastern South Australia. Australian Mammalogy 31:47–55.
Milewski, A. V. 1981. A comparison of reptile communities in relation to soil fertility in the mediterranean and adjacent arid parts of Australia and Southern Africa. Journal of Biogeography 8:493–503.
Mittleman, M. B. 1952. A generic synopsis of the lizards of the subfamily Lygosominae. Smithsonian Miscellaneous Collections 117:1–35.

Nyakatura, J. A., E. Andrada, S. Curth, and M. S. Fischer. 2014. Bridging “Romer’s Gap”: limb mechanics of an extant belly-dragging lizard inform debate on tetrapod locomotion during the early carboniferous. Evolutionary Biology 41:175–190.
O'Connor, D., and R. Shine. 2003. Lizards in ‘nuclear families’: a novel reptilian social system in *Egernia saxatilis* (Scincidae). Molecular Ecology 12:743–752.
Oliver, P. M., and K. L. Sanders. 2009. Molecular evidence for Gondwanan origins of multiple lineages within a diverse Australasian gecko radiation. Journal of Biogeography 36:2044–2055.
Page, R. D. M. 1993. On islands of trees and the efficacy of different methods of branch swapping in finding most-parsimonious trees. Systematic biology 42:200–210.
Pianka, E. R. 1986. Ecology and natural history of desert lizards: analyses of the ecological niche and community structure. Princeton University Press, Princeton, NJ.
Pledge, N. S. 1992. The Curramulka local fauna: a new late Tertiary fossil assemblage from Yorke Peninsula, South Australia. The Beagle, Records of the Northern Territory Museum of Arts and Sciences 9:115–142.
Poe, S., and J. J. Wiens. 2000. Character selection and the methodology of morphological phylogenetics; pp. 20–36 in J. J. Wiens (ed.), Phylogenetic analysis of morphological data. Smithsonian Institution Press, Washington, DC.
Price, G. J., and I. H. Sobbe. 2005. Pleistocene palaeoecology and environmental change on the Darling Downs, southeastern Queensland, Australia. Memoirs of the Queensland Museum 51:171–201.
Prideaux, G. J., J. A. Long, L. K. Ayliffe, J. C. Hellstrom, B. Pillans, W. E. Boles, M. N. Hutchinson, R. G. Roberts, M. L. Cupper, L. J. Arnold, P. D. Devine, and N. M. Warburton. 2007. An arid-adapted middle Pleistocene vertebrate fauna from south-central Australia. Nature 445:422–425.
Pyron, R. A., F. T. Burbrink, and J. J. Wiens. 2013. A phylogeny and revised classification of Squamata, including 4161 species of lizards and snakes. BMC Evolutionary Biology 13:93.
Rabosky, D. L., S. C. Donnellan, A. L. Talaba, and I. J. Lovette. 2007. Exceptional among-lineage variation in diversification rates during the radiation of Australia's most diverse vertebrate clade. Proceedings of the Royal Society of London B: Biological Sciences 274:2915–2923.
Rambaut, A., A. J. Drummond, D. Xie, G. Baele, and M. A. Suchard. 2018. Posterior summarisation in Bayesian phylogenetics using Tracer 1.7. Systematic biology 67:901–904.
Raup, D. M., S. J. Gould, T. J. M. Schopf, and D. S. Simberloff. 1973. Stochastic models of phylogeny and the evolution of diversity. The Journal of Geology 81:525–542.
Reed, E. H., and S. J. Bourne. 2000. Pleistocene fossil vertebrate sites of the South East region of South Australia. Transactions of the Royal Society of South Australia 124:61–90.
Reed, E. H., and S. J. Bourne. 2009. Pleistocene fossil vertebrate sites of the South East region of South Australia II. Transactions of the Royal Society of South Australia 133:30–40.
Reeder, T. W. 2003. A phylogeny of the Australian *Sphenomorphus* group (Scincidae: Squamata) and the phylogenetic placement of the crocodile skinks (*Tribolonotus*): Bayesian approaches to assessing congruence and obtaining confidence in maximum likelihood inferred relationships. Molecular Phylogenetics and Evolution 27:384–397.
Reeder, T. W., T. M. Townsend, D. G. Mulcahy, B. P. Noonan, P. L. Wood, Jr., J. W. Sites, Jr., and J. J. Wiens. 2015. Integrated analyses resolve conflicts over squamate reptile phylogeny and reveal unexpected placements for fossil taxa. PLoS ONE 10:e0118199.
Rich, T. H. 1991. Monotremes, placentals, and marsupials: their record in Australia and its biases; pp. 894–1057 in P. Vickers-Rich, J. M. Monaghan, R. F. Baird, and T. H. Rich (eds.), Vertebrate Palaeontology of Australasia. Pioneer Design Studio Pty Ltd, Melbourne, Australia.
Richter, A. 1994. Lacertilia aus der Unteren Kreide von Una und Galve (Spanien) und Anoual (Marokko). Berliner geowissenschaftliche Abhandlungen (E: Paläobiologie) 14:1–147.

Richter, A., and M. Wuttke. 2012. Analysing the taphonomy of Mesozoic lizard aggregates from Uña (eastern Spain) by X-ray controlled decay experiments. Palaeobiodiversity and Palaeoenvironments 92:5–28.
Ronquist, F., S. Klopfstein, L. Vilhelmsen, S. Schulmeister, D. L. Murray, and A. P. Rasnitsyn. 2012a. A total-evidence approach to dating with fossils, applied to the early radiation of the hymenoptera. Systematic biology 61:973–999.
Ronquist, F., M. Teslenko, P. Van Der Mark, D. L. Ayres, A. Darling, S. Höhna, B. Larget, L. Liu, M. A. Suchard, and J. P. Huelsenbeck. 2012b. MrBayes 3.2: efficient Bayesian phylogenetic inference and model choice across a large model space. Systematic biology 61:539–542.
Russell, A. P., and A. M. Bauer. 2008. The appendicular locomotor apparatus of *Sphenodon* and normal-limbed squamates; pp. in C. Gans, A. S. Gaunt, and K. Adler (eds.), The skull and appendicular locomotor apparatus of Lepidosauria. Society for the Study of Amphibians and Reptiles, Ithaca, New York, USA.
Schofield, J. A., A. L. Fenner, K. Pelgrim, and C. M. Bull. 2012. Male-biased movement in pygmy bluetongue lizards: implications for conservation. Wildlife Research 39:677–684.
Shea, G. M. 1990. The genera *Tiliqua* and *Cyclodomorphus* (Lacertilia: Scincidae): generic diagnoses and systematic relationships. Memoirs of the Queensland Museum 29:495–520.
Shea, G. M., and M. N. Hutchinson. 1992. A new species of lizard (*Tiliqua*) from the Miocene of Riversleigh, Queensland. Memoirs of the Queensland Museum 32:303–310.
Simões, T. R., M. W. Caldwell, A. Palci, and R. L. Nydam. 2017. Giant taxon-character matrices: quality of character constructions remains critical regardless of size. Cladistics 33:198–219.
Skinner, A., A. F. Hugall, and M. N. Hutchinson. 2011. Lygosomine phylogeny and the origins of Australian scincid lizards. Journal of Biogeography 38:1044–1058.
Smith, K. T., and M. Wuttke. 2012. From tree to shining sea: taphonomy of the arboreal lizard *Geiseltaliellus maarius* from Messel, Germany. Palaeobiodiversity and Palaeoenvironments 92:45–65.
Smith, M. A. 1937. A review of the genus *Lygosoma* (Scincidae: Reptilia) and its allies. Records of the Indian Museum 39:213–234.
Smith, M. J. 1976. Small fossil vertebrates from Victoria Cave, Naracoorte, South Austraia. IV, Reptiles. Transactions of the Royal Society of South Australia 100:39–51.
Smith, M. J. 1982. Reptiles from Late Pleistocene deposits on Kangaroo Island, South Australia. Transactions of the Royal Society of South Australia 106:61–66.
Storr, G. M. 1978. The genus *Egernia* (Lacertilia, Scincidae) in Western Australia. Records of the Western Australian Museum 6:147–187.
Swofford, D. L. 2003. PAUP*: Phylogenetic Analysis Using Parsimony (*and other methods). 4.0 b10. Sinauer Associates, Sunderland, Massachusetts.
Title, P. O., and D. L. Rabosky. 2016. Do macrophylogenies yield stable macroevolutionary inferences? An example from squamate reptiles. Systematic biology 66:843–856.
Tonini, J. F. R., K. H. Beard, R. B. Ferreira, W. Jetz, and R. A. Pyron. 2016. Fully-sampled phylogenies of squamates reveal evolutionary patterns in threat status. Biological Conservation 204, Part A:23–31.
Uetz, P. 2010. The original descriptions of reptiles. Zootaxa 2334:59–68.
Uetz, P., P. Freed, and J. e. Hošek. 2019. The Reptile Database.
Vickers-Rich, P., and P. V. Rich. 1991. Vertebrate palaeontology of Australasia. Pioneer Design Studio, Melbourne, Australia, 1437 pp.
Vidal, N., and S. B. Hedges. 2009. The molecular evolutionary tree of lizards, snakes, and amphisbaenians. Comptes rendus biologies 332:129–139.
Welch, K. 1982. Herpetology of the Old World II. Preliminary comments on the classification of skinks (Family Scincidae) with specific reference to those genera found in Africa, Europe, and southwest Asia. Herptile 7:25–27.
While, G. M., T. Uller, and E. Wapstra. 2009. Family conflict and the evolution of sociality in reptiles. Behavioral Ecology 20:245–250.

Wiens, J. J. 2004. The role of morphological data in phylogeny reconstruction. Systematic biology 53:653–661.
Wiens, J. J., C. R. Hutter, D. G. Mulcahy, B. P. Noonan, T. M. Townsend, J. W. Sites, and T. W. Reeder. 2012. Resolving the phylogeny of lizards and snakes (Squamata) with extensive sampling of genes and species. Biology Letters 8:1043–1046.
Wiley, E. O., D. Siguel-Causey, D. R. Brooks, and V. A. Funk. 1991. The Compleat Cladist: A primer of phylogenetic procedures. Museum of Natural History, The University of Kansas, Lawrence, Kansas, 158 pp.
Williams, D. L. G. 1980. Catalogue of Pleistocene vertebrate fossils and sites in South Australia. Transactions of the Royal Society of South Australia 104:101–115.
Wilson, S., and G. Swan. 2017. A complete guide to the Reptiles of Australia. 5th Edition. Reed New Holland Publishers, Sydney, Australia, 647 pp.
Wineski, L. E., and C. Gans. 1984. Morphological basis of the feeding mechanics in the shingle-back lizard *Trachydosaurus rugosus* (Scincidae, Reptilia). Journal of Morphology 181:271–295.
Wright, A. M., K. M. Lyons, M. C. Brandley, and D. M. Hillis. 2015b. Which came first: The lizard or the egg? Robustness in phylogenetic reconstruction of ancestral states. Journal of Experimental Zoology Part B: Molecular and Developmental Evolution 324:504–516.
Yang, Z., and B. Rannala. 1997. Bayesian phylogenetic inference using DNA sequences: a Markov Chain Monte Carlo Method. Molecular biology and evolution 14:717–724.
Yule, G. 1924. A mathematical theory of evolution, based on the conclusions of Dr. JC Willis, FRS. Philosophical Transactions of the Royal Society of London Series B 213:21–87.
Zheng, Y., and J. J. Wiens. 2016. Combining phylogenomic and supermatrix approaches, and a time-calibrated phylogeny for squamate reptiles (lizards and snakes) based on 52 genes and 4162 species. Molecular Phylogenetics and Evolution 94, Part B:537–547.

CHAPTER 2: THE ORIGINS OF AUSTRALIAN EGERNIINAE REVEALED BY A NEW SPECIES OF *PROEGERNIA* FROM THE NAMBA FORMATION IN SOUTH AUSTRALIA

K. M. Thorn[1, 2], M. H. Hutchinson[2], M. S. Y. Lee[1, 2], N. Brown[1], A. B. Camens[1], and T. H. Worthy[1]

[1] College of Science and Engineering, Flinders University, Bedford Park, SA 5047, Australia

[2] South Australian Museum, North Terrace, Adelaide, SA 5000, Australia

2.1 Context

This chapter examines the temporal origins of the Australian Egerniinae. I was actively involved in the collection of material for this chapter, participating in two field trips to Lake Pinpa and Billeroo Creek during my candidature. The addition of a second species within *Proegernia*, with stratigraphic context, provides an age calibration close to the base of the phylogeny of egerniines and aids in our investigation of the temporal origins of the crown Australian radiation.

Note: nomenclatural acts in thesis chapters are not considered published under ICZN rules.

2.2 Statement of authorship

KMT conceived the project, conducted fieldwork, collected the data, performed analyses, produced all figures and wrote the manuscript. THW and ABC funded the project, conducted field work, contributed to discussions, and commented on multiple drafts of the manuscript; MNH and MSYL commented on multiple drafts of the manuscript and contributed to discussions. NB collected the stratigraphic samples and information as part of a separate honours project.

2.3 Abstract

New Oligo-Miocene fossil vertebrates from the Namba Formation (east of Lake Frome, South Australia) were uncovered from multiple expeditions from 2007–2018. Two primary collection sites were systematically excavated, the sedimentology recorded, and fossiliferous layers screened. During the Oligo-Miocene the Tarkarooloo sub-basin contained a large lacustrine system, now exposed around Lake Pinpa, which had seasonal fluctuations in water level resulting in the precipitation of Palygorskite and dolomitic clays. Immediately above the dolomite layer exposed in Lake Pinpa, abundant disarticulated material of small vertebrates was concentrated in shallow channels and along lake edges and is now exposed on the western shore. This fossiliferous deposit, also known from Billeroo Creek to the north of Lake Pinpa, includes aquatic (such as osteichthyes, lungfish, platypus *Obdurodon*, and waterfowl) and terrestrial (such as possums, dasyurids, and scincids) vertebrates and is hereafter recognised as the Fish Lens. A new egerniine scincid taxon *Proegernia mikebulli* sp. nov. described herein, is based on a near-complete reconstructed mandible, maxilla, premaxilla, and pterygoid. Other scincid elements recovered with this material, which could not yet be confidently associated with *P. mikebulli*, include a vertebra and proximal femur fragment. This new taxon and sister species *P. palankarinnensis*, when added to a tip-dated total-evidence phylogenetic analysis, are recovered as stem Australian egerniines, representing a separate radiation to all extant egerniines.

2.4 Introduction

Major biogeographical events have shaped the Australian flora and fauna, from the separation from Antarctica ~45 million years ago, through to Pleistocene glacial cycles (Hall, 2002; White, 2006). Australia's herpetofauna can be broadly traced from two origins: true relics from Gondwana, the southern supercontinent, or recent arrivals from Asia to Sahul, the continental mass including Australia and New Guinea (Skinner et al., 2011; Oliver and Hugall, 2017). Gondwanan origins are recorded for diplodactyloids, chelids and some frogs (Oliver and Sanders, 2009; Vidal and Hedges, 2009). The Asian route appears to have been taken by agamids, elapids, and typhlopids sometime during the Oligo-Miocene (Hugall and Lee, 2004; Sanders and Lee, 2008; Skinner et al., 2011). The temporal origins of Australian scincid lizard radiations are still unresolved. Morphological data led Greer to conclude that "there is nothing in the distribution of skinks as a whole that suggests that any skink ever used a Gondwanaland dispersal route" (Greer, 1979, pg. 354). Greer's inferences are supported by molecular data that indicate Australian scincids' closest extant relatives are in south-east Asia (Lambert et al., 2015).

The Australian scincids comprise three subfamilies: the Egerniinae Welch, 1982, Sphenomorphinae Welch, 1982 and Eugongylinae Welch, 1982 (Uetz et al., 2019). Of these three clades, detailed molecular phylogenetic analyses have been conducted for the sphenomorphine (Rabosky et al., 2007; Skinner et al., 2013) and egerniine radiations (Gardner et al., 2008), but no recent molecular phylogeny of the Australian eugongyline skinks has been published (see Chapple et al., 2009, which includes some Australian taxa). A molecular phylogenetic analysis of Australian skinks (Skinner et al., 2011) produced a node-calibrated molecular clock estimate of the divergence of all three subfamilies. Those results suggested that the Australian Egerniinae arrived 18.2 Ma, Eugongylinae 22.9 Ma, and the Sphenomorphinae were the first group to reach Australia 25.3 Ma. However, analyses using mid-Miocene fossil calibrations established a much earlier origin, minimally 34.61 Ma, for the Australian egerniines (Thorn et al., 2019). This new date prompted this investigation to seek fossil evidence that might further demarcate the timing of the arrival of (potentially) Australia's first scincids.

The oldest Australian fossil with distinctive scincid characters, *Proegernia palankarinnensis* Martin et al., 2004, is from the Etadunna Formation, Lake Eyre Basin, at the Oligo-Miocene boundary 25-26 Ma (Martin et al., 2004). An Eocene femur loosely assigned to Scincomorpha by Hocknull (2000) is not convincingly scincid, so is not robust evidence for inferring the temporal origin of the Australian Scincidae. Other Oligo-Miocene Australian material from the Etadunna Formation were referred to Egerniinae but remain undescribed, as follows: a dentary (UCR 20814), broken parietal (UCR 20815), partial maxilla (UCR 20816), an assortment of vertebrae, and a

broken scapulocoracoid (Estes, 1984). Both the *Proegernia palankarinnensis* holotype and the material referred by Estes (1984) cannot currently be located.

New collections of Oligo-Miocene material are required to resolve the composition and relationships of Australia's oldest scincid faunas. Recent expeditions into central South Australia have unearthed new Oligo-Miocene fossil squamates from the Namba Formation at Lake Pinpa and Billeroo Creek, southeast of Lake Frome. The Namba Formation is of a similar age to the Etadunna Formation (Woodburne et al., 1994), and the vertebrate fossil material collected from the lowest layers of this Formation are termed the Pinpa Fauna (Tedford et al., 1977). This investigation places the new Oligo-Miocene fossil material into phylogenetic context, alongside *P. palankarinnensis* from the Etadunna, and the Miocene species of *Egernia* and *Tiliqua* analysed in Thorn et al. (2019), to infer a more robust date for the arrival of scincids to the continent of Sahul.

2.5 Material & Methods

2.5.20 Excavation and fossil collection

Some fossil specimens from the Namba Formation were collected from the ground surface having been exposed by erosion; most referred to in this investigation were recovered by sieving excavated sediment. Trenches were excavated to examine the stratigraphy of both Billeroo Creek (BC2) and Site 12, Lake Pinpa (LP12). Sediment samples were taken from these trenches. Mineral composition was determined by XRD (X-ray diffraction) and XRF (X-ray fluorescence) analyses conducted by Flinders Analytical. Nested sieves with mesh apertures of 6, 3 and 1 mm were used to create sediment fractions from which the fossil material was sorted from the dolomitic clays. The micro-vertebrate material was sorted into fish, mammal, bird, turtle, crocodile, frog, and squamate. Of the 48 squamate cranial specimens recovered, 43 were scincids, and 5 identified as geckos (see Appendix 4 for the complete microvertebrate specimen list excluding fish, mammals, anurans and birds).

All descriptive terminology of the cranial elements follows Evans (2008); and Richter (1994) and Kosma (2003) for tooth crown features. Appendicular skeleton terminology follows Russell and Bauer (2008), and Hoffstetter and Gasc (1969) for vertebrae.

2.5.21 Scanning electron microscopy

Cranial material identified to Scincidae was further cleaned in water, dried, and then imaged using Scanning Election Microscopy (SEM). The minute size of most specimens is beyond the capabilities of Micro CT for resolution of morphological features required for identification and descriptions. No specimens required sputter coating. All SEM work was conducted at Flinders

University Microscopy facilities using an Inspect FEI F50 SEM. Maximum voltage used for image taking was limited to 2kV and a spot size of 3–4. Measurements of tooth crowns and features of the dentary mentioned in the text were taken using the SEM software.

2.5.22 Phylogenetic analyses

In order to better understand the timing of the Australian colonisation by the Egerniinae, both molecular and morphological data (including fossils) are required to generate tip-dated phylogenies. Undated parsimony and tip-dated Bayesian analyses infer, respectively, the phylogeny with the least homoplasy, and the most probable dated phylogeny.

2.5.22.1 Morphological characters

Morphological characters used in the following analyses consisted of 102 discrete and 48 continuous traits, forming an expanded matrix from Thorn et al. (2019) as per methods for Chapter 2. Continuous characters, derived from the measurements of the individual bones or teeth from the dentaries and maxillae, were taken from either Micro-CT scan data in Avizo Lite (v. 9.0) or SEM at Flinders Microscopy, to the nearest micrometre, or with digital callipers to the nearest ten micrometres. All measurements were converted to ratios of either dentary or maxilla length to standardise for size. Continuous characters were converted to values spanning 0–2 to replicate the average number of discrete character states, for analyses in both TNT (Goloboff and Catalano, 2016) and BEAST 1.8.3 (Drummond et al., 2012), so that they do not have a disproportionate weight .

2.5.22.2 Molecular partitions

Molecular data sourced from Tonini et al. (2016) and Gardner et al. (2008) were analysed using PartitionFinder 2 (Lanfear et al., 2016) to find optimal partitions and substitution models. The same six molecular (gene) partitions, 12s (412 base pairs [bps]), 16s (681 bps), ND4 (693 bps), BDNF (699 bps), CMOS (835 bps) and B-fibrinogen (1051 alignable bps) and substitution models (Thorn et al. 2019) are used again here.

2.5.22.3 Maximum Parsimony

The parsimony analyses for the combined discrete morphological, continuous morphological, and molecular data were performed using TNT v.1.5 (Goloboff and Catalano 2016). *Eutropis multifasciata* was set as the most distant outgroup following the phylogenetic interpretations of Gardner et al. (2008) and Thorn et al. (2019). The most parsimonious tree (MPT) for the combined data was found using 1000 replicates of tree-bisection-reconnection (TBR) with up to 1000000 trees held.

To assess clade support, 200 partitioned bootstrap replicates (with discrete characters, continuous characters, and each gene locus treated as a separate resampling partition), were performed using TNT, using new search methods (XMULT) with 1000 replicates and 1000000 trees held. The MPT and bootstrap trees from TNT were exported in nexus format, and continuous and discrete characters were traced (in Mesquite; Maddison and Maddison, 2017). The executable files for finding the Most Parsimonious tree, and for performing 200 reps of Partitioned Bootstrap resamples can be found in the SI data files Namba_Egerniines_Topology.tnt (MPT file) and Namba_Egerniines_PartitionedBootstrap.tnt.

2.5.22.4 Bayesian analysis

The discrete and continuous morphological, and molecular data were simultaneously analysed in BEAST v1.8.4 using tip-dated Bayesian approaches (Drummond et al., 2012). *Eutropis multifasciata* was again set as the furthest outgroup. Polymorphic discrete morphological data was treated as coded, i.e. if coded as states 0,1, it was treated as 0 or 1, but not 2. The discrete character set was analysed using the Mkv-model with correction for non-sampling of constant characters (Lewis, 2001; Alekseyenko et al., 2008). Despite recent disputes over the effectiveness of this model (Goloboff et al., 2018), it is well-tested (Wright and Hillis, 2014; O'Reilly et al., 2016) and is still widely accepted and applied to morphological data (Harmon, 2019). Continuous characters, transformed to span values between 0 and 2, were analysed with the Brownian motion model. Bayes factors were used to test the need to accommodate among-character rate variability for both discrete and continuous morphological characters (i.e. gamma parameter).

The stratigraphic data used for tip-dating analyses were derived from fossil taxa and their associated stratigraphy noted in Table 2.1 below. No node age constraints were imposed in this analysis, all dates are retrieved from the morphological and stratigraphic age ranges from the noted fossil taxa (tips). The most appropriate available model in BEAST v.1.8.4, birth-death serial sampling (Stadler, 2010), was applied. An uncorrelated relaxed clock (Drummond et al., 2006) was separately applied to the molecular and morphological data.

Each Bayesian analysis was run for 100,000,000 generations with a burn-in of 20%. The analysis was conducted four times to confirm stationarity. The post-burnin samples of all four runs were examined in Tracer 1.7.1 (Rambaut et al., 2018). All four runs were combined in LogCombiner, and the consensus tree produced by TreeAnnotator (Drummond et al., 2012). The executable .xml file for BEAST, all output log files, and the final consensus tree file (.tree) are available in the supplementary information folder Namba_Egerniine_BayesianFiles.

Table 2.1: Fossil calibrations used, their minimum and maximum ages (Ma) and references for the age dates or species descriptions.

Fossil calibration	Min age	Max age	References for age
Zone A, Etadunna Formation	25.5	25.7	Woodburne et al. (1994)
Pinpa Local Fauna, Namba Formation	25.5	25.7	Woodburne et al. (1994)
AL 90 Locality, Carl Creek Limestone	14.17	15.11	Woodhead et al. (2016)
Gag Locality, Carl Creek Limestone	14.47	16.86	Woodhead et al. (2016)

2.6 Geological Setting

2.6.20 The Namba Formation

Five expeditions collected new material from the Namba formation from 2007–2018. Over this period, numerous squamate fragments were collected from multiple sites at Lake Pinpa and Billeroo Creek. Two sites have yielded the majority of the material described herein; Site 12 at Lake Pinpa, and Billeroo Creek's 'Fish Lens' (a specific part of Wells' Bog Site of Tedford's, and later Rich's, expeditions, which included an expansive area sampling the Namba Formation and the overlying Pleistocene Eurinilla and dune sediments). All of the sites from Lake Pinpa and Billeroo Creek yielding scincid material for this investigation expose and sample the fluvio-lacustrine Namba Formation from north-eastern South Australia (see Figure 2.1).

The Namba Formation shares an unconformable lower boundary with the Eyre Formation (Paleocene-Eocene) within our study area; and is unconformably overlain by the Pleistocene Eurinilla Formation (Figure 2.2). The Namba sequence is a lateral equivalent to the Etadunna formation from the north western Lake Eyre Basin (Callen, 1977; Woodburne et al., 1994). The Namba Formation was divided into two members discussed by Tedford et al. (1977). Green claystones and dolomitic claystones at the top of the lower member hosted a locally abundant vertebrate fauna, termed the Pinpa Fauna by Tedford et al. (1977) which is biostratigraphically correlated with Zone A of the Etadunna Formation to be 25.5–25.7 Ma (Woodburne et al., 1994). Sites visited by multiple teams during the late 1970s–early 1980s led by Tedford, Rich, and others, named multiple fossil localities; added to these are new numbered sites from expeditions carried out in 2007 and between 2015–2018 led by T. H. Worthy and A. B. Camens.

Deposits and the fossils therein contributing to the Pinpa Local Fauna may be classed into two clear taphonomic groups: those containing isolated bones or partial skeletons of terrestrial vertebrates (marsupials, predatory birds, wading birds, and meiolanid turtles), and those containing localized concentrated bone accumulations which were previously thought to be derived from crocodile coprolites, encompassing mostly aquatic vertebrates (mostly fish, but including also turtle, crocodile, dolphin and other rare vertebrates). Collection of both categories of this material was predominantly from surface exposures along the western edge of Lake Pinpa and north eastern Billeroo Creek (Rich, 1991), with the occasional excavation of articulated or associated marsupial skeletons. In slightly younger overlying/incised fluviatile units exposed as channel fill deposits, the Ericmas Local Fauna has been derived from large scale excavations at Ericmas and South Prospect quarries (Lake Namba, 5 km south of Lake Pinpa) in the 1970s and 1980s (Rich, 1991). Tom O's Quarries at Lake Tarkarooloo unearthed the biochronologically similar Tarkarooloo Local Fauna, by bulk processing and screening sediments with the help of the Australian Army on one of several expeditions led by T H Rich of Museums Victoria (Rich, 1984). The quarried Ericmas sites contained predominantly terrestrial vertebrate remains, but until the 2007 Worthy and Camens expedition, no squamate material was recorded from the Namba Formation. Two outcrops of Namba Formation have revealed most of the Oligo-Miocene fauna previously described: Lake Pinpa, and 'Wells' Bog Site' at Billeroo Creek. Squamate remains have predominantly been recovered with the smallest mammal taxa and associated with a concentration of aquatic vertebrates in lenses filled with fish bones and lungfish dental plates. Lenses of fossil bones together form a 'fish layer' in the upper part of a limonite-stained olive grey clay, overlain by massive non-fossiliferous grey clay (See section 2.6.22 for more details on the stratigraphy). The fish layer, variably up to 50 mm thick, is 200–300 mm above a mottled black and white dolomitic layer of unknown depth and crops out at a number of discrete sites on the western side of Lake Pinpa. There are fossils in the underlying dolomite, including associated or partly articulated skeletons of birds and mammals, but fish bones are rare. This dolomitic bed was exposed more towards the middle of the lake in the 1970s when it was extensively sampled, but has since at least 2007 been buried by inwashed Quaternary sands. Both layers contain the same mammal and bird species and so the faunas from each are collectively referred to the Pinpa Local Fauna (Tedford et al., 1977; Vickers-Rich and Rich, 1991). The upper fish layer can have very dense concentrations of bone, from the typically aquatic taphonomic groups mentioned above. Both the fish layer and underlying dolomites are exposed at Wells' Bog Site in Billeroo Creek shown in Figure 2.2.

2.6.21 Fossil sites

Fossil sites in the Lake Pinpa–Billeroo Creek area were numbered chronologically on the 2007 trip in order of discovery, not based on geographical location (Figure 2.1).

2.6.21.1 Billeroo Creek Site 2 Fish Lens

Billeroo Creek Site 2 (BC2) is located on the northern side of the creek (Figure 2.1) and is a part of the more expansive Wells Bog Site. Fossils derive from a concentrated lens of predominantly fish bone with limonite inclusions, within the top of Layer 3 of the Namba Formation (Figure 2). The base of this fossiliferous 'Fish Lens' is not flat, but undulated relating to depth of semi-discrete lenses exposed over an area of roughly 10 m by 3 m, excavated over three trips, with a maximum thickness of ~150 mm. The lens sits stratigraphically ~200 mm above Layer 5, another much more extensive bone layer in dolomite, from which the majority of skeletal fossils at the site have been collected. Numerous specimens were retrieved from this stratigraphic layer, see Appendix 3 for a complete list.

2.6.21.2 Lake Pinpa

Site 6 (LP6) SAMA P43058 a posterior fragment of a left scincid maxilla, was recovered from Site 6 on the 2007 expedition. The fish lens was observed eroding out in patches over a broad area (200 m by 50 m) here around the margins of the overlying massive grey clay (L2 on Figure 2.1).

Site 9 (LP9) SAMA P43057 a posterior fragment of a left scincid dentary, was recovered from Site 9 on the 2007 expedition. Here the fish lens was exposed in a narrow zone at the base and edge of eroding massive clay Layer 2.

Site 12 (LP12) Specimens LP12.1 (partial humerus) and LP12.2 (maxilla fragment) were found at Site 12 on the edge of Lake Pinpa. Bone was found eroding out on the surface, along the Lake edge, from the lowest silty clay layer. Associated and articulated skeletons occur in both this layer and the dolomitic clay (L5) beneath. An undulating clean erosional boundary was observed between these two units.

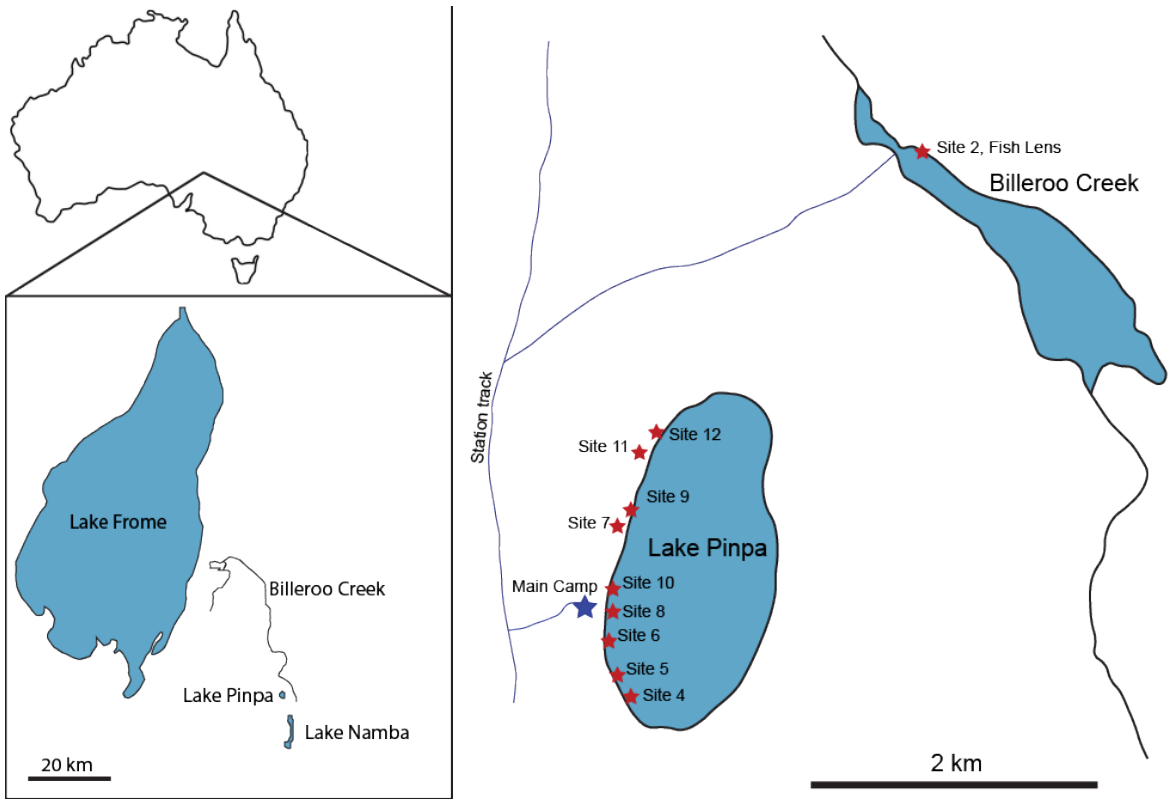

Figure 2.1: Map of the Lake Pinpa and Billeroo Creek sites, Frome Downs Station, South Australia. Stratigraphic columns in Figure 2 were compiled from locations marked above.

2.6.22 Stratigraphy of the Namba Formation

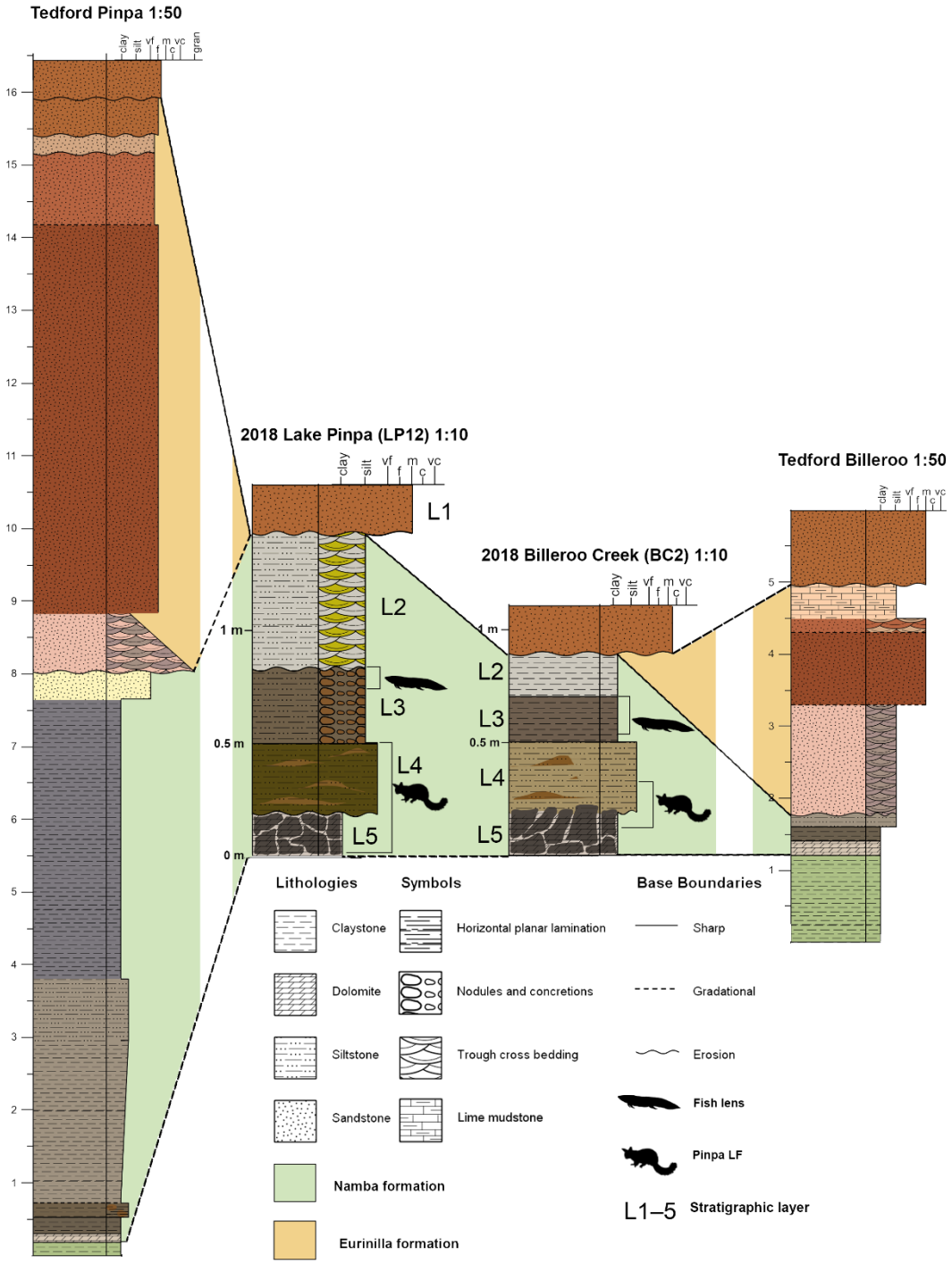

Figure 2.2: Stratigraphic sections representing Lake Pinpa at Site 12 (see Figure 1) and Billeroo Creek, Site 2, constructed in SedLog 3.1 from notes and figures in Callen and Tedford (1976); Tedford et al. (1977) illustrated to a 1:50 scale; and vertical sections excavated in 2018 by N. Brown illustrated at 1:10. Grain sizes were determined in the field. Colours are converted from Munsell figures to corresponding RGB values using Centore (2013).

Layer 1 The top layer of the stratigraphic section at LP12, designated Layer 1, is not part of the Namba Formation. The red sands are reworked sediment from the nearby Quaternary dunes that unconformably overlie the Namba exposures around many of the lakes in the area. At Billeroo Creek (BC2), the fluvial Eurinilla Formation lies unconformably on the Namba Formation and

eroded sediments from both it and overlying dunes mantled the Namba Formation where the section was excavated.

Layer 2 Erosion of Layer 2 means its original depth at both BC2 and LP12 cannot be assessed, but near LP07, exposures as documented in the section by Tedford et al. (1977), show it was minimally ~6 m thick. It sits unconformably on Layer 3. At LP12, layer 2 is composed of interbedded light green-grey (7/1/10Y) and yellow (5/1/10Y) medium silts that display cross bedding with very fine laminations. From a distance they have an overall uniform, pale-grey appearance. The layer at BC2 is similar but with white (8/1/10YR) medium silt rather than a yellow one. No inclusions or fossils have been found in this unit, but locally vertically aligned gypsum crystal plates occur.

Layer 3 The upper boundary of Layer 3 at LP12 is erosional, the troughs filled with sediments from Layer 2. Easily distinguishable from Layer 2, it is composed of an olive-grey (4/2/5Y) clay with strong brown (4/6/7.5YR) limonite inclusions throughout. Maximum thickness at Pinpa was 150 mm. The same layer at BC2 was a dark greyish-brown (4/2/2.5Y) clay that had a maximum thickness of ~100 mm and limonite presence was less consistent. The results of the XRD supported field observations of the clay content of the sediment, with clay minerals Smectite and Palygorskite combining to make up 79% of Layer 3 at Lake Pinpa. Iron minerals were noted in the stratigraphic section with the presence of Limonite inclusions in Layer 3. The XRD of Layer 3 at Pinpa picked up the iron ore mineral Goethite (9% of total mineral composition) a common component of Limonite, this is supported by the XRF reported 19.82% Iron (II). The Fish Lens at BC2 had variable thickness within the top 50 mm of this layer, in some cases Layer 2 has cut down through Layer 3 and sits directly on or has cut through the Fish Lens. At Lake Pinpa, the Fish Lens is usually much thinner (1–10 mm thick) and occurs near the top of Layer 3. However, at LP6, the Fish Lens is locally much thicker, sometimes up to 50-80 mm thick in areas of a couple square metres scattered over several hundred square meters on the lake bed. Layer 3 sits conformably on Layer 4 in stratigraphic sections at BC2, but the boundary is unconformable at LP12.

Layer 4 150 mm of an olive (5Y 5/3) and orange (10YR 4/6) mottled clay that sits unconformably on Layer 5 at LP12 and conformably on Layer 5 at BC2. Fossils were found in the lower portion of this layer, on the boundary with Layer 5 at both sites.

Layer 5 This layer is composed of a dolomitic white (10YR 8/1) mudstone with extensive black manganese staining leaving a mottled appearance. 66% of sediment in Layer 5 at Pinpa and 54% of Layer 5 at Billeroo Creek (Table 2.2) is derived of clay minerals Smectite and Palygorskite. Layer 5 had less Fe, but much more Mg, Ca and Mn than L3 (Table 2.2), reflecting that it included the minerals Dolomite/Ankerite (Table 2.3), not present in the Layer 3 at either site. The mottled

appearance of the dolomitic Layer 5 in both sections is explained by the transition from Dolomite ($CaMg(CO_3)2$) to Ankerite ($Ca(Fe,Mg,Mn)(CO_3)2$) with the partial replacement of magnesium with iron (II) and manganese. The primary source of fossils contributing to the Pinpa Local Fauna at Lake Pinpa and Billeroo Creek (excluding Fish Lens) is the assemblage occurring at the bottom of Layer 4 and in the top of Layer 5. Carbonate presence was confirmed with a dilute hydrochloric acid in the field. Bones were mostly restricted to upper levels of this layer, none were recorded >100 mm below the base of Layer 4.

Table 2.2 Major and trace elements detected by X-ray fluorescence analysis of sediments sampled Layer 3 and 5 from stratigraphic sections of Lake Pinpa Site 12 and Billeroo Creek Site 2. Values are %, minor trace elements making the total of each sample 100 are not shown.

	MgO	Al_2O_3	SiO_2	CaO	MnO	Fe_2O_3
Pinpa 12 L3	4.043	8.815	46.53	0.238	0.2303	19.82
Pinpa 12 L5	10.45	7.444	43.64	7.901	4.227	8.105
Billeroo Creek L5	13.65	5.875	36.08	13.02	1.634	6.982

Table 2.3 Mineral components of sediment samples taken from Layers 3 and 5 at Lake Pinpa and Layer 5 at Billeroo Creek Site 2.

	Clay Minerals	Dolomite/ Ankerite	Goethite	Quartz	Other	Total
Pinpa 12 L3	79	-	9	11	1	100
Pinpa 12 L5	66	23	3	6	2	100
Billeroo Creek L5	54	38	2	5	1	100

2.7 Results

2.7.20 New specimens collected

Additional material expanding the taxonomic sample of the Pinpa Local Fauna (first recorded by Tedford et al. (1977) was recovered in 2015-18 in the form of associated skeletons and isolated bones from the base of L4 and the top of the dolomitic clay layer (L5) at BC2 and LP12. The collection of this material by excavations at LP12 revealed predominantly terrestrial taxa with numerous marsupials and birds. In comparison, the fauna from the Fish Lens is more aquatic, a possible current-concentrated, lake-edge accumulation with bony fish abundant and lungfish, dolphins, flamingos, rails, turtles, crocodiles and the platypus *Obdurodon* represented, in addition to terrestrial marsupials and small scincids.

The age of the formation, concentration of terrestrial or aquatic fauna, dolomite formation, and presence of erosion surfaces, indicate periods of fluctuating water levels and water transportation.

2.7.21 Systematic Palaeontology

Order SQUAMATA Oppel, 1811

Family SCINCIDAE Gray, 1825

Subfamily EGERNIINAE Welch, 1982

Genus *PROEGERNIA* Martin et al., 2004

PROEGERNIA MIKEBULLI sp. nov.

Holotype—BCF2.8, a near complete right dentary; 27 tooth loci, 14 of which bear teeth.

2.7.21.1 Diagnosis

The holotype BCF2.8 represents a member of the subfamily Egerniinae, which is characterised by a dentary with a closed Meckel's groove and a large inferior alveolar foramen. The genus *Proegernia* has tooth crowns widening anteroposteriorly from the shaft, with near horizontal cristae, meeting at an apex slightly posterior to the centre of the tooth, and conspicuous angles in the anterior and posterior *culmen lateralis*. *Proegernia* can be distinguished from other members of the Egerniinae (*Egernia*, *Bellatorias*, *Liopholis*, *Cyclodomorphus*, *Tiliqua*, *Tribolonotus*, and *Corucia*) using the combination of the following traits: a more anteriorly positioned apex of the splenial notch at >50% the anteroposterior length of the dentary; a tooth count above 22 on the dentary tooth row, and 20 on the maxilla; minimal anteroposterior flaring of the tooth crown with lateral compression of the medial face; a 1 mm sliver of open Meckel's groove immediately posterior to the symphysis and a concavity of the ventral face of the pterygoid body. *Proegernia mikebulli* differs from *P. palankarinnensis* in lacking lateral tooth striae and having up to five more tooth loci for a total of 27. Fig 9 reveals that *P. mikebulli* has a much more medially inflected anterior tip to dentary; or conversely *P. palankarinnensis* is more linear in dorsal view.

Type locality—Fish Lens, BC2, Namba Formation, northern side of Billeroo Creek, GPS coordinates S 31°6'11.76" E 140°13'53.70", See Figure 1.

Age—Specimens were found in Layers 3–5 of the Namba Formation stratigraphy described in this report and are allocated to the Pinpa LF. This LF has been biostratigraphically correlated with the "Wynyardiid" or Minkina Fauna, (Zone A) of the Etadunna Formation, 25.5-25.7 Ma (Woodburne et al., 1994; Megirian et al., 2010).

Paratype—BCF2.5 a partial right dentary from BC2, with a complete coronoid process, 23 tooth loci and 10 teeth.

Referred specimens—The following specimens are referred to this taxon based on the combination of their appropriate size and having a general similarity to the represented elements in other

egerniines. Details of tooth crown shape also enable referral of tooth-bearing bones to the same taxon. Two right post-dentary compound bones; LP6.1 from Lake Pinpa (LP6) preserving the dorsal surface of the surangular and glenoid, broken part-way through the retroarticular process; and BCF2.48 from Billeroo Creek (BC2) which preserves the ventral and medial face of the articular, the glenoid entirely and most of the retroarticular process. Two right partial maxillae both from BC2, BCF2.47 representing an anterior fragment with premaxillary process intact and the first 9 tooth loci holding 3 teeth; and BCF2.9 which preserves the posterior majority of the maxilla with 16 loci and 9 teeth, the facial process is broken above the row of maxillary foramina. An intact left pre-maxilla, BCF2.48 from BC2, with osteoderm fragments on the internasal process, preserving two teeth from four loci. A right pterygoid BCF2.18 from BC2, the quadrate process broken beneath the epipterygoid notch.

2.7.21.2 **Etymology**

The species is named after Professor Michael Bull (1947-2016) of Flinders University, South Australia, who devoted decades to documenting the ecology of Australia's egerniine skinks. Mike Bull supervised a generation of Australian ecologists and his lectures inspired countless students to become biologists. Mike's studies of Australian egerniine skinks and their parasites are model long-term ecological studies, and led to major discoveries such as monogamous pairs in *Tiliqua rugosa*, parental care and family living in *Egernia* spp.; and the establishment of a successful breeding and reintroduction program for the endangered Pygmy Bluetongue, *Tiliqua adelaidensis*.

2.7.21.3 Description

Dentary—Seventeen incomplete dentaries were recovered from the 2007-2018 trips to Lake Pinpa and Billeroo Creek. Of these, a reconstruction of a near-complete dentary of *Proegernia mikebulli* was possible using BCF2.8 and BCF2.5 (See Figure 2.3). From the anterior tip of the symphysis to the posterior tip of the coronoid process, missing only the angular process, the dentary is 12.7 mm long. In medial aspect, the dentary is convex ventrally, 1.6 mm wide and 2.2 mm tall at mid-tooth row length, and the dental sulcus has a shallow concave curve. From occlusal view, the symphysis is directed medially to articulate with the opposing dentary at an angle of 32°. The dental sulcus is prominent, BCF2.8 preserving 14 pleurodont teeth from 27 loci. The tooth row is 10.8 mm long.

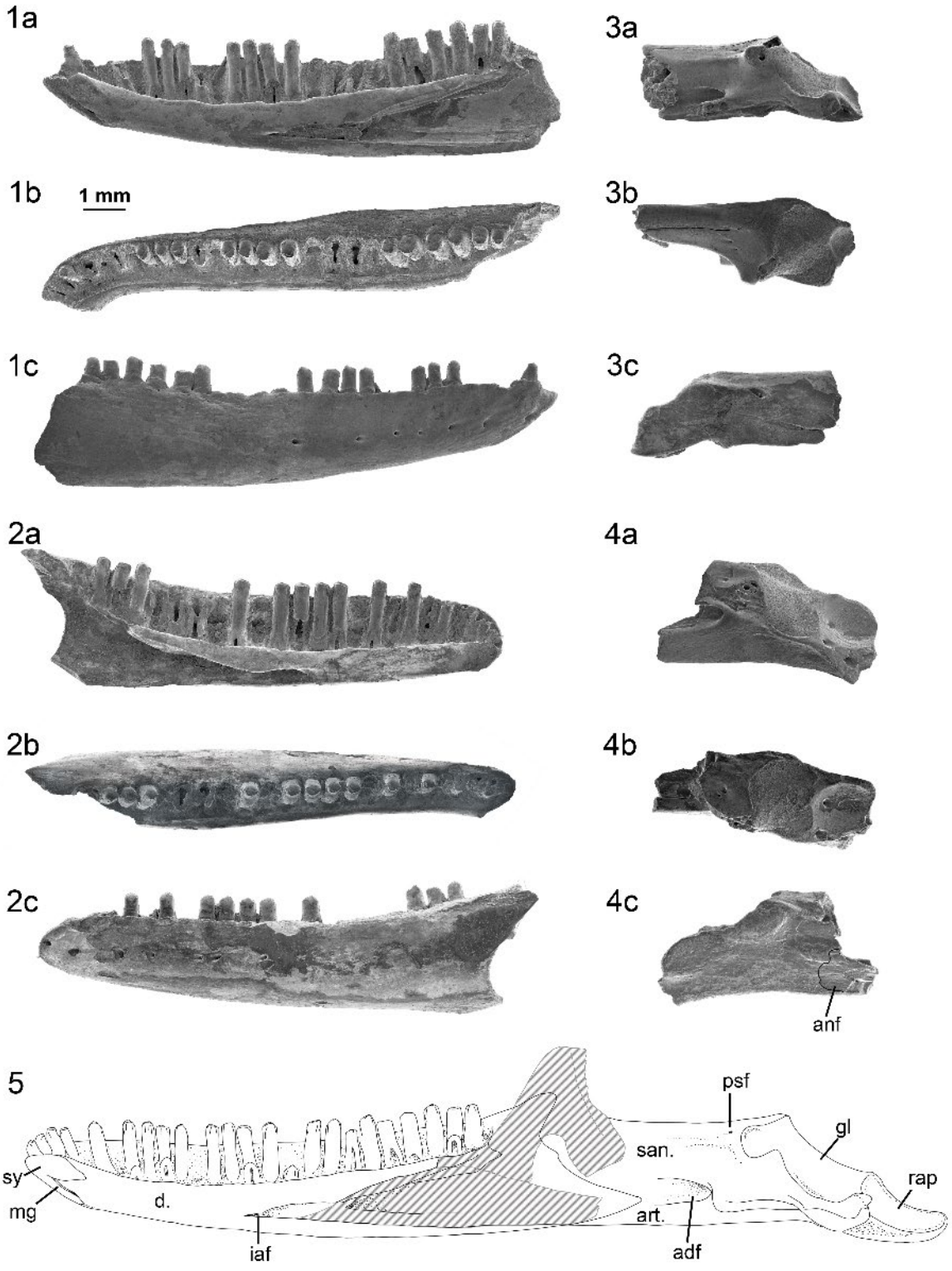

Figure 2.3: **1a-c Holotype, a right dentary, BCF2.8, 2a-c paratype; a left dentary BCF2.5; two right post-dentary compound bones 3a-c LP6.1 and 4a-c BCF2.48 of *Proegernia mikebulli* sp. nov. from the Fish Lens at BC2; and 5 a complete reconstruction in medial view of the right mandible of *Proegernia mikebulli*, the coronoid and splenial are drawn based on examination of the modern representative specimens, no fossil representatives of these elements are known. Abbreviations: adf, adductor fossa; anf, angular facet; art., articular; d., dentary; gl, glenoid; iaf, inferior alveolar foramen; mg, Meckel's groove; psf, posterior surangular foramen; rap, retroarticular process; san., surangular; and sy, symphysis.**

The anterior symphysis, preserved in its entirety on BCF2.8, has a flattened, reverse '7' shape in medial view. Posteriorly, the symphysis divides, a narrow sliver of the flattened face of

this feature runs posteroventrally along the anterior edge of the dentary. The dorsal body of this feature is an elongate ovular shape, becoming wider posteriorly and terminating at a sharp point. At its longest, the symphysis is 1.8 mm and is 1.3 mm deep. Posterior to the apex of the dorsal and ventral descending sections of the symphysis is the symphysial foramen, extending ventrally into a 1 mm long opening of Meckel's groove. The anterior opening of Meckel's Groove in this specimen is <0.2 mm wide. The groove is open and lies parallel with the dorsal side of the ventral section of the symphysis; further posteriorly it is enclosed.

The inferior alveolar foramen and the dorsal and ventral margin of the splenial notch are preserved to the posterior end of the tooth row in BCF2.8 (Figure 2.3). The inferior alveolar foramen lies on the ventral margin of the splenial notch, positioned approximately 50% along the tooth row. The shape of the splenial notch is narrow and roughly parallel-sided for the anterior 40% of the preserved length, expanding dorsoventrally with a convex upper edge and straight ventral margin for the remaining posterior section of length. Where the notch expands, the dorsal edge preserves a concave face, allowing the splenial to medially overlap the dentary. Posterior to this face, beneath the 3rd last tooth, the dental sulcus is broken.

The coronoid process of the dentary is preserved on the paratype BCF2.5. The coronoid process ascends posterodorsally from the position of the last tooth. The dorsal tip extends higher than the posterior tooth. The ventral margin of this process preserves the anteromedial articular facet for the coronoid, which therefore can be seen to overlap the splenial and dentary anterior of the 3rd last tooth position. The angular process, although not preserved entirely on either compound bone specimen, can be reconstructed with some confidence using the angle of the intact edge immediately beneath the coronoid process. The total length of this process is limited by the absence of a facet for its articulation on either of the recovered post-dentary compound bones.

The lateral face of the dentary is slightly convex and preserves a single row of eight mental foramina extending posteriorly from the anterior top of the dentary, to below the 17th tooth position. The largest foramen in the row is at the posterior end.

Post-dentary bones— Two right post-dentary complexes were recovered from the Namba Formation, LP6.1 from a right mandible at Lake Pinpa (LP6; Figure 2.3 3a–c) and BCF2.48 from Billeroo Creek (BC2; Figure 2.3 4a–c). These elements are referred to this taxon as they are of appropriate size, confirmed as scincid material by the presence of a facet for the angular bone, which is not present in gekkotans; and the angle of the retroarticular process. The retroarticular process shape similar to extant egerniines, and when aligned horizontally in in-vivo position the angular in egerniines is wide and ventures further laterally than the narrow ventrally positioned

angular of eugongylines (i.e. *Emoia longicauda* SAMA R2352, *Eugongylus rufescens* R36735). Sphenomorphines generally have a simple, straight post-dentary complex without medial torsion of the articular, and the retroarticular is not inflected medially posterior of the glenoid. All scincid bones from Billeroo Creek and Lake Pinpa are consistent with one egerniine taxon; there is no variation among elements that might indicate more than one species being represented, so both compound bones are referred to the taxon named from the dentaries. The post-dentary complex is the fused surangular and articular bones making up the posterior half of the scincid mandible. This fusion develops ontogenetically; complete fusion of the two elements with no traces of a suture internally is evidence of adulthood in extant Australian scincids (Gelnaw, 2011).

LP6.1 is a near complete right adult post-dentary preserving completely fused surangular and articular bones. Anteriorly the areas for articulation with the dentary and coronoid are not preserved, neither are the angular or the anterior edge of the adductor fossa. A facet for articulation of the angular is present on the ventral half of the lateral face of the articular, not extending to reach the posterior surangular process. The posterior majority of the retroarticular process is broken off LP6.1, a description of its complete shape is based on BCF2.48. A hairline crack in the surangular traces along the dorsal surface to just anterior of the dorsal tip of the glenoid. The dorsal surface of the surangular is relatively straight and rises slightly to meet the dorsal tip of the glenoid where the quadrate articulates with the mandible. The maximum preserved length of this dorsal surface is 2.9 mm. The glenoid faces posterodorsally, the surface is convex mediolaterally and concave anteroposteriorly, reaching a maximum of 1.8 mm long. The lower third of the glenoid becomes slightly concave ventrally, curving up to meet the medial articular process of the surangular. The surface of the glenoid has a pitted texture indicating attachment of cartilage in the mandibular cotyle. Posteroventrally the glenoid ends in a clearly defined ridge between it and the retroarticular process. What is preserved of the retroarticular process is concave (BCF2.48). Medially, the foramen for the chorda tympani is preserved in BCF2.48.

Two foramina are preserved dorsally in a flattened surface, and a posterior surangular foramen is on the lateral face immediately anterior of the glenoid. No anterior surangular foramen is preserved on either LP6.1 or BCF2.48. From the flattened dorsal surface of the surangular, the bone curves sharply ventrally, leaving a flat medial surface above the dorsal margin of the adductor fossa. The adductor fossa is in the lower 50% of the medial face of the complex. The anterior margin of the adductor fossa is not preserved on either post-dentary compound bone. Viewed medially, the posterior edge of the narrow, ovular, fossa terminates anterior to the glenoid. The lateral face of the post-dentary complex of the mandible is convex when viewed dorsally and anteriorly. A discernible ridge runs from just anterior of the posterior surangular foramen, anteriorly

to the broken anterior edge of LP6.1, marking the posteroventral edge of the *M. adductor mandibulae externis*.

Maxilla— Two incomplete right maxillae (BCF2.9, BCF2.47) were recovered from BC2 that are referred to *Proegernia mikebulli*. BCF2.9 (Figure 2.4, right) preserves a near complete tooth row, a bifid posterior termination of the suborbital process, and complete tooth crowns from both the anterior tooth form and posterior tooth form on the same row. This specimen was recovered from sieved material in two halves, that when articulated fitted together, and so was joined with Paraloid B72 before SEM images were taken. The smoothed hemispherical shape on the dorsal edge of the palatine process of the maxilla is Paraloid B72 and not a feature of the bone.

Anteriorly, the maxilla BCF2.9 lacks the tip of the premaxillary process. The anteriormost tooth positions are missing on BCF2.47; tooth and loci counts are based on the reconstruction also using BCF2.47. The facial process of the maxilla is incomplete preserving only 2.3 mm above the tooth row. The unbroken edge of the orbit can be traced from above the level of the 14th tooth position, to the broken dorsal tip of the suborbital process. The ventral tip of the bifid suborbital process is intact as are the last tooth positions. The tooth row preserves 16 of 20 loci, and 9 pleurodont teeth are still in position.

The lateral face of the maxilla is slightly convex from anterior to posterior when viewed dorsally, the facial process slightly mediolaterally concave until terminating at the broken dorsal edge. The maxilla preserves nine primary foramina on the lateral face, the largest is the most anterior. Above the primary row, 11 more foramina, the largest one-third the size of the primaries, are visible in the SEM in two rows. Medially, the dental shelf leading to the palatine process is broken. The dental shelf thins posteriorly and ends in a fine point at the ventral tip of the bifid suborbital process. The tooth row occlusal surface is slightly convex posteriorly, with larger teeth beginning at the ninth position. The last two teeth decrease in size posteriorly, creating the trailing edge of the convex occlusal line.

The reconstructed maxilla is 11.1 mm long from the premaxillary process to the suborbital process, with 20 tooth positions (see Figure 2.4). Height of the facial process was not preserved on any specimen.

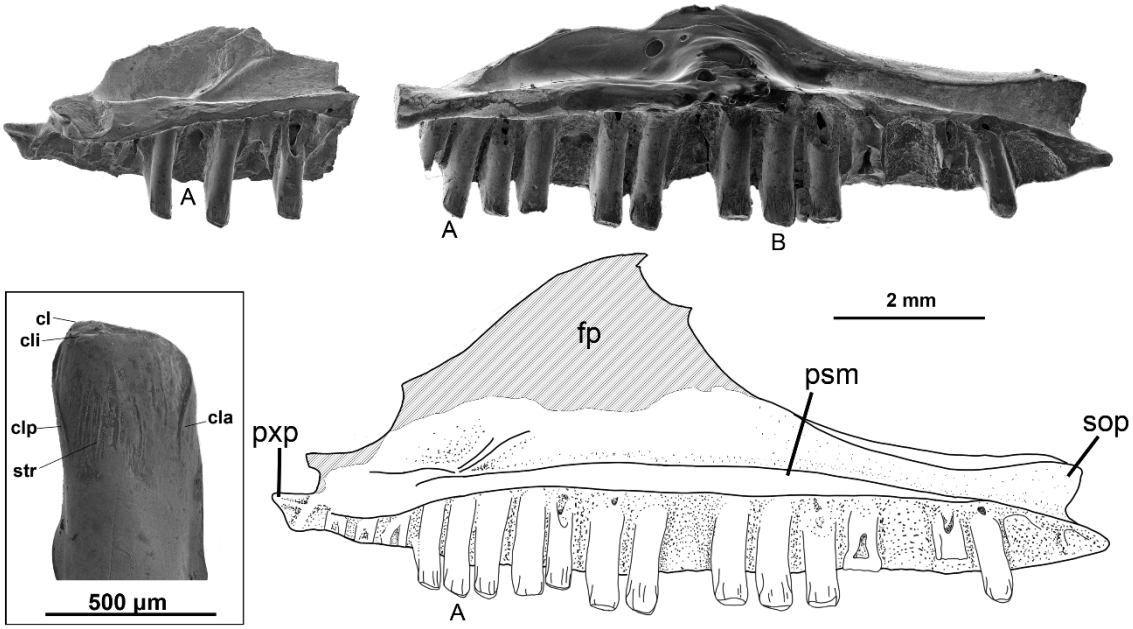

Figure 2.4: Right maxilla of *Proegernia mikebulli* sp. nov. reconstructed with BCF2.47 (anterior fragment) and BCF2.9 (near complete maxilla). A marks the same tooth locus on both specimens. Enclosed by the box is the tooth 'B'. Abbreviations: cl, *cuspis labialis*; cla, *culmen lateralis* anterior; cli, *cuspis lingualis*; clp, *culmen lateralis* posterior; fp, facial process; psm, palatine shelf of the maxilla; pxp, premaxillary process; sop, suborbital process; and str, striae.

Premaxilla— A single complete left premaxilla, BCF2.48, was recovered from Fish Lens at BC2 (Figure 2.5). An osteoderm is fused to the anterior face of the internasal process, and would have overlapped the right premaxilla when the pair were articulated. Paired, unfused premaxillae in adulthood eliminate the possibility that this element belongs to a gekkotan. The ascending internasal process has a flattened medial side for articulation with its paired element. Viewed laterally, a foramen for the longitudinal canal is situated immediately above the maxillary process in the lateral face of the internasal process. Sharply pointed dorsally, the internasal process widens ventrally and terminates at the notch for the exit of the ethmoidal foramen laterally, and tooth row medially. The internasal process of the premaxilla rises towards the nasals at a 40° angle. The total length of the internasal process is 3.1 mm. The maxillary process is curved posterolaterally towards the maxilla and is approximately 1/3 of the height of the internasal process, reaching 1.6 mm in mediolateral width. The lateral edge of the maxilla process curves ventrally to finish beside the fourth tooth position.

Four tooth loci are present and the first two teeth are preserved. These teeth are 0.53 mm long from the lateral face of the maxillary process and 0.28 mm wide. What remains of the worn crowns (see inset A, Figure 2.5) match those of the anterior-most teeth of the maxilla specimen BCF2.47. There are weak striae on the medial face of the crown, a mediolateral compression of the

crown below the *crista lingualis*, and a sharply curved, prominent, *culmen lateralis*.

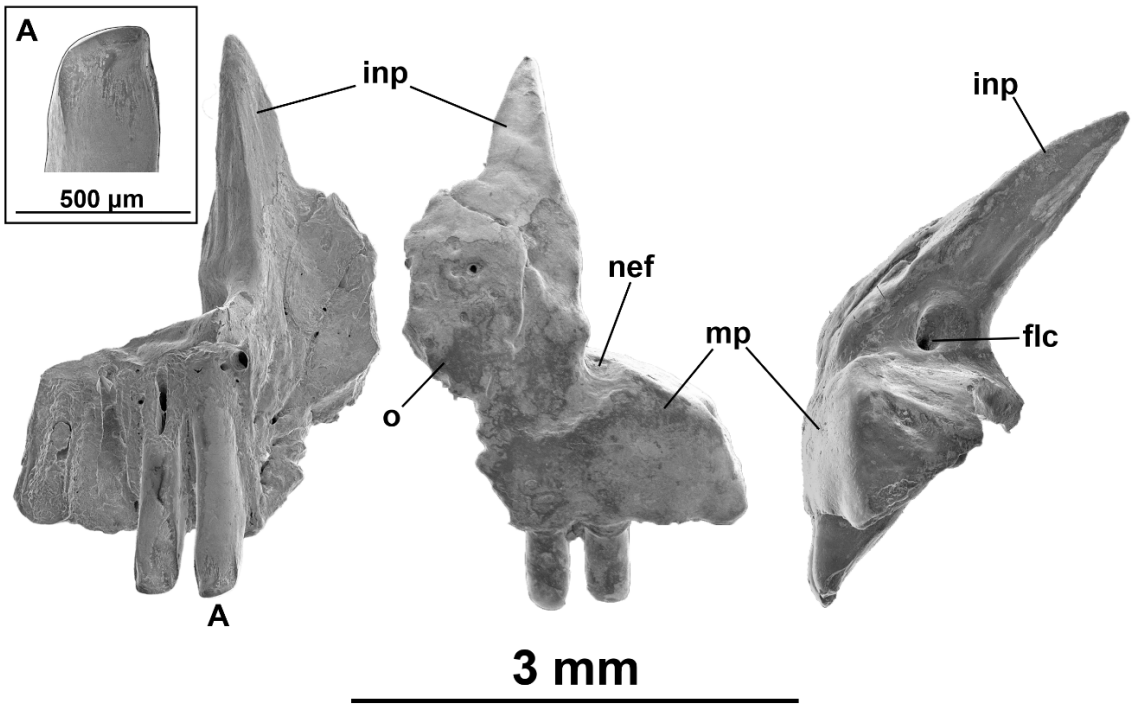

Figure 2.5: Left premaxilla (BCF2.48) of *Proegernia mikebulli* sp. nov. from posterior (left), anterior (centre), and lateral (right) view. A, tooth one, enlarged in box. Abbreviations: flc, foramen of longitudinal canal; inp, internasal process; mp, maxillary process; nef, notch of the ethmoidal foramen; and o, osteoderm.

Dentition— The dentition of *Proegernia mikebulli* is described using the two dentaries BCF2.8 and BCF2.5, the maxillae BCF2.47 and BCF2.9, and premaxilla BCF2.48, totalling a near-complete upper and lower tooth row. The upper tooth row contains a total of 24–25 teeth, 4 or 5 on the left and right premaxilla, and 20 on the maxilla. The dentary tooth row has 27 tooth positions, beginning above the symphysis anteriorly and terminating just anterior of the coronoid process. The occlusal profile of the maxilla and dentary are both convex, with slightly larger teeth in the posterior half of the tooth row.

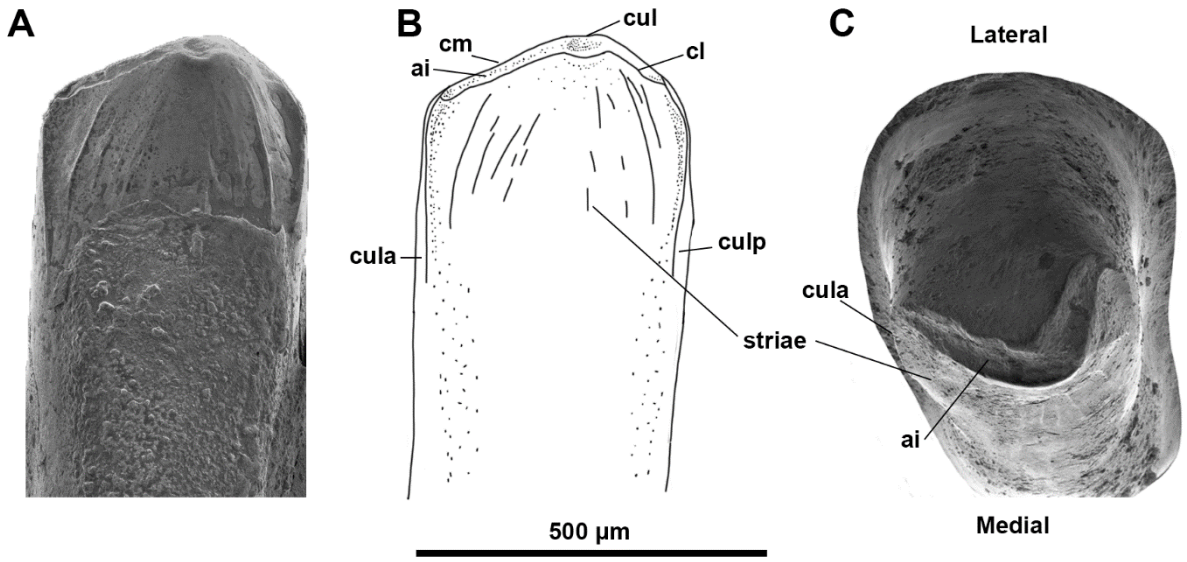

Figure 2.6: A and B: 24th tooth on the dentary BCF2.8, medial view, and C the 16th tooth in occlusal view, all to the scale of 500µm. Abbreviations: ai, *antrum intercristatum*; cl, *crista lingualis*; cm, *crista mesialis*; cul, *cuspis labialis*; cula, *culmen lateralis* anterior; and culp, *culmen lateralis* posterior.

The tooth crown on the dentary is similar in width to the shaft, expanding anteroposteriorly with slight mediolateral compression for the last 30% of the tooth height. Prominent anterior and posterior *culmen laterales* extend from the tips of the *crista mesialis*, turning medially and ventrally on the dentary, with a sharp angle producing 'shoulders' notable in medial view of the tooth (Figure 2.6). From the central cusp, the anterior cristae dip ventrally 20°, and posterior cristae 45°. The cusp (*cuspis labialis*; Figure 2.6*)* is slightly posterior of the centre of the tooth, and in occlusal view is positioned just posteromedial to the centre. This medial shift of the cusp creates a convex curve on the dorsal surface of the tooth, directing the both cristae medially. Striae are only located on the medial face of the tooth crown, running dorsoventrally angled from the off-centre cusp. The two most prominent striae run parallel to the *culmen lateralis* (both anterior and posterior), all others are weaker in profile with staggered lengths. Tooth crown morphology is similar on the maxilla and premaxilla.

Tooth wear begins at the cusp, forming a shallow rounded depression, gradually deepening medially. The *antrum intercristatum* expands in width from the central cusp. Wear is more prominent in the centre of the tooth crown between the cusps, than anteriorly or posteriorly along the cristae, creating a thickening 'v' shape.

Pterygoid— A single right pterygoid attributed to *P. mikebulli* was recovered from Fish Lens at BC2 (BCF2.18; Figure 2.7). It is near complete but missing the anterior-most tip of the palatine process and distal tip of the quadrate process. The pterygoid articulates with the palatine anteriorly with a pointed process extending anteriorly from a fanned, v-shaped pterygoid head to overlap with a similar feature from the anterior element. Laterally to the palatine process, the ectopterygoid

process extends towards the ectopterygoid with a concave, curved facet for articulation with this element on the dorsal surface of the pterygoid head. Between these two processes, the fan-shaped pterygoid head has a concavity on the ventral surface that is 0.7 mm wide and 1.7 mm long. Within this concavity are three foramina, one in the deepest area of the concavity, and two are paired anteriorly, near the palatine process. Posteriorly, the pterygoid head narrows to become a parallel-sided rod, before bending medially at an angle of 35° towards the epipterygoid notch. The epipterygoid notch is an ovular concavity, with raised margins, on the dorsal surface of the pterygoid at the anterior end of the quadrate process. A sharp ridge extends from the anterior edge of the epipterygoid notch to the corner of the bend towards the pterygoid head. Posterior to the epipterygoid notch, the quadrate process becomes L-shaped in cross section and extends 1.5 mm posteriorly before the broken edge. The pterygoid head is 2.7 mm wide between the palatine and ectopterygoid processes. Total length of this element is not preserved.

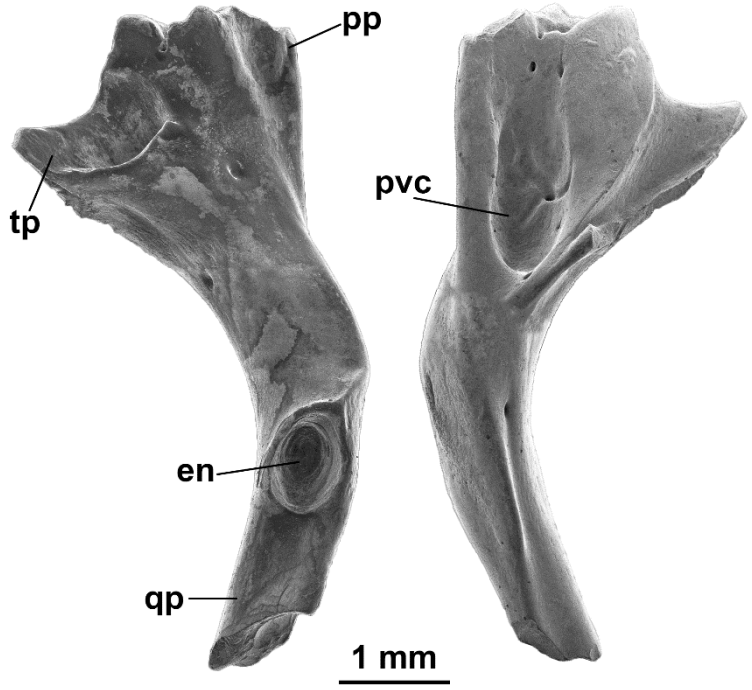

Figure 2.7: **Right pterygoid of *Proegernia mikebulli* sp. nov., BCF2.18 in dorsal (left) and ventral (right) views. Abbreviations: en, epipterygoid notch; pp, palatine process; pvc pterygoid ventral concavity; qp, quadrate process; and tp, ectopterygoid process.**

2.7.22 Postcranial material potentially attributable to *Proegernia mikebulli*

Several procoelous vertebrae and assorted vertebral fragments were recovered from the Fish Lens at BC2. The best preserved of these is BCF2.20, a pre-sacral vertebra (Figure 2.8). This specimen is near complete, missing only the posterodorsal tip of the neural spine and the lateral tip of the right postzygapophysis. A thin crack runs posterolaterally on the ventral face of the centrum from just posterior of the ventral foramina, to the broken zygapophysis. The vertebra has an elongate

centrum, the ventral surface is concave in lateral view. The neural canal is a similar diameter to the cotyle/condyle with a flat ventral surface broadening laterally before coming to a tear drop point when viewed anteriorly or posteriorly. Synapophyses are present immediately posterior to the prezygapophyses on the lateral facies. The neural spine rises posteriorly, steadily at an angle of 20°, from the dorsal margin of the neural canal until reaching the broken extremity. The prezygapophyses are angled at 32° and the postzygapophyses at 28°. Overall shape of the vertebra is relatively elongate, approximately one third longer than it is wide. Overall centrum length is 4.2 mm, the cotyle maximum width is 1.6 mm; the vertebra height anteriorly is 2.4 mm, posteriorly including the broken neural spine the height it is a maximum of 3.7 mm. The widest point of the vertebra is between the synapophyses, totalling 3.3 mm. This element is identified as scincid based on the minimal dorsoventral compression of the rounded cotyle and condyle, elongated centrum, absence of a zygosphene/zygantrum and the minimal size of the ventral foramina. Snake vertebrae have shorter centra, a round cotyle/condyle with no compression, a set of zygosphenes and zygantra, and a ventral hypapophysis. A procoelous centrum devoid of a hollow space for the notochord eliminates the possibility of the vertebra belonging to a non-pygopodid gekkotan. Gekkotans inclusive of pygopodids also have enlarged ventral foramina. Procoelous Gekkota vertebrae (mostly restricted to pygopodids) tend to have smaller condyles and cotyles, the cotylar hollow often not visible in ventral view because the dorsoventral inclination is minimal (Hoffstetter and Gasc, 1969).

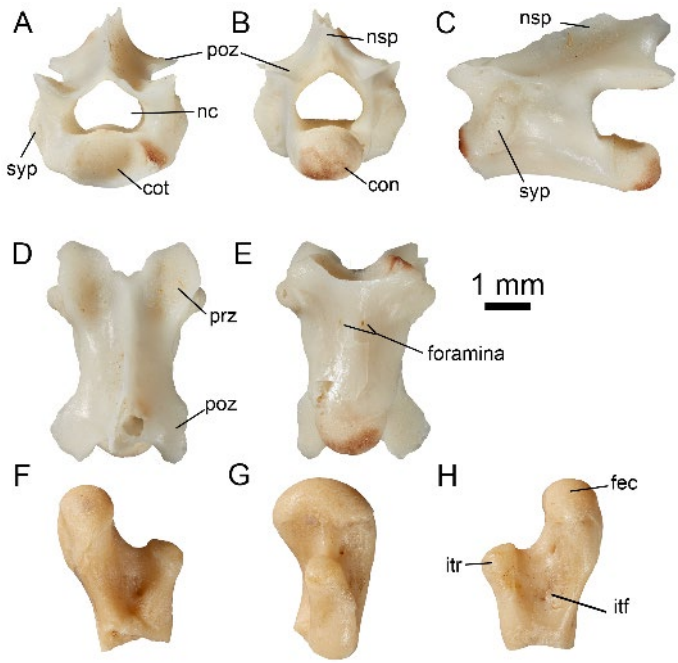

Figure 2.8: A single vertebra (BCF2.20) potentially referable to *Proegernia mikebulli* sp. nov., recovered from Fish Lens, BC2. A, anterior view; B, posterior view; C, lateral view, anterior to the left; D, dorsal view; and E, ventral view. A proximal fragment of a right femur assigned to *Proegernia mikebulli* sp. nov. BCF2.46. F, dorsal; G, anterior; and H, ventral views.

Abbreviations: con, condyle; cot, cotyle; fec, femoral condyle; itf, intertrochanteric fossa; itr, internal trochanter, nc, neural canal; nsp, neural spine, poz, postzygapophysis; prz, prezygapophysis; and syp, synapophysis.

A partial right proximal femur, BCF2.46 (F–H, Figure 2.8), was recovered from the Fish Lens at BC2. Broken immediately beneath the intertrochanteric fossa, no remnants of the shaft width or length are preserved. All other proximal features are intact. The femoral head extends medially to once have articulated with acetabulum. The specimen is most likely from an adult scincid as the epiphyses are fully ossified and fused to the diaphysis. The articular surface of the femoral condyle is semi-circular viewed anteriorly, and ovular in proximal profile. The femoral head extends medially away from the centre line of the shaft. The lateral trochanter is much shorter, only rising slightly above the edge of the intertrochanteric fossa. The intertrochanteric fossa is a concave surface between the condyle and trochanter on the ventral face of the proximal femur. The dorsal side also preserves a concave surface, but this is steeper-sided with a prominent 'v' marking where the femoral shaft begins. The width of the femoral condyle is widest in anterior view, measuring 2.2 mm at the suture with the epiphysis. The internal trochanter is 1.3 mm tall from the base of the intertrochanteric fossa. Total length preserved is 3.8 mm.

A fossil scincid femur was identified to family by Lee et al. (2009b) based on the trochanter major tapering gradually in height distally. The trochanter major is not visible on this specimen, the shaft is broken immediately proximal to it.

2.7.23 Comparing new taxon with *Proegernia palankarinnensis*

The type species of *Proegernia* (by monotypy) is *Proegernia palankarinnensis.* While the specimen is currently missing, the existing description (Martin et al., 2004) suggested *Proegernia* as being representative of a transitional form between a plesiomorphic lygosomine dentary morphology and the derived egerniine condition. The plesiomorphic traits shared by both *Proegernia palankarinnensis* and *P. mikebulli* are the small 1 mm long opening of Meckel's groove posterior of the symphysial foramen and the more anterior extent of the splenial notch into the anterior half of the tooth row length. Both species of *Proegernia* also have egerniine features emerging in the prominent 'shoulders' of the *culmen lateralis* on their unicuspid tooth crowns, and a relatively deep splenial notch at the posterior of the dentary, deeper than other Australasian scincids. *Proegernia palankarinnensis* was described as having 22 tooth loci, with a possible maximum of 23 teeth, uncertain due to a broken symphysial region. Specimens newly described above as *Proegernia mikebulli* preserve up to 27 dentary tooth positions (see BCF2.8, Figure 2.3). Both taxa share an anterior section of crowded, smaller teeth in their lower dentition. The spacing of teeth in *P. palankarinnensis* is marginally wider than *P. mikebulli* at the posterior end of the tooth row. Tooth shape varies between the two taxa, *P. palankarinnensis* has tooth shafts narrowing at the

base, *P. mikebulli* tooth shafts narrow beneath the crown and expand again at the base. Martin et al. (2004) noted that the tooth crowns of *Proegernia* SAMA P39204 preserve distinct striations on both the lateral and medial faces. *Proegernia mikebulli* tooth crowns have weakly lineated striae on the medial face of the crown beneath the *crista lingualis*, but the lateral tooth face is smooth.

Although occurring almost concurrently, comparisons of shape of the dentary bone between the holotype for *P. palankarinnensis* and *P. mikebulli* (see Figure 2.9) show that the two fossils are of quite different species based on the following characteristics: 1) The overall shape of the dentary of *P. palankarinnensis* is less robust, the dentary bone itself being narrower between the medial edge of the dental sulcus and lateral face at the height of the mental foramina; the medial inflection of the symphysis is also considerably less in *P. palankarinnensis* than *P. mikebulli*, even after taking into account the effects of erosion. 2) The medial face of the dentary, posterior to the symphysis and anterior of the splenial notch below the dental sulcus is deeper in *P. mikebulli*. 3) The inferior alveolar foramen is positioned more anteriorly in *P. palankarinnensis*, below the 12th tooth position, *P. mikebulli* extending only as far as posterior edge of the 14th tooth. 4) No short extension of Meckel's groove can be observed anterior of the inferior alveolar foramen in *P. mikebulli*, a plesiomorphic character representing a partial remnant of Meckel's groove that is noted on the holotype of *P. palankarinnensis* (Figure 2.9 A). 5) The internal septum of both specimens extends anteriorly to a similar degree. The facet for articulation of the coronoid terminates beneath the second-last tooth in *P. palankarinnensis* and the third last tooth locus in *P. mikebulli*. The dorsal edge of the splenial notch is widened more abruptly in *P. mikebulli* with a curve, in *P. palankarinnensis* the same space is sharply v-shaped. The coronoid process preserved on *P. palankarinnensis* does not extend above the height of the final tooth crown, unlike the process on BCF2.5 of *P. mikebulli*.

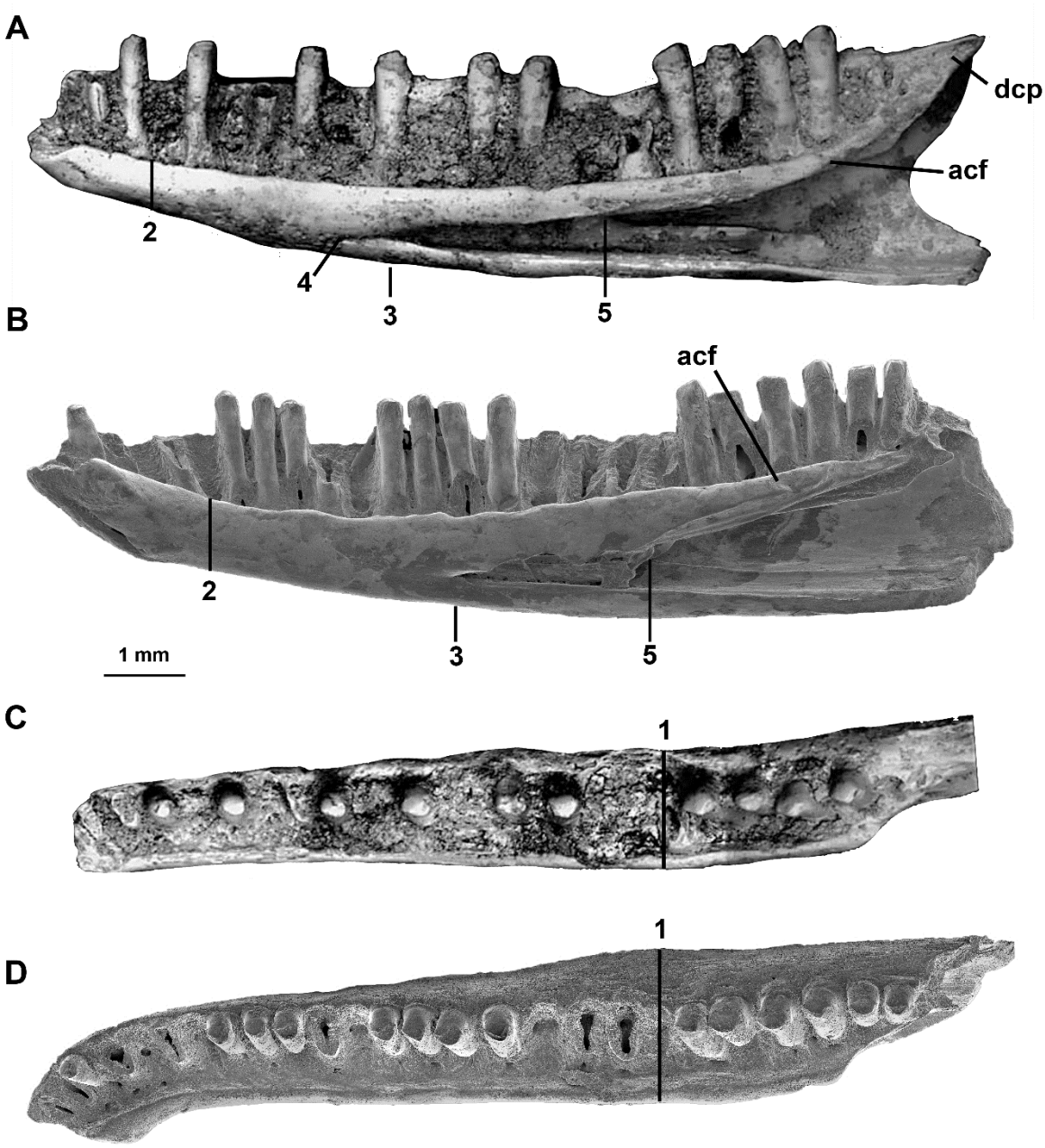

Figure 2.9: **Comparative SEM of *Proegernia mikebulli* sp. nov. (B,D) and microphotographs of *P. palankarinnensis* (A,C from Martin et al. 2004), in medial (above) and occlusal (below) views Note the anterior extension of the splenial notch in *P. palankarinnensis* and the increased the number of teeth/loci in *P. mikebulli*. Both share the 1 mm long anterior opening of Meckel's groove immediately posterior to the symphysis. Features described above are labelled, 1) Overall dentary robustness; 2) Dentary depth; 3) Position of the IAF; 4) Meckel's Groove extension anterior of the IAF, present in *P. palankarinnensis* and absent in *P. mikebulli*; and 5) anterior extent of the internal septum similar in both taxa. Abbreviations: acf, anterior coronoid facet; and dcp, dentary coronoid process.**

2.7.24 Other Egerniinae and other scincids

Comparisons between the extant egerniine taxa *Lissolepis coventryi* (SAMA R57317) and *Liopholis multiscutata* (FUR168), as well as a Southeast Asian outgroup representative *Eutropis multifasciata* (SAMA R35693), were conducted to determine how similar or derived the fossil taxon is from the inferred plesiomorphic lygosomine condition.

Four characters notably vary in the egerniine and outgroup lygosomine representatives chosen, and the extinct *P. mikebulli*. The anterior extent of the splenial notch and the inferior alveolar foramen; the shape and robustness of the symphysis, the dentary depth and overall width, and the number of teeth corresponding to tooth row length.

The anterior extent of the splenial notch varies within the egerniine radiation, both species of *Lissolepis* share a further anterior-reaching inferior alveolar foramen than any other genus in the extant group. The ancestral scincid condition, represented by the examined taxa *Eumeces schneideri* (SAMA R6695), *Brachymeles schadenbergi* (SAMA R8853), *Plestiodon fasciatus* (SAMA R66784), and *Eutropis multifasciata* (SAMA R35693) maintain a splenial notch present anteriorly further than 60% along the length of the tooth row, or one that stretches anteriorly into an elongate open Meckel's groove. The anterior extension of the splenial notch is a plesiomorphic state for this character, also shared by both *Proegernia* taxa.

The symphysial joint at the anterior extremity of the lower mandible in scincids varies between subfamilies in its overall size and robustness. Within egerniines, the variation is in the anteroposterior length of its posteroventral section, and the depth of the upper branch. In egerniine species that have a reinforced symphysial joint and manipulate harder food, the lower branch of the symphysis is extended posteriorly and sometimes ventromedially (especially in *Tiliqua*, *Cyclodomorphus* and larger species of *Egernia*), to form a 'chin'. The dorsal branch of the symphysis deepens in *Liopholis* and in larger, omnivorous and herbivorous *Egernia* spp. This may be related to functional morphology to handle stresses on the chin during feeding, rather than a phylogenetic signal as these taxa do not form a clade. *Proegernia mikebulli* is conservative in both the length and width of the posteroventral extension of the symphysis, possibly due to the foramen in the anterodorsal corner. This feature extends into the open Meckel's groove in sphenomorphines and scincines. In egerniines this foramen is usually absent. Both *P. palankarinnensis* and *P. mikebulli* preserve a small extension of this foremen into the open Meckel's groove, but neither extends beyond the posterior edge of the symphysis.

Increased dentary depth and width, in relation to overall length, increases the robustness of the scincid mandible. Variation in these measurements occur between genera of egerniines; species within *Liopholis* often have shorter, deeper faces and corresponding dentaries than similar-sized lizards within the genus *Egernia* (see Thorn et al. 2019; Supplementary information). *Lissolepis* has a more gracile dentary, with lesser height, and width compared to its length (see Figure 2.10). Outside of the egerniines, *Eutropis* and other SE Asian scincids with an unmodified insectivorous diet are more gracile again. *Eutropis multifasciata* has a longer dentary relative to snout-vent length

than all egerniines. Derived morphologies related to dietary adaptations as seen in the herbivorous and durophagous members of the Egerniinae (i.e. *Corucia zebrata*, *Tiliqua* and *Cyclodomorphus*) result in more robust dentary dimensions in conjunction with modified dental morphology. *Proegernia palankarinnensis* and *P. mikebulli* present dentary depths most similar to *Lissolepis* spp., between the ancestral shallow insectivorous *Eutropis,* and the deeper dentary typical of *Liopholis* spp. Deepening of the dentary bone and shortening of the snout noted in numerous species within the genus *Liopholis* is possibly due to the group's affinity for burrowing (Greer, 1989).

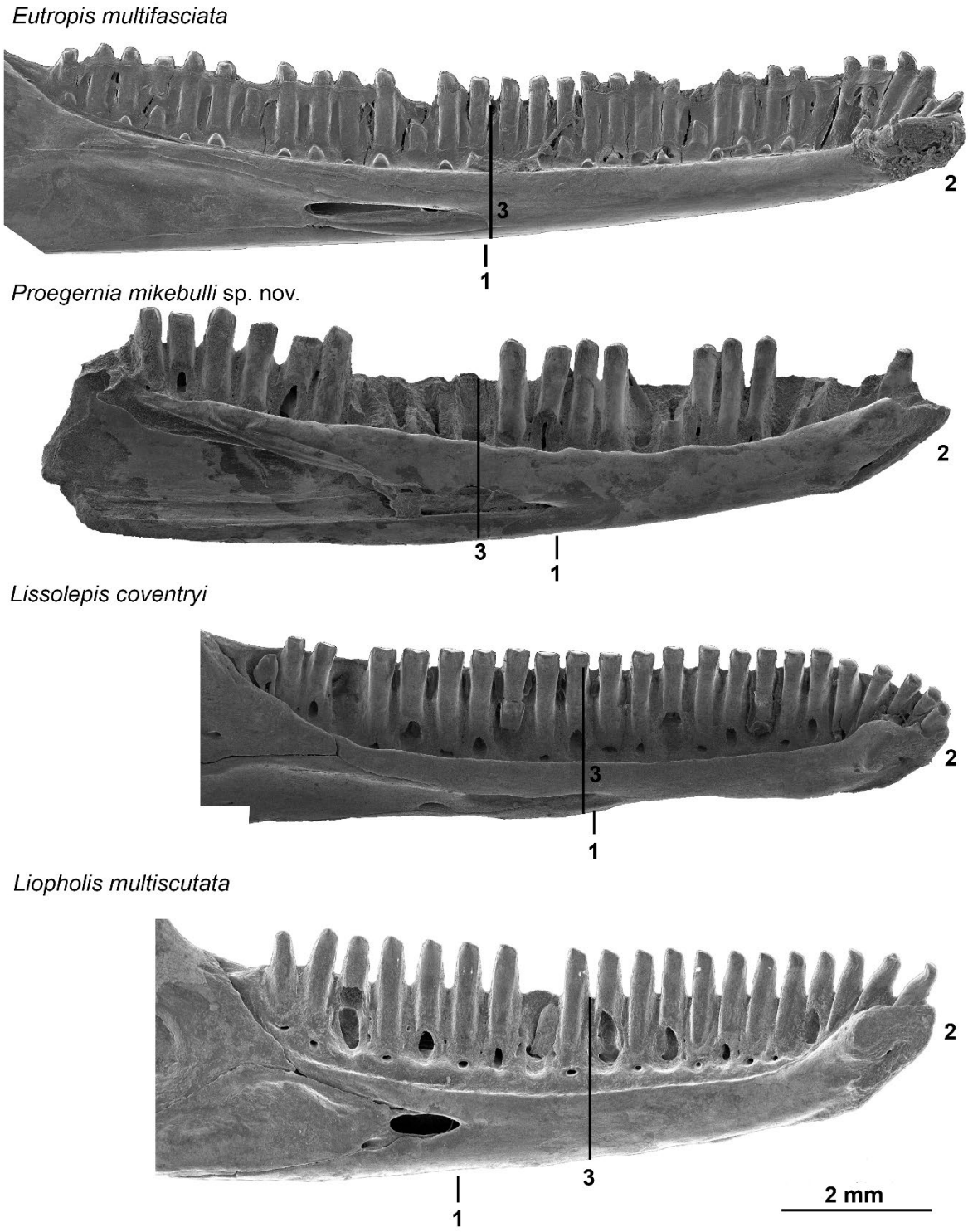

Figure 2.10: Comparative medial views of the dentaries of *Eutropis multifasciata* (SAMA R35693), *Proegernia mikebulli* sp. nov., *Lissolepis coventryi* (SAMA R57317) and *Liopholis multiscutata* (FUR168). 1 Anterior extent of splenial; 2 Symphysis shape and robustness; and 3 Dentary depth at mid-tooth row length.

2.7.24.1 Dentition

The teeth of *Eutropis multifasciata* (SAMA R35693) and *Proegernia mikebulli* show increasing derivation from the basal insectivorous skink tooth type as described by Richter (1994) and Kosma (2003) and represented by *Plestiodon fasciatus* (SAMA R66784; Figure 2.11). Although many species within the extant radiations of eugongyline, sphenomorphine and egerniine scincids have modified tooth shapes for dietary specialisations, taxa exhibiting the most plesiomorphic tooth crown shapes were chosen for comparisons with fossil taxa.

Proegernia mikebulli has departed from the crown shape of basal skinks (see Richter, 1994; Kosma, 2003) by having both cristae directing medially, creating a sharp angle with the *crista distales* and the *culmen laterales*, and less-prominent striae mark the medial face of the tooth. *Eutropis* retain the prominent striae running dorsoventrally on the medial face of the tooth, these striae are almost all equally prominent, while *P. mikebulli* appears to have slightly stronger striae immediately adjacent and parallel to the *culmen laterales*. The tooth crowns of *Eugongylus rufescens* also demonstrate prominent *culmen laterales* and weakened striae, although the tooth shape differs; the shaft widening beneath the crown slightly and wear patterns make obvious the less medially directed cristae. The basal sphenomorphine condition is that of a narrow tooth shaft and crown, with sharply angled cristae creating a more pointed tooth profile. The medial face of the sphenomorphine tooth is anteroposteriorly convex and marked with prominent striae that do not approach the height of the lingual cristae but sit a third of the depth of the crown lower. The striae on *P. mikebulli* extend from almost directly in contact with the lingual cristae to the ventral tips of the *culmen laterales.*

The tooth crown in *P. mikebulli* is similar to that of the extant *Lissolepis coventryi* sharing medially directed cristae, sharp 'shoulders' in the *culmen lateralis*, weak medial striae and absent lateral striae, and an expanded crown width on a narrower tooth shaft.

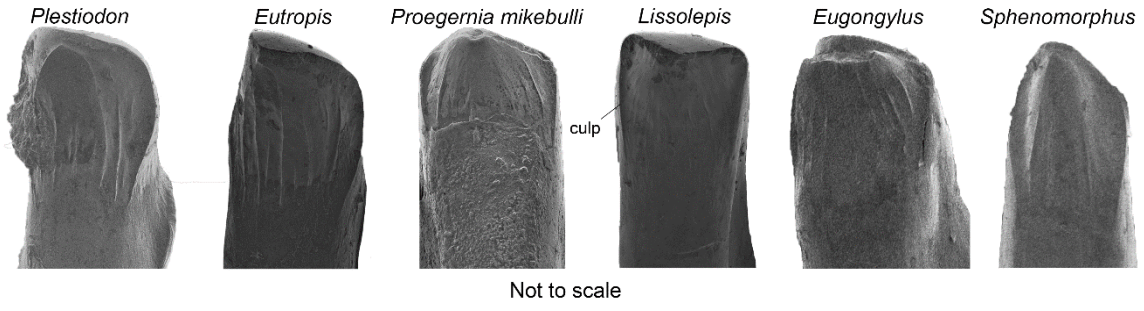

Figure 2.11: Medial view of dentary tooth crowns of *Plestiodon fasciatus* (SAMA R66784), *Eutropis multifasciata* (SAMA R35693), *Lissolepis coventryi* (SAMA R57317), *Proegernia mikebulli* sp. nov. (BCF2.8), *Eugongylus rufescens* (SAMA R36735) and *Sphenomorphus jobiensis* (SAMA R6736). *Plestiodon* represents the basal skink tooth condition as described by Richter (1994). *Culmen lateralis* posterior is labelled culp.

2.7.25 Phylogenetic Relationships

2.7.25.1 Maximum Parsimony

One most parsimonious tree was recovered from maximum parsimony analysis (Figure 2.12) of all morphological and molecular data with a best score of 4726.250, found 60/1000 times. Confidence on most of the nodes indicated by the bootstrap analyses is low; only support for the clades *Bellatorias*, *Liopholis* and *Tiliqua+Cyclodomorphus* are above 50. This is almost certainly due to unstable position of the fossils, which are missing all DNA and most morphological data (111 missing characters for *P. palankarinnensis* and 73 for *P. mikebulli*).

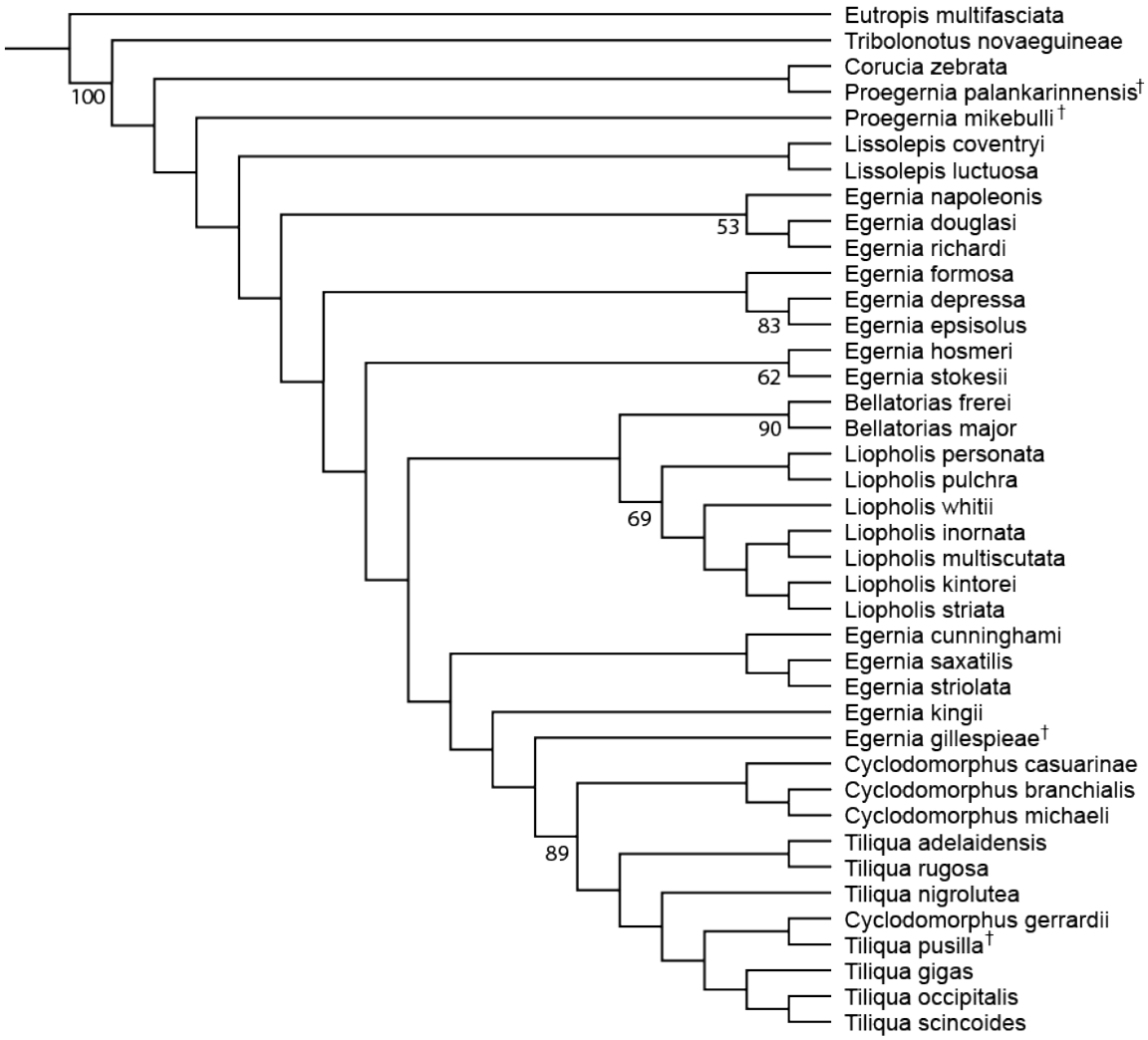

Figure 2.12: The single most parsimonious tree produced as a result of a search of 10,000 trees using new search methods (XMULT) in the phylogenetic analysis program TNT (Goloboff and Catalano, 2016). Bootstrap values >50 shown.

Proegernia mikebulli is recovered basal to the extant Australian Egerniinae defined by *Lissolepis and Tiliqua,* with no bootstrap support for their placement within crown Australian egerniines. *Proegernia palankarinnensis* is retrieved as sister to the Solomon Islands' *Corucia zebrata*, with bootstrap support <50%. These relationships are best interpreted as an effective

polytomy between crown egerniines, *Corucia*, *Proegernia*, and *Lissolepis*. Thus, rather than erect a new genus, we provisionally assign the new species to *Proegernia* (due to geographic and stratigraphic links with the type of that genus, and the Bayesian results below).

The position of both taxa outside the crown Australian egerniines is due to plesiomorphic scincid character states such as a partially open Meckel's groove (char. 11) in both fossil taxa. This feature is similar in *Eutropis multifasciata* which has an anteriorly extended splenial notch compared to *Proegernia* spp. The anterior extent of the splenial (char. 21), and the extension of Meckel's Groove anterior of the splenial notch are features supporting the split between crown *Lissolepis* and *Proegernia*; *Lissolepis* with a splenial reaching approximately 50% of the tooth row length anteriorly, and *Proegernia* reaching beyond to two-thirds the tooth row length.

The extant clade containing *Lissolepis* and *Tiliqua* and all intervening taxa is diagnosed by a completely closed Meckel's Groove (char. 11), an absence of pterygoid teeth (char. 131), and a pterygoid quadrate ramus that is arcuate in cross section (char. 134). *Proegernia* (and *Corucia*) have plesiomorphic or alternative states for these characters, resulting in their position outside the crown Australian egerniine clade. Morphological synapomorphies of the basal crown Australian group genus *Lissolepis* that are shared by both *Proegernia* taxa are the termination of the dentary coronoid process (char. 17), the orientation of the retroarticular process from dorsal view (char. 46), the plesiomorphic bicuspid tooth crown shape (char. 55), minimal dental cementum (char. 60), and the divot in the ventral surface of the pterygoid body that is also absent of pterygoid teeth (chars 135 and 131). These shared characters resulted in the interpreted polytomy between *Corucia*, *Proegernia* and *Lissolepis*.

2.7.25.2 Bayesian

The consensus of four separate runs of 100,000,000 generations, when combined in LogCombiner, then summarised with TreeAnnotator with a burnin of 20%, produced the topology shown in Figure 2.13.

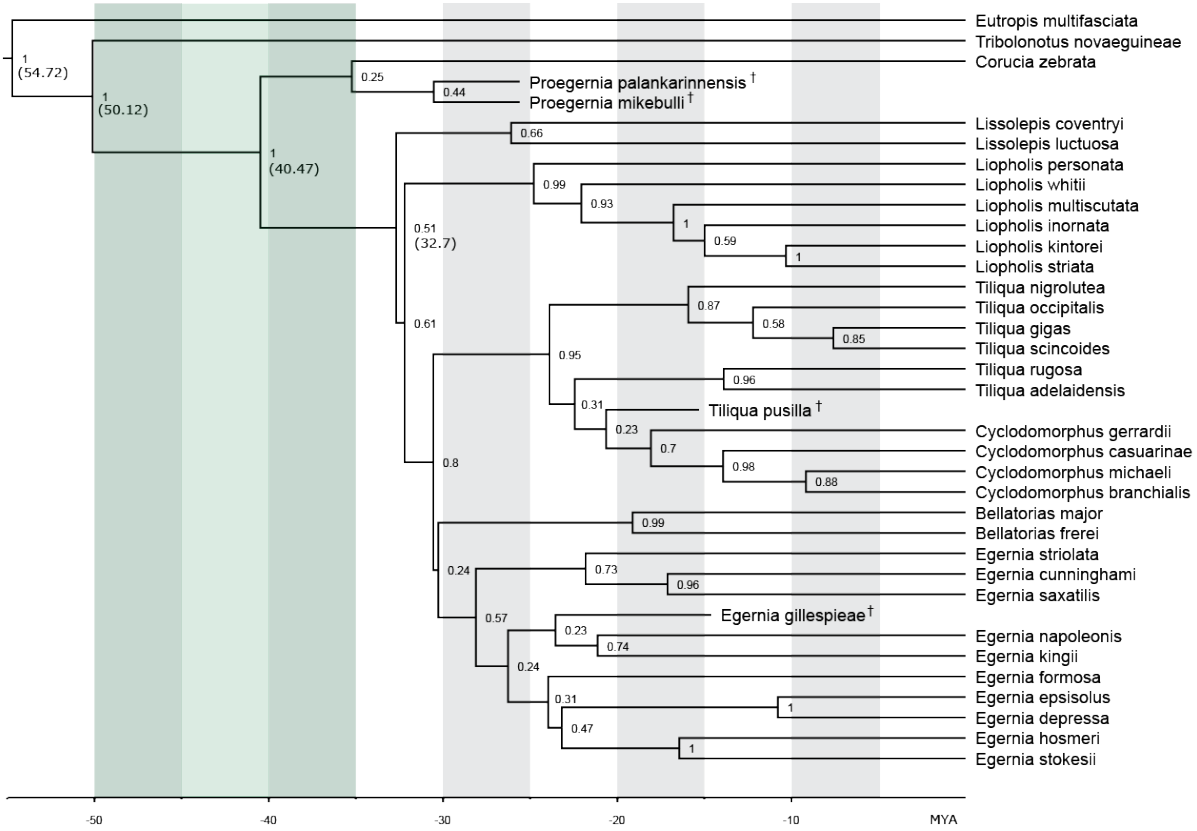

Figure 2.13: Consensus of four runs of tip-dated total evidence Bayesian analyses conducted in BEAST v. 1.8.4 using birth-death serial sampling and a relaxed clock with four fossil calibrations, combined in LogCombiner and consensus tree from TreeAnnotator. †denotes extinct taxon. Node ages are in brackets, the green shading denotes the Eocene isolation of Gondwanan Australia (Müller et al., 2016; Oliver and Hugall, 2017).

The extant egerniine radiation forms a well-supported clade. Within this, *Tribolonotus* is strongly supported as the sister to remaining taxa. Of those, *Corucia* is strongly supported as the sister of the remaining egerniines. Both late-Oligocene fossil *Proegernia* species are weakly supported as the sister to *Corucia* with a Prior Probability (PP) of 0.25. All Australian extant egerniines again form a clade that excludes both *Proegernia*. The extant Australian clade is a weakly supported (PP= 0.51) clade and retrieved as originating in the lower Oligocene (Figure 2.13).

Proegernia palankarinnensis and *P. mikebulli* are retrieved as sister taxa, but with little support (PP= 0.44), not unexpected given extensive missing data. Character changes affirming the sister relationship include the position of the mental foramina 50% along the length of the tooth row (char. 13), and the presence of less than 20 tooth crown striae (char. 61). Both of these features are also shared with *Lissolepis*, but not with their putative sister clade *Corucia zebrata*. The similar basal positioning of both taxa (i.e. outside crown Australian egerniines) is supported by the same characters as those noted after the parsimony analysis.

2.8 Discussion

2.8.20 Namba environment

Recent exploration of the Namba Formation outcrop at Lake Pinpa and Billeroo Creek has unearthed a new stem egerniine taxon, *Proegernia mikebulli*. Previous excavations and collection of surface material at these localities did not recover many squamate elements. This identification has increased the taxonomic diversity of the Namba Fauna to include at least one skink, with further material not described here-in also attributed to the Gekkota. The use of fine mesh-aperture sieves and bulk screening of concentrated lenses of fossiliferous sediments increased the sampled taxonomic richness of the Pinpa Local Fauna.

The excavation and subsequent analyses of the sediment profile at both Billeroo Creek (BC2) and Lake Pinpa (LP12) has allowed an interpretation of palaeoenvironmental conditions in the Frome Basin during the Oligo-Miocene. Dolomite requires a flooded alkaline environment to precipitate, most likely the result of the seasonal fluctuations of the water level of the palaeo-lakes that created the Namba Formation during the late Oligocene–early Miocene (see Callen, 1977). Fluctuations in the rainfall and evaporation contributed to the formation of palygorskite in the lower Layers 3–5. Smectite is the result of the weathering of minerals sourced from older rock outcrop (most likely from the nearby Flinders, Barrier, and Olary Ranges) deposited into the Namba area as swampy soils on the lake edge. Layers where dolomite is no longer present, i.e. Layer 3 according to the XRD result; demonstrate a dryer phase in the palaeo-environment without an alkaline waterbody at the surface. Deposition of the clay minerals still occurs, uplift of the Flinders Ranges began approximately in the middle Miocene, and semi-arid weathering sourced sediments from the foothills to fill the empty lake depression.

Callen (1977) noted that the Namba basin was once flooded, forming a larger palaeolake than the extant salt-outline. The palaeolake Namba supported a number of aquatic vertebrates including lungfish, *Obdurodon*, crocodiles, cetaceans and various waterbirds (Vickers-Rich and Rich, 1991; Fitzgerald, 2004; Worthy, 2009, 2011); their combined presence is indicative of a deeper aquatic environment. The lake was subject to varying rainfall and evaporation rates, resulting in receding lake edges, creating cycles of dolomite precipitation (recorded in Layer 5). Callen (1977) concluded that sufficient evaporation of surface water (conditions required for dolomite precipitation) could not occur in a consistently high-rainfall climate. Moderate seasonal rainfall and higher evaporation rates today result in dolomite deposits exemplified in the Coorong system in southern South Australia (Borch and Lock, 1979), with cool moist winters and hot dry summers. Lake levels rise after dry summers due to groundwater recharge, resulting in the dolomite

precipitation. Unexpectedly, *Proegernia mikebulli* and other small terrestrial vertebrates are preserved in lenses within this same seasonal lake layer. An explanation for this provenance is found in the concentration of the small vertebrate material found in Fish Lens at BC2. These lens deposits, visible intermittently at Lake Pinpa and in one large stretch at Billeroo Creek, are possibly the result of lake edge surface-current eddy pools, or shallow fluvial channels that formed when the water level changed around the lake.

Bones belonging to aquatic vertebrates (fish, turtle, and crocodiles) are mixed with small terrestrial vertebrates (scincids, gekkotans, birds and possums) in these concentrated lenses. The material would have to have been transported in order to mix two starkly different environments. Accumulation of small vertebrate material alongside associated larger vertebrate skeletons (at LP12) indicate that the transportation of material was not from a flash flood typical of tropical monsoon seasonality. The small terrestrial vertebrate material is within a size range attributable to raptor predation (Andrews, 1990; McDowell and Medlin, 2009). Predatory birds have been recorded from the Etadunna and Namba formations (Rich, 1991). The material concentration may be due to raptor pellet accumulations washing into the lake when water levels rose around the bases of raptor nests. As the water receded, raptor pellets filled with small vertebrates were transported either down small channels or to the receding lake edge with the precipitating dolomite and palygorskite deposits.

2.8.21 *Proegernia mikebulli* and crown group egerniines

Proegernia mikebulli was small and gracile by extant egerniine standards. Based on dentary length, an adult individual would be of a similar size to living *Lissolepis coventryi*, around 100 mm SVL (Wilson and Swan, 2017). Examinations of tooth crown features across the type specimens reveals they share features with both *Lissolepis* and species of *Liopholis* (cf. *L. multiscutata* and *L. whitii* both have a cusp slightly posterior to the centre of the tooth crown). Tooth crown features of scincids potentially preserve phylogenetic and dietary signals. Detailed studies across, within, and between the extant subfamilies may help elucidate any dietary preferences suggested by fossil dentition. Tooth striae are present on teeth specialised for most dietary preferences and we could not see a pattern in the number of striae between insectivorous, durophagous, or herbivorous species (see Kosma, 2003). Within genera, the number and patterning of striae was fairly similar. *Cyclodomorphus* and *Tiliqua* increase the number of striae from other egerniines, partly due to the change in tooth shape leading to striae radiating on all sides from a central cusp. *Lissolepis* and *Liopholis* have fewer striae and all are restricted to the lingual face of the tooth crown, below the lingual cristae. The two fossil species of *Proegernia* have few striae, similar to *Lissolepis* and *Liopholis*. The buccal striae on the crowns of *Proegernia palankarinnensis* are unusual and weren't

observed on extant *Eutropis multiscutata*, *Sphenomorphus jobiensis* or *Eugongylus rufescens*. Examination of fine-scale tooth crown features may prove useful characters for morphological phylogenetic analyses of fragmentary or incomplete tooth-bearing scincid material in future.

From what can be deduced of the palaeoenvironment surrounding Lake Pinpa and Billeroo Creek in the late Oligocene–early Miocene, *Proegernia mikebulli* lived in a cool, moist climate region with seasonal hot, dry summers with high evaporation rates. *Proegernia* and other small terrestrial vertebrates were likely prey of a raptor species; an undescribed accipitrid was excavated from LP12 by Worthy/Camens-led expeditions. Other squamates known from this region and time period include a small gekkotan, and a possible constricting snake (Vickers-Rich and Rich, 1991). Although no evidence of *Proegernia palankarinnensis* was found at either Namba site, the presence of at least two Australian scincids, from neighbouring basins, covering similar time periods and environments may be an indication of the early diversity of Australian squamates. Extant Australian scincids are difficult to separate based on isolated cranial material. The same cryptic diversity may have been present in the Oligo-Miocene, so more than two species may be present in the Etadunna and Namba Formations.

Although neither analysis produced firm support for the phylogenetic position of *Proegernia mikebulli*, both parsimony and Bayesian investigations placed the new taxon outside of crown Australian Egerniinae. *Proegernia* have a larger tooth count than crown Australian egerniines, a splenial notch placed more anteriorly, and a 1 mm long opening of Meckel's groove anterior to the splenial notch. Each of these character states are representative of the predicted transitional form between the plesiomorphic outgroup morphology and the majority of crown Australian egerniines. These characters have pulled *Proegernia* outside of the Australian crown group, but not beyond the Sahul stem genera *Corucia* and *Tribolonotus*. However, their precise position outside this crown group is uncertain. The node age for all Egerniinae is resolved as 50.12 Ma, with *Tribolonotus* as the extant stem taxon representing the arrival of the subfamily to northern Sahul (Australia, New Guinea and surrounding islands). The stem clade last shared a common ancestor with the crown Australian egerniines 40.47 million years ago. If relationships of one or both *Proegernia* with *Corucia* are correct (Figure 2.12–Figure 2.13), then there were either two migrations of Egerniinae into southern Sahul 40.47–32.7 Ma, or a single dispersal followed by extinction of *Proegernia* spp. and mainland species of *Corucia* and *Tribolonotus*. However, a large amount of missing data for these fossil taxa and low support for precise relationships means that it is possible that these trees are wrong, and that homoplasy with *Corucia* is what pulls these taxa away from the crown Australian group. It is thus possible that *Proegernia* lies on the stem to the Australian crown group, in which case only a single dispersal event to Australia need be assumed.

2.8.22 The origins of Australian scincids

The tip-dated phylogeny inclusive of the two Oligo-Miocene *Proegernia* taxa retrieves the age of the Egerniinae as 50.12 Ma. The last common ancestor of Egerniinae and Lygosominae was mostly likely living in the far south-eastern edge of Asia during the early Eocene. There is no fossil evidence of egerniines in Australia at this time, but records of similar sized squamates and marsupials in the Tingamarra Fauna (Godthelp et al., 1992) and Rundle Formation (Hocknull, 2000) demonstrate that fossil preservation is possible. Crown Egerniinae most likely originated either in south-eastern Asia or dispersed via rafting to Australia somewhere between 50.12 Ma and the connection with the Australian landmass in the late Eocene (32.7Ma). Miocene origins, after the migration of Sahul closer to south east Asia, have been hypothesised for agamids (22 Ma; Hugall et al., 2008), pythons (c. 35 Ma; Sanders and Lee, 2008), sphenomorphine skinks (Rabosky et al., 2007), and elapids (Sanders and Lee, 2008).

The current analysis indicates that egerniines are the oldest skinks in Australia. The diversification of the crown Australian egerniines (~33Ma) occurred nearly 10 million years before the estimated diversification of other Australian skinks, i.e. the Sphenomorphinae (c. 25 Ma) and Eugongylinae (c. 20 Ma; Skinner et al., 2011). The first egerniines would have shared the continent with pygopodid, diplodactylid and carphodactylid geckos, and madtsoiid snakes (Oliver and Sanders, 2009; Oliver and Hugall, 2017). Whether or not they began to diversify before or after arrival into Sahul, is not yet supported with fossil evidence. The search for older scincid material in Australia continues, with investigations of Eocene collections from Murgon in northern Queensland (Godthelp et al., 1992), early Oligocene vertebrates from Pwerte Marnte Marnte (Murray and Megirian, 2006), and mid-Miocene material from Bullock Creek (Murray and Megirian, 1992).

The current diversity of Australian skinks in the context of their fairly recent arrival compared to Gondwanan endemic marsupials and passerine birds, is notably impressive. After only ~33 million years in Australia, skinks have speciated remarkably into 461 species (Uetz et al., 2019), modified their body plans to disparate extremes, tried and tested numerous life history strategies, and colonised virtually every terrestrial habitat.

2.9 Acknowledgments

KMT is supported by an Australian Postgraduate Research Training Stipend. The Mark Mitchell Foundation funded both the fieldwork component of this project, and SEM time. Sue Double and Jenny Worthy for screening and sorting the fossil material. Rod Wells, Colin Doudy, Bob and Sue Tulloch, Amy Tschirn, Warren Handley, Jacob Blokland, Carey Burke and Ellen Mather were all part of the collaborative field team. Dr Jason Gascooke for training on, and use of, the SEM at Flinders Microscopy, an Australian Microscopy and Microanalysis Research Facility. Mary-Anne Binnie and Carolyn Kovach of the South Australian Museum, and Tim Ziegler from Museums Victoria, for access to collections, and loans of fossil and extant comparative material. The Willi Hennig Society for making TNT freely available.

2.10 References

Alekseyenko, A. V., C. J. Lee, and M. A. Suchard. 2008. Wagner and Dollo: a stochastic duet by composing two parsimonious solos. Systematic biology 57:772–784.

Andrews, P. 1990. Owls, caves and fossils. The Natural History Museum, London, 230 pp.

Borch, C. C. V. D., and D. Lock. 1979. Geological significance of Coorong dolomites. Sedimentology 26:813–824.

Callen, R. A. 1977. Late Cainozoic environments of part of northeastern South Australia. Journal of the Geological Society of Australia: An International Geoscience Journal of the Geological Society of Australia 24:151–169.

Callen, R. A., and R. H. Tedford. 1976. New Late Cainozoic rock units and depositional environments, Lake Frome area, South Australia. Transactions of the Royal Society of South Australia 100:125–167.

Chapple, D. G., P. A. Ritchie, and C. H. Daugherty. 2009. Origin, diversification, and systematics of the New Zealand skink fauna (Reptilia: Scincidae). Molecular Phylogenetics and Evolution 52:470–487.

Drummond, A. J., S. Y. W. Ho, M. J. Phillips, and A. Rambaut. 2006. Relaxed phylogenetics and dating with confidence. PLOS Biology 4:e88.

Drummond, A. J., M. A. Suchard, D. Xie, and A. Rambaut. 2012. Bayesian phylogenetics with BEAUti and the BEAST 1.7. Molecular biology and evolution 29:1969–1973.

Estes, R. 1984. Fish, amphibians and reptiles from the Etadunna Formation, Miocene of South Australia. Australian Zoologist 21:335–343.

Evans, S. E. 2008. The skull of lizards and Tuatara; pp. 1–343 in C. Gans, A. S. Gaunt, and K. Adler (eds.), Biology of the Reptilia 20, Morphology H The skull of Lepidosauria. Society for the Study of Amphibians and Reptiles, Ithaca, NY.

Fitzgerald, E. M. G. 2004. A review of the Tertiary fossil Cetacea (Mammalia) localities in Australia. Memoirs of Museum Victoria 61:183–208.

Gardner, M. G., A. F. Hugall, S. C. Donnellan, M. N. Hutchinson, and R. Foster. 2008. Molecular systematics of social skinks: phylogeny and taxonomy of the *Egernia* group (Reptilia: Scincidae). Zoological Journal of the Linnean Society 154:781–794.

Gelnaw, W. B. 2011. On the cranial osteology of *Eremiascincus* and its use for identification. Biological Sciences, East Tennessee State University, 253 pp.

Godthelp, H., M. Archer, R. Cifelli, S. J. Hand, and C. F. Gilkeson. 1992. Earliest known Australian Tertiary mammal fauna. Nature 356:514–516.

Goloboff, P. A., and S. A. Catalano. 2016. TNT version 1.5, including a full implementation of phylogenetic morphometrics. Cladistics 32:221–238.

Goloboff, P. A., M. Pittman, D. Pol, and X. Xu. 2018. Morphological data sets fit a common mechanism much more poorly than DNA sequences and call into question the Mkv model. Systematic biology 68:494–504.

Gray, J. E. 1825. A synopsis of the genera of reptiles and Amphibia, with a description of some new species. Annals of Philosophy 10:193–217.

Greer, A. E. 1979. A phylogenetic subdivision of Australian skinks. Records of the Australian Museum 32:339–371.

Greer, A. E. 1989. The biology and evolution of Australian lizards. Surrey Beatty & Sons, Chipping Norton, NSW, 264 pp.

Hall, R. 2002. Cenozoic geological and plate tectonic evolution of SE Asia and the SW Pacific: computer-based reconstructions, model and animations. Journal of Asian Earth Sciences 20:353–431.

Harmon, L. J. 2019. Phylogenetic comparative methods. 1.4 Edition. Luke Harmon, Published Online, 234 pp.

Hocknull, S. A. 2000. Remains of an Eocene skink from Queensland. Alcheringa: An Australasian Journal of Palaeontology 24:63–64.

Hoffstetter, R., and J.-P. Gasc. 1969. Vertebrae and ribs of modern reptiles; pp. 201–310 in C. Gans (ed.), Biology of the Reptilia. Academic Press, New York.
Hugall, A. F., and M. S. Y. Lee. 2004. Molecular claims of Gondwanan age for Australian agamid lizards are untenable. Molecular biology and evolution 21:2102–2110.
Hugall, A. F., R. Foster, M. Hutchinson, and M. S. Y. Lee. 2008. Phylogeny of Australasian agamid lizards based on nuclear and mitochondrial genes: implications for morphological evolution and biogeography. Biological Journal of the Linnean Society 93:343–358.
Kosma, R. 2003. The dentitions of recent and fossil scincomorphan lizards (Lacertilia, Squamata) - Systematics, Functional Morphology, Palecology. Department of Geosciences and Geography, University Hannover, Hanover, Germany, 231 pp.
Lambert, S. M., T. W. Reeder, and J. J. Wiens. 2015. When do species-tree and concatenated estimates disagree? An empirical analysis with higher-level scincid lizard phylogeny. Molecular Phylogenetics and Evolution 82:146–155.
Lanfear, R., P. B. Frandsen, A. M. Wright, T. Senfeld, and B. Calcott. 2016. PartitionFinder 2: new methods for selecting partitioned models of evolution for molecular and morphological phylogenetic analyses. Molecular biology and evolution 34:772–773.
Lee, M. S. Y., M. N. Hutchinson, T. H. Worthy, M. Archer, A. J. D. Tennyson, J. P. Worthy, and R. P. Scofield. 2009b. Miocene skinks and geckos reveal long-term conservatism of New Zealand's lizard fauna. Biology Letters 5:833–837.
Lewis, P. O. 2001. A likelihood approach to estimating phylogeny from discrete morphological character data. Systematic biology 50:913–925.
Maddison, W., and D. Maddison. 2017. Mesquite: a modular system for evolutionary analysis. Version 3.2.
Martin, J. E., M. N. Hutchinson, R. Meredith, J. A. Case, and N. S. Pledge. 2004. The oldest genus of scincid lizard (Squamata) from the Tertiary Etadunna Formation of South Australia. Journal of Herpetology 38:180–187.
McDowell, M. C., and G. C. Medlin. 2009. The effects of drought on prey selection of the barn owl (*Tyto alba*) in the Strzelecki Regional Reserve, north-eastern South Australia. Australian Mammalogy 31:47–55.
Megirian, D., G. Prideaux, P. Murray, and N. Smit. 2010. An Australian land mammal age biochronological scheme. Paleobiology 36:658–671.
Müller, R. D., M. Seton, S. Zahirovic, S. E. Williams, K. J. Matthews, N. M. Wright, G. E. Shephard, K. T. Maloney, N. Barnett-Moore, M. Hosseinpour, D. J. Bower, and J. Cannon. 2016. Ocean basin evolution and global-scale plate reorganization events since Pangea breakup. Annual Review of Earth and Planetary Sciences 44:107–138.
Murray, P., and D. Megirian. 1992. Continuity and contrast in Middle and Late Miocene vertebrate communities from the Northern Territory. The Beagle, Records of the Northern Territory Museum of Arts and Sciences 9:195–218.
Murray, P. F., and D. Megirian. 2006. The Pwerte Marnte Marnte Local Fauna: a new vertebrate assemblage of presumed Oligocene age from the Northern Territory of Australia. Alcheringa: An Australasian Journal of Palaeontology 30:211–228.
O'Reilly, J. E., M. N. Puttick, L. Parry, A. R. Tanner, J. E. Tarver, J. Fleming, D. Pisani, and P. C. Donoghue. 2016. Bayesian methods outperform parsimony but at the expense of precision in the estimation of phylogeny from discrete morphological data. Biology Letters 12:20160081.
Oliver, P., and A. Hugall. 2017. Phylogenetic evidence for mid-Cenozoic turnover of a diverse continental biota. Nat Ecol Evol 1:1896–1902.
Oliver, P. M., and K. L. Sanders. 2009. Molecular evidence for Gondwanan origins of multiple lineages within a diverse Australasian gecko radiation. Journal of Biogeography 36:2044–2055.
Oppel, M. 1811. Die Ordnungen, Familien und Gattungen der Reptilien, als Prodrom einer Naturgeschichte derselben. Joseph Lindauer, München, 86 pp.

Rabosky, D. L., S. C. Donnellan, A. L. Talaba, and I. J. Lovette. 2007. Exceptional among-lineage variation in diversification rates during the radiation of Australia's most diverse vertebrate clade. Proceedings of the Royal Society of London B: Biological Sciences 274:2915–2923.
Rambaut, A., A. J. Drummond, D. Xie, G. Baele, and M. A. Suchard. 2018. Posterior summarisation in Bayesian phylogenetics using Tracer 1.7. Systematic biology 67:901–904.
Rich, T. 1984. News from Foreign members: Australia, Museum of Victoria, Melbourne. Society of Vertebrate Paleontology News Bulletin 130:28.
Rich, T. H. 1991. Monotremes, placentals, and marsupials: their record in Australia and its biases; pp. 894–1057 in P. Vickers-Rich, J. M. Monaghan, R. F. Baird, and T. H. Rich (eds.), Vertebrate Palaeontology of Australasia. Pioneer Design Studio Pty Ltd, Melbourne, Australia.
Richter, A. 1994. Lacertilia aus der Unteren Kreide von Una und Galve (Spanien) und Anoual (Marokko). Berliner geowissenschaftliche Abhandlungen (E: Paläobiologie) 14:1–147.
Russell, A. P., and A. M. Bauer. 2008. The appendicular locomotor apparatus of *Sphenodon* and normal-limbed squamates; pp. in C. Gans, A. S. Gaunt, and K. Adler (eds.), The skull and appendicular locomotor apparatus of Lepidosauria. Society for the Study of Amphibians and Reptiles, Ithaca, New York, USA.
Sanders, K. L., and M. S. Y. Lee. 2008. Molecular evidence for a rapid late-Miocene radiation of Australasian venomous snakes (Elapidae, Colubroidea). Molecular Phylogenetics and Evolution 46:1165–1173.
Skinner, A., A. F. Hugall, and M. N. Hutchinson. 2011. Lygosomine phylogeny and the origins of Australian scincid lizards. Journal of Biogeography 38:1044–1058.
Skinner, A., M. N. Hutchinson, and M. S. Y. Lee. 2013. Phylogeny and divergence times of Australian *Sphenomorphus* group skinks (Scincidae, Squamata). Molecular Phylogenetics and Evolution 69:906–918.
Stadler, T. 2010. Sampling-through-time in birth–death trees. Journal of Theoretical Biology 267:396–404.
Tedford, R. H., M. Archer, A. Bartholomai, M. Plane, N. S. Pledge, T. Rich, P. Rich, and R. T. Wells. 1977. The discovery of Miocene vertebrates, Lake Frome area, South Australia. BMR Journal of Australian Geology & Geophysics 2:53–57.
Thorn, K. M., M. N. Hutchinson, M. Archer, and M. S. Y. Lee. 2019. A new scincid lizard from the Miocene of Northern Australia, and the evolutionary history of social skinks (Scincidae: Egerniinae). Journal of Vertebrate Paleontology 39:e1577873.
Uetz, P., P. Freed, and J. e. Hošek. 2019. The Reptile Database.
Vickers-Rich, P., and P. V. Rich. 1991. Vertebrate palaeontology of Australasia. Pioneer Design Studio, Melbourne, Australia, 1437 pp.
Vidal, N., and S. B. Hedges. 2009. The molecular evolutionary tree of lizards, snakes, and amphisbaenians. Comptes rendus biologies 332:129–139.
Welch, K. 1982. Herpetology of the Old World II. Preliminary comments on the classification of skinks (Family Scincidae) with specific reference to those genera found in Africa, Europe, and southwest Asia. Herptile 7:25–27.
White, M. E. 2006. Environments of the geological past; pp. 17–48 in J. R. Merrick, Archer, A., Hickey, G. M., Lee, M. S. Y. (ed.), Evolution and biogeography of Australasian vertebrates. Auscipub, Oatlands, NSW.
Wilson, S., and G. Swan. 2017. A complete guide to the Reptiles of Australia. 5th Edition. Reed New Holland Publishers, Sydney, Australia, 647 pp.
Woodburne, M. O., B. J. Macfadden, J. A. Case, M. S. Springer, N. S. Pledge, J. D. Power, J. M. Woodburne, and K. B. Springer. 1994. Land mammal biostratigraphy and magnetostratigraphy of the Etadunna Formation (late Oligocene) of South Australia. Journal of Vertebrate Paleontology 13:483–515.
Woodhead, J., S. J. Hand, M. Archer, I. Graham, K. Sniderman, D. A. Arena, K. H. Black, H. Godthelp, P. Creaser, and E. Price. 2016. Developing a radiometrically-dated chronologic

sequence for Neogene biotic change in Australia, from the Riversleigh World Heritage Area of Queensland. Gondwana Research 29:153–167.
Worthy, T. H. 2009. Descriptions and phylogenetic relationships of two new genera and four new species of Oligo-Miocene waterfowl (Aves: Anatidae) from Australia. Zoological Journal of the Linnean Society 156:411–454.
Worthy, T. H. 2011. Descriptions and phylogenetic relationships of a new genus and two new species of Oligo-Miocene cormorants (Aves: Phalacrocoracidae) from Australia. Zoological Journal of the Linnean Society 163:277–314.
Wright, A. M., and D. M. Hillis. 2014. Bayesian analysis using a simple likelihood model outperforms parsimony for estimation of phylogeny from discrete morphological data. PLoS ONE 9:e109210.

CHAPTER 3: A NEW SCINCID LIZARD FROM THE MIOCENE OF NORTHERN AUSTRALIA, AND THE EVOLUTIONARY HISTORY OF SOCIAL SKINKS (SCINCIDAE: EGERNIINAE)

KAILAH M. THORN,[1,2] MARK N. HUTCHINSON, [1,2] MICHAEL ARCHER, [3] and MICHAEL S.Y. LEE [1,2]

[1] College of Science and Engineering, Flinders University, GPO Box 5100, Adelaide, South Australia 5001, kailah.thorn@flinders.edu.au;

[2] South Australian Museum, North Terrace, Adelaide, South Australia 5000;

[3] Palaeontology, Geobiology and Earth Archives Research Centre (PANGEA), The University of New South Wales, Sydney, New South Wales, Australia 2052

3.1 Context

This chapter involved the creation and testing of the initial morphological character set and represents the first total-evidence phylogeny for the Egerniinae. A new fossil taxon is described: *Egernia gillespieae,* the first fossil *Egernia* acting as a calibration alongside *Tiliqua pusilla* for the divide between this genus and the blue- and pink-tongued skinks of *Tiliqua* and *Cyclodomorphus*.

This work was published in the peer-reviewed Journal of Vertebrate Paleontology in May 2019 and has been reformatted to be consistent with this thesis.

3.2 Statement of authorship

KMT built the character matrix, collected the morphological data, prepared all figures and wrote the manuscript; MNH conceived the project and edited manuscript drafts; MA recovered the specimen and provided information on specimen provenance; MSYL ran the phylogenetic analyses and edited manuscript drafts.

3.3 Abstract

The Egerniinae (formerly the *Egernia* group) is a morphologically diverse clade of skinks comprising 61 extant species from eight genera, spread across Australia, New Guinea and the Solomon Islands. The relatively large size and robustness of many egerniines has meant that they fossilize more readily than other Australian skinks, and have been more frequently recorded from palaeontological excavations. The Riversleigh World Heritage Area of north-eastern Australia has yielded multiple egerniine fossils, but most are isolated jaw elements, and only one taxon (“*Tiliqua” pusilla*) has been formally described. Articulated remains recently recovered from the mid-Miocene AL90 site (14.8 Ma) at Riversleigh are here described as *Egernia gillespieae,* and represent the first opportunity to describe the morphology of a significant portion of a single individual of a fossil member of the Egerniinae. We include this fossil and *“T”. pusilla* in an integrated analysis of morphology and published molecular data to assess their relationships and to provide calibration points for the timing of the egerniine radiation. Our calibrated tree combining molecular and morphological data suggests that the modern Australian radiation dates to the end of the Eocene (34.1 Ma). Both fossils are within the Australian crown clade Egerniinae: *Egernia gillespieae* is placed close to species of the living genus *Egernia,* while “*Tiliqua” pusilla* likely sits basal to the divergence of the clade inclusive of *Tiliqua* and *Cyclodomorphus*. The fossils thus provide direct evidence that the Australian radiation of the Egerniinae was well underway by the mid-Miocene.

3.4 Introduction

Explanations for both present biodiversity and the history of species radiations are increasingly derived from large-scale, detailed molecular analyses that sample only extant lineages. Although methodological refinements and expanding genomic data are increasing confidence in these analyses, phenotypic and palaeontological evidence remains crucial. To accurately infer evolutionary timescales and dynamics using these phylogenies, integration of fossil material with morphological and molecular data for living taxa is required (e.g. Rabosky, 2010; Lee and Palci, 2015).

Skinks (scincid lizards) represent a large component of the terrestrial Australian vertebrate fauna with over 448 named species across 46 genera (Uetz et al., 2019), compared to 315 native mammal species (pre-European settlement: Woinarski et al., 2014). All Australian skinks had been regarded as belonging to a well-supported monophyletic lineage (Pyron et al., 2013; Lambert et al., 2015) referred to as the Lygosominae, distributed across southern Asia, southern Africa, Madagascar and Central and South America. Within Australia "lygosomine" skinks fall into three monophyletic radiations, as elucidated by morphology (Greer, 1979) and DNA (Honda et al., 2000; Pyron et al., 2013); the *Sphenomorphus, Eugongylus* and *Egernia* groups. A re-classification proposal (Hedges, 2014) for family status for these 'groups' has not been widely accepted, but a consensus is emerging (Uetz et al., 2019) that now treats these major clades as subfamilies within the Scincidae: Sphenomorphinae, Eugongylinae and Egerniinae.

The egerniine skinks are an integral part of the modern Australian herpetofauna, occupying most terrestrial habitats ranging across alpine mountain ranges, deserts, coastal dunes, mesic woodlands and tropical rainforests (Greer, 1989; Hagen et al., 2012; Cogger, 2018). Diverse morphotypes, ecologies and life history strategies have led the members of the group to be subjects of numerous investigations, including morphology (Estes and Williams, 1984; Shea, 1990), behaviour (Bull, 2000; Gardner et al., 2002; Chapple, 2003) and conservation (Fordham et al., 2012; Schofield et al., 2012). Yet all previous works were completed without a dated phylogenetic context. The potential contribution of fossil data to our understanding of the evolution of the egerniines has yet to be explored. Of the few fossil skink species named from Australia, all are larger-body-sized egerniine skinks, and most are based on tooth-bearing elements, often the only lizard material recovered due to the mammalian focus of many excavations (Hollenshead et al., 2011; Bell and Mead, 2014).

Previous attempts to produce a molecular phylogeny for the Egerniinae have resulted in conflicting or poorly-resolved trees from parsimony, maximum likelihood analyses and Bayesian

inferences (Honda et al., 1999; Gardner et al., 2008). The previously broadly-defined genus of *Egernia* Gray, 1838 was shown to be potentially paraphyletic with respect to *Tiliqua* and *Cyclodomorphus*, and split by Gardner et al. (2008) into four genera: *Lissolepis* Peters, 1872, *Liopholis* Fitzinger, 1843, *Bellatorias*, Wells and Wellington, 1984, and *Egernia* Gray, 1838. The age of the Australian radiation has also been poorly constrained: either calibrated with egerniine fossils that have not been analysed phylogenetically (Skinner et al., 2011), or with fossils from far outside the group (e.g. Wright et al., 2015a; Tonini et al., 2016). The retrieved age varies widely: between 52.37 (Wright et al., 2015a) and 23.76 (Tonini et al., 2016) million years.

We here present a combined morphological and molecular phylogeny of the Egerniinae. We reassess the variation in cranial features across all seven extant genera of the group, expanding and reassessing many of the defining characters used in current taxonomies (see Hedges, 2014) and in higher-level squamate phylogenetics (e.g. Gauthier et al., 2012). This phylogeny is dated using the two most important egerniine fossils. Both are from the mid-Miocene of Riversleigh World Heritage Area of NW Queensland, Australia, which has provided a wealth of lizard material that is yet to be studied in detail (Hutchinson, 1992). The first is "*Tiliqua" pusilla* (Shea and Hutchinson, 1992) from the Gag locality (see Discussion for explanation of quotes). The second is the most complete egerniine fossil yet known, an articulated partial skull from Allan's Ledge 1990 (AL90) site, which we describe and name herein. We assess the combined living and fossil, morphological and molecular data using parsimony and tip-dated Bayesian approaches, to infer the phylogeny, divergence times, and the evolution of key morphological features in the Egerniinae.

3.5 Methods

3.5.20 Fossil Material

The new associated and partly articulated specimen is from Alan's Ledge 1990 (AL90) Site, Riversleigh World Heritage Area, north western Queensland. This material was discovered in 1994 and recovered using acid preparation of limestone blocks at the University of New South Wales. The Systematic Palaeontology section lists full details of the specimen, locality and preparation.

3.5.21 Morphological and Molecular Data

Thirty four extant species were included for the morphological analysis in this study, chosen based on the need to sample all major lineages, the availability of museum specimens for Micro-CT scanning, and previously collected molecular data for each taxon. If the same specimen could not be used for both morphology and molecular characterisation, specimens from the same geographic region were sourced in an effort to avoid conflating potential cryptic species. Dry skeletal specimens were primarily from the herpetology collections of the South Australian Museum

(SAM), as well as Museum Victoria (NMV) and the Western Australian Museum (WAM); see the Supplementary Information (SI) for catalogue numbers. Micro computed tomography (Micro-CT) scans of all specimens were generated using the Skyscan-1076 at Adelaide Microscopy. Resulting files were reconstructed in NRecon (Bruker), and rendered and measured in Avizo Light (version 9.0). Two resolutions were used (8.5µ and 17µ) across the sample taxa, due to size variation across the group. Voxel size was recorded and defined in Avizo to standardise measurements. All measurements were recorded in micrometres as continuous characters.

Characters coded for this study include those previously used in squamate phylogeny, as well as newly-identified traits variable in the Egerniinae. Most of the characters were used or modified from Gauthier et al. (2012), who provided the most exhaustive list of osteological characters that vary among squamates; all those which we observed to vary within egerniines were included. New characters variable across the group were added based on direct observations and the literature on the osteology of the group (Greer, 1979; Shea, 1990; Hollenshead et al., 2011). General osteological terminology followed Evans (2008), and morphological terminology for describing the teeth is from Kosma (2003). An exception is that we term the foramina for the nerve branches innervating the *intermandibularis* musculature as the *intermandibularis* foramina, not 'mylohyoid foramina' as many previous authors have used (the *mylohyoideus* musculature is unique to mammals, derived in part from the posterior *intermandibularis* of other vertebrates; Schwenk, 2000; Diogo and Abdala, 2010). A total of 135 characters were identified for the skull and mandible, including 95 discrete and 40 continuous traits. Discrete characters which formed clear morphoclines were ordered (e.g. as in Gauthier et al., 2012). For continuous characters, raw measurements were standardised using either dentary or maxilla length to correct for size. All continuous characters were then log transformed, and standardised to range between 0 (min) and 2 (max), i.e. equivalent to a 3-state discrete (012) character. The average number of states for the 95 discrete characters was ~3 states, so this rescaling makes each continuous character roughly equivalent to an average discrete character. A full character list, and details of ordering and standardisation, are in the Supplementary Information with detailed images illustrating all new characters, as well as sources for characters used in previous studies. Character numbers referred to henceforth in the text relate to this file; within the TNT files character numbers will be one less due to the program numbering characters starting at 0 rather than 1.

The molecular alignment was derived from concatenating loci in Tonini et al. (2016) (T12S 412bp, 16S 681bp, ND4 693bp BDNF 699bp, CMOS 835bp) and Gardner et al. (2008; B-fibrinogen intron, 1051 alignable bp), and is available in the analysis files described below. Gaps were coded as missing data, not a separate state.

3.5.22 Phylogenetic Analyses

Analyses were performed using parsimony and Bayesian methods, using the combined data as well as the morphological and molecular data separately. The discussion below first focuses on the combined analyses; the separate analyses are detailed afterwards.

The parsimony analyses for the combined discrete morphological, continuous morphological, and DNA data were performed using TNT v.1.1 (Goloboff et al., 2008). *Eutropis* was set as the most distant outgroup (as in Gardner et al., 2008; see also Pyron et al., 2013). The most parsimonious tree for the combined data was found using 1000 replicates of tree-bisection-reconnection (TBR) with up to 1000000 trees held. To assess clade support, 200 partitioned bootstrap replicates were performed using TNT (with discrete characters, continuous characters, and each gene locus treated as a separate resampling partition), using new search methods (XMULT) with 1000 replicates and 1000000 trees held. The MPT and bootstrap trees from TNT were exported as nexus format, and continuous and discrete characters were mapped by TNT (SI file 'Mapped_Character_Optimisations.log') as well as visualised in Mesquite v3.2 (Maddison and Maddison, 2017). Consensus trees and clade frequencies were calculated in PAUP* (Swofford, 2003). The executable file for finding the most parsimonious tree (and optimising characters), and doing 200 reps of partitioned bootstrap resamples can be found in the SI data files Egernia_35_4506_MP.tnt and Egernia_35_4506_PartitionedBootstrap.tnt.

The discrete morphological, continuous morphological, and DNA data were simultaneously analysed using tip-dated Bayesian analyses (Drummond and Suchard, 2010; Ronquist et al., 2012a; Gavryushkina et al., 2017). *Eutropis* was again chosen as the outgroup. The optimal evolutionary histories that explain all three data sources - along with fossil/tip ages - were inferred using Markov-chain Monte Carlo (MCMC) approaches as implemented in the BEAST 1.8.4 package with post-processing modules LogCombiner and TreeAnnotator (Drummond et al., 2012). BEAST is increasingly widely employed for tip-dated phylogenetic analysis of time-sampled data including fossils (e.g. Drummond and Suchard, 2010; Gavryushkina et al., 2017). The executable BEAST xml files, with annotations describing exact model, prior, MCMC, burn-in and logging settings, are in SI data file Egernia_35asc_4506_Cont40UCLN_DisGammaUCLN_For_SI.xml. The description below summarises the major points.

The most appropriate partitioning scheme, substitution matrices, and among-site rate variability model for the molecular loci was identified via PartitionFinder 2 (Lanfear et al., 2016), using BIC with all loci and codons treated as candidate partitions. Discrete morphological characters were analysed using the Mk-model with correction for non-sampling of constant

characters (Lewis, 2001; Alekseyenko et al., 2008), which has been well-tested (Wright and Hillis, 2014; O'Reilly et al., 2016). Polymorphic morphological data (e.g. 0&1) could be treated exactly as coded (e.g. 0 or 1 but *not* 2), rather than as total uncertainty (0 or 1 or 2): an improvement over earlier versions of BEAST. Continuous morphological characters were analysed using Brownian motion model bounded between 0 and 2, since all characters were rescaled to span these values. Bayes Factors were used to test the need to accommodate rate variability among discrete and continuous morphological characters (i.e. gamma parameter).

For dating, the root age was loosely constrained to lie between the most extreme values found across multiple recent studies (see Title and Rabosky, 2016). No other node age constraints were imposed; the retrieved dates are generated from the phenotypic and stratigraphic information contained in the fossil taxa (tips). The most appropriate available tree prior in BEAST (1) (birth-death serial sampling) was employed. The significance of rate variation across lineages (strict versus relaxed clocks), in each of the three character sets, was tested using Bayes Factors. Each Bayesian analysis was repeated four times to confirm stationarity, with the post-burnin samples of all four runs combined for statistical analyses and consensus trees.

The parsimony and Bayesian analyses above were also repeated for the morphological data alone, and for the molecular data alone, using the same models and settings (except those which were no longer relevant given the exclusion of either morphology or molecules).

3.6 Systematic palaeontology

Order SQUAMATA Oppel, 1811
Family SCINCIDAE Gray, 1825
Subfamily EGERNIINAE Welch, 1982
Genus *EGERNIA* Gray, 1838
EGERNIA GILLESPIEAE, sp. nov.
(Figure 3.1, Figure 3.3, and Figure 3.5)

Holotype—Left articulated mandible (nearly complete; Figure 3.1) QM F57957a. Other elements listed below can be confidently associated with this holotype: all material was found in a single block 94H from AL90 site and designated one specimen number as an associated skeleton of one individual. Associated cranial elements: Left premaxilla (57957b), left maxilla (57957c), frontal (57957d), left nasal (57957e), left quadrate (57957f), left (57957g) and right (57957h) pterygoid,

left and right squamosal (57957i & 57957j). Associated post-cranial elements described in the SI: left humerus (57957k) and left ulna (57957l).

Type Locality—Riversleigh World Heritage area, Queensland. System C, site AL90. Radiometric dating of flowstone has identified Allan's Ledge 1990 (AL90) as middle Miocene in age, 14.82 ± 0.29 MA (Woodhead et al., 2016). AL90 has been identified as a likely pitfall trap (Arena et al., 2014) with a number of other articulated and associated skeletons previously recovered i.e. *Nimbadon lavarackorum* from K. H. Black et al. (2012), a new Miocene bandicoot reported in Black et al. (2015), and the post-crania of *Ganguroo bilamena* of Kear et al. (2001). Palaeoecological analyses of the faunal remains from AL90 and surrounding sites of similar age (i.e. Ringtail and D4) suggest that the local environment was warm, wet, closed forest environment during this period (Travouillon et al., 2009).

Etymology—Named in honour of researcher Dr Anna Gillespie, who played a central role in the recovery and preparation of this specimen and countless other Riversleigh fossils.

3.7 Diagnosis

Egernia gillespieae is a skink with a single frontal, Meckelian groove overgrown by the dentary and a dorsoventrally tall splenial notch, a combination typical of an egerniine skink. Among egerniines it is most similar to other species currently assigned to the genus *Egernia* in possessing mediolaterally compressed tooth crowns each surmounted by a single apical crest, and weakly concave, to flattened, lingual surfaces (char. 55 in SI). It is distinguished from all other *Egernia* species in the degree of progression from moderate to very robust teeth in the posterior half of the jaw, the largest teeth having a distinctively enlarged and flattened crown morphology transected by a weak remnant of the apical crest. The posteromedial ramus of the coronoid extends further along the surangular and consists of a dorsal and lingual protruding ridge, connected by a broad sheet of bone not present in any other *Egernia*. The surangular fills less than half of the visible space between the anteromedial and posteromedial rami of the coronoid.

3.8 Description

The holotype is a near-complete left adult mandible QM F57957a in Figure 3.1, missing the retroarticular process and an anterior fragment of the symphysis. Varying stages of tooth replacement and posterior loss of the suture line between the articular and surangular indicates this is an adult mandible. The other cranial elements associated with the holotype include the complete frontal, left nasal and both squamosals, partial remains of both pterygoids, and a fragmented left

maxilla. A left humerus (QM F57957k) and ulna (QM F57957l) are described in the online Supplementary Information.

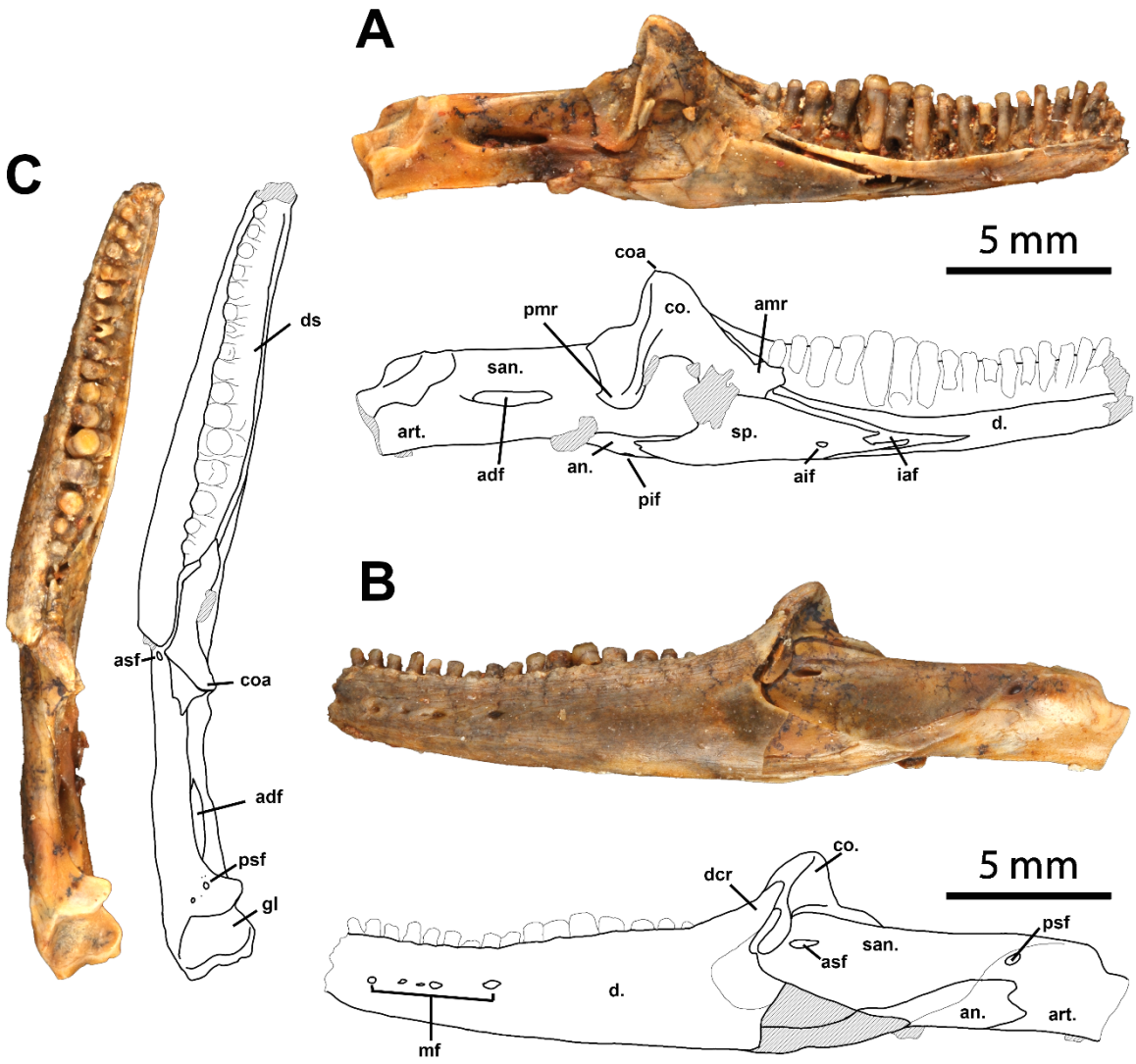

Figure 3.1: Clockwise from left; Occlusal, lingual and labial views of left mandible of QM F59757a, the holotype for *Egernia gillespieae* sp. nov. Abbreviations: adf, adductor fossa; aif, anterior intermandibularis foramen; amr, anterior medial ramus of the coronoid; an., angular; art., articular; asf, anterior surangular foramen; co., coronoid; coa, coronoid apex; d., dentary; dcr, dentary coronoid ramus; ds, dental sulcus; gl, glenoid; iaf, inferior alveolar foramen; mf, mental foramina; pif, posterior intermandibularis foramen; pmr, posterior mandibular ramus of coronoid; psf, posterior surangular foramina; san., surangular; sp., splenial.

3.8.20 Mandible

The mandible remains articulated, with only a slight displacement of the splenial. A small amount of bone is missing from the symphysis and posterior process of the dentary. The extent of the posterior process is still traceable due to the surface scarring across the surangular/articular. Length as preserved 23.62 mm. Estimated total length from the (inferred) anterior-most point of the symphysis to the (inferred) posterior of the articular is 26.5 mm. Length of the tooth row as

preserved is 10.61 mm with alveoli suggesting 19 dentary teeth. Dentary height (Character 2) is 2.80 mm. Maximum dentary width, measured in occlusal view at the midpoint of the dentary length is 2.16 mm. No symphysial ridge extends posterior to the articulation with the right dentary. The splenial notch extends 50% along the length of the tooth row. The notch is sharply v-shaped and preserves the location of the inferior alveolar foramen well, with the location of the splenial only slightly shifted ventrally. *Egernia gillespieae* preserves five visible mental foramina, although some are clogged with matrix.

3.8.20.1 Splenial

Preserved in its entirety, extends anteriorly approximately one-half the length of the dentary and posteriorly to in line with the coronoid apex. The anterior intermandibularis foramen (AIF) sits posterior but relatively in line with the inferior alveolar foramen, a common feature in *Egernia*. The splenial height is 74.2% the height of the total dentary.

3.8.20.2 Coronoid

Apex is broad and rounded in shape, with two large posterior crests and extensive overlap of the surangular. Two small posterior crests on the coronoid are present in half of the species examined in this study, with no clear phylogenetic pattern. However, *Egernia gillespieae* is unique in that the two crests extend far posteriorly along the surangular and are connected by a broad flange of bone. The medial exposure of the surangular only fills one-third of the space between the anteromedial and posteromedial rami of the coronoid; this too is unique - in all other sampled *Egernia* specimens, the surangular fills approximately two-thirds of that space.

3.8.20.3 Surangular and Articular

Completely fused in this specimen; no sutures are visible externally or in the Micro CT scan. The posterior *intermandibularis* foramen (*mylohyoideus*, see Schwenk, 2000) lies on the ventral surface of the mandible; this trait appears highly variable in *Egernia*, opening on the lingual surface in some species. The position slightly posterior to the coronoid apex is also very typical of the genus, only varying in *Egernia depressa* and *E. epsisolus* where it is directly below the apex. Although the retroarticular process is broken off, the general shape of the preserved articular cotyle (glenoid) is similar to extant *Egernia*.

3.8.20.4 Comparisons

The surangular and articular are proportionally deeper in lingual profile and wider in occlusal view when contrasted with extant *Egernia*, making the overall structure more robust in form. The dentary generally resembles extant *Egernia* but has a more robust general appearance (e.g. than extant *E. striolata*, see Figure 3.2), evident in the ratio of width and height to the length of

the bone. The presence of only five mental foramina is a relatively low number within *Egernia*, but shared with some species such as *E. depressa* and *E. saxatilis*. The splenial notch extends 50% along the length of the tooth row, uncommon within *Egernia* (*s.s*), present only in *E. hosmeri*, all others are closer to one third the length of the dentary. The splenial height of 74.2% is higher than in any other *Egernia* excluding *E. pilbarensis* (77.7%); the only other sampled species close to this value is *E. formosa* (71.4%). This dimension is directly proportional to overall jaw depth, quantifying some of the observed shape changes seen in Figure 3.2. Finally, the medial exposure of the surangular is less than in other sampled *Egernia.*

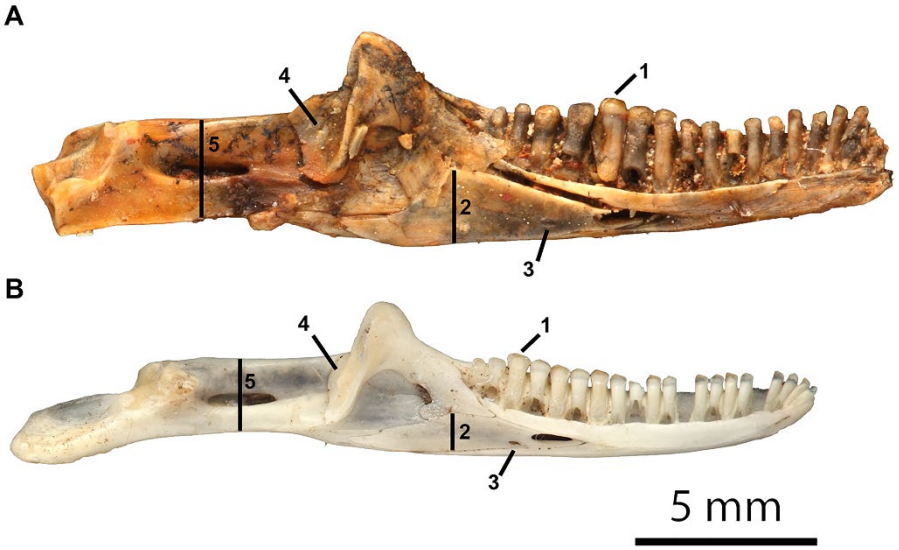

Figure 3.2: Comparative lingual views of A *Egernia gillespieae* sp. nov. and B *Egernia striolata* (SAMA R24877) highlighting differences. (1) The enlargement of the 5th tooth at the rear of the jaw of *E. gillespieae*, but the 3rd last tooth in *E. striolata*; (2) the depth of the splenial, much greater in *E. gillespieae* than *E. striolata*; (3) the positioning of the anterior intermandibularis foramen directly posterior to the inferior alveolar foramen in *E. gillespieae* but posteroventral to it in *E. striolata*; (4) the considerable posterior expansion of the posterior coronoid crests in *E. gillespieae* compared to their much lesser development in *E. striolata*; (5) the more robust surangular and articular depth in *E. gillespieae*.

3.8.21 Dentition

The dentary preserves 17 loci (alveoli) containing 16 teeth, with likely two more loci anterior to the break near the symphysis. The first preserved position is hereafter considered to be the 3rd tooth, and the last preserved position, the 19th tooth. Four stages of tooth replacement are visible, from an emerging tooth below the old 16th, the uncemented but fully erupted 15th tooth (Figure 3.3), the 13th tooth is firmly ankylosed to the dental sulcus with a visible resorption pit beneath it and the 10th and 12th teeth getting ready to be shed. Teeth increase in size towards the posterior section of the dentary, with the largest tooth, 2.3 mm in height and 0.75 mm in diameter, in the 15th position (Figure 3.4). The apices of the teeth do not form a straight horizontal line,

suggesting the occlusion with the maxillary teeth is not uniform and a complementary size disparity occurs on the upper tooth row.

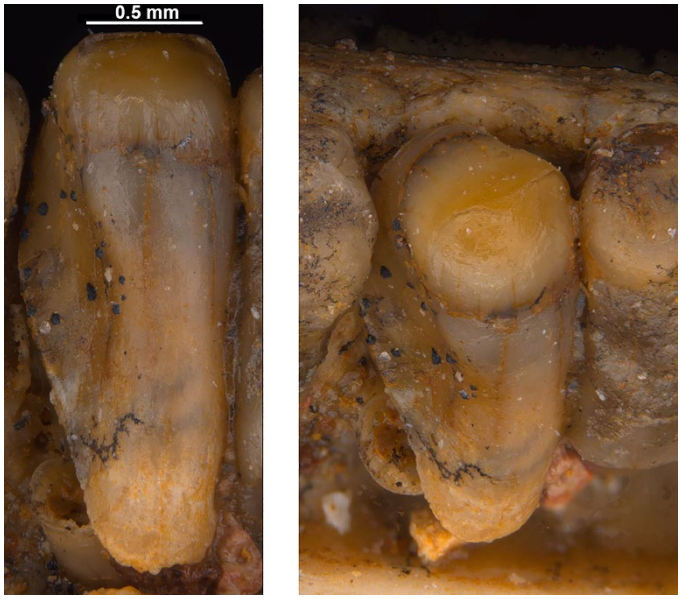

Figure 3.3: 15th dentary tooth of *Egernia gillespieae* sp. nov., the largest on the lower tooth row, under light microscopy. Left image shows expansion of the crown from the shaft and relative size. Right image taken from occlusal view highlights the weak apical crest traced across the near-rounded crown.

The anterior-most teeth in *Egernia gillespieae* are in poor condition, the first three missing entirely. Teeth are fairly evenly-spaced in the anterior of the dentary. Anterior tooth size remains fairly uniform until the 12th position, and all are taller in profile than the dentary wall, visible from the labial view. These teeth are narrow, pillar-like in shape with minimal crown diameter expansion from the shaft. The enamel covers the entire crown and extends approximately ¼ the vertical length of the tooth. Teeth 13 to 16 on the dentary row are tightly packed, the crowns almost touching as new teeth emerge. Wear is visible on the 16th tooth, generated by occlusion with the maxillary tooth row, opening lingually-oriented, long and shallow intercristatum across the top of the crown. Slightly smaller in diameter than the 15th tooth, this tooth also sits lower in profile on the tooth row, while still showing evidence of occlusion with the maxillary teeth.

The remarkably well preserved 15th tooth of *E. gillespieae* (Figure 3.3) exhibits a crown diameter that is 10-20% greater than that of the shaft, with minor mediolateral compression of the crown creating a slightly concave lingual face. This tooth is also unusual in being the largest, with four teeth behind it, rather than the typical two or three in other *Egernia*. The apical groove of the crown is weak in profile, with a residual crest compiled of the *crista mesialis* and *crista distalis* visible on the unworn tooth reaching across an otherwise rounded structure (Figure 3.4). The *culmines laterales* are prominent and frame the lingual face of the tooth crown. No striations are visible on any of the teeth.

Tooth crown shape varies across the species of *Egernia*, but all species have some mediolateral compression, and anteroposterior widening of the crown from the shaft. The number of dentary teeth vary ontogenetically (not uncommon, see Brown et al., 2015) and interspecifically. Three dentition profiles are observed in genus *Egernia*: simple bicuspid crowns with tall pillar-like shafts and higher tooth count (i.e. *Egernia formosa*); bicuspid crowns with slight lateral compression, enlarged teeth at the rear of the tooth row (i.e. *Egernia striolata*); and heavily modified herbivorous dentition as observed in *E. cunninghami* with singular cusped, triangular crowns and high tooth counts. *Egernia gillespieae* is a modified form of the *E. striolata* type dentition, some of the teeth anterior to the enlarged 15th tooth on QM F57957a are very similar in crown shape.

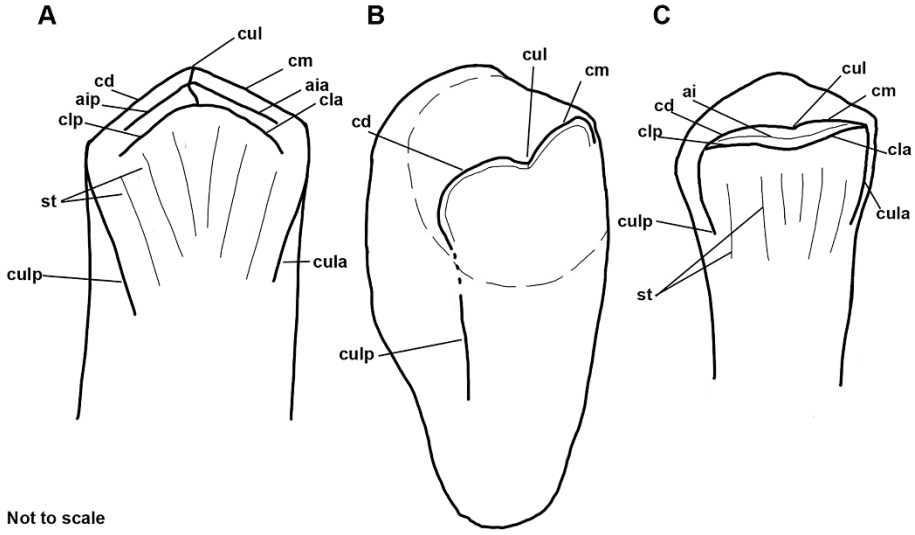

Figure 3.4: Tooth crown morphology of A a typical scincid (adapted from Kosma, 2003), B *Egernia gillespieae* sp. nov. and C a typical *Egernia* (modelled after *E. striolata*). Abbreviations: ai, antrum intercristatum; aia, antrum intercristatum (anterior portion); aip, antrum intercristatum (posterior portion); cd, crista distalis; cla, crista lingualis anterior; clp, crista lingualis posterior; cm, crista mesialis; cul, cuspis labialis; cula, culmen lateralis anterior; culp, culmen lateralis posterior; st, striae.

3.8.22 Skull

3.8.22.1 *Maxilla*

The single recovered left maxilla (QM F59757c; Figure 3.5) was exposed on the surface of the limestone block and therefore exhibits broken tooth crowns, missing teeth and is missing most of the facial process. The length of the maxilla as preserved is 12.27 mm and the tooth row 10.04 mm. The tooth row has 16 loci and 13 remaining tooth shafts. The three anterior teeth appear slightly narrower than the remaining tooth row, but due to poor preservation of the remaining teeth, size differences cannot be quantified. Remaining features consistent with *Egernia* are the v-shaped jugal articulation (the modal condition in *Tiliqua* is a jugal articulation that tapers to a single point), and a narrow tooth shaft relative to the crown.

3.8.22.2 Premaxilla

The left premaxilla (QM F59757b; Figure 3.5) has four tooth loci that retain three peg-like teeth. The nasal process reaches 3.51 mm in height and remains intact to the point of nasal suture. No ventral ethmoidal foramina are visible, and from anterior view, no notch is present in the ascending nasal process. The maxillary process extends 1.91 mm, suggesting an average length snout, relative to the maxilla length, for *Egernia*. Seven or eight total (left and right) premaxillary teeth are typical of *Egernia,* which (excepting *E. cunninghami*) all have four teeth on the left premaxilla.

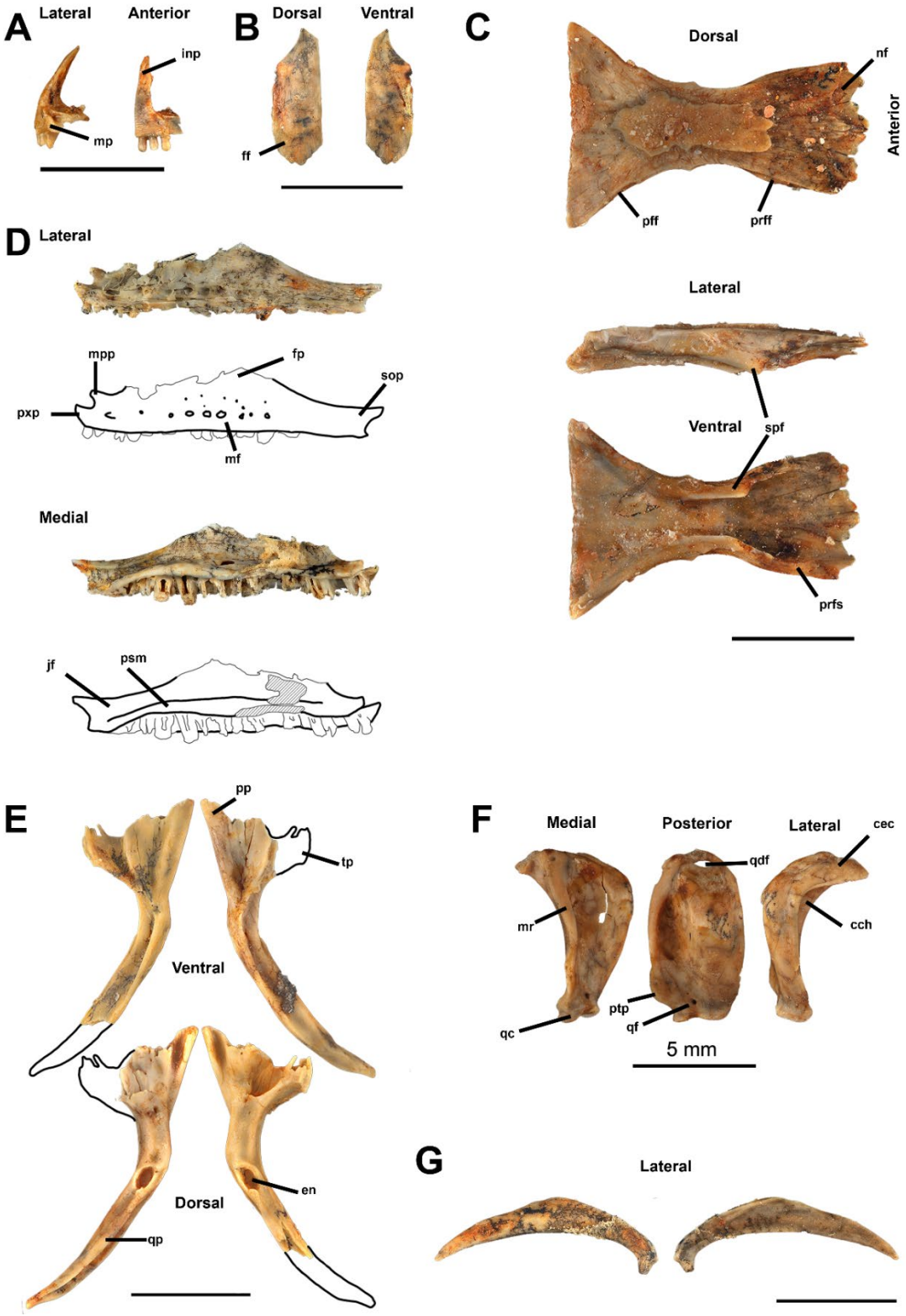

Figure 3.5: ***Egernia gillespieae*** **sp. nov., elements associated with holotype specimen and attributed to the same individual. A QM F59757b (premaxilla), B 59757e (left nasal), C 59757d (frontal), D 59757c (left maxilla), E left (59757g) and right (59757h) pterygoids, F left quadrate (59757f), and G left (59757i) and right (59757j) squamosals. Abbreviations: cch, tympanic conch; cec, cephalic condyle; en, epipterygoid notch; ff, frontal facet; fp, facial process; inp, internasal process; jf, jugal facet; mf, maxillary foramina; mp, maxillary process; mpp, medial premaxillary process; mr, medial ridge; nf, nasal facet; pff, postfrontal facet; pp, palatine process; prff, prefrontal facet; psm, palatine shelf of the maxilla; ptp, pterygoid process of the quadrate; pxp, premaxillary process; qc, quadrate condyle; qdf, quadrate dorsal foramen; qf, quadrate foramen; qp, quadrate process; sop, suborbital process of the maxilla; spf, suborbital process of the frontal; tp, ectopterygoid process.**

3.8.22.3 Nasal

The nasals are paired; the recovered left nasal (QM F59757e; Figure 3.5) is complete, 5.65 mm in length. The nasal is equal in width at the anterior and posterior ends, creating a flat, straight nasal roof bridging from the premaxilla to the anterior of the frontal. The posterior dorsal surface preserves a facet for the frontal suture.

3.8.22.4 Frontal

The frontal (QM F59757d; Figure 3.5) is a fused single bone, hourglass in shape, broader posteriorly at the frontoparietal suture. It has a relatively broad interorbital width of 2.98 mm, and is anteroposteriorly 10.84 mm long. Extent of the notch for the prefrontal indicates that the prefrontal would extend posteriorly beyond 50% of the length of the orbit. Although no parietal was recovered, the frontal does record a frontoparietal suture width of 8.04 mm.

3.8.22.5 Quadrate

Only the left quadrate (QM F59757f; Figure 3.5) was recovered from this individual. It remains entirely intact, with a small fracture running down the centre of the tympanic conch. The bone is posteriorly curved, with the tympanic conch open anteriorly, the mandibular-quadrate condyle is ventral and cephalic condyle on the dorsal surface. The quadrate is mediolaterally broad for the entire length of the bone, only narrowing at the two opposing condyles. Most of the curvature in the bone is constrained to the dorsal half when viewed laterally, the conch straightening ventrally along the medial ridge. The total quadrate height is 6.83 mm, the widest point of the conch is 3.89 mm and the mandibular-quadrate condyle is 2.31 mm across.

Shape of the tympanic conch is similar in all respects to that of other *Egernia*. Relative height compared to maxilla length is similar to other *Egernia* species. The conch is thin and lightly built, not as robust in appearance as in some species such as *E. cunninghami* or *E. formosa*.

3.8.22.6 Pterygoids

The pterygoids (left QM F59757g, and right 59757h; Figure 3.5) lack teeth. The shaft extending from the epipterygoid notch to the quadrate is not particularly robust, and is narrow and rod-shaped, not broad or strongly concaved along its length. The pterygoid is relatively long, roughly 116% of maxilla length. Extension of the pterygoid relates to a longer posterior skull region, lengthening the section beyond the maxilla beneath the braincase. Average pterygoid length in *Egernia* is 105% of the maxilla length. *Egernia gillespieae* is most similar to *E. kingii* (113.4%), *E. napoleonis* (114.5%) and *E. cunninghami* (119.3%), among species considered here.

3.8.22.7 Squamosal

The squamosals (QM F59757i and 59757j; Figure 3.5) are 9.28 mm long, and lightly curved, exhibiting the typical shape of all lygosomines. The anterior end is featureless and comes to a fine point, the posterior end that articulates with the supratemporal has a flattened surface but is not much larger in diameter from the rest of the bone. There is no expansion or flattening of the bone, as observed on the more robust egerniines, *Tiliqua* and *Cyclodomorphus*.

3.9 Variation in Cranial Osteology across the Egerniinae

Having recorded character states from exemplars of multiple species in each genus within the Egerniinae, new potential characters differentiating genera emerged that have then been examined further using multiple individuals for many species.

The splenial notch shape diagnostic character (char. 16) used by Hollenshead et al. (2011) held true with the v-shaped notch present in all *Egernia* (*s.l.*). Although *Bellatorias* was described as being unique in having a 'u-shaped' notch in Hollenshead's study, *Bellatorias frerei* (SAMA R 21133) has a 'v-shaped' notch. This character warrants further investigation as variability is present.

Pterygoid length proved to vary across the entire group with *Tiliqua* exhibiting a relatively shortened post-orbital region of the cranium in comparison to other genera, evident from the ratio of pterygoid length to maxilla length (char. 123). *Tiliqua* recording an average pterygoid:maxilla ratio of 91% in comparison to *Cyclodomorphus* with 103%, *Egernia* 105%, *Liopholis* 106%, *Bellatorias* 102% and *Lissolepis* with 106%. All *Tiliqua* with the exception of *T. rugosa* have a maxilla longer than their pterygoid (*T. rugosa* is 103% maxilla length).

Quadrate height compared to maxilla length (char. 108) varies between genera, with *Tiliqua* and *Cyclodomorphus* having a fairly short quadrate around 50% or less of the maxilla length, compared with all other genera which have 50% or more, usually closer to 60% and as high as 70% in *Liopholis striata* (as expected as *Liopholis* has a fairly short maxilla).

3.10 Phylogeny

The combined morphological and molecular parsimony analysis in TNT produced a single tree of 4325.124 steps (Figure 3.6; CI=0.45, RI=0.574), likely due to the remote possibility of there being more than one equally-parsimonious result from analyses involving continuous characters. As predicted based on previous (molecular) work, *Tribolonotus* is sister to all other Egerniinae, and *Corucia zebrata* is the sister to Australian forms. *Lissolepis* retains the basal position for the Australian clade, as found by Gardner et al. (2008). *Bellatorias* and *Liopholis* also form separate

basal clades, bootstrap figures >50% providing some justification for their taxonomic allocations to separate genera. *Egernia* (*sensu stricto*) groups with *Cyclodomorphus* and *Tiliqua.* However, *Egernia* is paraphyletic, with *Tiliqua* and *Cyclodomorphus* deeply nested inside, confidently separated from *Egernia* with a bootstrap value of 90. *Egernia gillespieae* is placed within the *Egernia* grade, near *Egernia napoleonis* and the *Tiliqua+Cyclodomorphus* clade. Though *Tiliqua* and *Cyclodomorphus* together form a clade, the two genera are not reciprocally monophyletic. The morphologically unexpected clade composed of the disparate *T. adelaidensis* and *T. rugosa* (found in previous molecular analyses: Gardner et al., 2008) is retrieved and is the sister to all other *Tiliqua* plus *Cyclodomorphus. "Tiliqua" pusilla* nests in *Cyclodomorphus,* sister to *C. branchialis*.

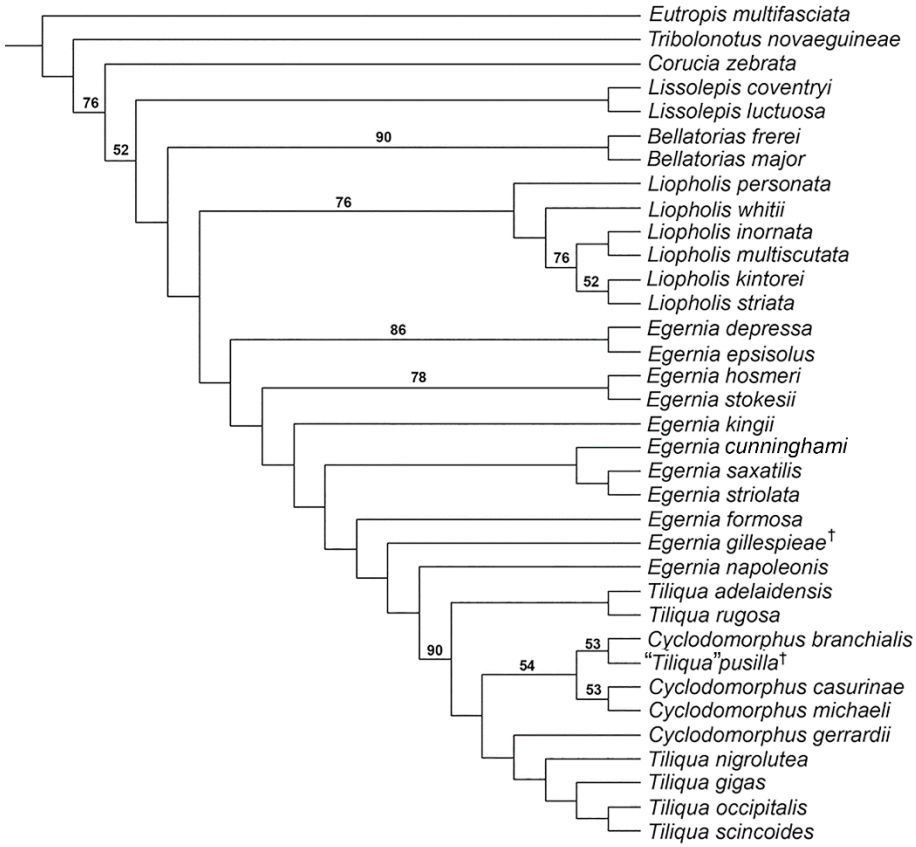

Figure 3.6: Phylogeny of the Egerniinae, based on parsimony analysis of combined continuous morphological, discrete morphological and DNA characters. Bootstrap values >50% indicated. Tree length of 4325.142 steps, CI=0.45, RI=0.574. Executable file and character optimizations are in the SI.

The Bayesian total evidence analysis gives results which are broadly similar to the combined parsimony tree, but with some notable differences (Figure 3.7). The same primary clades in egerniines are again retrieved: *Corucia* is sister to the Australian egerniines, and *Lissolepis* is basal to all other Australian egerniines, followed by *Liopholis* and *Bellatorias. Egernia* (*sensu stricto*) again groups with *Tiliqua* and *Cyclodomorphus*, and the latter two genera again form a clade. However, *Egernia* is now a clade (supported by a posterior probability of 0.83) rather than a grade. *Egernia gillespieae* again nests within *Egernia.* "*Tiliqua" pusilla* again groups with the

Tiliqua-Cyclodomorphus group, but is basal to all living species (rather than nested within *Cyclodomorphus*). Divergence times are in the middle of the range of previous estimates based on other studies, with that of the Australian egerniines being 34.61 Ma, and the *Tiliqua-Cyclodomorphus* group, 25.43 Ma.

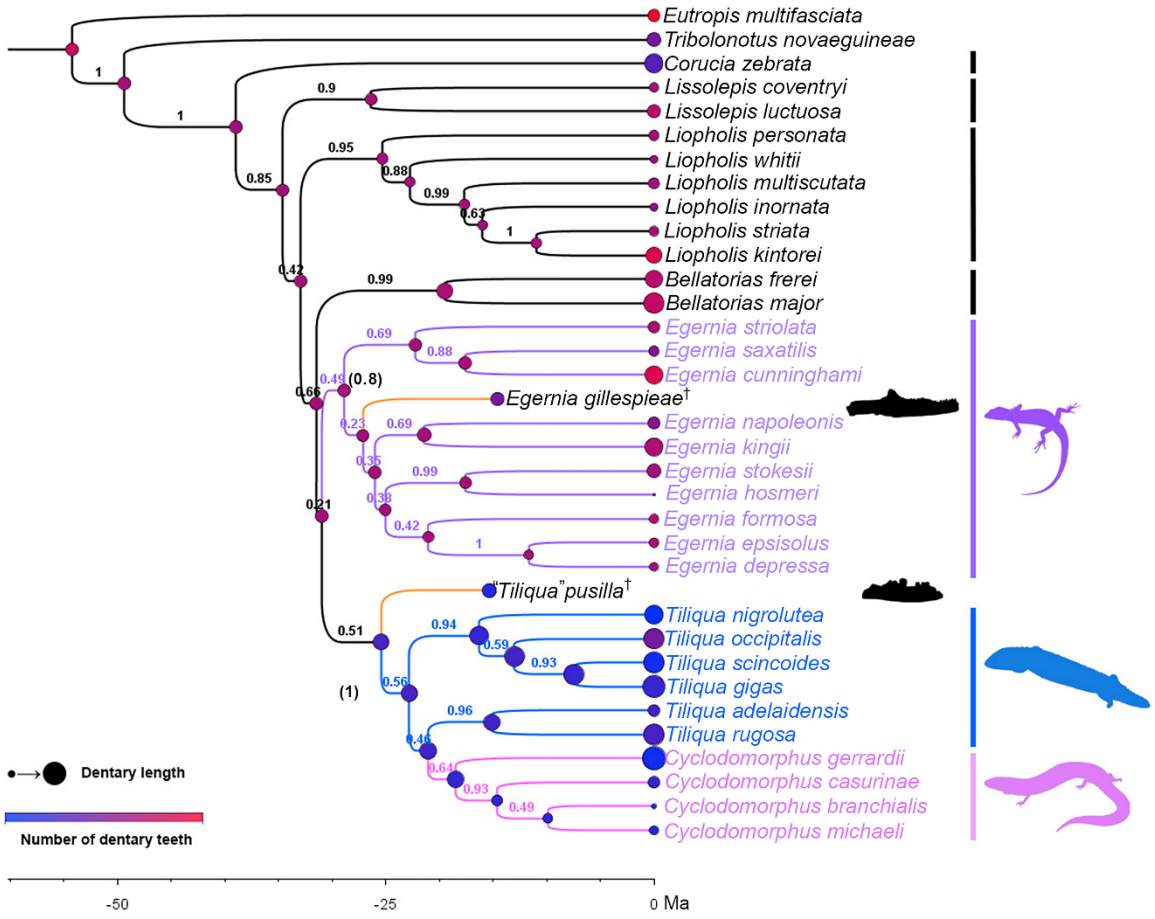

Figure 3.7: Phylogeny of the Egerniinae, based on a tip-dated Bayesian analysis of combined continuous morphological, discrete morphological and DNA characters. Maximum clade consensus tree from BEAST analysis, numbers refer to posterior probabilities of clades. Numbers in brackets referrer to the posterior probability scores recovered in the analysis (Fig. S4 in SI file 'Alternate Topologies) excluding the two fossil species, which lower resolution in parts of the tree due to their lack of DNA data and resultant 'wildcard' nature. Dentary length (an index of overall size) indicated by the size of the node circle, and the number of dentary teeth are indicated by colour of that circle. The three key crown clades, *Egernia*, *Tiliqua* and *Cyclodomorphus* are colour coded, as are the two fossils. Photo sources are listed in the SI.

Trees resulting from the morphological data alone produced highly implausible topologies, both in parsimony and Bayesian analyses (Figs. S1 and S2 in online SI file 'Alternate Topologies'). For instance, in the MP morphology tree, the Solomon Islands *Corucia* and the New Guinea *Tribolonotus* were nested in Australian egerniines as sister to *Tiliqua*+*Cyclodomorphus*, a biogeographically discordant arrangement which contradicts all DNA studies to date (Gardner et al., 2008; Tonini et al., 2016). The Bayesian morphology tree manages to retrieve the accepted position of *Tribolonotus* outside Egerniinae, but *Corucia* still nests within the Australian forms. Attempting to interpret the position of fossils in trees where many extant taxa are clearly misplaced is unlikely

to be worthwhile: for this reason, we do not discuss these trees in detail but present them in SI for completeness. Nevertheless, the morphological data alone did consistently retrieve some widely-accepted clades (e.g. *Tiliqua* + *Cyclodomorphus*, *E. depressa*+*epsisolus*, *Liopholis* [MP], Lissolepis [Bayesian]), suggesting the data did have some phylogenetic signal.

The Bayesian topology from molecular data alone produced the same topology (for extant taxa) to the respective combined data trees (Figs. S3 and S4 in online SI file 'Alternate Topologies'), with higher prior probability scores for most clades, likely due to the exclusion of fossil 'wildcards' lacking DNA. The *Tiliqua*+*Cyclodomorphus* clade was retrieved with a score of 1, and the *Egernia* clade with 0.98.

Our analyses do not conclusively resolve the monophyly or paraphyly of *Egernia,* so we continue to provisionally use the name without quotes; this was the approach also used in Gardner et al. (2008) who had similarly equivocal results. Using quotes ("*Egernia*") potentially gives the unintended message that there is strong evidence the genus is invalid, but given that likelihood/Bayesian methods are generally preferred for DNA data (which dominates the current dataset), the results could be seen as more favourable towards *Egernia* monophyly.

3.11 Discussion

3.11.20 Affinities and Biology of Fossil Taxa

Both fossils are robustly retrieved within the Australian crown Egerniinae, thus providing direct evidence for the antiquity of this clade. *Egernia gillespieae* groups near other species of *Egernia* in both analyses: it was placed in a grade with other *Egernia* in the parsimony tree, and in a clade with other *Egernia* in the Bayesian analysis. In part this is because *Egernia* species lack some of the specialised morphology that defines the *Tiliqua* lineage, with the result that *E. gillespieae* has more symplesiomorphies of *Egernia,* than *Tiliqua*. The fossil shares the following similarities with *Egernia* (*s.s*) which optimise on the Bayesian phylogeny as synapomorphies: a rounded coronoid apex (char. 36; synapomorphy of all *Egernia* species excluding *stokesii* and *depressa*); and the posterior *intermandibularis* foramen is located slightly posterior to the coronoid apex as in all *Egernia* (*sensu lato*) and not in *Tiliqua* or *Cyclodomorphus* (char. 30); the frontal of *E. gillespieae* has a longer anteroposterior dimension (char. 70) than any *Tiliqua* but similar to the proportions seen in *Egernia*; a premaxillary process length (char. 63) closer to the average value for *Egernia* (16.91% maxilla length) than *Tiliqua* (15.3% maxilla length); and close to the longest total pterygoid length (char, 123) at 116.7% maxilla length (second only to *E. cunninghami* at 119.2%). Although we have no parietal for this species, it appears as though the skull shape is generally longer in profile than *Tiliqua*, similar in shape to some *Egernia* such as *E. saxatilis*.

Egernia gillespieae presents an expanded tooth crown shape that is derived compared to the typical *Egernia* mediolaterally compressed shape, but has not fully expressed the rounded or conical crown of *Tiliqua* or *Cyclodomorphus*. The detail preserved in the well-preserved 15th tooth (Figure 3.3) shows a single crest along what would otherwise have been an apical groove in modern *Egernia*. The tooth still has a concave lingual face, as in *Egernia*, but the loss of the paired labial and lingual cusps demonstrates what a possible intermediate form from *Egernia* to *Tiliqua* dentition would have looked like. This intermediate stage suggests a shift towards a crushing dentition, also highlighted in the increased dentary width and rounder symphysis shape. The overall increase in density and robust form of the mandible of this species suggests a stronger more rigid structure for a durophagous diet. A heavy, robust jaw with less mobility in favour of increased strength by means of bony overlap is typical of durophagous species of *Tiliqua* and *Cyclodomorphus* (see Kosma, 2003) but also of primarily herbivorous species such as *Corucia zebrata* or *Egernia cunninghami*.

"*Tiliqua" pusilla* has affinities with the *Tiliqua+Cyclodomorphus* clade. It is nested within this clade in the parsimony analysis, and is sister to this clade in the Bayesian analysis. "*Tiliqua" pusilla* presents a combination of durophagous and robustness characters shared with both *Tiliqua* and *Cyclodomorphus* such as a decreased number of teeth (chars. 50 and 79), enlarged symphysis (chars. 5 and 6), and increased tooth crown widths >50% of the 'typical' tooth (char. 54). However, with fewer characters available for analysis, its exact position within the *Tiliqua+Cyclodomorphus* clade is less well established than that of *E. gillespieae*. Our use of "*Tiliqua*" in quotes is to reflect the uncertainty of its phylogenetic position - though there are broader questions relating to the potential non-monophyly of both *Tiliqua* and *Cyclodomorphus*. Shea and Hutchinson (1992) placed *pusilla* within *Tiliqua* based on two synapomorphies; the posterior extension of the symphysial crest almost 1/3 the length of the dentary, and the angulate nature of the coronoid margin of the dorsal medial lamina. The tooth crown shape exhibited by *T. pusilla* is like no other species from the *Tiliqua+Cyclodomorphus* clade. A distinct notch is present on the crown of *T. pusilla*, which is not present on any other species. The rounded crowns are much narrower and taller than those of *Cyclodomorphus gerrardii*, lack the striate, turban-shaped crown morphology of *T. scincoides* and *T. gigas*, and are not conical in shape as those of many *Cyclodomorphus* and *Tiliqua*.

The two species of fossil egerniine skinks have affinities to different modern genera and occur roughly contemporaneously and at the same location in northern Queensland, with fragments of other egerniines (Hutchinson, 1992). This demonstrates that the major lineages of this clade had diversified by the mid-Miocene, and that the group had a longer prior history in Australia. In the tip-dated Bayesian analyses, the position of *Egernia gillespieae* within the *Egernia* (retrieved as a clade), along with the position of "*Tiliqua*" *pusilla* with the *Tiliqua-Cyclodomorphus* clade, pushes

the divergence of *Egernia* and the *Tiliqua-Cyclodomorphus* clade beyond 30 Ma, and with the crown ages of *Egernia* and the *Tiliqua-Cyclodomorphus* clade each exceeding 25Ma (Figure 3.7).

3.11.21 Phylogeny, Biogeography and Evolution of the Egerniinae

Although the combined-data parsimony and Bayesian trees differ in some respects, they exhibit important similarities which contribute to a slightly more resolved phylogeny of the living Egerniinae. Gardner et al. (2008)'s MP analysis presented a polytomy between *Liopholis, Bellatorias, Egernia,* and a *Tiliqua-Cyclodomorphus* clade. Low posterior probability scores in their Bayesian analysis also resulted in no clear branching order for *Lissolepis*, *Liopholis* or *Bellatorias*. The new analyses here - which include morphological and additional molecular data - identify *Lissolepis* as the most basal Australian clade, and support a relationship between *Egernia* and the *Tiliqua-Cyclodomorphus* clade: *Egernia* is either the sister-group (Bayesian) or paraphyletic stem group (Parsimony) to *Tiliqua-Cyclodomorphus*. The new Bayesian phylogeny also provides divergence date estimates, allowing a more precise chronology of the evolutionary history and biogeography of this group. Our discussion below therefore focuses on the dated Bayesian tree, though differences in the MP tree are discussed.

The position of *Tribolonotus* and *Corucia zebrata* of New Guinea as successively closer relatives of the Australian egerniines in both analyses suggests northern origins, but not necessarily origins on Sunda. The Bayesian analysis suggests that the mainland Australian radiation within the Egerniinae began around ~35 Ma, during the late Eocene/early Oligocene, more than ten million years earlier than previously predicted by Hagen et al. (2012). As egerniines are completely confined to the Sahul side of Wallace's line, the earlier splits of *Tribolonotus* and *Corucia* between 40 and 50 Ma provide the latest dates that the ancestral form that gave rise to egerniines could have crossed the deep water barrier between Sunda and Sahul. The branch length representing the molecular divergence of the Australian egerniines from *Corucia*, *Tribolonotus* and *Eutropis* is relatively short compared to the molecular gap between egerniines and the other two Australian skink clades, the Eugongylinae and the Sphenomorphinae (Reeder, 2003). It is possible, given modern clade distributions, that the initial divergences within the Egerniinae occurred south of Wallace's Line, but north of Australia (see Oliver et al., 2018) with the ancestor of the Australian radiation subsequently making the crossing further south to mainland Australia. These dates suggest that the Egerniinae may have been one of the earliest of the several clades of squamates that crossed from Asia to Australia as it drifted northward during the Cenozoic (Oliver and Hugall, 2017).

Lissolepis is the earliest-branching Australian subclade of the Egerniinae; the two extant species, *Lissolepis luctuosa* and *L. coventryi* diverged at approximately 26 MA, indicating that the

two represent long-disjunct sisters, potentially surviving in (respectively) southwest and southeast refugia (both are confined to swampy habitats). The early branching point for *Lissolepis* is associated with retaining a generalized scincid body shape, and the typical scincid insectivorous dentition (Kosma, 2003), the teeth having slender, bicuspid crowns and tooth counts that are rather high compared to most *Egernia* group taxa.

With strong support scores concurring with both our parsimony result, and that of Gardner et al. (2008), the species previously designated *Liopholis* form a well-supported clade. These species all share narrow, pillar like teeth with the typical bicuspid crowns (char. 55), and the position of the splenial extends less than 50% along the length of the dentary (char. 21), this combination of features are not present in either *Lissolepis* (more basal) or *Bellatorias*. The mid-Miocene age of the node containing the modern arid-adapted *Liopholis* species (*L. inornata, L. striata* and *L. kintorei*) appears to pre-date Australia's late Miocene aridification. *Liopholis multiscutata*'s intermediate position, and its modern dry-coastal-environment adaptations, may support a single-origin colonisation of the arid interior by an ancestor similar to this species (Chapple and Keogh, 2004).

Although forming their own clade in both the MP and Bayesian trees, the validity of *Bellatorias* (*B. major* and *B. frerei*) from *Liopholis* and *Egernia* could be better tested with the inclusion of *Bellatorias obiri*. The character based on the shape of the splenial notch, previously identified by Hollenshead et al. (2011), remained a synapomorphy for *Bellatorias major*, but the notch of *B. frerei* appeared v-shaped, typical of *Egernia* and *Lissolepis*. Only one synapomorphy for this clade could be traced, the retroarticular process of the mandible of *Bellatorias* is mildly inflected dorsally (<30°), contrary to both *Liopholis* and *Egernia* which are either horizontal or ventrally angled (char. 47). The divergence date calculated for this clade is 31.49 MA from *Liopholis* and *Egernia*. When more nuclear DNA sequences are available, adding both the Australian *B. obiri* and a sample of the New Guinean population to the phylogeny may help assess the morphological distinctiveness of *Bellatorias* from *Liopholis* and *Egernia*.

The large clade consisting of *Egernia*+*Tiliqua*+*Cyclodomorphus* contains numerous derived morphologies, diets and behaviours. The fossil calibrations establish that this group diverged over 30 MA. This is particularly significant as it also highlights the antiquity of the splits between the three genera, and suggests that more fossil bluetongue material could be present in other Miocene sites, helping better elucidate the palaeobiogeography of the group. In future, adding already-known but poorly studied fossil material that can be assigned to either *Tiliqua* or *Cyclodomorphus* (i.e.

Pliocene *T. wilkinsonorum* and cf. *Cyclodomorphus* of Hutchinson and Mackness, 2002) might further refine and constrain the timing of the divergence of the species currently assigned to these two genera.

The species of *Tiliqua* and *Cyclodomorphus* were grouped as a monophyletic assemblage distinct from those assigned to *Egernia* in both the MP and Bayesian analyses. Both discrete and continuous morphological characters, i.e. maxilla suborbital ramus extension (char. 87), the ramus extending to the posterior quarter of the orbit in *Tiliqua+Cyclodomorphus,* and the low number of dentary teeth (char. 50, Figure 3.7) supported this division. Within *Egernia,* there are several strikingly disparate body plans, from smooth-scaled arboreal skinks to stub-tailed, spiny-scaled saxicolous species. One of the primary aims of this investigation was to further explore the monophyly of *Egernia*, something that was left uncertain by Gardner et al. (2008). The Bayesian analysis did result in the retrieval of a monophyletic *Egernia* as sister to the *Tiliqua+Cyclodomorphus* clade, however *Egernia* is only weakly supported (pp=0.49). This appears be artificially lowered due to the two fossil taxa acting as 'wildcards'; when they were excluded (Fig. S4 in online SI file 'Alternate Topologies'), the support increased to 0.8 (*Egernia*). Thus, the combined morphological and molecular data seem to favour a monophyletic *Egernia.*

Characters uniting the members of *Egernia* (i.e. consistent when traced in Mesquite across the Bayesian tree) include most notably those relating to dentition. Although some variation occurs across diets, all *Egernia* share the laterally-compressed tooth crowns, a dentary tooth count of 19-23, and minimal heterodonty (tooth crown ≤25% larger than the 'typical' tooth). Characters which conversely support the paraphyly of *Egernia* divisions in the MP phylogeny include: the degree of vomer fusion (Char. 112), which is complete in *Tiliqua* and *Cyclodomorphus*, *Egernia napoleonis*, *E. epsisolus* and *E. pilbarensis*, but only partial in the rest of *Egernia;* and the presence of a prefrontal projection (Char. 90) in the *Tiliqua+Cyclodomorphus* clade and *E. formosa*.

The lack of reciprocal monophyly between *Tiliqua* and *Cyclodomorphus* was one of the findings of the study of Gardner et al. (2008). This had not been expected, given the numerous morphological characters that differentiate the two clades (Shea, 1990). We added additional species, molecular sequences and morphological data, but still found that reciprocal monophyly was not well-supported. *Tiliqua scincoides*, *T. gigas, T. occipitalis* and *T. nigrolutea* form a close-knit clade in both analyses, while *T. adelaidensis* and *T. rugosa* which show striking morphological disparity but are strongly united by both the Bayesian and MP analyses, are sister to all other *Tiliqua* and *Cyclodomorphus* (parsimony) or on the *Cyclodomorphus* branch (Bayesian). This same topology was recovered in the analyses of the molecular data alone (online SI file 'Alternate

Topologies' Fig. S3), and previous molecular analyses (Gardner et al., 2008). *Cyclodomorphus gerrardii* is only weakly retained with other *Cyclodomorphus* in the Bayesian analysis, the parsimony result pushing it into a position as sister to *Tiliqua*. Historically members of these two genera have been combined or separated several times (Mitchell, 1950; Cogger et al., 1983; Shea, 1990), or certain species have been placed in monotypic genera (e.g. *Hemisphaeriodon gerrardii, Trachydosaurus rugosus*). Further work with genomic DNA studies on all living species of Australian egerniines is nearly complete (S. Donnellan, pers. comm.) and this may provide the large-scale data needed to clarify the historical branching pattern within this significant lizard group. The results of a robust genomic investigation of this clade may require revisiting the generic taxonomy of *Tiliqua* and *Cyclodomorphus*.

The least morphologically consistent pairing of species within this tree is that of *Tiliqua adelaidensis* (the pygmy bluetongue) and *Tiliqua rugosa* (the shingleback skink) (Gardner et al., 2008). Their external characteristics are highly discordant: a small (20g), smooth scaled, hole-dweller, in comparison with the very large (up to 1kg), heavily armoured, surface dweller. Nevertheless, some morphological support for this odd pairing exists, including a much shorter retroarticular processes (proportionally to dentary length, char. 49), and the count of 16 dentary teeth. Both species have more in common with *Tiliqua* than *Cyclodomorphus*: they have a dentitional pattern of a greater number of mildly enlarged teeth, rather than a single massive tooth, and the presence of the elongated symphysial ridge. However, their position closer to *Cyclodomorphus* rather than *Tiliqua* has some support in the patterns of mental foramina size along the dentary (char. 14).

The results of this investigation highlight the utility of integrating morphology, fossils and molecular data for taxonomic analyses. When analysed separately, the morphology gives a highly implausible topology, while the DNA gives a phylogeny which cannot explicitly accommodate fossil taxa. A tip-dated total evidence assessment inclusive of multiple fossils as well as morphology and DNA has produced a more detailed and dated phylogeny, providing a robust framework for inferring the group's biogeography and diversification. The AL90 specimen of *Egernia gillespieae* is the best preserved and most complete pre-Pleistocene lizard fossil in Australia and demonstrates the potential of sites such as Riversleigh to shed light on the origins of the continent's most diverse group of land vertebrates.

3.12 Acknowledgements

Support for The Riversleigh Fossil Project comes from the Australian Research Council (LE0989067, DP0985214, DP0664621, LP0989969, LP100200486, DP1094569, DP130100197,

DE130100467, DP170101420), Xstrata Community Partnership Program North Queensland, Outback at Isa, Mount Isa City Council, Queensland Museum, University of New South Wales, Environment Australia, Queensland Parks and Wildlife Service, the CREATE fund at UNSW, and the Waanyi people of north-western Queensland. The authors would like to acknowledge the numerous field teams that have collected fossils from Riversleigh World Heritage area over the last 40 years; P. Stokes for photographing the *Egernia gillespieae* specimens and comparative material; Adelaide Microscopy for access to their Skyscan-1076 for Micro-CT; I. Douvartzidis for assisting with the Micro-CT scanning; M. Gardner for discussions on *Egernia* diversity; Australian Biological Resources Study - National Taxonomy Research Grant Program for a Student Travel Grant to KMT, and the Society of Vertebrate Palaeontology for the Jackson School of Geosciences Travel Award to KMT, to present this research at the 77th Annual Meeting of Society of Vertebrate Palaeontology in Calgary. Thanks also to the Willi Hennig Society for making TNT freely available, and Andrej Čerňanský, an anonymous reviewer, and the editor Juliana Sterli for their comments and suggestions which improved this manuscript. KMT is supported by an Australian Government Research Training Program Scholarship.

3.13 References

Alekseyenko, A. V., C. J. Lee, and M. A. Suchard. 2008. Wagner and Dollo: a stochastic duet by composing two parsimonious solos. Systematic biology 57:772–784.

Arena, D. A., K. H. Black, M. Archer, S. J. Hand, H. Godthelp, and P. Creaser. 2014. Reconstructing a Miocene pitfall trap: Recognition and interpretation of fossiliferous Cenozoic palaeokarst. Sedimentary Geology 304:28–43.

Bell, C. J., and J. I. Mead. 2014. Not enough skeletons in the closet: Collections-based anatomical research in an age of conservation conscience. The Anatomical Record 297:344–348.

Black, K. H., A. B. Camens, M. Archer, and S. J. Hand. 2012. Herds overhead: *Nimbadon lavarackorum* (Diprotodontidae) heavyweight marsupial herbivores in the Miocene rainforests of Australia. PLoS ONE 7:e48213.

Black, K. H., K. J. Travouillon, T. J. Myers, M. Archer, S. J. Hand, and L. A. B. Wilson. 2015. Functional and geometric morphometric analysis of a middle Miocene bandicoot (Marsupialia, Peramelemorphia) skeleton from the Riversleigh World Heritage Area, Australia. Journal of Vertebrate Paleontology Program and Abstracts, 2015:91.

Brown, C. M., C. S. van Buren, D. W. Larson, K. S. Brink, N. E. Campione, M. J. Vavrek, and D. C. Evans. 2015. Tooth counts through growth in diapsid reptiles: implications for interpreting individual and size-related variation in the fossil record. Journal of Anatomy 226:322–333.

Bull, C. M. 2000. Monogamy in lizards. Behavioural Processes 51:7–20.

Chapple, D. G. 2003. Ecology, life-history, and behavior in the Australian scincid genus *Egernia*, with comments on the evolution of complex sociality in lizards. Herpetological Monographs 17:145–180.

Chapple, D. G., and J. S. Keogh. 2004. Parallel adaptive radiations in arid and temperate Australia: molecular phylogeography and systematics of the *Egernia whitii* (Lacertilia: Scincidae) species group. Biological Journal of the Linnean Society 83:157–173.

Cogger, H., E. Cameron, and H. Cogger. 1983. Zoological catalogue of Australia. Vol. 1. Amphibia and Reptilia. Bureau of Flora and Fauna: Canberra:313.

Cogger, H. G. 2018. Reptiles & Amphibians of Australia. Updated 7th Edition. CSIRO Publishing, Clayton South, Victoria, Australia.

Diogo, R., and V. Abdala. 2010. The head muscles of Dipnoans - a review on the homologies and evolution of these muscles within vertebrates; pp. 169–218 in J. M. Jorgensen and J. Joss (eds.), Biology of Lungfishes. Science Publishers and Taylor and Francis, Oxford, UK.

Drummond, A. J., and M. Suchard. 2010. Bayesian random local clocks, or one rate to rule them all. BMC Biology 8:114.

Drummond, A. J., M. A. Suchard, D. Xie, and A. Rambaut. 2012. Bayesian phylogenetics with BEAUti and the BEAST 1.7. Molecular biology and evolution 29:1969–1973.

Estes, R., and E. E. Williams. 1984. Ontogenetic variation in the molariform teeth of lizards. Journal of Vertebrate Paleontology 4:96–107.

Evans, S. E. 2008. The skull of lizards and Tuatara; pp. 1–343 in C. Gans, A. S. Gaunt, and K. Adler (eds.), Biology of the Reptilia 20, Morphology H The skull of Lepidosauria. Society for the Study of Amphibians and Reptiles, Ithaca, NY.

Fitzinger, L. 1843. Systema reptilium. Fasciculus primus, Amblyglossae. Braumüller et Seidel, Vienna, Austria.

Fordham, D. A., M. J. Watts, S. Delean, B. W. Brook, L. M. B. Heard, and C. M. Bull. 2012. Managed relocation as an adaptation strategy for mitigating climate change threats to the persistence of an endangered lizard. Global Change Biology 18:2743–2755.

Gardner, M. G., C. M. Bull, and S. J. B. Cooper. 2002. High levels of genetic monogamy in the group-living Australian lizard Egernia stokesii. Molecular Ecology 11:1787–1794.

Gardner, M. G., A. F. Hugall, S. C. Donnellan, M. N. Hutchinson, and R. Foster. 2008. Molecular systematics of social skinks: phylogeny and taxonomy of the *Egernia* group (Reptilia: Scincidae). Zoological Journal of the Linnean Society 154:781–794.

Gauthier, J. A., M. Kearney, J. A. Maisano, O. Rieppel, and A. D. B. Behlke. 2012. Assembling the Squamate Tree of Life: Perspectives from the Phenotype and the Fossil Record. Bulletin of the Peabody Museum of Natural History 53:3–308.

Gavryushkina, A., T. A. Heath, D. T. Ksepka, T. Stadler, D. Welch, and A. J. Drummond. 2017. Bayesian total-evidence dating reveals the recent crown radiation of penguins. Systematic biology 66:57–73.

Goloboff, P. A., J. Farris, and K. Nixon. 2008. TNT, a free program for phylogenetic analysis. Cladistics 24:774–786.

Gray, J. E. 1825. A synopsis of the genera of reptiles and Amphibia, with a description of some new species. Annals of Philosophy 10:193–217.

Gray, J. E. 1838. Catalogue of the slender-tongued saurians, with descriptions of many new genera and species (continued). Annals and Magazine of Natural History 2:287–293.

Greer, A. E. 1979. A phylogenetic subdivision of Australian skinks. Records of the Australian Museum 32:339–371.

Greer, A. E. 1989. The biology and evolution of Australian lizards. Surrey Beatty & Sons, Chipping Norton, NSW, 264 pp.

Hagen, I. J., S. C. Donnellan, and C. M. Bull. 2012. Phylogeography of the prehensile-tailed skink *Corucia zebrata* on the Solomon Archipelago. Ecology and evolution 2:1220–1234.

Hedges, S. B. 2014. The high-level classification of skinks (Reptilia, Squamata, Scincomorpha). Zootaxa 3765:317–338.

Hollenshead, M. G., J. I. Mead, and S. L. Swift. 2011. Late Pleistocene *Egernia* group skinks (Squamata: Scincidae) from Devils Lair, Western Australia. Alcheringa: An Australasian Journal of Palaeontology 35:31–51.

Honda, M., H. Ota, M. Kobayashi, and T. Hikida. 1999. Phylogenetic relationships of Australian skinks of the *Mabuya* group (Reptilia: Scincidae) inferred from mitochondrial DNA sequences. Genes and Genetics Systems 74:135–139.

Honda, M., H. Ota, M. Kobayashi, J. Nabhitabhata, H.-S. Yong, and T. Hikida. 2000. Phylogenetic relationships, character evolution, and biogeography of the subfamily Lygosominae (Reptilia: Scincidae) inferred from mitochondrial DNA sequences. Molecular Phylogenetics and Evolution 15:452–461.

Hutchinson, M. N. 1992. Origins of the Australian scincid lizards: a preliminary report on the skinks of Riversleigh. The Beagle, Records of the Northern Territory Museum of Arts and Sciences 9:61–70.

Hutchinson, M. N., and B. S. Mackness. 2002. Fossil lizards from the Pliocene Chinchilla Local Fauna, Queensland. Records of the South Australian Museum 35:169–184.

Kear, B. P., M. Archer, and T. F. Flannery. 2001. Postcranial morphology of *Ganguroo bilamena* Cooke,1997 (Marsupialia: Macropodidae) from the Middle Miocene of Riversleigh, northwestern Queensland. Memoirs of the Association of Australasian Palaeontologists 25:123–138.

Kosma, R. 2003. The dentitions of recent and fossil scincomorphan lizards (Lacertilia, Squamata) - Systematics, Functional Morphology, Palecology. Department of Geosciences and Geography, University Hannover, Hanover, Germany, 231 pp.

Lambert, S. M., T. W. Reeder, and J. J. Wiens. 2015. When do species-tree and concatenated estimates disagree? An empirical analysis with higher-level scincid lizard phylogeny. Molecular Phylogenetics and Evolution 82:146–155.

Lanfear, R., P. B. Frandsen, A. M. Wright, T. Senfeld, and B. Calcott. 2016. PartitionFinder 2: new methods for selecting partitioned models of evolution for molecular and morphological phylogenetic analyses. Molecular biology and evolution 34:772–773.

Lee, M. S. Y., and A. Palci. 2015. Morphological phylogenetics in the genomic age. Current Biology 25:R922–R929.
Lewis, P. O. 2001. A likelihood approach to estimating phylogeny from discrete morphological character data. Systematic biology 50:913–925.
Maddison, W., and D. Maddison. 2017. Mesquite: a modular system for evolutionary analysis. Version 3.2.
Mitchell, F. J. 1950. The scincid genera *Egernia* and *Tiliqua* (Lacertilia). Records of the South Australian Museum 9:275–308.
O'Reilly, J. E., M. N. Puttick, L. Parry, A. R. Tanner, J. E. Tarver, J. Fleming, D. Pisani, and P. C. Donoghue. 2016. Bayesian methods outperform parsimony but at the expense of precision in the estimation of phylogeny from discrete morphological data. Biology Letters 12:20160081.
Oliver, P., and A. Hugall. 2017. Phylogenetic evidence for mid-Cenozoic turnover of a diverse continental biota. Nat Ecol Evol 1:1896–1902.
Oliver, P. M., R. M. Brown, F. Kraus, E. Rittmeyer, S. L. Travers, and C. D. Siler. 2018. Lizards of the lost arcs: mid-Cenozoic diversification, persistence and ecological marginalization in the West Pacific. Proceedings of the Royal Society B 285:20171760.
Oppel, M. 1811. Die Ordnungen, Familien und Gattungen der Reptilien, als Prodrom einer Naturgeschichte derselben. Joseph Lindauer, München, 86 pp.
Peters, W. 1872. Untitled [Mr. W. Peters made a statement about new collections of Batrachians (of Dr. O Wucherer from Bahia), as well as some new or lesser known saurians]. Monatsberichte der Königlichen Preussische Akademie des Wissenschaften zu Berlin 1872:776.
Pyron, R. A., F. T. Burbrink, and J. J. Wiens. 2013. A phylogeny and revised classification of Squamata, including 4161 species of lizards and snakes. BMC Evolutionary Biology 13:93.
Rabosky, D. L. 2010. Extinction rates should not be estimated from molecular phylogenies. Evolution 6:1816–1824.
Reeder, T. W. 2003. A phylogeny of the Australian *Sphenomorphus* group (Scincidae: Squamata) and the phylogenetic placement of the crocodile skinks (*Tribolonotus*): Bayesian approaches to assessing congruence and obtaining confidence in maximum likelihood inferred relationships. Molecular Phylogenetics and Evolution 27:384–397.
Ronquist, F., S. Klopfstein, L. Vilhelmsen, S. Schulmeister, D. L. Murray, and A. P. Rasnitsyn. 2012a. A total-evidence approach to dating with fossils, applied to the early radiation of the hymenoptera. Systematic biology 61:973–999.
Schofield, J. A., A. L. Fenner, K. Pelgrim, and C. M. Bull. 2012. Male-biased movement in pygmy bluetongue lizards: implications for conservation. Wildlife Research 39:677–684.
Schwenk, K. 2000. Feeding in lepidosaurs; pp. in K. Schwenk (ed.), Feeding, form, function and evolution in tetrapod vertebrates. Academic Press, San Diego, U.S.A.
Shea, G. M. 1990. The genera *Tiliqua* and *Cyclodomorphus* (Lacertilia: Scincidae): generic diagnoses and systematic relationships. Memoirs of the Queensland Museum 29:495–520.
Shea, G. M., and M. N. Hutchinson. 1992. A new species of lizard (*Tiliqua*) from the Miocene of Riversleigh, Queensland. Memoirs of the Queensland Museum 32:303–310.
Skinner, A., A. F. Hugall, and M. N. Hutchinson. 2011. Lygosomine phylogeny and the origins of Australian scincid lizards. Journal of Biogeography 38:1044–1058.
Swofford, D. L. 2003. PAUP*: Phylogenetic Analysis Using Parsimony (*and other methods). 4.0 b10. Sinauer Associates, Sunderland, Massachusetts.
Title, P. O., and D. L. Rabosky. 2016. Do macrophylogenies yield stable macroevolutionary inferences? An example from squamate reptiles. Systematic biology 66:843–856.
Tonini, J. F. R., K. H. Beard, R. B. Ferreira, W. Jetz, and R. A. Pyron. 2016. Fully-sampled phylogenies of squamates reveal evolutionary patterns in threat status. Biological Conservation 204, Part A:23–31.

Travouillon, K. J., S. Legendre, M. Archer, and S. J. Hand. 2009. Palaeoecological analyses of Riversleigh's Oligo-Miocene sites: Implications for Oligo-Miocene climate change in Australia. Palaeogeography, Palaeoclimatology, Palaeoecology 276:24–37.
Uetz, P., P. Freed, and J. e. Hošek. 2019. The Reptile Database.
Welch, K. 1982. Herpetology of the Old World II. Preliminary comments on the classification of skinks (Family Scincidae) with specific reference to those genera found in Africa, Europe, and southwest Asia. Herptile 7:25–27.
Wells, R. W., and R. C. Wellington. 1984. A synopsis of the class Reptilia in Australia. Australian Journal of Herpetology 1:73–129.
Woinarski, J. C. Z., A. A. Burbidge, and P. L. Harrison. 2014. The action plan for Australian mammals 2012. CSIRO Publishing, Clayton, Victoria, Australia, 1038 pp.
Woodhead, J., S. J. Hand, M. Archer, I. Graham, K. Sniderman, D. A. Arena, K. H. Black, H. Godthelp, P. Creaser, and E. Price. 2016. Developing a radiometrically-dated chronologic sequence for Neogene biotic change in Australia, from the Riversleigh World Heritage Area of Queensland. Gondwana Research 29:153–167.
Wright, A. M., and D. M. Hillis. 2014. Bayesian analysis using a simple likelihood model outperforms parsimony for estimation of phylogeny from discrete morphological data. PLoS ONE 9:e109210.
Wright, A. M., G. T. Lloyd, and D. M. Hillis. 2015a. Modeling character change heterogeneity in phylogenetic analyses of morphology through the use of priors. Systematic biology 65:602–611.

CHAPTER 4: AN ARMORED MEGAFAUNAL SKINK FROM THE PLEISTOCENE OF AUSTRALIA EXPANDS THE LIMITS OF LIZARD DIVERSITY

K. M. Thorn, D. A. Fusco, M. H. Hutchinson, M. G. Gardner, J. L. Clayton, G. J. Prideaux, and M. S. Y. Lee

[1] College of Science and Engineering, Flinders University, Bedford Park, SA 5047, Australia

[2] South Australian Museum, North Terrace, Adelaide, SA 5000, Australia

4.1 Context

This chapter is formatted for submission to the journal *Science*. This project demonstrates the morphological extremes attained by the Egerniinae. The taxa *Aethesia frangens* Hutchinson and Scanlon, 2009 and *Tiliqua laticephala* Čerňanský and Hutchinson 2013 are redescribed as a single giant species, *Tiliqua frangens* (Hutchinson and Scanlon, 2009). This newly reassembled skink's armour plating and herbivore skull structure converges on that of terrestrial tortoises (absent from modern Australia, but found on other continents). This niche in eastern Australia is now filled by extant *Tiliqua rugosa*, after *T. frangens* went extinct with the rest of the Pleistocene megafauna in the Late Pleistocene. The extinction of this taxon suggests that not only did mammals, birds, monitors and snakes lose larger representatives, but Australia's presently most speciose vertebrate family, the Scincidae was also impacted by the Pleistocene mass extinction.

Note: nomenclatural acts in thesis chapters are not considered published under ICZN rules.

4.2 Statement of authorship

KMT conceived the project, collected the data, performed analyses and wrote the manuscript. DAF collected the Wellington material and provided stratigraphic context; MNH and MSYL commented on multiple drafts of the manuscript and contributed to discussions; MGG and JLC coordinated and conducted the Sleepy Lizard surveys contributing all of the *Tiliqua rugosa* measurements. MSYL assisted with analyses. MSYL and GJP commented on the manuscript. GJP and MSYL provided the project funding.

4.3 Abstract

Squamate reptiles (lizards and snakes) are the most speciose extant land vertebrates, yet their fossil record has been poorly documented compared with other groups, meaning that key aspects of their biogeography and evolution have remained unknown. Here we expand our understanding of the adaptive potential of squamates by describing the largest-ever skink, a giant species with spiked dermal armour, which we resolve as the sister taxon to the shingleback, *Tiliqua rugosa*. At an estimated 2.38 kg, *Tiliqua frangens* was more than double the body mass of the world's largest living skink, with a robust body form, a broad head and squat limbs. We interpret it as an analogue of a small land tortoise, an herbivore niche unfilled in Australia today. This species expands the known morphological and ecological diversity of squamates, and adds Scincidae to the long list of Australian vertebrate families that lost their largest representatives in the late Pleistocene 'megafauna' extinction.

4.4 Main text

Fossil taxa provide unique insights for understanding the evolution of living groups, often exhibiting unexpected morphologies, ecologies or geographic distributions, and acting as calibrations for anchoring molecular phylogenies in time. The Australian Quaternary (last 2.5 million years) fossil record preserves diverse clades of mammals and birds with unfamiliar morphologies. Short-faced kangaroos (Prideaux, 2004), giant dromornithid birds (Murray and Vickers-Rich, 2004), and browsing diprotodontids (Price and Piper, 2009) contributed to an entirely different ecosystem to that of modern Australia. These recently-extinct Quaternary species show that current mammal and bird diversity is in many ways depauperate due to late Pleistocene extinctions (Roberts et al., 2001). The relatively few described Australian Quaternary squamates largely mirror extant morphologies; aside from only two known extinct giants, the monitor lizard *'*Megalania*'* *Varanus priscus* (Owen, 1859) and primitive snake *Wonambi naracoortensis* (Smith, 1976).

The Wellington Caves of New South Wales in central eastern Australia provided the first Australian vertebrate fossils (Mitchell, 1838). Along with producing fossils of both '*Megalania*' and *Wonambi*, two other large Pleistocene squamates have been identified from this area, both skinks. *Aethesia frangens* Hutchinson and Scanlon, 2009 of indeterminate relationships was described from a partial anatomically extreme mandible, known only from sediments retrieved from Phosphate Mine-Bone Cave, an early Pliocene to late Pleistocene complex (Hutchinson and Scanlon, 2009). *Tiliqua laticephala* Čerňanský and Hutchinson, 2013 a putative egerniine skink, was described from an unusually broad frontal found on the cave floor (hence lacking stratigraphic provenance) at Big Sink locality, which has both Pliocene and Pleistocene infills (Hutchinson and Scanlon, 2009; Čerňanský and Hutchinson, 2013). When *T. laticephala* was described, conspecificity with *A. frangens* was excluded because the holotype mandible of the latter was considered too unlike an egerniine such as *Tiliqua laticephala*. Neither taxon could be referred to the other, due to lack of overlapping elements, and morphological oddity. New excavations in Wellington Caves beginning in 2016, and a detailed inspection of museum collections has unearthed new fossil material expanding our knowledge of both taxa, revealing that the two names pertain to a single and very unusual species. *Tiliqua laticephala* is a junior synonym of *Aethesia frangens* but this taxon is a member of the genus *Tiliqua*. Therefore, the new taxonomic position for *Aethesia frangens* is here determined as *Tiliqua frangens.* The new material includes much of the skull (complete mandibles, maxillae, frontals, premaxillae, nasal, prefrontals, postfrontal, squamosal, braincase, and quadrate) and postcranium; it also includes specimens spanning almost all postembryonic ontogeny. This material is described and illustrated in Appendix 3, and reveals a taxon with features in

common with modern species of *Tiliqua* (blue-tongued lizards of Australasia). *Tiliqua frangens* is most similar to *Tiliqua rugosa* the shingleback skink, but twice as heavy as even the largest living skinks, and with hypertrophied and spiny osteodermal armour plating creating a unique silhouette for this Pleistocene giant. This species is further characterized by extreme cranial morphology, with a deep skull profile, flat wide skull roof, and a robust quadrate tympanic conch for increased jaw adductor attachment. We here describe the new fossil material and assess the morphology, ontogeny, phylogenetic relationships and ecological role of this giant aberrant Pleistocene skink. Skinks are one of the most speciose lizard clades (1669 species globally; Uetz et al., 2019), but are also famous for being stereotypically small, unadorned and nondescript; the new taxon thus dramatically expands their known diversity, and indeed lizard diversity as a whole.

Parsimony and Bayesian analyses of the combined discrete morphological and DNA data united *T. frangens* with *Tiliqua rugosa* (Figure 3.1). The tip-dated Bayesian analyses retrieved a divergence date of 11.2 Ma. More broadly, the fossil falls within the *Tiliqua-Cyclodomorphus* clade, i.e. blue-tongue and pink-tongued skinks. The tip-dated Bayesian analyses retrieved a divergence date of 21.1 Ma for this divergence, and an age of 34.9 Ma for the crown Australian egerniine radiation.

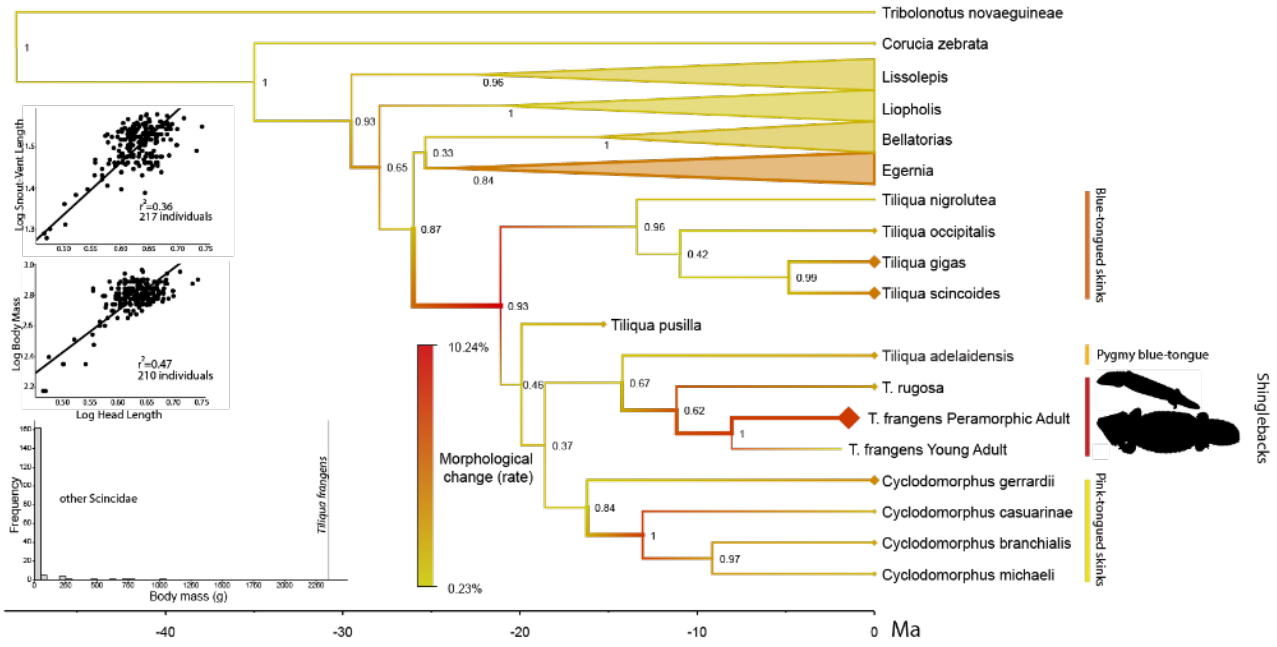

Figure 3.1: Results of the Bayesian analysis from BEAST v.1.8.4 using both ontogenetic units for *Tiliqua frangens, the 'Young adult' and 'Peramorphic adult')*. Node values are posterior probabilities. Colour represents morphological rate of change (% per Ma). Major Axis Regressions for log-transformed values of *Tiliqua rugosa* head length against snout-vent length (above) and body mass (below). Data (Data S1.xlsx) includes adult males, females, and unsexed sub-adults. Frequency histogram of scincid body mass (grams), data from Meiri (2010). Detailed versions of the major axis regression plots are in Figure A3.15, in Appendix 3.

Continuous characters were also initially considered but were highly homoplasic and generated problematic (e.g. biogeographically highly discordant) phylogenetic relationships, which are discussed in Appendix 3.

Head length of living individuals of *Tiliqua rugosa* correlate (with some minor sexual dimorphism) with snout-vent length (Bull and Pamula, 1996), and with body mass. A major axis regression of the log-transformed head length (mm) and snout-vent (SVL, mm) of extant *T. rugosa* specimens (Figure 3.1) produced the relationship: SVL = 1.274 (Head Length) + 0.697 (see Appendix 3). With a skull length of 70 mm, the inferred total SVL of *T. frangens* is ~594 mm. A major axis regression of the log-transformed head length (mm) and body mass (grams) of extant *T. rugosa* specimens (Figure 3.1) produced the relationship: Body Mass = 2.767 x (Head Length) + 1.0395. When the reconstructed head length figure for *T. frangens* is inserted into the body mass equation for its *T. rugosa* its sister taxon, the total body mass of *T. frangens* is ~2387 grams (see calculations in SI data file 'Data S1. Measurements.xlsx').

Figure 3.2: Artist reconstruction of *Tiliqua frangens* outside Cathedral Cave, Wellington. Informed by the fossils described in this thesis and body size analyses. Extant *Lampropholis* sp. for scale. Artist: Katrina Kenny.

The new excavation of the Quaternary sediments of Cathedral Cave in Wellington, New South Wales, has unearthed a wealth of new material of a giant spiky armoured skink *Tiliqua frangens,* which unequivocally unites the poorly-known taxa *Aethesia frangens* and *Tiliqua laticephala* from NSW, as well as a partial skeleton from Queensland. This newly reconstituted taxon is now the best-known Australian fossil lizard, in terms of overall morphology, and ontogeny.

Tiliqua frangens is most closely related to the living armour-plated Shingleback skink, *Tiliqua rugosa* (Figure 3.1). Both *T. rugosa* and *T. frangens* are large, armoured skinks: however, *T. frangens* takes these trends to the extreme, and is the largest and most bizarre skink (and arguably lizard) to have ever existed. This extends to dentition: unique dental traits not found in any other skinks include pleuro-acrodont dentition in adults and a halt in tooth replacement for the last two teeth in each row in peramorphic adults.

With an inferred weight well in excess of 2kgs, *Tiliqua frangens* is by far heaviest known scincid ever (see histogram in Figure 3.1). The egerniines *Bellatorias major* (Land Mullet: 670 g) and *Corucia zebrata* (Prehensile-tailed Skink: 1 kg) are the two largest living skinks (Klingenböck et al., 2000; Meiri, 2010; Hagen et al., 2012). The Australian Cenozoic record preserves two other extinct egerniine giants from further north, *Tiliqua wilkinsonorum* Hutchinson and Mackness, 2002 from Chinchilla, and a *Tiliqua* sp. mentioned from the Mt Etna collection (Hocknull, 2005). These taxa are represented solely by isolated dentaries with unique dentitions. *Tiliqua wilkinsonorum* has a longer, but less robust dentary than *Tiliqua rugosa*.

Even the largest and oldest *Tiliqua rugosa* individuals do not approach the shape and size of the peramorphic *T. frangens*. The early life stages represented by the neonate dentaries are similar, but with age *T. frangens* acquires a number of automorphic features through disproportionate bone growth. The peramorphic *T. frangens* holotype SAM P43196, introduces new autapomorphies at each life stage from the neonate AM F145608, young adult AM F143322 to adult AM F143321; but without this ontogenetic progression, P43196 was previously not recognised as *Tiliqua* (Hutchinson and Scanlon, 2009).

Tiliqua frangens greatly extends the 'land tortoise' niche theory proposed for *T. rugosa* (Milewski, 1981). The increased body mass and heavy spiky armour on *T. frangens* demonstrates a peramorphic extreme over its closest (and already peramorphic) relative, *T. rugosa*. A heavy but flexible carapace covers the animal dorsally, laterally and ventrally, the short stocky limbs are geared for power over speed, and gigantic body size (for a skink) allows efficient processing of herbivorous matter (see Table A3 for other tortoise similarities). Armour plating has been hypothesised to be an adaptation to aridity in other scincomorphs (Broeckhoven et al., 2018); but without detailed palaeoclimate information for the sites preserving *T. frangens* this relationship cannot be confirmed here. Solid ossified dorsal spines are not present on any other Australian squamates. The spiny tails of *Egernia* project posteriorly and are localised to the tail region, the osteoderms within the spiny scales are not single but composed of multiple narrow plates. Australian agamid lizards have soft spines (without osteoderms) running in a dorsal row or as

lateral lines. One suggestion (A. Palci pers. comm.), is that solid spines make it less comfortable for predators to constrict *T. frangens*. *Wonambi naracoortensis* and a *Morelia* sp. are found in the same deposits as *T. frangens*; spines would also make swallowing this large lizard more difficult for *Wonambi* as it had a smaller gape than modern constrictors (Palci et al., 2018).

The increase in body size may correlate with diet, tough plant matter requiring a stronger bite force (Metzger and Herrel, 2005), and low-quality plant matter requiring larger digestive tracts (King, 1996). The deep jaw and tall skull profile of *Tiliqua frangens* is similar to those observed in other herbivorous lizards such as *Corucia zebrata,* and iguanians like the Indian spiny-tailed lizard *Uromastyx hardwickii,* and the marine iguana *Amblyrhynchus cristatus*. A deeper mandible profile paired with shorter dentary length allocates force over a shorter lever, generating a stronger bite at the anterior of the dentary in herbivorous lizards and land tortoises (King, 1996; see Table A3). The comparative depth of the anterior tip of the mandible to other egerniines, and the increased surface area of the symphysis due to the posterior elongation of the 'chin', also suggests this increase in force. Although the feeding mechanics of *Tiliqua rugosa* are well documented (Wineski and Gans, 1984), no study has examined the role of tooth crown shape in relation to diet in extant egerniines. A common trait associated with a durophagous diet, present in many *Tiliqua* and *Cyclodomorphus* species, are blunt posterior teeth, suggesting a crushing rather than cutting action (Gans et al., 1985). *Tiliqua frangens'* teeth retain a fairly blunt profile with a single ridge, similar to *T. rugosa*, providing a single pressure point to puncture the surface of a hard object rather than crush it with brute force. *Tiliqua rugosa* are predominantly herbivorous, seasonally relying on small flowers for 88.2–93.7% of their adult diet (Brown, 1991).

Fossil fragments identifiable as *Tiliqua frangens* are localised to the western side of the Great Dividing Range, north of the Murray River, and to as far north as the Darling Downs area in southern Queensland. These sites are not restricted to a particular extant Köppen climatic zone (Stern and Hoedt, 2000), instead spread over current grassland, temperate and subtropical regions (see Figure A3.14 in Appendix 3). Shifting climatic areas in the late Pleistocene may provide a better indicator of *T. frangens* preferred habitat, possibly analogous to the northern population of *T. rugosa* which prefers a mosaic of open understorey vegetation (usually composed of bluebush/saltbush; Norval and Gardner, 2019). Land tortoises, a potential analogue of *T. frangens,* are absent from Australia today, and the relict forms present in the Pleistocene (meiolaniids) were considerably larger at an estimated >200 kgs (Appendix 1, page 251 in Flannery and Roberts, 1999) allowing dietary niche separation from *T. frangens*. *Tiliqua frangens* had no competition from true terrestrial tortoises, instead exploiting the empty niche highlighted in Table A3: the open habitat, slow-moving, armoured, herbivorous, reptile on the Australian continent during the late Pleistocene.

In none of the recorded fossil sites do *T. frangens* and *T. rugosa* occur concurrently, despite modern populations of *T. rugosa* existing in these areas today (see Figure A3.14 in Appendix 3). Fossil calibrated molecular phylogeography of extant *T. rugosa* populations estimate a fast radiation of the northern population sometime during the Pleistocene (Ansari et al., 2019). The largest recorded specimens of *T. rugosa* are localised to north-eastern extremities of their extant distribution. The range expansion, rapid diversification and body size increase for this population may be correlated with the extinction of *T. frangens* leaving an open niche to fill in this area.

The incredible size, peramorphy, unusual shape and intense armour plating of *Tiliqua frangens* is unlike any lizard in the world, greatly expanding the diversity of skinks, and squamate reptiles as a whole. This bizarre Pleistocene skink also highlights that, just like mammals and birds, Australia's reptile fauna exhibited a much greater diversity of forms before human colonisation. This highlights a major gap in our understanding of Quaternary Australian herpetofaunal diversity: squamate reptiles are this continent's most speciose terrestrial vertebrates, but our knowledge of their pre-human diversity lags substantially behind that of mammals and birds. A new excavation of the Quaternary sediments of Cathedral Cave in Wellington, New South Wales, has unearthed a wealth of new material of a giant spiky armoured skink *Tiliqua frangens,* which unites the poorly-known taxa *Aethesia frangens* and *Tiliqua laticephala* from NSW*,* and a partial skeleton from Queensland. This newly reconstituted taxon is now the best-known Australian fossil lizard, in terms of overall morphology, and ontogeny.

4.5 Acknowledgements

Thanks to Wellington field work teams and Flinders University Palaeontology Society volunteers. The curators and collection managers of eastern Australia; M. McCurry, M.-A. Binnie, C. Kovach, T. Ziegler, and S. Hocknull for access to fossil and comparative material. P. Stokes for assistance with photography; Adelaide Microscopy for access to their Micro CT facilities; I. Douvartzidis for assisting with the Micro-CT scanning. Microscopy Australia, J. Gascooke and the Australian National Fabrication Facility (ANFF) at Flinders University for use of the Inspect F SEM.
Funding: This project was funded by Australian Research Council DP150100264 grant to GJP and MH; a MAXIM Foundation research grant to GJP, TW and DAF; and a Small Research Grant from the Royal Society of South Australia to KMT. KMT and DAF are supported by Australian Government Research Training Program Scholarships. The Sleepy Lizard Project is funded by the Sleepy Lizard Survey Fund, Hermon Slade Foundation (HSF190559) and an Australian Research Council DP200102880 grant to MGG.

4.6 References

Broeckhoven, C., C. De Kock, and C. Hui. 2018. Sexual dimorphism in the dermal armour of cordyline lizards (Squamata: Cordylinae). Biological Journal of the Linnean Society 125:30–36.

Brown, G. 1991. Ecological feeding analysis of south-eastern Australian scincids (Reptilia, Lacertilia). Australian Journal of Zoology 39:9–29.

Bull, C. M., and Y. Pamula. 1996. Sexually dimorphic head sizes and reproductive success in the sleepy lizard *Tiliqua rugosa*. Journal of Zoology 240:511–521.

Čerňanský, A., and M. N. Hutchinson. 2013. A new large fossil species of *Tiliqua* (Squamata: Scincidae) from the Pliocene of the Wellington Caves (New South Wales, Australia). Alcheringa: An Australasian Journal of Palaeontology 37:131–136.

Flannery, T. F., and R. G. Roberts. 1999. Late Quaternary extinctions in Australasia; pp. 248–260 in R. D. E. MacPhee and H.-D. Sues (eds.), Extinctions in near time. Springer Science & Business Media, United States of America.

Gans, C., F. De Vree, and D. Carrier. 1985. Usage pattern of the complex masticatory muscles in the Shingleback lizard, *Trachydosaurus rugosus*: a model for muscle placement. The American Journal of Anatomy 173:219–240.

Hagen, I. J., S. C. Donnellan, and C. M. Bull. 2012. Phylogeography of the prehensile-tailed skink *Corucia zebrata* on the Solomon Archipelago. Ecology and evolution 2:1220–1234.

Hocknull, S. A. 2005. Ecological succession during the late Cainozoic of central eastern Queensland: extinction of a diverse rainforest community. Memoirs of the Queensland Museum 51:39–122.

Hocknull, S. A. 2009. Late Cainozoic rainforest vertebrates from Australopapua: evolution, biogeography and extinction. Biological, Earth and Environmental Sciences, Faculty of Science, University of New South Wales, 628 pp.

Hutchinson, M. N., and B. S. Mackness. 2002. Fossil lizards from the Pliocene Chinchilla Local Fauna, Queensland. Records of the South Australian Museum 35:169–184.

Hutchinson, M. N., and J. D. Scanlon. 2009. New and unusual Plio-Pleistocene lizard (Reptilia: Scincidae) from Wellington Caves, New South Wales, Australia. Journal of Herpetology 43:139–147.

King, G. 1996. Reptiles and herbivory. Chapman & Hall, London, UK, 160 pp.

Klingenböck, A., K. Osterwalder, and R. Shine. 2000. Habitat use and thermal biology of the "Land mullet" *Egernia major*, a large Scincid lizard from remnant rain forest in southeastern Australia. Copeia 2000:931–939.

Meiri, S. 2010. Length–weight allometries in lizards. Journal of Zoology 281:218–226.

Metzger, K. A., and A. Herrel. 2005. Correlations between lizard cranial shape and diet: a quantitative, phylogenetically informed analysis. Biological Journal of the Linnean Society 86:433–466.

Milewski, A. V. 1981. A comparison of reptile communities in relation to soil fertility in the mediterranean and adjacent arid parts of Australia and Southern Africa. Journal of Biogeography 8:493–503.

Mitchell, T. L. 1838. Three expeditions into the interior of eastern Australia, with descriptions of the recently explored region of Australia Felix, and of the present colony of New South Wales, Volume 1 and 2. T & W Boone, London.

Murray, P. F., and P. Vickers-Rich. 2004. Magnificent mihirungs: the colossal flightless birds of the Australian dreamtime. Indiana University Press, Bloomington, Indiana, 410 pp.

Norval, G., and M. G. Gardner. 2019. The natural history of the sleepy lizard, *Tiliqua rugosa* (Gray, 1825) – Insight from chance observations and long-term research on a common Australian skink species. Austral Ecology:doi:10.1111/aec.12715.

Owen, R. 1859. Description of some remains of a gigantic land-lizard (*Megalania prisca*, Owen) from Australia. Philosophical Transactions of the Royal Society of London 149:43–48.

Palci, A., M. N. Hutchinson, M. W. Caldwell, J. D. Scanlon, and M. S. Lee. 2018. Palaeoecological inferences for the fossil Australian snakes *Yurlunggur* and *Wonambi* (Serpentes, Madtsoiidae). Royal Society open science 5:172012.

Price, G. J., and K. J. Piper. 2009. Gigantism of the Australian *Diprotodon* Owen 1838 (Marsupialia, Dirptodontoidea) through the Pleistocene. Journal of Quaternary Science 24:1029–1038.

Prideaux, G. 2004. Systematics and evolution of the sthenurine kangaroos, Volume 146. University of California Press, Oaklands, California.

Roberts, R. G., T. F. Flannery, L. K. Ayliffe, H. Yoshida, J. M. Olley, G. J. Prideaux, G. M. Laslett, A. Baynes, M. A. Smith, R. Jones, and B. L. Smith. 2001. New ages for the last Australian megafauna: continent-wide extinction about 46,000 years ago. Science 292:1888–1892.

Smith, M. J. 1976. Small fossil vertebrates from Victoria Cave, Naracoorte, South Austraia. IV, Reptiles. Transactions of the Royal Society of South Australia 100:39–51.

Stern, H., and G. d. Hoedt. 2000. Objective classification of Australian climates. Australian Meteorological Magazine 49:87–96.

Uetz, P., P. Freed, and J. e. Hošek. 2019. The Reptile Database.

Wineski, L. E., and C. Gans. 1984. Morphological basis of the feeding mechanics in the shingle-back lizard *Trachydosaurus rugosus* (Scincidae, Reptilia). Journal of Morphology 181:271–295.

CHAPTER 5: DISCUSSION
THE FOSSIL RECORD OF THE EGERNIINAE AND ITS IMPLICATIONS FOR UNDERSTANDING THEIR EVOLUTIONARY HISTORY

5.1 The fossil record of the Egerniinae

The description of three new fossil Egerniinae taxa, spanning the Neogene and Paleogene in Australia, contributes to filling gaps in the sparse fossil record of Australian squamates. The search for these fossils uncovered a wealth of undescribed squamate material from numerous other palaeontological sites across the continent that deserve equal future attention. These sites are summarised in Table A5 in Appendix 5.

While palaeoherpetology in North America and Europe has produced numerous ecological inferences using squamate taxa in the last 20 years (Bell et al., 2004; Blain et al., 2008; Blain et al., 2018; Villa et al., 2018), Australian palaeontology is lacking significant contributions to this field (Prideaux, 2007). The high alpha diversity of Australian squamates in comparison to the relatively low diversity of higher ('family' level) groups has meant that identification of morphological autapomorphies between fossil taxa are more difficult. Most papers referring to the existence of unidentified Australian herpetofauna reference the inadequacy of museum skeletal collections or a lack of published methods for the identification of most family groups to genus or species level (Archer, 1978; Bell and Mead, 2014). Some refer to consulting other herpetologists for assistance with identifications (Pledge, 1992), and others send material to said herpetologists to investigate independently (Dawson and Augee, 1997). Overwhelmingly, in many large scale vertebrate palaeontological collections that include herpetofauna, the mammals alone are the focus of the primary publication from that site (Douglas et al., 1966; Dortch and Merrilees, 1971; Travouillon et al., 2009; Prideaux et al., 2010; McDowell et al., 2012). Archaeological excavations that present fauna lists are usually inclusive of family level identification of lizards (Balme, 1995; Maloney et al., 2018), but many of these note only the larger species of the Varanidae, Agamidae and Egerniinae that are relevant 'economic fauna' and of a size to be retrieved by 3 mm screens (Baynes et al., 2019). The difference in vertebrate diversity between what exists in a collection of vertebrate palaeontological material and what is published, is an area needing attention. Australia's fossil avifauna have been highlighted by the works of Boles, Worthy, Nguyen and Shute in recent decades and may be equally as diverse as the mammal communities they existed with (Worthy, 2009, 2011; Nguyen et al., 2013; Nguyen, 2016; Shute et al., 2016; Boles, 2017; Shute et al., 2017). Efforts to describe and identify fossil frogs have demonstrated that their remains are useful for

palaeoecological interpretations (Hocknull, 2005; Price et al., 2005; Hocknull, 2009; Tyler and Prideaux, 2016). The 'megafauna' squamate taxa and crocodylomorphs are commonly identified to genus in major site-specific publications (e.g. Tedford et al., 1992; Hocknull, 2005; Price and Sobbe, 2005; Hocknull, 2009; Louys and Price, 2013), and the snakes of Cenozoic Australia were intensively published by John Scanlon (Scanlon, 1992, 1993, 1997; Scanlon and Lee, 2000; Scanlon, 2006) and Alessandro Palci (Palci et al., 2014; Palci et al., 2018). When underrepresentation of the Scincidae is rectified, the identification of our most diverse terrestrial vertebrate family from palaeontological investigations might eventually present a more accurate reflection of prehistoric diversity on the Australian continent.

The three extinct taxa investigated in this thesis each contribute new information to the phylogeny of the Egerniinae, and they are each new elements in the palaeoecological investigations of the sites they came from. *Egernia gillespieae* is Australia's oldest species of *Egernia*, and its contemporaneous existence with *Tiliqua pusilla* calibrates the divergence of these genera to ~30 million years ago. The reinvestigation of material from Wellington Caves in New South Wales brought to light the morphological extremes of *Tiliqua frangens*, driving a three-state museum search for more of this intriguing animal, now recognised as the world's largest ever scincid and one of the most bizarre lizards. The Oligo-Miocene of central South Australia hosts at least two early egerniine taxa, *Proegernia palankarinnensis* and *P. mikebulli*, a possible stem clade to the extant Australian radiation. Each of these taxa were chosen as focal points to this thesis because they form succinct bodies of work as individual chapters and when brought together they greatly elucidate the history of Australia's scincid evolution.

5.2 The ongoing importance of morphological data in phylogenetics

It's becoming cheaper and easier to generate and share skeletal anatomical data of vertebrates thanks to micro-computed tomography (Micro-CT) and surface scanning contributing to massive digital databases. With the increasing uptake of digitisation of palaeontological collections and CT scanning of extant species, we are presented with an opportunity to further our knowledge of the evolution of vertebrates, by creating morphological matrices to input this data into a phylogenetic framework. Digitally presented morphology allows for precise recording of continuous morphological characters as measurements or morphometric landmarks. This precision reduces bias in morphological character coding (Simões et al., 2017), and better informs Bayesian analyses by creating numerous species-level apomorphic traits (Lee and Palci, 2015).

New analytical programs have been developed with more sophisticated models for phylogenetic inferences using morphological or fossil data. Application of new methods permitted

by the use of these programs has produced the most robust assessment of egerniine phylogenetic history to date, including time-calibration. Despite this, the limited preservation of *Proegernia* spp. has resulted in the resolution of detail at the base of the tree remaining equivocal. The positions resolved for the extinct taxa, although not always well supported, did help to elucidate the branching order of extant lineages that were unresolved with molecular data alone. A more precise and better developed phylogeny of crown egerniines will allow palaeontology to better inform the diversification timing and rates of this clade throughout the Neogene of Australasia during a period of major climatic changes and vertebrate lineage extinctions.

5.3 The evolution of the Egerniinae

The last common ancestor of all Australian scincids is hypothesised to live somewhere in southern Asia, sometime during the Paleogene (Skinner et al., 2011). Both the sphenomorphines and eugongylines dispersed into Australia relatively recently with numerous basal taxa still occupying areas of south-eastern Asia and the southern Pacific (Skinner et al., 2011; Skinner et al., 2013; Thorn et al., 2017). The timing of the arrival of the Egerniinae to the Sahul landmass was uncertain, with both super-tree and 'lygosomine-focused' analyses producing large confidence intervals on suggested node ages (Skinner et al., 2011; Title and Rabosky, 2016). By adding multiple fossil taxa as calibrating 'tips' in a total-evidence phylogeny of the Egerniinae, the Australian clade is retrieved as ~33Ma million years old. This age pre-dates the crown Australian clades of the other extant scincid groups; Sphenomorphinae is the closest at c. 30Ma (Skinner et al., 2013). The stem positioning of *Proegernia* in Chapter 4 demonstrates the existence of extinct Australian lineages outside of the living (crown) group, and possible multiple Australian colonisation events. The date of arrival of egerniines to Australia can still not be confirmed with phylogeny alone, node ages for *Corucia* and *Tribolonotus* and their lack of fossil taxa on the Australian continent suggest that the beginning of diversification of the Egerniinae could have begun on an island archipelago that today forms the Solomon Islands. Geologically, these land masses formed an arc with Southeast Asia during the late Paleocene, as the gap between Southeast Asia and Australia began to close. These terranes don't become part of the Sahul landmass until the Miocene–Pliocene (Hall, 2002; Müller et al., 2016) and may not have emerged above sea level to form terrestrial habitats, so the egerniine radiation cannot be explained by vicariance; dispersal to Sahul via rafting or floating must have occurred at some stage during the mid-late Paleogene. Dispersal of lizards over great distances of salt water is not unique (Rieppel, 2002; Carranza and Arnold, 2003), or physically impossible (Houle, 1998). This period of isolation from the southeast Asian lygosomines on a continent devoid of endemic scincomorphs, was accommodating of morphological experimentation and radiation resulting in the distinctive morphology of egerniine

skinks. The New Guinean and Solomon Islands taxa are the result of a second dispersal, or are survivors of an extinction that wiped out any southern species of *Corucia* or *Tribolonotus* and all representatives of *Proegernia*. Surviving Australian egerniines then underwent rapid morphological evolution, possibly the result of the earlier extinction (Benton and Emerson, 2007; Crisp and Cook, 2009). The paucity of earlier Palaeogene fossil evidence for this conclusion is not unexpected (Benton and Emerson, 2007), concluding with another ghost lineage for this continent alongside numerous marsupial clades (Karen H Black et al., 2012), some shorebirds (De Pietri et al., 2016), and diplodactyloid geckos (Oliver and Sanders, 2009).

The remarkable variation in shape and size across this scincid clade is the result of 60 million years of niche specialisation, changing climates and the resulting biome shifts. The fossil record provides evidence of the timing of deep divergences driven by dietary shifts (*Bellatorias, Egernia* and *Tiliqua*) in the mid-Miocene, with one branch of egerniines developing durophagous dentition (*Tiliqua*+*Cyclodomorphus*). There are also multiple homoplasious examples of lanceolate tooth cusp adaptations for herbivory (*Corucia*, *Egernia* spp. and *Bellatorias* spp.). The evolution of herbivory in scincomorphs is infrequent (King, 1996), but when mapped across the new phylogeny of egerniines is shown to have occurred repeatedly within the subfamily. Changing climates and vegetation (Martin, 2006; Byrne et al., 2008; Byrne et al., 2011) led to the extinctions of Oligo–Miocene lineages from the mainland (*Corucia* and *Tribolonotus*), or entirely (*Proegernia*). Vicariance caused by expanding aridification in central Australia resulted in a deep divergence between the two species of *Lissolepis* (Greer, 1979; Atkins et al., 2019).

Continued investigation of the timing and causes of the rapid morphological radiation of the group may be further investigated by examining finer details in skull shape, and external morphology. Variations in the shape of egerniine skulls is noted in extant (i.e. the *Egernia depressa* group; Hollenshead, 2011) and extinct forms (*Tiliqua frangens*), but the timing and drivers of these changes in shape have not been thoroughly investigated. Osteoderm shapes vary across this group through time, space, and the phylogeny. Spiny tails within *Egernia* spp. appear to be analogous in crevice-dwelling species as they occur in the *E. depressa*/*E. stokesii*/*E. hosmeri*/*E. epsisolus* clade and have either been lost in all other *Egernia,* or more likely evolved a second time in *Egernia cunninghami*. While the use of these moveable spines in *Egernia* spp. is well recorded (Greer, 1989; Chapple, 2003; Arida and Bull, 2008), any selective pressures for the evolution of immovable spines on the osteoderms of *Tiliqua frangens* are unknown. Recording these morphological variables and mapping them across the phylogeny may provide information on the timing and any associated driving factors of their evolution.

5.4 Conclusions

This thesis achieved its stated aims that together built a better understanding of the origins and phenotypic diversity of the Egerniinae:

- A new tip-dated phylogeny for the group is published (Chapter 2; Thorn et al., 2019), morphological diversity can be mapped across this tree through time.
- Phenotypic extremes were observed in dentition (*Egernia gillespieae*; Chapter 2) and body size and shape (*Tiliqua frangens*; Chapter 3)
- The origins of Australia's scincid diversity are calibrated by the oldest described Australian scincid clade *Proegernia* (Chapter 4)
- The fossil diversity of the Australian Egerniinae is expanded to include two new taxa: *Egernia gillespieae* and *Proegernia mikebulli*, and a redescription of the world's largest scincid *Tiliqua frangens*.

5.5 Future work

The phylogenetic results in each chapter have highlighted the ongoing paraphyletic organisation within the genera *Tiliqua*+*Cyclodomorphus*. In every tree the two extant species *Tiliqua adelaidensis* and *T. rugosa* are related to extant *Cyclodomorphus*. This relationship is retrieved by the molecular data and is supported by some morphological characters (characters 44, 139, and 142). The implications of this paraphyly might eventually lead to the renaming of both extant taxa and the extinct sister taxon *T. frangens* to the genus *Trachydosaurus* Gray, 1825. The nomenclatural act has not been formalised in this thesis, but should be addressed appropriately in the near future when further genomic data for the remaining not yet sampled *Tiliqua* and *Cyclodomorphus* taxa is made available to better support or refute this taxonomic change.

There are changes that I would make to the final morphological character set used in this thesis. These changes are based on further reading (Simões et al., 2017) and testing of these characters late in the writing of this thesis, after the publication of Chapter 2. Characters 13, 46, 47, and 109 could be converted to continuous characters as they deal with sizes, and the size classes defined in the original characters may not suit new taxa entered into the matrix. Characters 28–29, 100–101, and 110–111 record presence/absence of a feature, and then the following character relates to its size or location. Contingent characters such as these can lead to ancestral node optimisation in Parsimony analyses when absence is a plesiomorphic trait. If absence is recorded by the first character and then N/A for the second, N/A also becomes plesiomorphic (Simões et al.,

2017). Potentially, these characters should be rewritten as a multistate coding with absent as the first state (0).

Herpetofaunal palaeodiversity in Australia has not been summarised on a continent-wide scale, previous publications only including only 'Reptilia', a family name within a broader vertebrate 'laundry list' (Rich, 1991), or diversity sampled within state boundaries (Williams, 1980; Molnar, 1982) or regions (Molnar and Kurz, 1997; Reed and Bourne, 2000; Reed and Bourne, 2009). The most detailed investigations of herpetofaunal diversity in single sites in Australia are those by Smith (1976), Hocknull (2005), Fraser and Wells (2006), and Hollenshead et al. (2011). These publications include genus and sometimes species-level identifications that are quantified through stratigraphic succession representing time. Other publications have included species-level identifications, but only for the total site list, not covering changes through time in taxonomic richness (Prideaux et al., 2007). An important step forward in palaeoecological research in Australia will be the identification and integration of any species-level apomorphies for identifications (Bell et al., 2010). Character optimisation in parsimony and Bayesian analyses are rigorous means of testing which morphological autapomorphies make suitable diagnostic characters, between taxa and ontogenetic stages. Total-evidence trees also provide the framework to trace characters through time, aiding in the identification of fossil taxa much older than those found in quaternary deposits. In the future, taxa not available for morphological coding in this study will need to be added to inform the analyses for identification of quaternary fossils with more certainty. Exploration of postcranial material and whether or not it can be used to identify fossil taxa to family and genus level may also assist in increasing the number of identified specimens of reptiles in fossil deposits. Osteologically cryptic extant species identified using these methods highlight the underestimated diversity of Australian fossil lizards. While this issue may not be possible to overcome in taxa too old to be picked out by ancient DNA, recognition of how often cryptic species occur in different clades can provide an estimation of past species diversity.

The implications of recognising this increase in Australia's palaeoherpetofaunal diversity has contextualised extant diversity, and the possible rate of extinctions after human arrival and colonisation. It has been well-established that Australia's mammalian faunal richness decreased after both anthropogenic events, with the largest body size classes more likely to die off. The only two reptile species considered in these analyses are the giant snake *Wonambi* and giant goanna Megalania. With the addition of *Tiliqua frangens*—which does not survive in the fossil record beyond the same megafauna extinction event—it appears that scincid lizard diversity may also have been impacted by the arrival of humans to Sahul. With the identification of smaller (in terms of body size) and presently the more diverse herpetofauna clades, future research should concentrate

on providing data to accurately estimate the role of humans in driving population and species extinctions, using non-mammalian data. Identification of Holocene squamates pre- and post-European invasion of Australia may provide an estimate of the resilience of these animals to rapid extinction drivers, informing models used to test the effect of other factors such as human-induced climate change, invasive pests, and disease.

Questions driven from the results of this thesis relate to the significate rate of body size change in the Egerniinae. *Tiliqua frangens* and *T. wilkinsonorum* stand out as two Plio-Pleistocene giants, but their smaller extant relatives still represent the world's largest scincid lizards. Australia has more than its fair share of large bodied skinks, most of them within the Egerniinae. What is driving this increase in body size in Australia, and why only this group and not (to the same extent) in the Eugongylinae and Sphenomorphinae? When did Australian skinks begin growing so large, is this morphological change driven by a change in climate and resource availability or competition? How are multiple lineages able to grow so large in a relatively short period of time?

The total-evidence phylogeny produced in this thesis has inspired as many new questions as it set out to answer. With the addition of more taxa, trials of alternative phylogenetic and biogeographic models, or integration with larger e.g. genomic data sets, these results will continue to unravel large palaeoecological questions in Australian scincid diversity.

5.6 References

Archer, M. 1978. Quaternary vertebrate faunas from the Texas Caves of southeastern Queensland. Memoirs of the Queensland Museum 19:61–109.

Arida, E. A., and M. Bull. 2008. Optimising the design of artificial refuges for the Australian skink, Egernia stokesii. Applied Herpetology 5:161–172.

Atkins, Z. S., M. D. Amor, N. Clemann, D. G. Chapple, G. M. While, M. G. Gardner, M. L. Haines, K. A. Harrisson, M. Schroder, and K. A. Robert. 2019. Allopatric divergence drives the genetic structuring of an endangered alpine endemic lizard with a sky-island distribution. Animal Conservation.

Balme, J. 1995. 30,000 years of fishery in western New South Wales. Archaeology in Oceania 30:1–21.

Baynes, A., C. Piper, and K. M. Thorn. 2019. An experimental investigation of differential recovery of native rodent remains from Australian palaeontological and archaeological deposits. Records of the Western Australian Museum 34:1–30.

Bell, C. J., and J. I. Mead. 2014. Not enough skeletons in the closet: Collections-based anatomical research in an age of conservation conscience. The Anatomical Record 297:344–348.

Bell, C. J., J. J. Head, and J. I. Mead. 2004. Synopsis of the herpetofauna from Porcupine Cave; pp. 117–126 in A. D. Barnosky (ed.), Biodiveristy response to climate change in the Middle Pleistocene: The Porcupine Cave Fauna from Colorado. University of California Press, Oakland, California.

Bell, C. J., J. A. Gauthier, and G. S. Bever. 2010. Covert biases, circularity, and apomorphies: A critical look at the North American Quaternary Herpetofaunal Stability Hypothesis. Quaternary International 217:30–36.

Benton, M. J., and B. C. Emerson. 2007. How did life become so diverse? The dynamics of diversification according to the fossil record and molecular phylogenetics. Palaeontology 50:23–40.

Black, K. H., M. Archer, S. J. Hand, and H. Godthelp. 2012. The rise of Australian marsupials: a synopsis of biostratigraphic, phylogenetic, palaeoecologic and palaeobiogeographic understanding; pp. 983–1078 in J. A. Talent (ed.), Earth and Life. Springer Science.

Blain, H.-A., S. Bailon, and G. Cuenca-BescГis. 2008. The Early to Middle Pleistocene palaeoenvironmental change based on the squamate reptile and amphibian proxies at the Gran Dolina site, Atapuerca, Spain. Palaeogeography, Palaeoclimatology, Palaeoecology 261:177–192.

Blain, H.-A., J. A. C. Silva, J. M. J. Arenas, V. Margari, and K. Roucoux. 2018. Towards a Middle Pleistocene terrestrial climate reconstruction based on herpetofaunal assemblages from the Iberian Peninsula: State of the art and perspectives. Quaternary Science Reviews 191:167–188.

Boles, W. E. 2017. A brief history of avian palaeontology in Australia; pp. 265–362 in Memoirs of the Nuttal Ornithological Club, Vol. III The Nuttal Ornithological Club, Cambridge, Massachusetts.

Byrne, M., D. K. Yeates, L. Joseph, M. Kearney, J. Bowler, M. A. J. Williams, S. Cooper, S. C. Donnellan, J. S. Keogh, R. Leys, J. Melville, D. J. Murphy, N. Porch, and K. H. Wyrwoll. 2008. Birth of a biome: insights into the assembly and maintenance of the Australian arid zone biota. Molecular Ecology 17:4398–4417.

Byrne, M., D. A. Steane, L. Joseph, D. K. Yeates, G. J. Jordan, D. Crayn, K. Aplin, D. J. Cantrill, L. G. Cook, M. D. Crisp, J. S. Keogh, J. Melville, C. Moritz, N. Porch, J. M. K. Sniderman, P. Sunnucks, and P. H. Weston. 2011. Decline of a biome: evolution, contraction, fragmentation, extinction and invasion of the Australian mesic zone biota. Journal of Biogeography 38:1635–1656.

Carranza, S., and E. N. Arnold. 2003. Investigating the origin of transoceanic distributions: Mtdna shows *Mabuya* lizards (Reptilia, Scincidae) crossed the Atlantic twice. Systematics and Biodiversity 1:275–282.

Chapple, D. G. 2003. Ecology, life-history, and behavior in the Australian scincid genus *Egernia*, with comments on the evolution of complex sociality in lizards. Herpetological Monographs 17:145–180.

Crisp, M. D., and L. G. Cook. 2009. EXPLOSIVE RADIATION OR CRYPTIC MASS EXTINCTION? INTERPRETING SIGNATURES IN MOLECULAR PHYLOGENIES. Evolution 63:2257-2265.

Dawson, L., and M. Augee. 1997. The late Quaternary sediments and fossil vertebrate fauna from Cathedral Cave, Wellington Caves, New South Wales. Proceedings-Linnean Society of New South Wales 117:51–78.

De Pietri, V. L., R. P. Scofield, S. J. Hand, A. J. D. Tennyson, and T. H. Worthy. 2016. Sheathbill-like birds (Charadriiformes: Chionoidea) from the Oligocene and Miocene of Australasia. Journal of the Royal Society of New Zealand 46:181-199.

Dortch, C. E., and D. Merrilees. 1971. A salvage excavation in Devils Lair, Western Australia. Journal of The Royal Society of Western Australia 54:103–113.

Douglas, A. M., G. W. Kendrick, and D. Merrilees. 1966. A fossil bone deposit near Perth, Western Australia, interpreted as a carnivore's den after feeding tests on living *Sarcophilus* (Marsupialia, Dasyuridae). Journal of The Royal Society of Western Australia 49:88–90.

Drummond, A. J., M. A. Suchard, D. Xie, and A. Rambaut. 2012. Bayesian phylogenetics with BEAUti and the BEAST 1.7. Molecular biology and evolution 29:1969–1973.

Fraser, R. A., and R. T. Wells. 2006. Palaeontological excavation and taphonomic investigation of the late Pleistocene fossil deposit in Grant Hall, Victoria Fossil Cave, Naracoorte, South Australia. Alcheringa: An Australasian Journal of Palaeontology 30:147–161.

Gavryushkina, A., D. Welch, T. Stadler, and A. J. Drummond. 2014. Bayesian inference of sampled ancestor trees for epidemiology and fossil calibration. PLOS Computational Biology 10:e1003919.

Goloboff, P. A., and S. A. Catalano. 2016. TNT version 1.5, including a full implementation of phylogenetic morphometrics. Cladistics 32:221–238.

Goloboff, P. A., C. I. Mattoni, and A. S. Quinteros. 2006. Continuous characters analyzed as such. Cladistics 22:589–601.

Gray, J. E. 1825. A synopsis of the genera of reptiles and Amphibia, with a description of some new species. Annals of Philosophy 10:193–217.

Greer, A. E. 1979. A phylogenetic subdivision of Australian skinks. Records of the Australian Museum 32:339–371.

Hall, R. 2002. Cenozoic geological and plate tectonic evolution of SE Asia and the SW Pacific: computer-based reconstructions, model and animations. Journal of Asian Earth Sciences 20:353–431.

Heath, T. A., J. P. Huelsenbeck, and T. Stadler. 2014. The fossilized birth–death process for coherent calibration of divergence-time estimates. Proceedings of the National Academy of Sciences 111:E2957–E2966.

Hocknull, S. A. 2005. Ecological succession during the late Cainozoic of central eastern Queensland: extinction of a diverse rainforest community. Memoirs of the Queensland Museum 51:39–122.

Hocknull, S. A. 2009. Late Cainozoic rainforest vertebrates from Australopapua: evolution, biogeography and extinction. Biological, Earth and Environmental Sciences, Faculty of Science, University of New South Wales, 628 pp.

Hollenshead, M. G. 2011. Geometric morphometric analysis of cranial variation in the *Egernia depressa* (Reptilia: Squamata: Scincidae) species complex. Records of the Western Australian Museum 26:138–153.

Hollenshead, M. G., J. I. Mead, and S. L. Swift. 2011. Late Pleistocene *Egernia* group skinks (Squamata: Scincidae) from Devils Lair, Western Australia. Alcheringa: An Australasian Journal of Palaeontology 35:31–51.
Houle, A. 1998. Floating Islands: A mode of long-distance dispersal for small and medium- sized terrestrial vertebrates. Diversity and Distributions 4:201–216.
King, G. 1996. Reptiles and herbivory. Chapman & Hall, London, UK, 160 pp.
Lee, M. S. Y., and A. Palci. 2015. Morphological phylogenetics in the genomic age. Current Biology 25:R922–R929.
Lemey, P., A. Rambaut, J. J. Welch, and M. A. Suchard. 2010. Phylogeography takes a relaxed random walk in continuous space and time. Molecular biology and evolution 27:1877–1885.
Louys, J., and G. J. Price. 2013. The Chinchilla Local Fauna: an exceptionally rich and well-preserved Pliocene vertebrate assemblage from fluviatile deposits of south-eastern Queensland, Australia. Acta Palaeontologica Polonica 60:551–573.
Maloney, T., S. O'Connor, R. Wood, K. Aplin, and J. Balme. 2018. Carpenters Gap 1: A 47,000 year old record of indigenous adaption and innovation. Quaternary Science Reviews 191:204–228.
Martin, H. A. 2006. Cenozoic climatic change and the development of the arid vegetation in Australia. Journal of Arid Environments 66:533–563.
McDowell, M. C., A. Baynes, G. C. Medlin, and G. J. Prideaux. 2012. The impact of European colonization on the late-Holocene non-volant mammals of Yorke Peninsula, South Australia. The Holocene 22:1441–1450.
Molnar, R. E. 1982. A catalogue of fossil amphibians and reptiles in Queensland. Memoirs of the Queensland Museum 20:613–633.
Molnar, R. E., and C. Kurz. 1997. The distribution of Pleistocene vertebrates on the eastern Darling Downs, based on the Queensland Museum collections. Proceedings of the Linnean Society of New South Wales 117:107–129.
Müller, R. D., M. Seton, S. Zahirovic, S. E. Williams, K. J. Matthews, N. M. Wright, G. E. Shephard, K. T. Maloney, N. Barnett-Moore, M. Hosseinpour, D. J. Bower, and J. Cannon. 2016. Ocean basin evolution and global-scale plate reorganization events since Pangea breakup. Annual Review of Earth and Planetary Sciences 44:107–138.
Nguyen, J. M. 2016. Australo-Papuan treecreepers (Passeriformes: Climacteridae) and a new species of sittella (Neosittidae: Daphoenositta) from the Miocene of Australia. Palaeontologia Electronica 19:1–13.
Nguyen, J. M., T. H. Worthy, W. E. Boles, S. J. Hand, and M. Archer. 2013. A new cracticid (Passeriformes: Cracticidae) from the Early Miocene of Australia. Emu-Austral Ornithology 113:374–382.
Oliver, P. M., and K. L. Sanders. 2009. Molecular evidence for Gondwanan origins of multiple lineages within a diverse Australasian gecko radiation. Journal of Biogeography 36:2044–2055.
Palci, A., M. W. Caldwell, and J. D. Scanlon. 2014. First report of a pelvic girdle in the fossil snake *Wonambi naracoortensis* Smith, 1976, and a revised diagnosis for the genus. Journal of Vertebrate Paleontology 34:965–969.
Palci, A., M. N. Hutchinson, M. W. Caldwell, J. D. Scanlon, and M. S. Lee. 2018. Palaeoecological inferences for the fossil Australian snakes *Yurlunggur* and *Wonambi* (Serpentes, Madtsoiidae). Royal Society open science 5:172012.
Pledge, N. S. 1992. The Curramulka local fauna: a new late Tertiary fossil assemblage from Yorke Peninsula, South Australia. The Beagle, Records of the Northern Territory Museum of Arts and Sciences 9:115–142.
Price, G. J., and I. H. Sobbe. 2005. Pleistocene palaeoecology and environmental change on the Darling Downs, southeastern Queensland, Australia. Memoirs of the Queensland Museum 51:171–201.

Price, G. J., M. J. Tyler, and B. N. Cooke. 2005. Pleistocene frogs from the Darling Downs, southeastern Queensland, and their palaeoenvironmental significance. Alcheringa 29:171–182.

Prideaux, G. J. 2007. MID-PLEISTOCENE VERTEBRATE RECORDS | Australia; pp. 1517-1537 in S. A. Elias (ed.), Encyclopedia of Quaternary Science. Elsevier, Oxford.

Prideaux, G. J., G. A. Gully, A. M. C. Couzens, L. K. Ayliffe, N. R. Jankowski, Z. Jacobs, R. G. Roberts, J. C. Hellstrom, M. K. Gagan, and L. M. Hatcher. 2010. Timing and dynamics of Late Pleistocene mammal extinctions in southwestern Australia. Proceedings of the National Academy of Sciences of the United States of America 107:22157–22162.

Prideaux, G. J., J. A. Long, L. K. Ayliffe, J. C. Hellstrom, B. Pillans, W. E. Boles, M. N. Hutchinson, R. G. Roberts, M. L. Cupper, L. J. Arnold, P. D. Devine, and N. M. Warburton. 2007. An arid-adapted middle Pleistocene vertebrate fauna from south-central Australia. Nature 445:422–425.

Reed, E. H., and S. J. Bourne. 2000. Pleistocene fossil vertebrate sites of the South East region of South Australia. Transactions of the Royal Society of South Australia 124:61–90.

Reed, E. H., and S. J. Bourne. 2009. Pleistocene fossil vertebrate sites of the South East region of South Australia II. Transactions of the Royal Society of South Australia 133:30–40.

Rich, T. H. 1991. Monotremes, placentals, and marsupials: their record in Australia and its biases; pp. 894–1057 in P. Vickers-Rich, J. M. Monaghan, R. F. Baird, and T. H. Rich (eds.), Vertebrate Palaeontology of Australasia. Pioneer Design Studio Pty Ltd, Melbourne, Australia.

Rieppel, O. 2002. A case of dispersing chameleons. Nature 415:744–5.

Scanlon, J. D. 1992. A new large madtsoiid snake from the Miocene of the Northern Territory. The Beagle: Records of the Museums and Art Galleries of the Northern Territory 9:49.

Scanlon, J. D. 1993. Madtsoiid snakes from the Eocene Tingamarra Fauna of eastern Queensland. Kaupia 3:3–8.

Scanlon, J. D. 1997. *Nanowana* gen. nov., small madtsoiid snakes from the Miocene of Riversleigh: Sympatric species with divergently specialised dentition Memoirs of the Queensland Museum 41:393–412.

Scanlon, J. D. 2006. Skull of the large non-macrostomatan snake *Yurlunggur* from the Australian Oligo-Miocene. Nature 439:839.

Scanlon, J. D., and M. S. Lee. 2000. The Pleistocene serpent *Wonambi* and the early evolution of snakes. Nature 403:416.

Shute, E., G. J. Prideaux, and T. H. Worthy. 2016. Three terrestrial Pleistocene coucals (Centropus: Cuculidae) from southern Australia: biogeographical and ecological significance. Zoological Journal of the Linnean Society 177:964–1002.

Shute, E., G. J. Prideaux, and T. H. Worthy. 2017. Taxonomic review of the late Cenozoic megapodes (Galliformes: Megapodiidae) of Australia. Royal Society open science 4:170233.

Simões, T. R., M. W. Caldwell, A. Palci, and R. L. Nydam. 2017. Giant taxon-character matrices: quality of character constructions remains critical regardless of size. Cladistics 33:198–219.

Skinner, A., A. F. Hugall, and M. N. Hutchinson. 2011. Lygosomine phylogeny and the origins of Australian scincid lizards. Journal of Biogeography 38:1044–1058.

Skinner, A., M. N. Hutchinson, and M. S. Y. Lee. 2013. Phylogeny and divergence times of Australian *Sphenomorphus* group skinks (Scincidae, Squamata). Molecular Phylogenetics and Evolution 69:906–918.

Smith, M. J. 1976. Small fossil vertebrates from Victoria Cave, Naracoorte, South Austraia. IV, Reptiles. Transactions of the Royal Society of South Australia 100:39–51.

Stadler, T. 2010. Sampling-through-time in birth–death trees. Journal of Theoretical Biology 267:396–404.

Tedford, R., R. Wells, and S. Barghoorn. 1992. Tirari Formation and contained faunas, Pliocene of the Lake Eyre Basin, South Australia. The Beagle: Records of the Museums and Art Galleries of the Northern Territory 9:173–194.

Thorn, K. M., M. N. Hutchinson, M. Archer, and M. S. Y. Lee. 2019. A new scincid lizard from the Miocene of Northern Australia, and the evolutionary history of social skinks (Scincidae: Egerniinae). Journal of Vertebrate Paleontology 39:e1577873.

Thorn, K. M., C. I. Nielsen, M. Archer, M. N. Hutchinson, and M. S. Y. Lee. 2017. Dating Australian skink diversification: fossil *Sphenomorphus* and *Egernia* group skinks from Riversleigh World Heritage Area (Queensland, Australia). Geological Society of Australia Abstracts 125:39.

Title, P. O., and D. L. Rabosky. 2016. Do macrophylogenies yield stable macroevolutionary inferences? An example from squamate reptiles. Systematic biology 66:843–856.

Travouillon, K. J., S. Legendre, M. Archer, and S. J. Hand. 2009. Palaeoecological analyses of Riversleigh's Oligo-Miocene sites: Implications for Oligo-Miocene climate change in Australia. Palaeogeography, Palaeoclimatology, Palaeoecology 276:24–37.

Tyler, M. J., and G. J. Prideaux. 2016. Early to middle Pleistocene occurrences of *Litoria*, *Neobatrachus* and *Pseudophryne* (Anura) from the Nullarbor Plain, Australia: first frogs from the "frog-free zone". Memoirs of Museum Victoria 74:403–408.

Villa, A., H.-A. Blain, and M. Delfino. 2018. The Early Pleistocene herpetofauna of Rivoli Veronese (Northern Italy) as evidence for humid and forested glacial phases in the Gelasian of Southern Alps. Palaeogeography, Palaeoclimatology, Palaeoecology 490:393-403.

Williams, D. L. G. 1980. Catalogue of Pleistocene vertebrate fossils and sites in South Australia. Transactions of the Royal Society of South Australia 104:101–115.

Worthy, T. H. 2009. Descriptions and phylogenetic relationships of two new genera and four new species of Oligo-Miocene waterfowl (Aves: Anatidae) from Australia. Zoological Journal of the Linnean Society 156:411–454.

Worthy, T. H. 2011. Descriptions and phylogenetic relationships of a new genus and two new species of Oligo-Miocene cormorants (Aves: Phalacrocoracidae) from Australia. Zoological Journal of the Linnean Society 163:277–314.

BIBLIOGRAPHY

Alekseyenko, A. V., C. J. Lee, and M. A. Suchard. 2008. Wagner and Dollo: a stochastic duet by composing two parsimonious solos. Systematic biology 57:772–784.

Andrews, P. 1990. Owls, caves and fossils. The Natural History Museum, London, 230 pp.

Ansari, M. H., S. J. Cooper, M. P. Schwarz, M. Ebrahimi, G. Dolman, L. Reinberger, K. M. Saint, S. C. Donnellan, C. M. Bull, and M. G. Gardner. 2019. Plio-Pleistocene diversification and biogeographic barriers in southern Australia reflected in the phylogeography of a widespread and common lizard species. Molecular Phylogenetics and Evolution 133:107–119.

Archer, M. 1972. *Phascolarctos* (Marsupialia, Vombatoidea) and an associated fossil fauna from Koala Cave near Yanchep, Western Australia. Helictite 10:49–59.

Archer, M. 1974. Excavations in the Orchestra Shell Cave, Wanneroo, Western Australia: Part III. Fossil vertebrate remains. Archaeology & Physical Anthropology in Oceania 9:156–162.

Archer, M. 1978. Quaternary vertebrate faunas from the Texas Caves of southeastern Queensland. Memoirs of the Queensland Museum 19:61–109.

Archer, M., D. A. Arena, M. Bassarova, R. M. D. Beck, K. Black, W. E. Boles, P. Brewer, B. N. Cooke, K. Crosby, A. Gillespie, H. Godthelp, S. J. Hand, B. P. Kear, J. Louys, A. Morrell, J. Muirhead, K. K. Roberts, J. D. Scanlon, K. J. Travouillon, and S. Wroe. 2006. Current status of species-level representation in faunas from selected fossil localities in the Riversleigh World Heritage Area, northwestern Queensland. Alcheringa: An Australasian Journal of Palaeontology 30:1–17.

Arena, D. A., K. H. Black, M. Archer, S. J. Hand, H. Godthelp, and P. Creaser. 2014. Reconstructing a Miocene pitfall trap: Recognition and interpretation of fossiliferous Cenozoic palaeokarst. Sedimentary Geology 304:28–43.

Arida, E. A., and M. Bull. 2008. Optimising the design of artificial refuges for the Australian skink, Egernia stokesii. Applied Herpetology 5:161–172.

Atkins, Z. S., M. D. Amor, N. Clemann, D. G. Chapple, G. M. While, M. G. Gardner, M. L. Haines, K. A. Harrisson, M. Schroder, and K. A. Robert. 2019. Allopatric divergence drives the genetic structuring of an endangered alpine endemic lizard with a sky-island distribution. Animal Conservation.

Atlas of Living Australia. 2019. Mapping and Analyses Spatial Portal;Commonwealth Scientific and Industrial Research Organisation.

Austin, J. J., and E. N. Arnold. 2006. Using ancient and recent DNA to explore relationships of extinct and endangered *Leiolopisma* skinks (Reptilia: Scincidae) in the Mascarene islands. Molecular Phylogenetics and Evolution 39:503–511.

Australian Bureau of Meteorology. 2006. Koeppen climate classification (base climate related classification datasets) Commonwealth of Australia ed Atlas of Living Australia, Victoria, Australia.

Balme, J. 1995. 30,000 years of fishery in western New South Wales. Archaeology in Oceania 30:1–21.

Bartholomai, A. 1977. The fossil vertebrate fauna from Pleistocene deposits at Cement Mills, Gore, Queensland. Memoirs of the Queensland Museum 18:41–51.

Baynes, A., and R. Baird. 1992. The original mammal fauna and some information on the original bird fauna of Uluru National Park, Northern Territory. The Rangeland Journal 14:92–106.

Baynes, A., C. Piper, and K. M. Thorn. 2019. An experimental investigation of differential recovery of native rodent remains from Australian palaeontological and archaeological deposits. Records of the Western Australian Museum 34:1–30.

Bell, C. J., and J. I. Mead. 2014. Not enough skeletons in the closet: Collections-based anatomical research in an age of conservation conscience. The Anatomical Record 297:344–348.

Bell, C. J., J. J. Head, and J. I. Mead. 2004. Synopsis of the herpetofauna from Porcupine Cave; pp. 117–126 in A. D. Barnosky (ed.), Biodiveristy response to climate change in the Middle Pleistocene: The Porcupine Cave Fauna from Colorado. University of California Press, Oakland, California.

Bell, C. J., J. A. Gauthier, and G. S. Bever. 2010. Covert biases, circularity, and apomorphies: A critical look at the North American Quaternary Herpetofaunal Stability Hypothesis. Quaternary International 217:30–36.

Benton, M. J. 1984. The relationships and early evolution of the Diapsida; pp. 575–596 in M. W. J. Ferguson (ed.), The Structure, Development and Evolution of Reptiles. Cambridge University Press, London, United Kingdom.

Benton, M. J., and B. C. Emerson. 2007. How did life become so diverse? The dynamics of diversification according to the fossil record and molecular phylogenetics. Palaeontology 50:23–40.

Black, K. H., A. B. Camens, M. Archer, and S. J. Hand. 2012. Herds overhead: *Nimbadon lavarackorum* (Diprotodontidae) heavyweight marsupial herbivores in the Miocene rainforests of Australia. PLoS ONE 7:e48213.

Black, K. H., M. Archer, S. J. Hand, and H. Godthelp. 2012. The rise of Australian marsupials: a synopsis of biostratigraphic, phylogenetic, palaeoecologic and palaeobiogeographic understanding; pp. 983–1078 in J. A. Talent (ed.), Earth and Life. Springer Science.

Black, K. H., K. J. Travouillon, T. J. Myers, M. Archer, S. J. Hand, and L. A. B. Wilson. 2015. Functional and geometric morphometric analysis of a middle Miocene bandicoot (Marsupialia, Peramelemorphia) skeleton from the Riversleigh World Heritage Area, Australia. Journal of Vertebrate Paleontology Program and Abstracts, 2015:91.

Blain, H.-A., S. Bailon, and G. Cuenca-BescГis. 2008. The Early to Middle Pleistocene palaeoenvironmental change based on the squamate reptile and amphibian proxies at the Gran Dolina site, Atapuerca, Spain. Palaeogeography, Palaeoclimatology, Palaeoecology 261:177–192.

Blain, H.-A., J. A. C. Silva, J. M. J. Arenas, V. Margari, and K. Roucoux. 2018. Towards a Middle Pleistocene terrestrial climate reconstruction based on herpetofaunal assemblages from the Iberian Peninsula: State of the art and perspectives. Quaternary Science Reviews 191:167–188.

Boles, W. E. 2017. A brief history of avian palaeontology in Australia; pp. 265–362 in Memoirs of the Nuttal Ornithological Club, Vol. III The Nuttal Ornithological Club, Cambridge, Massachusetts.

Borch, C. C. V. D., and D. Lock. 1979. Geological significance of Coorong dolomites. Sedimentology 26:813–824.

Bremer, K. 1988. The limits of amino acid sequence data in angiosperm phylogenetic reconstruction. Evolution 42:795–803.

Broeckhoven, C., C. De Kock, and C. Hui. 2018. Sexual dimorphism in the dermal armour of cordyline lizards (Squamata: Cordylinae). Biological Journal of the Linnean Society 125:30–36.

Brown, C. M., C. S. van Buren, D. W. Larson, K. S. Brink, N. E. Campione, M. J. Vavrek, and D. C. Evans. 2015. Tooth counts through growth in diapsid reptiles: implications for interpreting individual and size-related variation in the fossil record. Journal of Anatomy 226:322–333.

Brown, G. 1991. Ecological feeding analysis of south-eastern Australian scincids (Reptilia, Lacertilia). Australian Journal of Zoology 39:9–29.

Bull, C. M. 2000. Monogamy in lizards. Behavioural Processes 51:7–20.

Bull, C. M., and Y. Pamula. 1996. Sexually dimorphic head sizes and reproductive success in the sleepy lizard *Tiliqua rugosa*. Journal of Zoology 240:511–521.

Bull, M., M. Hutchinson, and A. Fenner. 2007. Omnivorous diet of the endangered Pygmy Bluetongue Lizard, *Tiliqua adelaidensis*. Amphibia-Reptilia 28:560–565.

Burbrink, F. T., F. G. Grazziotin, R. A. Pyron, D. Cundall, S. Donnellan, F. Irish, J. S. Keogh, F. Kraus, R. W. Murphy, B. Noonan, C. J. Raxworthy, S. Ruane, A. R. Lemmon, E. M. Lemmon, and H. Zaher. 2019. Interrogating genomic-scale data for Squamata (lizards, snakes, and amphisbaenians) shows no support for key traditional morphological relationships. Systematic biology.

Butler, W. H., and D. Merrilees. 1971. Remains of *Potorous platyops* (Marsupialia, Macropodidae) and other mammals from Bremer Bay, Western Australia. Journal of The Royal Society of Western Australia 54:53–58.

Byrne, M., D. K. Yeates, L. Joseph, M. Kearney, J. Bowler, M. A. J. Williams, S. Cooper, S. C. Donnellan, J. S. Keogh, R. Leys, J. Melville, D. J. Murphy, N. Porch, and K. H. Wyrwoll. 2008. Birth of a biome: insights into the assembly and maintenance of the Australian arid zone biota. Molecular Ecology 17:4398–4417.

Byrne, M., D. A. Steane, L. Joseph, D. K. Yeates, G. J. Jordan, D. Crayn, K. Aplin, D. J. Cantrill, L. G. Cook, M. D. Crisp, J. S. Keogh, J. Melville, C. Moritz, N. Porch, J. M. K. Sniderman, P. Sunnucks, and P. H. Weston. 2011. Decline of a biome: evolution, contraction, fragmentation, extinction and invasion of the Australian mesic zone biota. Journal of Biogeography 38:1635–1656.

Callen, R. A. 1977. Late Cainozoic environments of part of northeastern South Australia. Journal of the Geological Society of Australia: An International Geoscience Journal of the Geological Society of Australia 24:151–169.

Callen, R. A., and R. H. Tedford. 1976. New Late Cainozoic rock units and depositional environments, Lake Frome area, South Australia. Transactions of the Royal Society of South Australia 100:125–167.

Camin, J. H., and R. R. Sokal. 1965. A method for deducing branching sequences in phylogeny. Evolution 19:311–326.

Camp, C. L. 1923. Classification of lizards. Bulletin of the American Museum of Natural History 48:289–481.

Carranza, S., and E. N. Arnold. 2003. Investigating the origin of transoceanic distributions: Mtdna shows *Mabuya* lizards (Reptilia, Scincidae) crossed the Atlantic twice. Systematics and Biodiversity 1:275–282.

Čerňanský, A., and M. N. Hutchinson. 2013. A new large fossil species of *Tiliqua* (Squamata: Scincidae) from the Pliocene of the Wellington Caves (New South Wales, Australia). Alcheringa: An Australasian Journal of Palaeontology 37:131–136.

Chapman, A. D. 2009. Numbers of living species in Australia and the world. Australian Biological Resources Study, Toowoomba, Australia.

Chapple, D. G. 2003. Ecology, life-history, and behavior in the Australian scincid genus *Egernia*, with comments on the evolution of complex sociality in lizards. Herpetological Monographs 17:145–180.

Chapple, D. G., and J. S. Keogh. 2004. Parallel adaptive radiations in arid and temperate Australia: molecular phylogeography and systematics of the *Egernia whitii* (Lacertilia: Scincidae) species group. Biological Journal of the Linnean Society 83:157–173.

Chapple, D. G., and J. S. Keogh. 2005. Complex mating system and dispersal patterns in a social lizard, Egernia whitii. Molecular Ecology 14:1215–1227.

Chapple, D. G., J. S. Keogh, and M. N. Hutchinson. 2004. Molecular phylogeography and systematics of the arid-zone members fo the *Egernia whitii* (Lacertilia: Scincidae) species group. Molecular Phylogenetics and Evolution 33:549–561.

Chapple, D. G., P. A. Ritchie, and C. H. Daugherty. 2009. Origin, diversification, and systematics of the New Zealand skink fauna (Reptilia: Scincidae). Molecular Phylogenetics and Evolution 52:470–487.

Clemann, N., M. Hutchinson, P. Robertson, D. C. Chapple, G. Gillespie, J. Melville, and D. Michael. 2018. *Liopholis montana*; pp. e.T109478522A109478529 The IUCN Red List of Threatened Species.

Cogger, H., E. Cameron, and H. Cogger. 1983. Zoological catalogue of Australia. Vol. 1. Amphibia and Reptilia. Bureau of Flora and Fauna: Canberra:313.
Cogger, H. G. 2018. Reptiles & Amphibians of Australia. Updated 7th Edition. CSIRO Publishing, Clayton South, Victoria, Australia.
Conrad, J. L. 2008. Phylogeny and systematics of Squamata (Reptilia) based on morphology. Bulletin of the American Museum of Natural History:1–182.
Cosgrove, R. 1995. Late Pleistocene behavioural variation and time trends: the case from Tasmania. Archaeology in Oceania 30:83–104.
Crisp, M. D., and L. G. Cook. 2009. EXPLOSIVE RADIATION OR CRYPTIC MASS EXTINCTION? INTERPRETING SIGNATURES IN MOLECULAR PHYLOGENIES. Evolution 63:2257-2265.
Darwin, C. 1859. The origin of species by means of natural selection or the preservations of favoured races in the struggle for life. 1st Edition. John Murray, London, 502 pp.
Dawson, L., and M. Augee. 1997. The late Quaternary sediments and fossil vertebrate fauna from Cathedral Cave, Wellington Caves, New South Wales. Proceedings-Linnean Society of New South Wales 117:51–78.
De Pietri, V. L., R. P. Scofield, S. J. Hand, A. J. D. Tennyson, and T. H. Worthy. 2016. Sheathbill-like birds (Charadriiformes: Chionoidea) from the Oligocene and Miocene of Australasia. Journal of the Royal Society of New Zealand 46:181-199.
Diogo, R., and V. Abdala. 2010. The head muscles of Dipnoans - a review on the homologies and evolution of these muscles within vertebrates; pp. 169–218 in J. M. Jorgensen and J. Joss (eds.), Biology of Lungfishes. Science Publishers and Taylor and Francis, Oxford, UK.
Dodson, J., R. Fullagar, J. Furby, R. Jones, and I. Prosser. 1993. Humans and megafauna in a late Pleistocene environment from Cuddie Springs, north western New South Wales. Archaeology in Oceania 28:94–99.
Dortch, C. E., and D. Merrilees. 1971. A salvage excavation in Devils Lair, Western Australia. Journal of The Royal Society of Western Australia 54:103–113.
Dortch, J., and R. Wright. 2010. Identifying palaeo-environments and changes in Aboriginal subsistence from dual-patterned faunal assemblages, south-western Australia. Journal of Archaeological Science 37:1053–1064.
Doughty, P., L. Kealley, and S. C. Donnellan. 2011. Revision of the Pygmy Spiny-tailed Skinks (*Egernia depressa* species-group) from Western Australia, with descriptions of three new species. Records of the Western Australian Museum 26:115–137.
Douglas, A. M., G. W. Kendrick, and D. Merrilees. 1966. A fossil bone deposit near Perth, Western Australia, interpreted as a carnivore's den after feeding tests on living *Sarcophilus* (Marsupialia, Dasyuridae). Journal of The Royal Society of Western Australia 49:88–90.
Drummond, A. J., and M. Suchard. 2010. Bayesian random local clocks, or one rate to rule them all. BMC Biology 8:114.
Drummond, A. J., S. Y. W. Ho, M. J. Phillips, and A. Rambaut. 2006. Relaxed phylogenetics and dating with confidence. PLOS Biology 4:e88.
Drummond, A. J., M. A. Suchard, D. Xie, and A. Rambaut. 2012. Bayesian phylogenetics with BEAUti and the BEAST 1.7. Molecular biology and evolution 29:1969–1973.
Dubas, G., and C. Bull. 1991. Diet choice and food availability in the omnivorous lizard, *Trachydosaurus rugosus*. Wildlife Research 18:147–155.
Edgecombe, G. D. 2010. Palaeomorphology: fossils and the inference of cladistic relationships. Acta Zoologica 91:72-80.
Edwards, A. W. F., and L. L. Cavalli-Sforza. 1963. The reconstruction of evolution. Annals of Human Genetics 27:105–106.
Estes, R. 1984. Fish, amphibians and reptiles from the Etadunna Formation, Miocene of South Australia. Australian Zoologist 21:335–343.
Estes, R., and E. E. Williams. 1984. Ontogenetic variation in the molariform teeth of lizards. Journal of Vertebrate Paleontology 4:96–107.

Estes, R., K. De Queiroz, and J. Gauthier. 1988. Phylogenetic relationships of the lizard families. Stanford Univ Press, Stanford, CA, Stanford, California, 648 pp.
Etheridge, R., and K. de Queiroz. 1988. A phylogeny of Iguanidae; pp. 283–367 in R. Estes and G. Pregill (eds.), Phylogenetic relationships of the lizard families. Stanford University Press, Stanford, California.
Etheridge, R. J. 1917. *Megalania prisca*, Owen and *Notiosaurus dentatus*, Owen; lacertilian dermal armour; opalised remains from Lightening Ridge. Proceedings of the Royal Society of Victoria 29:127–133.
Evans, S. E. 2003. At the feet of the dinosaurs: the early history and radiation of lizards. Biological Reviews 78:513–551.
Evans, S. E. 2008. The skull of lizards and Tuatara; pp. 1–343 in C. Gans, A. S. Gaunt, and K. Adler (eds.), Biology of the Reptilia 20, Morphology H The skull of Lepidosauria. Society for the Study of Amphibians and Reptiles, Ithaca, NY.
Evans, S. E., and M. E. Jones. 2010. The origin, early history and diversification of lepidosauromorph reptiles; pp. 27–44, New aspects of Mesozoic biodiversity. Springer Berlin Heidelberg.
Felsenstein, J. 1985. Confidence limits on phylogenies: An approach using the bootstrap. Evolution 39:783–791.
Felsenstein, J. 2004. Inferring Phylogenies. Sinauer Associates, Sunderland, Massachusetts.
Fitzgerald, E. M. G. 2004. A review of the Tertiary fossil Cetacea (Mammalia) localities in Australia. Memoirs of Museum Victoria 61:183–208.
Fitzinger, L. 1843. Systema reptilium. Fasciculus primus, Amblyglossae. Braumüller et Seidel, Vienna, Austria.
Flannery, T. F., and R. G. Roberts. 1999. Late Quaternary extinctions in Australasia; pp. 248–260 in R. D. E. MacPhee and H.-D. Sues (eds.), Extinctions in near time. Springer Science & Business Media, United States of America.
Fordham, D. A., M. J. Watts, S. Delean, B. W. Brook, L. M. B. Heard, and C. M. Bull. 2012. Managed relocation as an adaptation strategy for mitigating climate change threats to the persistence of an endangered lizard. Global Change Biology 18:2743–2755.
Fraser, R. A., and R. T. Wells. 2006. Palaeontological excavation and taphonomic investigation of the late Pleistocene fossil deposit in Grant Hall, Victoria Fossil Cave, Naracoorte, South Australia. Alcheringa: An Australasian Journal of Palaeontology 30:147–161.
Frost, D. R., and R. Etheridge. 1989. A phylogenetic analysis and taxonomy of iguanian lizards (Reptilia: Squamata). Miscellaneous Publication of the University of Kansas Museum of Natural History 81:1–65.
Gans, C., F. De Vree, and D. Carrier. 1985. Usage pattern of the complex masticatory muscles in the Shingleback lizard, *Trachydosaurus rugosus*: a model for muscle placement. The American Journal of Anatomy 173:219–240.
Gardner, M. G., C. M. Bull, and S. J. B. Cooper. 2002. High levels of genetic monogamy in the group-living Australian lizard Egernia stokesii. Molecular Ecology 11:1787–1794.
Gardner, M. G., A. F. Hugall, S. C. Donnellan, M. N. Hutchinson, and R. Foster. 2008. Molecular systematics of social skinks: phylogeny and taxonomy of the *Egernia* group (Reptilia: Scincidae). Zoological Journal of the Linnean Society 154:781–794.
Gauthier, J. 1984. A cladistic analysis of the higher systematic categories of the Diapsida. University of California, Berkley, California, USA.
Gauthier, J., A. G. Kluge, and T. Rowe. 1988. Amniote phylogeny and the importance of fossils. Cladistics 4:105–209.
Gauthier, J. A., M. Kearney, J. A. Maisano, O. Rieppel, and A. D. B. Behlke. 2012. Assembling the Squamate Tree of Life: Perspectives from the Phenotype and the Fossil Record. Bulletin of the Peabody Museum of Natural History 53:3–308.

Gavryushkina, A., D. Welch, T. Stadler, and A. J. Drummond. 2014. Bayesian inference of sampled ancestor trees for epidemiology and fossil calibration. PLOS Computational Biology 10:e1003919.
Gavryushkina, A., T. A. Heath, D. T. Ksepka, T. Stadler, D. Welch, and A. J. Drummond. 2017. Bayesian total-evidence dating reveals the recent crown radiation of penguins. Systematic biology 66:57–73.
Gelnaw, W. B. 2011. On the cranial osteology of *Eremiascincus* and its use for identification. Biological Sciences, East Tennessee State University, 253 pp.
Germano, D. J. 1994. Growth and age at maturity of North American tortoises in relation to regional climates. Canadian Journal of Zoology 72:918–931.
Gillespie, G., J. Woinarski, P. McDonald, H. Cogger, and A. Fenner. 2018. *Bellatorias obiri*; pp. e.T47155317A47155335 The IUCN Red List of Threatened Species.
Godthelp, H., M. Archer, R. Cifelli, S. J. Hand, and C. F. Gilkeson. 1992. Earliest known Australian Tertiary mammal fauna. Nature 356:514–516.
Goloboff, P. A., and S. A. Catalano. 2016. TNT version 1.5, including a full implementation of phylogenetic morphometrics. Cladistics 32:221–238.
Goloboff, P. A., C. I. Mattoni, and A. S. Quinteros. 2006. Continuous characters analyzed as such. Cladistics 22:589–601.
Goloboff, P. A., J. Farris, and K. Nixon. 2008. TNT, a free program for phylogenetic analysis. Cladistics 24:774–786.
Goloboff, P. A., M. Pittman, D. Pol, and X. Xu. 2018. Morphological data sets fit a common mechanism much more poorly than DNA sequences and call into question the Mkv model. Systematic biology 68:494–504.
Gray, J. E. 1825. A synopsis of the genera of reptiles and Amphibia, with a description of some new species. Annals of Philosophy 10:193–217.
Gray, J. E. 1838. Catalogue of the slender-tongued saurians, with descriptions of many new genera and species (continued). Annals and Magazine of Natural History 2:287–293.
Greer, A. E. 1970. A subfamilial classification of scincid lizards. Bulletin of the Museum of Comparative Zoology at Harvard College 139:151–183.
Greer, A. E. 1979. A phylogenetic subdivision of Australian skinks. Records of the Australian Museum 32:339–371.
Greer, A. E. 1989. The biology and evolution of Australian lizards. Surrey Beatty & Sons, Chipping Norton, NSW, 264 pp.
Greer, A. E. 2001. Distribution of maximum snout-vent length among species of scincid lizards. Journal of Herpetology 35:383–395.
Gunther, A. 1877. Notice on two large extinct lizards, formerly inhabiting the Mascarence Islands. Journal of the Linnean Society of Zoology 13:323–327.
Haas, G. 1974. Muscles of the jaws and associated structures in the Rhynchocephalia and Squamata; pp. 285–490 in C. Gans (ed.), Biology of the Reptilia. Academic Press, London and New York.
Hagen, I. J., S. C. Donnellan, and C. M. Bull. 2012. Phylogeography of the prehensile-tailed skink *Corucia zebrata* on the Solomon Archipelago. Ecology and evolution 2:1220–1234.
Hall, B. K. 2007. Fins Into Limbs: Evolution, Development, and Transformation. University of Chicago Press, Chicago, Illinois, 433 pp.
Hall, R. 2002. Cenozoic geological and plate tectonic evolution of SE Asia and the SW Pacific: computer-based reconstructions, model and animations. Journal of Asian Earth Sciences 20:353–431.
Hamilton, A. 2013. The evolution of phylogenetic systematics. University of California Press, Oakland, California, 320 pp.
Hammer, Ø., D. A. T. Harper, and P. D. Ryans. 2001. PAST: Paleontological statistics software package for education and data analysis. Paleontologia Electronica 4:9.

Harmon, L. J. 2019. Phylogenetic comparative methods. 1.4 Edition. Luke Harmon, Published Online, 234 pp.
Heath, T. A., J. P. Huelsenbeck, and T. Stadler. 2014. The fossilized birth–death process for coherent calibration of divergence-time estimates. Proceedings of the National Academy of Sciences 111:E2957–E2966.
Hedges, S. B. 2014. The high-level classification of skinks (Reptilia, Squamata, Scincomorpha). Zootaxa 3765:317–338.
Hedges, S. B., J. Marin, M. Suleski, M. Paymer, and S. Kumar. 2015. Tree of life reveals clock-like speciation and diversification. Molecular biology and evolution 32:835–845.
Hennig, W. 1966. Phylogenetic systematics. University of Illinois Press, Chicago, USA, 263 pp.
Hildebrand, M., and G. E. Goslow. 2001. Analysis of vertebrate structure. 5th Edition. Wiley, New York, 635 pp.
Hocknull, S. A. 2000. Remains of an Eocene skink from Queensland. Alcheringa: An Australasian Journal of Palaeontology 24:63–64.
Hocknull, S. A. 2005. Ecological succession during the late Cainozoic of central eastern Queensland: extinction of a diverse rainforest community. Memoirs of the Queensland Museum 51:39–122.
Hocknull, S. A. 2009. Late Cainozoic rainforest vertebrates from Australopapua: evolution, biogeography and extinction. Biological, Earth and Environmental Sciences, Faculty of Science, University of New South Wales, 628 pp.
Hoffstetter, R. 1949. Les reptiles subfossils de L'ile Maurice: 1. Les Scincidae. Annales de Paleontologie 35:43–72.
Hoffstetter, R., and J.-P. Gasc. 1969. Vertebrae and ribs of modern reptiles; pp. 201–310 in C. Gans (ed.), Biology of the Reptilia. Academic Press, New York.
Hollenshead, M. G. 2011. Geometric morphometric analysis of cranial variation in the *Egernia depressa* (Reptilia: Squamata: Scincidae) species complex. Records of the Western Australian Museum 26:138–153.
Hollenshead, M. G., J. I. Mead, and S. L. Swift. 2011. Late Pleistocene *Egernia* group skinks (Squamata: Scincidae) from Devils Lair, Western Australia. Alcheringa: An Australasian Journal of Palaeontology 35:31–51.
Honda, M., H. Ota, M. Kobayashi, and T. Hikida. 1999. Phylogenetic relationships of Australian skinks of the *Mabuya* group (Reptilia: Scincidae) inferred from mitochondrial DNA sequences. Genes and Genetics Systems 74:135–139.
Honda, M., H. Ota, M. Kobayashi, J. Nabhitabhata, H.-S. Yong, and T. Hikida. 2000. Phylogenetic relationships, character evolution, and biogeography of the subfamily Lygosominae (Reptilia: Scincidae) inferred from mitochondrial DNA sequences. Molecular Phylogenetics and Evolution 15:452–461.
Hope, J. H. 1978. Pleistocene mammal extinctions: the problem of Mungo and Menindee, New South Wales. Alcheringa: An Australasian Journal of Palaeontology 2:65–82.
Hope, J. H., R. J. Lampert, E. Edmondson, M. J. Smith, and G. F. Van Tets. 1977. Late Pleistocene faunal remains from Seton Rock Shelter, Kangaroo Island, South Australia. Journal of Biogeography:363–385.
Horton, D. R. 1972. Evolution in the genus *Egernia* (Lacertilia:Scincidae). Journal of Herpetology 6:101–109.
Houle, A. 1998. Floating Islands: A mode of long-distance dispersal for small and medium- sized terrestrial vertebrates. Diversity and Distributions 4:201–216.
Hugall, A. F., and M. S. Y. Lee. 2004. Molecular claims of Gondwanan age for Australian agamid lizards are untenable. Molecular biology and evolution 21:2102–2110.
Hugall, A. F., R. Foster, M. Hutchinson, and M. S. Y. Lee. 2008. Phylogeny of Australasian agamid lizards based on nuclear and mitochondrial genes: implications for morphological evolution and biogeography. Biological Journal of the Linnean Society 93:343–358.

Hutchinson, M. N. 1981: The systematic relationships of the genera *Egernia* and *Tiliqua* (Lacertilia: Scincidae). A review and immunological reassessment. Proceedings of the Melbourne Herpetological Symposium, 1981.
Hutchinson, M. N. 1992. Origins of the Australian scincid lizards: a preliminary report on the skinks of Riversleigh. The Beagle, Records of the Northern Territory Museum of Arts and Sciences 9:61–70.
Hutchinson, M. N., and B. S. Mackness. 2002. Fossil lizards from the Pliocene Chinchilla Local Fauna, Queensland. Records of the South Australian Museum 35:169–184.
Hutchinson, M. N., and J. D. Scanlon. 2009. New and unusual Plio-Pleistocene lizard (Reptilia: Scincidae) from Wellington Caves, New South Wales, Australia. Journal of Herpetology 43:139–147.
John-Alder, H. B., T. G. Jr., and A. F. Bennett. 1986. Locomotory capacities, oxygen consumption, and the cost of locomotion of the shingle-back lizard (*Trachydosaurus rugosus*). Physiologial Zoology 59:523–531.
Kear, B. P., and R. J. Hamilton-Bruce. 2011. Dinosaurs in Australia: Mesozoic life from the southern continent. CSIRO Publishing, Australia.
Kear, B. P., M. Archer, and T. F. Flannery. 2001. Postcranial morphology of *Ganguroo bilamena* Cooke,1997 (Marsupialia: Macropodidae) from the Middle Miocene of Riversleigh, northwestern Queensland. Memoirs of the Association of Australasian Palaeontologists 25:123–138.
Kendrick, G. W., and J. K. Porter. 1973. Remains of a thylacine (Marsupialia: Dasyuroidea) and other fauna from Caves in the Cape Range, Western Australia. Journal of The Royal Society of Western Australia 56:116–122.
King, B., and M. S. Y. Lee. 2015. Ancestral state reconstruction, rate heterogeneity, and the evolution of reptile viviparity. Systematic biology 64:532–544.
King, G. 1996. Reptiles and herbivory. Chapman & Hall, London, UK, 160 pp.
Klingenböck, A., K. Osterwalder, and R. Shine. 2000. Habitat use and thermal biology of the “Land mullet” *Egernia major*, a large Scincid lizard from remnant rain forest in southeastern Australia. Copeia 2000:931–939.
Kluge, A. G., and T. Grant. 2006. From conviction to anti-superfluity: old and new justifications of parsimony in phylogenetic inference. Cladistics 22:276–288.
Kosma, R. 2003. The dentitions of recent and fossil scincomorphan lizards (Lacertilia, Squamata) - Systematics, Functional Morphology, Palecology. Department of Geosciences and Geography, University Hannover, Hanover, Germany, 231 pp.
Lagarde, F., X. Bonnet, J. Corbin, B. Henen, K. Nagy, B. Mardonov, and G. Naulleau. 2003. Foraging behaviour and diet of an ecotothermic herbivore: *Testudo horsfieldi*. Ecography 26:236–242.
Lambert, S. M., T. W. Reeder, and J. J. Wiens. 2015. When do species-tree and concatenated estimates disagree? An empirical analysis with higher-level scincid lizard phylogeny. Molecular Phylogenetics and Evolution 82:146–155.
Lanfear, R., P. B. Frandsen, A. M. Wright, T. Senfeld, and B. Calcott. 2016. PartitionFinder 2: new methods for selecting partitioned models of evolution for molecular and morphological phylogenetic analyses. Molecular biology and evolution 34:772–773.
Lang, M. 1991. Generic relationships within Cordyliformes (Reptilia: Squamata). Bulletin de l’Institut Royal des Sciences Naturelles de Belgique. Biologie 61:121–188.
Laurin, M. 2012. Recent progress in paleontological methods for dating the Tree of Life. Frontiers in Genetics 3.
Lécuru, S. 1969: Étude morphologique de l’humérus des lacertiliens. Annales des Sciences Naturelles, Zoologie (12), 1969.
Lee, M. S. Y. 1998. Convergent evolution and character correlation in burrowing reptiles: towards a resolution of squamate relationships. Biological Journal of the Linnean Society 65:369–453.

Lee, M. S. Y. 2000. Soft anatomy, diffuse homoplasy, and the relationships of lizards and snakes. Zoologica scripta 29:101–130.
Lee, M. S. Y., and A. Palci. 2015. Morphological phylogenetics in the genomic age. Current Biology 25:R922–R929.
Lee, M. S. Y., P. M. Oliver, and M. N. Hutchinson. 2009a. Phylogenetic uncertainty and molecular clock calibrations: A case study of legless lizards (Pygopodidae, Gekkota). Molecular Phylogenetics and Evolution 50:661–666.
Lee, M. S. Y., A. Cau, D. Naish, and G. J. Dyke. 2014. Morphological Clocks in Paleontology, and a Mid-Cretaceous Origin of Crown Aves. Systematic biology 63:442–449.
Lee, M. S. Y., M. N. Hutchinson, T. H. Worthy, M. Archer, A. J. D. Tennyson, J. P. Worthy, and R. P. Scofield. 2009b. Miocene skinks and geckos reveal long-term conservatism of New Zealand's lizard fauna. Biology Letters 5:833–837.
Lemey, P., A. Rambaut, J. J. Welch, and M. A. Suchard. 2010. Phylogeography takes a relaxed random walk in continuous space and time. Molecular biology and evolution 27:1877–1885.
Lewis, P. O. 2001. A likelihood approach to estimating phylogeny from discrete morphological character data. Systematic biology 50:913–925.
Louys, J., and G. J. Price. 2013. The Chinchilla Local Fauna: an exceptionally rich and well-preserved Pliocene vertebrate assemblage from fluviatile deposits of south-eastern Queensland, Australia. Acta Palaeontologica Polonica 60:551–573.
Lyman, R. L. 1994. Vertebrate Taphonomy. Cambridge University Press, Cambridge, 555 pp.
Mackness, B. S., and M. N. Hutchinson. 2000. Fossil lizards from the Early Pliocene Bluff Downs Local Fauna. Transactions of the Royal Society of South Australia 124:17–30.
Maddison, W., and D. Maddison. 2017. Mesquite: a modular system for evolutionary analysis. Version 3.2.
Maloney, T., S. O'Connor, R. Wood, K. Aplin, and J. Balme. 2018. Carpenters Gap 1: A 47,000 year old record of indigenous adaption and innovation. Quaternary Science Reviews 191:204–228.
Marianelli, P. C. 1995. Palaeoenvironmental study of Quaternary fossiliferous fissure fills of the Katherine Area, N. T., Faculty of Science and Engineering, Flinders University.
Martin, H. A. 2006. Cenozoic climatic change and the development of the arid vegetation in Australia. Journal of Arid Environments 66:533–563.
Martin, J. E., M. N. Hutchinson, R. Meredith, J. A. Case, and N. S. Pledge. 2004. The oldest genus of scincid lizard (Squamata) from the Tertiary Etadunna Formation of South Australia. Journal of Herpetology 38:180–187.
McDowell, M. C., and G. C. Medlin. 2009. The effects of drought on prey selection of the barn owl (*Tyto alba*) in the Strzelecki Regional Reserve, north-eastern South Australia. Australian Mammalogy 31:47–55.
McDowell, M. C., A. Baynes, G. C. Medlin, and G. J. Prideaux. 2012. The impact of European colonization on the late-Holocene non-volant mammals of Yorke Peninsula, South Australia. The Holocene 22:1441–1450.
Megirian, D., G. Prideaux, P. Murray, and N. Smit. 2010. An Australian land mammal age biochronological scheme. Paleobiology 36:658–671.
Meiri, S. 2010. Length–weight allometries in lizards. Journal of Zoology 281:218–226.
Metzger, K. A., and A. Herrel. 2005. Correlations between lizard cranial shape and diet: a quantitative, phylogenetically informed analysis. Biological Journal of the Linnean Society 86:433–466.
Milewski, A. V. 1981. A comparison of reptile communities in relation to soil fertility in the mediterranean and adjacent arid parts of Australia and Southern Africa. Journal of Biogeography 8:493–503.
Mitchell, F. J. 1950. The scincid genera *Egernia* and *Tiliqua* (Lacertilia). Records of the South Australian Museum 9:275–308.

Mitchell, T. L. 1838. Three expeditions into the interior of eastern Australia, with descriptions of the recently explored region of Australia Felix, and of the present colony of New South Wales, Volume 1 and 2. T & W Boone, London.
Mittleman, M. B. 1952. A generic synopsis of the lizards of the subfamily Lygosominae. Smithsonian Miscellaneous Collections 117:1–35.
Molnar, R. E. 1982. A catalogue of fossil amphibians and reptiles in Queensland. Memoirs of the Queensland Museum 20:613–633.
Molnar, R. E., and C. Kurz. 1997. The distribution of Pleistocene vertebrates on the eastern Darling Downs, based on the Queensland Museum collections. Proceedings of the Linnean Society of New South Wales 117:107–129.
Morris, D. A., M. Augee, D. Gillieson, and J. Head. 1997. Analysis of a late Quaternary deposit and small mammal fauna from Nettle Cave, Jenolan, New South Wales. Proceedings of the Linnean Society of New South Wales 117.
Müller, R. D., M. Seton, S. Zahirovic, S. E. Williams, K. J. Matthews, N. M. Wright, G. E. Shephard, K. T. Maloney, N. Barnett-Moore, M. Hosseinpour, D. J. Bower, and J. Cannon. 2016. Ocean basin evolution and global-scale plate reorganization events since Pangea breakup. Annual Review of Earth and Planetary Sciences 44:107–138.
Murray, P., and D. Megirian. 1992. Continuity and contrast in Middle and Late Miocene vertebrate communities from the Northern Territory. The Beagle, Records of the Northern Territory Museum of Arts and Sciences 9:195–218.
Murray, P. F., and P. Vickers-Rich. 2004. Magnificent mihirungs: the colossal flightless birds of the Australian dreamtime. Indiana University Press, Bloomington, Indiana, 410 pp.
Murray, P. F., and D. Megirian. 2006. The Pwerte Marnte Marnte Local Fauna: a new vertebrate assemblage of presumed Oligocene age from the Northern Territory of Australia. Alcheringa: An Australasian Journal of Palaeontology 30:211–228.
Nguyen, J. M. 2016. Australo-Papuan treecreepers (Passeriformes: Climacteridae) and a new species of sittella (Neosittidae: Daphoenositta) from the Miocene of Australia. Palaeontologia Electronica 19:1–13.
Nguyen, J. M., T. H. Worthy, W. E. Boles, S. J. Hand, and M. Archer. 2013. A new cracticid (Passeriformes: Cracticidae) from the Early Miocene of Australia. Emu-Austral Ornithology 113:374–382.
Norval, G., and M. G. Gardner. 2019. The natural history of the sleepy lizard, *Tiliqua rugosa* (Gray, 1825) – Insight from chance observations and long-term research on a common Australian skink species. Austral Ecology:doi:10.1111/aec.12715.
Nyakatura, J. A., E. Andrada, S. Curth, and M. S. Fischer. 2014. Bridging “Romer’s Gap”: limb mechanics of an extant belly-dragging lizard inform debate on tetrapod locomotion during the early carboniferous. Evolutionary Biology 41:175–190.
O'Connor, D., and R. Shine. 2003. Lizards in ‘nuclear families’: a novel reptilian social system in *Egernia saxatilis* (Scincidae). Molecular Ecology 12:743–752.
O'Reilly, J. E., M. N. Puttick, L. Parry, A. R. Tanner, J. E. Tarver, J. Fleming, D. Pisani, and P. C. Donoghue. 2016. Bayesian methods outperform parsimony but at the expense of precision in the estimation of phylogeny from discrete morphological data. Biology Letters 12:20160081.
Oliver, P., and A. Hugall. 2017. Phylogenetic evidence for mid-Cenozoic turnover of a diverse continental biota. Nat Ecol Evol 1:1896–1902.
Oliver, P. M., and K. L. Sanders. 2009. Molecular evidence for Gondwanan origins of multiple lineages within a diverse Australasian gecko radiation. Journal of Biogeography 36:2044–2055.
Oliver, P. M., R. M. Brown, F. Kraus, E. Rittmeyer, S. L. Travers, and C. D. Siler. 2018. Lizards of the lost arcs: mid-Cenozoic diversification, persistence and ecological marginalization in the West Pacific. Proceedings of the Royal Society B 285:20171760.

Oppel, M. 1811. Die Ordnungen, Familien und Gattungen der Reptilien, als Prodrom einer Naturgeschichte derselben. Joseph Lindauer, München, 86 pp.
Owen, R. 1859. Description of some remains of a gigantic land-lizard (*Megalania prisca*, Owen) from Australia. Philosophical Transactions of the Royal Society of London 149:43–48.
Page, R. D. M. 1993. On islands of trees and the efficacy of different methods of branch swapping in finding most-parsimonious trees. Systematic biology 42:200–210.
Palci, A., M. W. Caldwell, and J. D. Scanlon. 2014. First report of a pelvic girdle in the fossil snake *Wonambi naracoortensis* Smith, 1976, and a revised diagnosis for the genus. Journal of Vertebrate Paleontology 34:965–969.
Palci, A., M. N. Hutchinson, M. W. Caldwell, J. D. Scanlon, and M. S. Lee. 2018. Palaeoecological inferences for the fossil Australian snakes *Yurlunggur* and *Wonambi* (Serpentes, Madtsoiidae). Royal Society open science 5:172012.
Paluh, D. J., and A. M. Bauer. 2017. Comparative skull anatomy of terrestrial and crevice-dwelling *Trachylepis* skinks (Squamata: Scincidae) with a survey of resources in scincid cranial osteology. PLoS ONE 12:e0184414.
Peters, W. 1872. Untitled [Mr. W. Peters made a statement about new collections of Batrachians (of Dr. O Wucherer from Bahia), as well as some new or lesser known saurians]. Monatsberichte der Königlichen Preussische Akademie des Wissenschaften zu Berlin 1872:776.
Pianka, E. R. 1986. Ecology and natural history of desert lizards: analyses of the ecological niche and community structure. Princeton University Press, Princeton, NJ.
Pledge, N. S. 1992. The Curramulka local fauna: a new late Tertiary fossil assemblage from Yorke Peninsula, South Australia. The Beagle, Records of the Northern Territory Museum of Arts and Sciences 9:115–142.
Poe, S., and J. J. Wiens. 2000. Character selection and the methodology of morphological phylogenetics; pp. 20–36 in J. J. Wiens (ed.), Phylogenetic analysis of morphological data. Smithsonian Institution Press, Washington, DC.
Price, G. J., and I. H. Sobbe. 2005. Pleistocene palaeoecology and environmental change on the Darling Downs, southeastern Queensland, Australia. Memoirs of the Queensland Museum 51:171–201.
Price, G. J., and K. J. Piper. 2009. Gigantism of the Australian *Diprotodon* Owen 1838 (Marsupialia, Dirptodontoidea) through the Pleistocene. Journal of Quaternary Science 24:1029–1038.
Price, G. J., M. J. Tyler, and B. N. Cooke. 2005. Pleistocene frogs from the Darling Downs, southeastern Queensland, and their palaeoenvironmental significance. Alcheringa 29:171–182.
Price, G. J., J. Louys, G. K. Smith, and J. Cramb. 2019. Shifting faunal baselines through the Quaternary revealed by cave fossils of eastern Australia. PeerJ 6:e6099.
Prideaux, G. 2004. Systematics and evolution of the sthenurine kangaroos, Volume 146. University of California Press, Oaklands, California.
Prideaux, G. J. 2007. Mid-Pleistocene vertebrate records: Australia; pp. 1517-1537 in S. A. Elias (ed.), Encyclopedia of Quaternary Science. Elsevier, Oxford.
Prideaux, G. J., G. A. Gully, A. M. C. Couzens, L. K. Ayliffe, N. R. Jankowski, Z. Jacobs, R. G. Roberts, J. C. Hellstrom, M. K. Gagan, and L. M. Hatcher. 2010. Timing and dynamics of Late Pleistocene mammal extinctions in southwestern Australia. Proceedings of the National Academy of Sciences of the United States of America 107:22157–22162.
Prideaux, G. J., J. A. Long, L. K. Ayliffe, J. C. Hellstrom, B. Pillans, W. E. Boles, M. N. Hutchinson, R. G. Roberts, M. L. Cupper, L. J. Arnold, P. D. Devine, and N. M. Warburton. 2007. An arid-adapted middle Pleistocene vertebrate fauna from south-central Australia. Nature 445:422–425.
Pyron, R. A., F. T. Burbrink, and J. J. Wiens. 2013. A phylogeny and revised classification of Squamata, including 4161 species of lizards and snakes. BMC Evolutionary Biology 13:93.

Rabosky, D. L. 2010. Extinction rates should not be estimated from molecular phylogenies. Evolution 6:1816–1824.
Rabosky, D. L., S. C. Donnellan, A. L. Talaba, and I. J. Lovette. 2007. Exceptional among-lineage variation in diversification rates during the radiation of Australia's most diverse vertebrate clade. Proceedings of the Royal Society of London B: Biological Sciences 274:2915–2923.
Rambaut, A., A. Drummond, and M. Suchard. 2014. Tracer v1. 6
Rambaut, A., A. J. Drummond, D. Xie, G. Baele, and M. A. Suchard. 2018. Posterior summarisation in Bayesian phylogenetics using Tracer 1.7. Systematic biology 67:901–904.
Raup, D. M., S. J. Gould, T. J. M. Schopf, and D. S. Simberloff. 1973. Stochastic models of phylogeny and the evolution of diversity. The Journal of Geology 81:525–542.
Reed, E. H., and S. J. Bourne. 2000. Pleistocene fossil vertebrate sites of the South East region of South Australia. Transactions of the Royal Society of South Australia 124:61–90.
Reed, E. H., and S. J. Bourne. 2009. Pleistocene fossil vertebrate sites of the South East region of South Australia II. Transactions of the Royal Society of South Australia 133:30–40.
Reeder, T. W. 2003. A phylogeny of the Australian *Sphenomorphus* group (Scincidae: Squamata) and the phylogenetic placement of the crocodile skinks (*Tribolonotus*): Bayesian approaches to assessing congruence and obtaining confidence in maximum likelihood inferred relationships. Molecular Phylogenetics and Evolution 27:384–397.
Reeder, T. W., T. M. Townsend, D. G. Mulcahy, B. P. Noonan, P. L. Wood, Jr., J. W. Sites, Jr., and J. J. Wiens. 2015. Integrated analyses resolve conflicts over squamate reptile phylogeny and reveal unexpected placements for fossil taxa. PLoS ONE 10:e0118199.
Rich, T. 1984. News from Foreign members: Australia, Museum of Victoria, Melbourne. Society of Vertebrate Paleontology News Bulletin 130:28.
Rich, T. H. 1991. Monotremes, placentals, and marsupials: their record in Australia and its biases; pp. 894–1057 in P. Vickers-Rich, J. M. Monaghan, R. F. Baird, and T. H. Rich (eds.), Vertebrate Palaeontology of Australasia. Pioneer Design Studio Pty Ltd, Melbourne, Australia.
Richter, A. 1994. Lacertilia aus der Unteren Kreide von Una und Galve (Spanien) und Anoual (Marokko). Berliner geowissenschaftliche Abhandlungen (E: Paläobiologie) 14:1–147.
Richter, A., and M. Wuttke. 2012. Analysing the taphonomy of Mesozoic lizard aggregates from Uña (eastern Spain) by X-ray controlled decay experiments. Palaeobiodiversity and Palaeoenvironments 92:5–28.
Rieppel, O. 1981. The skull and the jaw adductor musculature in some burrowing scincomorph lizards of the genera *Acontias*, *Typhlosaurus* and *Feylinia*. Journal of Zoology 195:493–528.
Rieppel, O. 2002. A case of dispersing chameleons. Nature 415:744–5.
Rieppel, O., J. Gauthier, and J. Maisano. 2008. Comparative morphology of the dermal palate in squamate reptiles, with comments on phylogenetic implications. Zoological Journal of the Linnean Society 152:131–152.
Roberts, R. G., T. F. Flannery, L. K. Ayliffe, H. Yoshida, J. M. Olley, G. J. Prideaux, G. M. Laslett, A. Baynes, M. A. Smith, R. Jones, and B. L. Smith. 2001. New ages for the last Australian megafauna: continent-wide extinction about 46,000 years ago. Science 292:1888–1892.
Ronquist, F., S. Klopfstein, L. Vilhelmsen, S. Schulmeister, D. L. Murray, and A. P. Rasnitsyn. 2012a. A total-evidence approach to dating with fossils, applied to the early radiation of the hymenoptera. Systematic biology 61:973–999.
Ronquist, F., M. Teslenko, P. Van Der Mark, D. L. Ayres, A. Darling, S. Höhna, B. Larget, L. Liu, M. A. Suchard, and J. P. Huelsenbeck. 2012b. MrBayes 3.2: efficient Bayesian phylogenetic inference and model choice across a large model space. Systematic biology 61:539–542.
RStudio Team. 2016. RStudio: Integrated development for R. RStudio Inc., Boston, USA.
Russell, A. P., and A. M. Bauer. 2008. The appendicular locomotor apparatus of *Sphenodon* and normal-limbed squamates; pp. in C. Gans, A. S. Gaunt, and K. Adler (eds.), The skull and appendicular locomotor apparatus of Lepidosauria. Society for the Study of Amphibians and Reptiles, Ithaca, New York, USA.

Sanders, K. L., and M. S. Y. Lee. 2008. Molecular evidence for a rapid late-Miocene radiation of Australasian venomous snakes (Elapidae, Colubroidea). Molecular Phylogenetics and Evolution 46:1165–1173.
Scanlon, J. D. 1992. A new large madtsoiid snake from the Miocene of the Northern Territory. The Beagle: Records of the Museums and Art Galleries of the Northern Territory 9:49.
Scanlon, J. D. 1993. Madtsoiid snakes from the Eocene Tingamarra Fauna of eastern Queensland. Kaupia 3:3–8.
Scanlon, J. D. 1997. *Nanowana* gen. nov., small madtsoiid snakes from the Miocene of Riversleigh: Sympatric species with divergently specialised dentition Memoirs of the Queensland Museum 41:393–412.
Scanlon, J. D. 2006. Skull of the large non-macrostomatan snake *Yurlunggur* from the Australian Oligo-Miocene. Nature 439:839.
Scanlon, J. D., and M. S. Lee. 2000. The Pleistocene serpent *Wonambi* and the early evolution of snakes. Nature 403:416.
Schofield, J. A., A. L. Fenner, K. Pelgrim, and C. M. Bull. 2012. Male-biased movement in pygmy bluetongue lizards: implications for conservation. Wildlife Research 39:677–684.
Schwenk, K. 2000. Feeding in lepidosaurs; pp. in K. Schwenk (ed.), Feeding, form, function and evolution in tetrapod vertebrates. Academic Press, San Diego, U.S.A.
Shea, G. M. 1990. The genera *Tiliqua* and *Cyclodomorphus* (Lacertilia: Scincidae): generic diagnoses and systematic relationships. Memoirs of the Queensland Museum 29:495–520.
Shea, G. M., and M. N. Hutchinson. 1992. A new species of lizard (*Tiliqua*) from the Miocene of Riversleigh, Queensland. Memoirs of the Queensland Museum 32:303–310.
Shute, E., G. J. Prideaux, and T. H. Worthy. 2016. Three terrestrial Pleistocene coucals (Centropus: Cuculidae) from southern Australia: biogeographical and ecological significance. Zoological Journal of the Linnean Society 177:964–1002.
Shute, E., G. J. Prideaux, and T. H. Worthy. 2017. Taxonomic review of the late Cenozoic megapodes (Galliformes: Megapodiidae) of Australia. Royal Society open science 4:170233.
Simões, T. R., M. W. Caldwell, A. Palci, and R. L. Nydam. 2017. Giant taxon-character matrices: quality of character constructions remains critical regardless of size. Cladistics 33:198–219.
Skinner, A., A. F. Hugall, and M. N. Hutchinson. 2011. Lygosomine phylogeny and the origins of Australian scincid lizards. Journal of Biogeography 38:1044–1058.
Skinner, A., M. N. Hutchinson, and M. S. Y. Lee. 2013. Phylogeny and divergence times of Australian *Sphenomorphus* group skinks (Scincidae, Squamata). Molecular Phylogenetics and Evolution 69:906–918.
Smith, K. T. 2009. Eocene lizards of the clade *Geiseltaliellus* from Messel and Geiseltal, Germany, and the early radiation of Iguanidae (Reptilia: Squamata). Bulletin of the Peabody Museum of Natural History 50:219–306.
Smith, K. T., and M. Wuttke. 2012. From tree to shining sea: taphonomy of the arboreal lizard *Geiseltaliellus maarius* from Messel, Germany. Palaeobiodiversity and Palaeoenvironments 92:45–65.
Smith, M. A. 1937. A review of the genus *Lygosoma* (Scincidae: Reptilia) and its allies. Records of the Indian Museum 39:213–234.
Smith, M. J. 1976. Small fossil vertebrates from Victoria Cave, Naracoorte, South Austraia. IV, Reptiles. Transactions of the Royal Society of South Australia 100:39–51.
Smith, M. J. 1982. Reptiles from Late Pleistocene deposits on Kangaroo Island, South Australia. Transactions of the Royal Society of South Australia 106:61–66.
Stadler, T. 2010. Sampling-through-time in birth–death trees. Journal of Theoretical Biology 267:396–404.
Stern, H., and G. d. Hoedt. 2000. Objective classification of Australian climates. Australian Meteorological Magazine 49:87–96.

Storr, G. M. 1978. The genus *Egernia* (Lacertilia, Scincidae) in Western Australia. Records of the Western Australian Museum 6:147–187.
Swofford, D. L. 2003. PAUP*: Phylogenetic Analysis Using Parsimony (*and other methods). 4.0 b10. Sinauer Associates, Sunderland, Massachusetts.
Taylor, J. A. 1986. Food and foraging behaviour of the lizard, *Ctenotus taeniolatus*. Australian Jorunal of Ecology 11:49–54.
Tchernov, E., O. Rieppel, H. Zaher, M. J. Polcyn, and L. L. Jacobs. 2000. A fossil snake with limbs. Science 287:2010–2012.
Tedford, R., R. Wells, and S. Barghoorn. 1992. Tirari Formation and contained faunas, Pliocene of the Lake Eyre Basin, South Australia. The Beagle: Records of the Museums and Art Galleries of the Northern Territory 9:173–194.
Tedford, R. H., M. Archer, A. Bartholomai, M. Plane, N. S. Pledge, T. Rich, P. Rich, and R. T. Wells. 1977. The discovery of Miocene vertebrates, Lake Frome area, South Australia. BMR Journal of Australian Geology & Geophysics 2:53–57.
Thorn, K. M., M. N. Hutchinson, M. Archer, and M. S. Y. Lee. 2019. A new scincid lizard from the Miocene of Northern Australia, and the evolutionary history of social skinks (Scincidae: Egerniinae). Journal of Vertebrate Paleontology 39:e1577873.
Thorn, K. M., C. I. Nielsen, M. Archer, M. N. Hutchinson, and M. S. Y. Lee. 2017. Dating Australian skink diversification: fossil *Sphenomorphus* and *Egernia* group skinks from Riversleigh World Heritage Area (Queensland, Australia). Geological Society of Australia Abstracts 125:39.
Title, P. O., and D. L. Rabosky. 2016. Do macrophylogenies yield stable macroevolutionary inferences? An example from squamate reptiles. Systematic biology 66:843–856.
Tonini, J. F. R., K. H. Beard, R. B. Ferreira, W. Jetz, and R. A. Pyron. 2016. Fully-sampled phylogenies of squamates reveal evolutionary patterns in threat status. Biological Conservation 204, Part A:23–31.
Travouillon, K. J., S. Legendre, M. Archer, and S. J. Hand. 2009. Palaeoecological analyses of Riversleigh's Oligo-Miocene sites: Implications for Oligo-Miocene climate change in Australia. Palaeogeography, Palaeoclimatology, Palaeoecology 276:24–37.
Tyler, M. J., and G. J. Prideaux. 2016. Early to middle Pleistocene occurrences of *Litoria*, *Neobatrachus* and *Pseudophryne* (Anura) from the Nullarbor Plain, Australia: first frogs from the "frog-free zone". Memoirs of Museum Victoria 74:403–408.
Uetz, P. 2010. The original descriptions of reptiles. Zootaxa 2334:59–68.
Uetz, P., P. Freed, and J. e. Hošek. 2019. The Reptile Database.
Vickers-Rich, P., and P. V. Rich. 1991. Vertebrate palaeontology of Australasia. Pioneer Design Studio, Melbourne, Australia, 1437 pp.
Vidal, N., and S. B. Hedges. 2009. The molecular evolutionary tree of lizards, snakes, and amphisbaenians. Comptes rendus biologies 332:129–139.
Villa, A., H.-A. Blain, and M. Delfino. 2018. The Early Pleistocene herpetofauna of Rivoli Veronese (Northern Italy) as evidence for humid and forested glacial phases in the Gelasian of Southern Alps. Palaeogeography, Palaeoclimatology, Palaeoecology 490:393-403.
Warton, D., R. Duursma, D. Falster, and S. Taskinen. 2018. (Standardised) Major axis estimation and testing routines. 3.4-8, Randwick, Australia.
Watson, C. M., and D. R. Formanowicz. 2012. A comparison of maximum sprint speed among the five-lined skinks (*Plestiodon*) of the southeastern United States at ecologically relevant temperatures. Herpetological Conservation and Biology 7:75–82.
Welch, K. 1982. Herpetology of the Old World II. Preliminary comments on the classification of skinks (Family Scincidae) with specific reference to those genera found in Africa, Europe, and southwest Asia. Herptile 7:25–27.
Wells, R. W., and R. C. Wellington. 1984. A synopsis of the class Reptilia in Australia. Australian Journal of Herpetology 1:73–129.

While, G. M., T. Uller, and E. Wapstra. 2009. Family conflict and the evolution of sociality in reptiles. Behavioral Ecology 20:245–250.
White, J. 1790. Journal of a voyage to New South Wales, with sixty-five plates of non descript animals, birds, lizards, serpents, curious cones of trees and other natural productions. Debrett, London, 229 pp.
White, M. E. 2006. Environments of the geological past; pp. 17–48 in J. R. Merrick, Archer, A., Hickey, G. M., Lee, M. S. Y. (ed.), Evolution and biogeography of Australasian vertebrates. Auscipub, Oatlands, NSW.
Whitelaw, M. J. 1991. Magnetic polarity stratigraphy of the Fisherman's Cliff and Bone Gulch vertebrate fossil faunas from the Murray Basin, New South Wales, Australia. Earth and Planetary Science Letters 104:417–423.
Wickham, H. 2016. ggplot2: Elegant graphics for data analysis. Springer-Verlag, New York.
Wiens, J. J. 2004. The role of morphological data in phylogeny reconstruction. Systematic biology 53:653–661.
Wiens, J. J., C. R. Hutter, D. G. Mulcahy, B. P. Noonan, T. M. Townsend, J. W. Sites, and T. W. Reeder. 2012. Resolving the phylogeny of lizards and snakes (Squamata) with extensive sampling of genes and species. Biology Letters 8:1043–1046.
Wiley, E. O., D. Siguel-Causey, D. R. Brooks, and V. A. Funk. 1991. The Compleat Cladist: A primer of phylogenetic procedures. Museum of Natural History, The University of Kansas, Lawrence, Kansas, 158 pp.
Williams, D. L. G. 1980. Catalogue of Pleistocene vertebrate fossils and sites in South Australia. Transactions of the Royal Society of South Australia 104:101–115.
Wilson, S., and G. Swan. 2017. A complete guide to the Reptiles of Australia. 5th Edition. Reed New Holland Publishers, Sydney, Australia, 647 pp.
Wineski, L. E., and C. Gans. 1984. Morphological basis of the feeding mechanics in the shingle-back lizard *Trachydosaurus rugosus* (Scincidae, Reptilia). Journal of Morphology 181:271–295.
Woinarski, J. C. Z., A. A. Burbidge, and P. L. Harrison. 2014. The action plan for Australian mammals 2012. CSIRO Publishing, Clayton, Victoria, Australia, 1038 pp.
Woodburne, M. O., B. J. Macfadden, J. A. Case, M. S. Springer, N. S. Pledge, J. D. Power, J. M. Woodburne, and K. B. Springer. 1994. Land mammal biostratigraphy and magnetostratigraphy of the Etadunna Formation (late Oligocene) of South Australia. Journal of Vertebrate Paleontology 13:483–515.
Woodbury, A. M. 1948. Studies of the desert tortoise, *Gopherus agassizii*. Ecological Monographs 18:145–200.
Woodhead, J., S. J. Hand, M. Archer, I. Graham, K. Sniderman, D. A. Arena, K. H. Black, H. Godthelp, P. Creaser, and E. Price. 2016. Developing a radiometrically-dated chronologic sequence for Neogene biotic change in Australia, from the Riversleigh World Heritage Area of Queensland. Gondwana Research 29:153–167.
Worthy, T. H. 2009. Descriptions and phylogenetic relationships of two new genera and four new species of Oligo-Miocene waterfowl (Aves: Anatidae) from Australia. Zoological Journal of the Linnean Society 156:411–454.
Worthy, T. H. 2011. Descriptions and phylogenetic relationships of a new genus and two new species of Oligo-Miocene cormorants (Aves: Phalacrocoracidae) from Australia. Zoological Journal of the Linnean Society 163:277–314.
Wright, A. M., and D. M. Hillis. 2014. Bayesian analysis using a simple likelihood model outperforms parsimony for estimation of phylogeny from discrete morphological data. PLoS ONE 9:e109210.
Wright, A. M., G. T. Lloyd, and D. M. Hillis. 2015a. Modeling character change heterogeneity in phylogenetic analyses of morphology through the use of priors. Systematic biology 65:602–611.

Wright, A. M., K. M. Lyons, M. C. Brandley, and D. M. Hillis. 2015b. Which came first: The lizard or the egg? Robustness in phylogenetic reconstruction of ancestral states. Journal of Experimental Zoology Part B: Molecular and Developmental Evolution 324:504–516.

Wu, N., L. A. Alton, C. J. Clemente, M. R. Kearney, and C. R. White. 2015. Morphology and burrowing energetics of semi-fossorial skinks (*Liopholis* spp.). Journal of Experimental Biology 218:2416–2426.

Wu, X.-C., D. B. Brinkman, and A. P. Russell. 1996. *Sineoamphisbaena hexatabularis*, an amphisbaenian (Diapsida: Squamata) from the Upper Cretaceous redbeds at Bayan Mandahu (Inner Mongolia, People's Republic of China), and comments on the phylogenetic relationships of the Amphisbaenia. Canadian Journal of Earth Sciences 33:541–577.

Yang, Z., and B. Rannala. 1997. Bayesian phylogenetic inference using DNA sequences: a Markov Chain Monte Carlo Method. Molecular biology and evolution 14:717–724.

Yule, G. 1924. A mathematical theory of evolution, based on the conclusions of Dr. JC Willis, FRS. Philosophical Transactions of the Royal Society of London Series B 213:21–87.

Zheng, Y., and J. J. Wiens. 2016. Combining phylogenomic and supermatrix approaches, and a time-calibrated phylogeny for squamate reptiles (lizards and snakes) based on 52 genes and 4162 species. Molecular Phylogenetics and Evolution 94, Part B:537–547.

APPENDICES

Appendix 1: Reference specimen list

Table A1: List of all egerniine specimens and the outgroup taxon, used in this thesis to generate morphological data set for phylogenetic analyses and as comparative specimens for identifications, body size and ontogeny. *denotes specimens prepared or collected by K. M. Thorn. # denotes specimens used to check ontogenetic or individual variation

Genus	species	Ethanol specimen	Skeletal specimen
Bellatorias	*frerei*	SAMA R21133	
	major		SAMA R35762
Brachymeles	*schadenbergi*		SAMA R8853
Corucia	*zebrata*		SAMA R35765
Cyclodomorphus	*branchialis*		WAM R71052
	casuarinae		SAMA R8798
	gerrardii		SAMA R47699
	melanops		SAMA R35681
	michaeli		SAMA R35682
Egernia	*cunninghami*		NMV D7815, SAMA R27151
	depressa	SAMA R29356	
	epsisolus		SAMA R3433H
	formosa		WAM R72681, R72681#, R65803#
	hosmeri		SAMA R22510
	kingii		WAM R36376, R89269#, R89270#
	napoleonis		WAM R45350, R45350#, R44673#
	rugosa		QM J24010
	saxatilis		SAMA R43961
	stokesii		WAM R28909, R16571#, R29068#
	striolata	SAMA R42740	FUR167*
Eugongylus	*rufescens*		SAMA R36735
Eumeces	*schneideri*		SAMA R6695
Eutropis	*multifasciata*		SAMA R35693
Liopholis	*inornata*		SAMA R35687, juv. R7238#
	kintorei		SAMA R29220
	margaretae		SAMA R24435
	personata		
	multiscutata		SAMA R25245, FUR168*
	striata		SAMA R7198
	whitii		SAMA R35688, juv. R35691#
Lissolepis	*coventryi*		SAMA R35686, R57317
	luctuosa		WAM R36018
Plestiodon	*fasciatus*		SAMA R66784

Sphenomorphus	*jobiensis*		SAMA R6736
Tiliqua	*adelaidensis*	R50714[#], R68380[#], R68381[#]	SAMA R40738
	gigas		SAMA R11419
	nigrolutea		SAMA R67631
	occipitalis		SAMA R35758
	rugosa		SAMA R27027, FUR055, FUR155*, FUR157*
	scincoides		SAMA R27036, R27040, FUR071*, FUR191*, FUR130*
Tribolonotus	*novaeguineae*		SAMA R33286

Appendix 2: Morphological character list

Blue text are continuous characters, measurements taken of Micro-CT scans in micrometres in Avizo Lite (v.9.0.0) and converted to millimetres. Raw measurements were later converted to percentages based on dentary or maxilla length to remove overall size biases, and then log transformed. Grey text are characters that were used in other studies but not applicable to egerniines. Red text represent the added or modified characters incorporated for Chapters 2 and 4, not present in Chapter 3 or the published SI for Thorn et al. (2019).

Dentary and Symphysis

1. Overall length of dentary, measured from posterior of angular process to tip of symphysis (*Corucia zebrata*, labial and occlusal views): keep raw measurements.
2. Length, height ratio of dentary (H/L), measured perpendicular to length at midpoint of dentary: (keep raw measurements).
3. Length, width ratio of dentary (W/L), measured at midpoint, perpendicular to height: (keep raw measurements).
4. Dentary, anterodorsal edge of dental parapet at tip (Gauthier et al., 2012): (0) straight; (1) tipped down.
5. Length of symphysis, along longest axis: (keep raw measurements, greatest length, as ratio of dentary length).
6. Width of symphysis, measured perpendicular to length at widest point, as ratio of length (*Egernia stokesii*, lingual view): keep raw measurements.
7. Symphysis shape: (0) Not bifid posteriorly (A, *Egernia stokesii,* medial view); (1) Bifid posteriorly (B, *Tiliqua adelaidensis*, medial view). 'Bifid' refers to when the primary horizontal and secondary posteroventral, sections of the symphysis are equal in width.

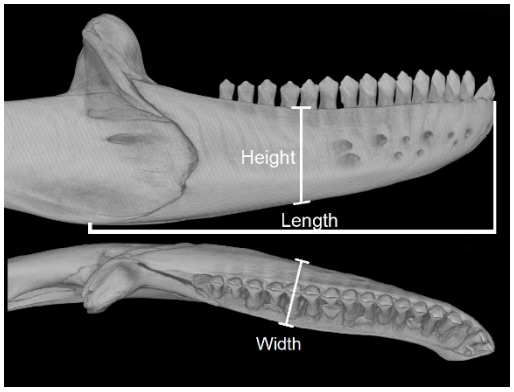

Figure A2.1: Measurement points for dentary height and width, at 50% along the length of the dentary. Specimen pictured is *Corucia zebrata* SAMA R35765 lateral and occlusal view.

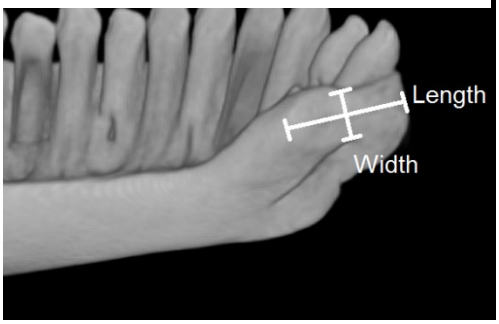

Figure A2.2: Measurement of the symphysis length and width. Specimen figured is *Egernia stokesii* WAM R28909 in medial view.

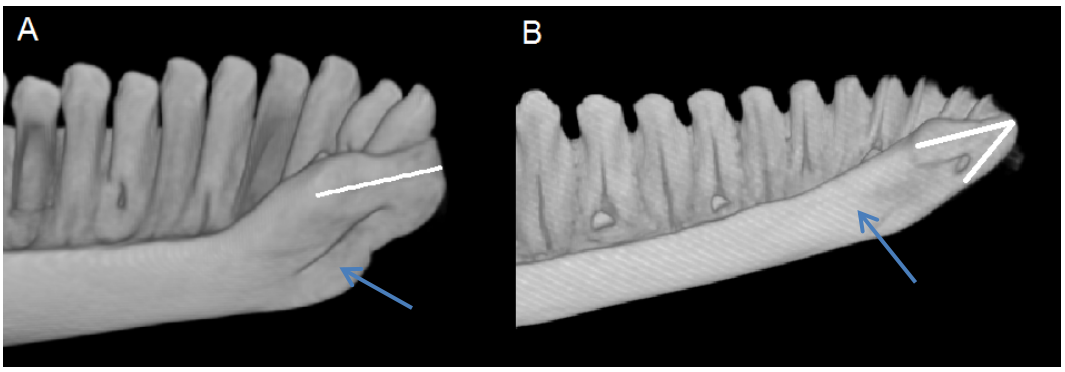

Figure A2.3: Symphysis shape (white line) as state A is straight without a ventral extension of a medial surface of articulation or B is bifid posteriorly with a ventral extension of the symphysial surface. Blue arrows show a prominent (A) chin or absence/weak (B) chin. Specimens figured are *Egernia stokesii* WAM R 28909(A) and *Tiliqua adelaidensis* SAMA R40738 (B); both in medial view.

8. Symphysis 'ledge' where bone protrudes towards opposing symphysis forming a posteriorly-directed 'chin': (0) absent/weak (B above right, *Tiliqua adelaidensis*); (1) prominent (A above left, *Egernia stokesii*).
9. Angle between dentaries at the symphysis: keep raw measurement (measured from single dentary from line of tooth row and along symphysis plane, and then doubled, *Corucia zebrata*, occlusal view).

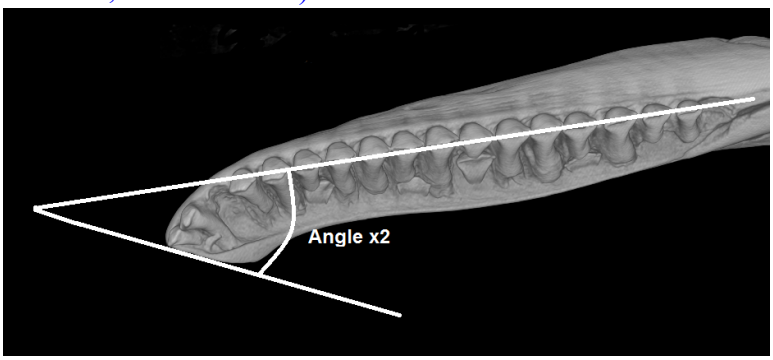

Figure A2.4: How to measure the angle between dentaries. Follow the line of the tooth cusps from the posterior-most tooth until this line of reference meets the line representing the surface of the symphysis. The 2D angle tool in Avizo can be used to trace this if specimen is viewed in occlusal view as pictured. This angle is then duplicated to represent the angle between two dentaries. Figured specimen is *Corucia zebrata* SAMA R35765.

10. Dentary subdental shelf/gutter development posteriorly (modified from Estes et al., 1988): (0) subdental shelf absent; (1) weakly developed subdental shelf; (2) pronounced subdental gutter. (ordered).
11. Meckel's groove: (0) open; (1) partially closed; (2) closed. (ordered).
12. Mental foramina: number of mental foramina: (keep raw values, if variable within species, use median value and keep left and right counts)
13. Mental foramina: posterior extent along length of tooth row (0) 25%; (1) 33%; (2) 50%; (3) 66%; (4) >66%. (ordered)
14. Mental foramina: size variation: (0) all foramina roughly the same size; (1) anteriormost foramen at least 2x larger than majority; (2) posteriormost foramen at least 2x larger than majority. Unordered.
15. Arrangement and rows of mental foramina: (0) mental foramina not arranged in regular horizontal row(s) on lateral face of dentary; (1) single horizontal row of foramina, A (*Lissolepis luctuosa*, labial view); (2) two horizontal rows of foramina, B (*Corucia zebrata*, labial view).

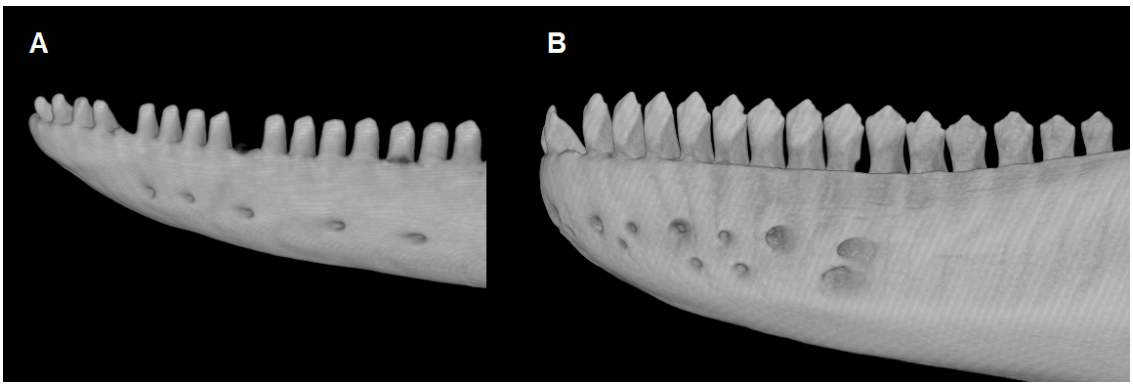

Figure A2.5: If arranged in a clear linear pattern, mental foramina on the lateral face of the dentary can be as a singular row (A) or two rows (B). Specimens figured are *Lissolepis luctuosa* WAM R36018 and *Corucia zebrata* SAMA R35765; both in lateral view.

16. Shape of splenial notch in dentary (Hollenshead et al., 2011): (0) triangular, V-shaped (A, B and C below); (1) Rounded, U-shaped, with concave margin to subdental shelf, beginning with a near perpendicular edge rising from the anterior inferior alveolar foramen, and a concave edge on the lower margin of the splenial notch (D, below).

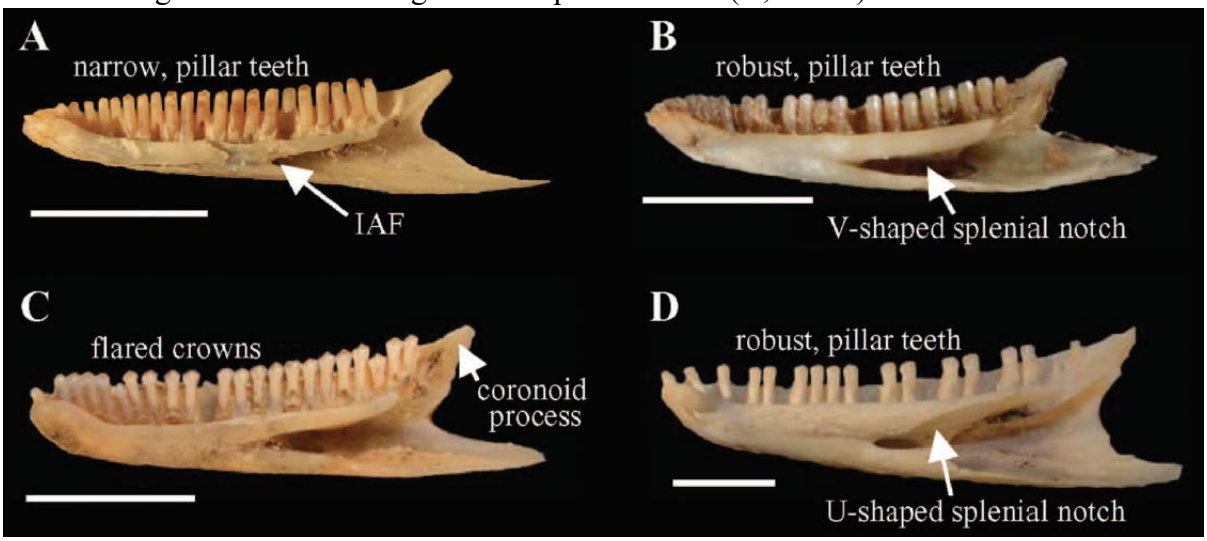

Figure A2.6: A: *Liopholis*, B: *Lissolepis*, C: *Egernia*, D: *Bellatorias*. From Hollenshead et al. (2011), p 35.

17. Posterior process of dentary on lateral surface of mandible (*Lissolepis luctuosa*, lateral view below) posterior termination (modified from Gauthier et al., 2012): (0) absent; (1) extends only to below (or anterior) to level of coronoid apex; (2) extends slightly behind level of coronoid apex; (3) extends posterior of visible coronoid in lateral view. (ordered)
18. Dentary Coronoid Ramus (DCR) posterodorsal extension (Estes et al., 1988): (0) absent or with only small dorsal extension; (1) large, but extending between lateral and medial processes of coronoid bone; (2) large, but extending dorsally to overlap most of anterolateral surface of coronoid bone; (3) extremely well developed, covering almost entire lateral surface of coronoid bone. (ordered)

Figure A2.7: Location of posterior process examined in Character 17. Specimen figured is *Lissolepis luctuosa* WAM R36018 in lateral view.

19. Reach of DCR up coronoid: (0) Less than or up to ¼ of apex height. (1) Between ¼ and ½ coronoid height. (2) Between ½ and ¾ coronoid height. (3) Between ¾ coronoid height and apex. (4) Dentary's coronoid ramus is taller than the apex of the coronoid bone. (ordered)
20. Dentary, angular process posterior termination on lateral face of mandible (Etheridge and de Queiroz, 1988): (0) below (or anterior to) level of coronoid apex; (1) just posterior to coronoid apex (less than half the distance across surangular to surangular foramen); (2) well posterior to level of coronoid apex but not approaching posterior surangular foramen; (3) near to posterior surangular foramen. (ordered)

Splenial

21. Anterior extent of the splenial in medial view (modified from Estes et al., 1988; Gauthier et al., 2012): (0) extends along one-third (or less) of the length of the dentary tooth row; (1) extends between one third and one-half; (2) extends approximately one half (3) extends two-thirds (or more). (ordered)
22. Posterior extent of splenial (modified from Gauthier et al. 2012): (0) anterior of coronoid process apex (A, *Eutropis multifasciata*); (1) to coronoid apex (B, *Cyclodomorphus melanops*); (2) beyond coronoid apex (C, *Egernia stokesii*). (ordered)

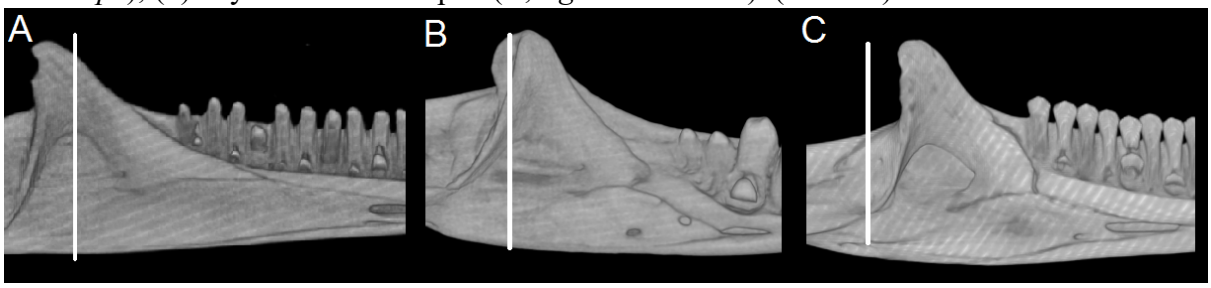

Figure A2.8: The posterior extent of the splenial, either terminating anterior of the coronoid apex (A); beneath the coronoid apex (B), or posterior of the coronoid apex (C). Figured specimens are *Eutropis multifasciata* SAMA R35693 (A), *Cyclodomorphus melanops* SAMA R35681 (B), and *Egernia stokesii* WAM R28909 (C); all in medial view.

23. Splenial inferior alveolar foramen (iaf) position relative to dentary in medial view: (0) enclosed entirely in splenial (1) >75% of margin is splenial, the rest dentary; (2) 50-74% of margin is splenial; (3) 50% or more of margin is dentary. (ordered)
24. Splenial inferior alveolar foramen position relative to anterior intermandibularis foramen: (0) anterior; (1) anterodorsal; (2) dorsal; (3) posterodorsal. (ordered)
25. Splenial maximum height as ratio of dentary height (measured from maximum dorsoventral dimension of splenial, keep raw measurements).

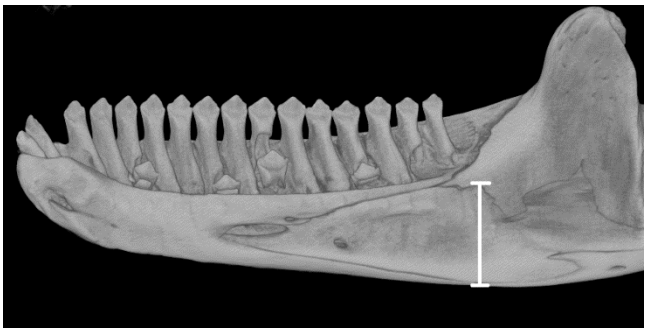

Figure A2.9: Splenial depth measured at greatest point visible externally in lateral view. Specimen figured is *Corucia zebrata* SAMA R35765.

Angular

26. Angular posterior extent: (0) reaches mandibular cotyle; (1) approaches, but does not reach mandibular cotyle; (2) extends more than 50% along length of surangular towards mandibular cotyle but does not approach it; (3) extends between 25-49% along length of surangular towards mandibular cotyle. (ordered)

27. Angular medial exposure (modified from Lee, 1998). Relative degree of medial exposure scored with mandible oriented so teeth pointing vertically up: (0) broad, >50% of total angular width exposed medially; (1) reduced, between 25-50% of angular width exposed; (2) narrow, less than 25% angular width exposed. (ordered)
28. Posterior intermandibularis foramen occurrence: (0) absent; (1) present
29. Posterior intermandibularis foramen - mediolateral position (Gauthier et al., 2012): (0) medial; (1) ventral; (2) lateral. (ordered) NA for species without foramen.
30. Posterior intermandibularis foramen - anteroposterior position, relative to coronoid apex (Frost and Etheridge, 1989): (0) anterior of apex; (1) directly below, A; (2) slightly posterior, B; (3) well posterior, beyond posteromedial coronoid process, C. (*Corucia zebrata*, *Liopholis whitii*, *Cyclodomorphus melanops*, all medial view) NA for species without foramen. (ordered)

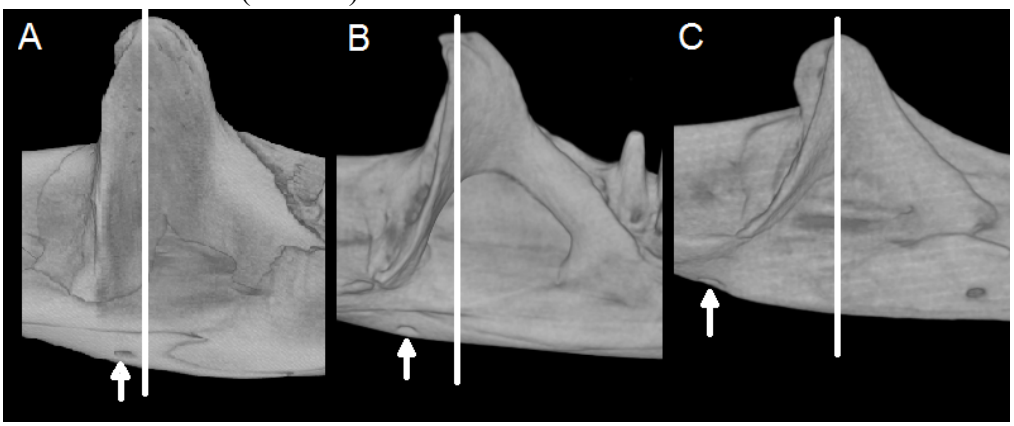

Figure A2.10: Possible locations of the posterior intermandibularis foramen either anterior of the apex or below the aoex (A), posterior of the apex (B), or posterior of the medially visible coronoid (C). Specimens figured are *Corucia zebrata* SAMA R35765 (A), *Liopholis whitii* SAMA R35688 (B), and *Cyclodomorphus melanops* SAMA R36681 (C) all in medial view.

Coronoid

31. Exposure of surangular between anteromedial and posteromedial rami of coronoid bone (in medial view): (0) absent; (1) present, fills <33% of space between base of anteromedial and posteromedial rami; (2) fills 33-66% of space; (3) fills > 66% of space. (ordered)
32. Coronoid anteromedial process fits into sulcus beneath tooth-bearing border of dentary, at or behind end of tooth row (Smith, 2009; Gauthier et al., 2012): (0) absent; (1) present, but not wrapping around the ventral margin dentary tooth bearing sulcus; (2) present and wraps around ventral margin of dentary tooth-bearing border at apex posteriorly.
33. Coronoid articulation with the dorsal margin of the surangular (Estes et al., 1988): (0) coronoid restricted to medial aspect of mandible; (1) coronoid extends onto dorsal surface of surangular; (2) coronoid arches over dorsal margin of mandible to reach lateral surface of surangular. (ordered)
34. Coronoid, anteromedial process, ventral margin, at/behind end of tooth row (Gauthier et al., 2012): (0) overlapped by splenial; (1) abuts splenial.
35. Coronoid, posteromedial ramus shape: (0) narrow, with no anterior flat surface (see 36A); (1) broad, with anterior and posterior flat surface (see 36B).
36. Coronoid apex shape: (0) sharp (*Egernia stokesii*, A); (1) blunt, rounded (*Corucia zebrata*, B); (2) flat or concave (*Tiliqua adelaidensis*, C).

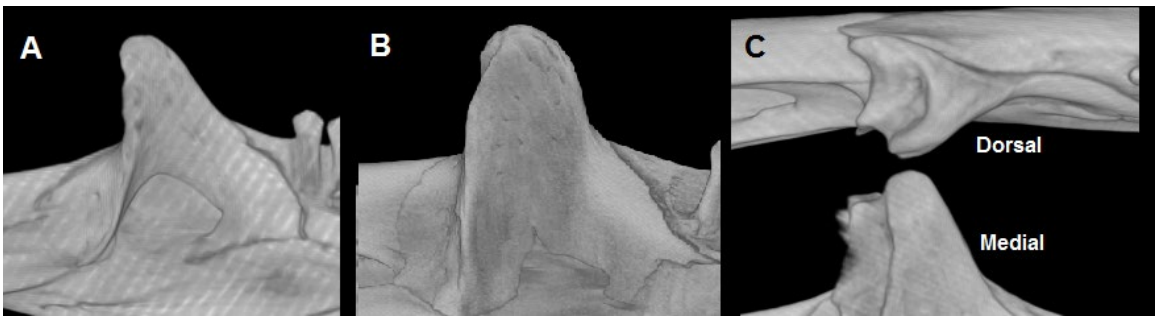

Figure A2.11: Variations in the shape of the coronoid apex demonstrated by *Egernia stokesii* WAM R28909 (A), *Corucia zebrata* SAMA R35765 (B) in medial view, and *Tiliqua adelaidensis* SAMA R 40738 (C) shown in medial and dorsal view to demonstrate the 'bucket'.

37. Coronoid, height from base of posteromedial ramus to apex as ratio of dentary height (A, *Corucia zebrata*, medial view), measured from point to point along ramus: keep raw measurement.

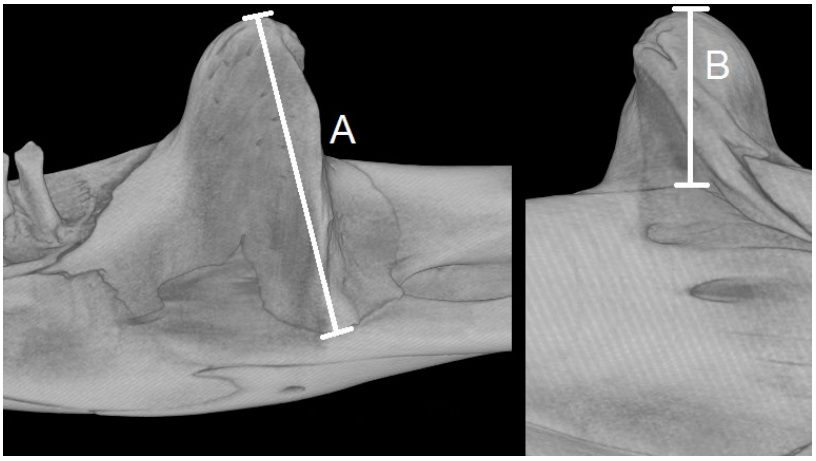

Figure A2.12: Measurements of coronoid height at taken from the centre of the apex to the lowest point on the posteromedial ramus (A). The height of the coronoid apex (Character 38) is measured from the centre of the apex to the dorsal surface of the surangular beneath it, this may require viewing in cross section if obscured by lateral wing of coronoid. Figured specimen is *Corucia zebrata* SAMA R35765 in medial (A) and lateral (B) views.

38. Coronoid, height of apex above surangular as ratio of dentary height (B, *Corucia zebrata* lateral view above): keep raw measurements. Measured from the middle of the dorsal surface of surangular directly below the apex of the coronoid (some species require measuring from a cross section if the surangular is not exposed at this location).
39. Coronoid, prominent posteriorly-directed ridge on posteromedial ramus: (0) absent, A; (1) present, B or C.

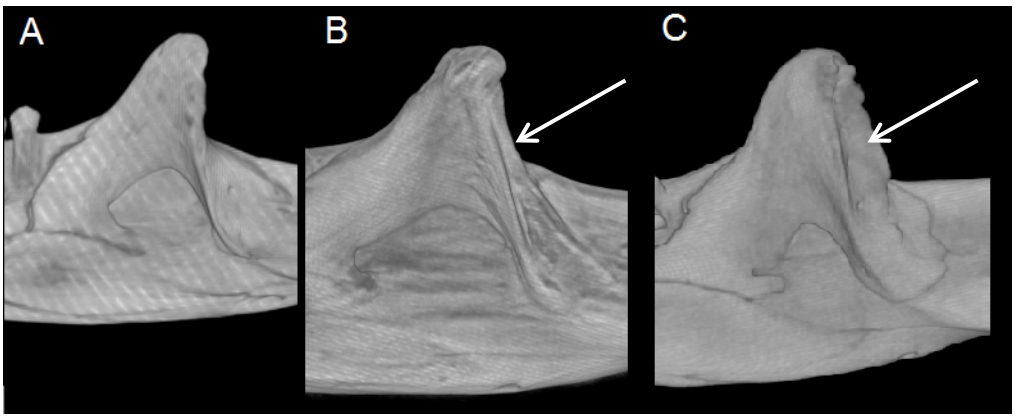

Figure A2.13: The appearance of the posteriorly directed 'wing' on the coronoid process and posterior coronoid ramus. The 'wing' is absent on (A) *Egernia stokesii* WAM R28909; present (B) but weak on *Bellatorias major* SAMA R35762 and present (B) and prominant on *Lissolepis luctuosa* WAM R36018. Prominence of the ridge can show ontogenetic variation but presence/absence is obvious in all adult phases.

Surangular and Articular

40. Surangular inserts into dentary lateral to the intramandibular septum, entering the intramandibular canal (Gauthier et al. 2012): (0) absent, A (*Liopholis whitii*); (1) present slightly, <25% of cavity filled in cross-section, B (*Corucia zebrata*); (2) present deeper 25-50% of cavity filled, C (*Tiliqua adelaidensis*); (3) present deeply >50% of cavity filled (ordered).

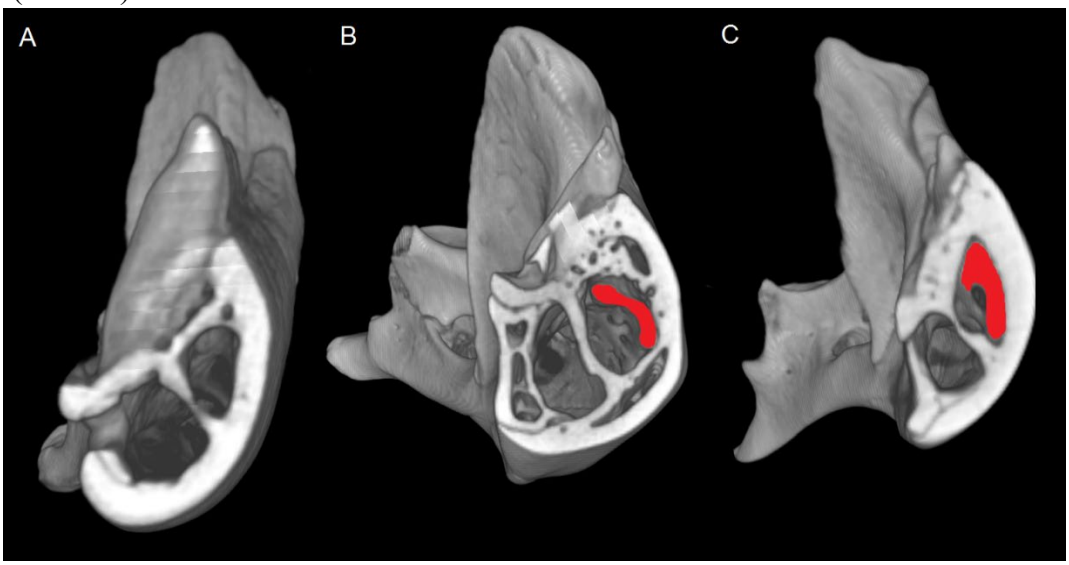

Figure A2.14: Viewed in cross section from the anterior, the absence or progression of the dentary posteriorly into the intramandibular canal. Each image marks the most anterior slice showing the closed intramandibular septum, the red section is the dentary. The dentary is absent in the septum in (A) *Liopholis whitii* SAMA R35688; the dentary is present but only fills <25% of the cavity in *Corucia zebrata* SAMA R35765 and present and filling 25–50% of the cavity in cross section in *Tiliqua adelaidensis* SAMA R40738.

41. Surangular, insertion area for adductor muscles on external face of mandible: (0) area not delineated; (1) faintly delineated, A (*Liopholis whitii*, posterodorsal view); (2) prominent/deeply delineated, B (*Lissolepis luctuosa*, posterolateral view).

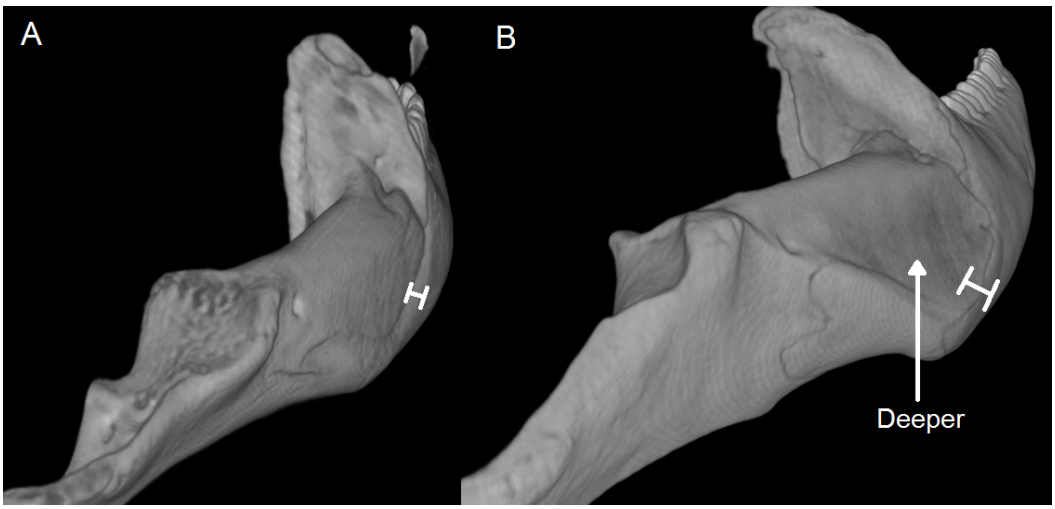

Figure A2.15: Delineation of the insertion area of the adductor muscles on the lateral face of the surangular appears either shallow/weak as in A represented by *Liopholis whitii* SAMA R35688, or the delineation is more prominent as shown by B *Lissolepis luctuosa* WAM R36018.

42. Number of anterior surangular foramina: (0) one; (1) two.
43. Number of posterior surangular foramina: (0) one; (1) two (both sides of mandibular cotyle); (2) more than two, with additional foramen in centre (*Tiliqua nigrolutea,* dorsal view).

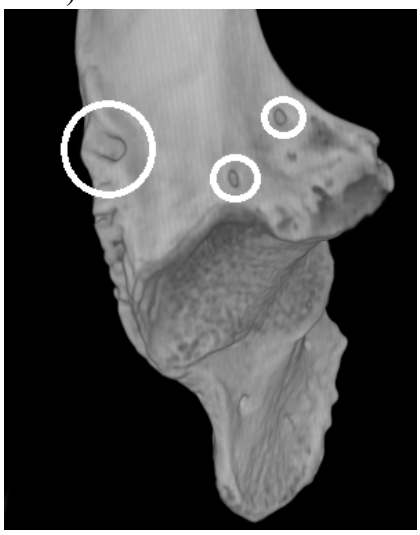

Figure A2.16: Posterior surangular foramina are visible on the dorsal surface of the surangular and include those on both sides of the ridge leading to the edge of the mandibular cotyle. Three are circled on *Tiliqua nigrolutea* SAMA R67631.

44. Adductor fossa, length viewed medially, as ratio of dentary length (*Corucia zebrata*, medial view): keep raw measurement.

Figure A2.17: Length of the adductor fossa is measured from the internal edges of the fossa anteriorly and posteriorly. Specimen figured is *Corucia zebrata* SAMA R35767.

45. Prearticular broadly contacts surangular behind posteromedial process of coronoid, restricting mandibular adductor fossa anteriorly (Gauthier et al., 2012): (0) absent; (1) present.

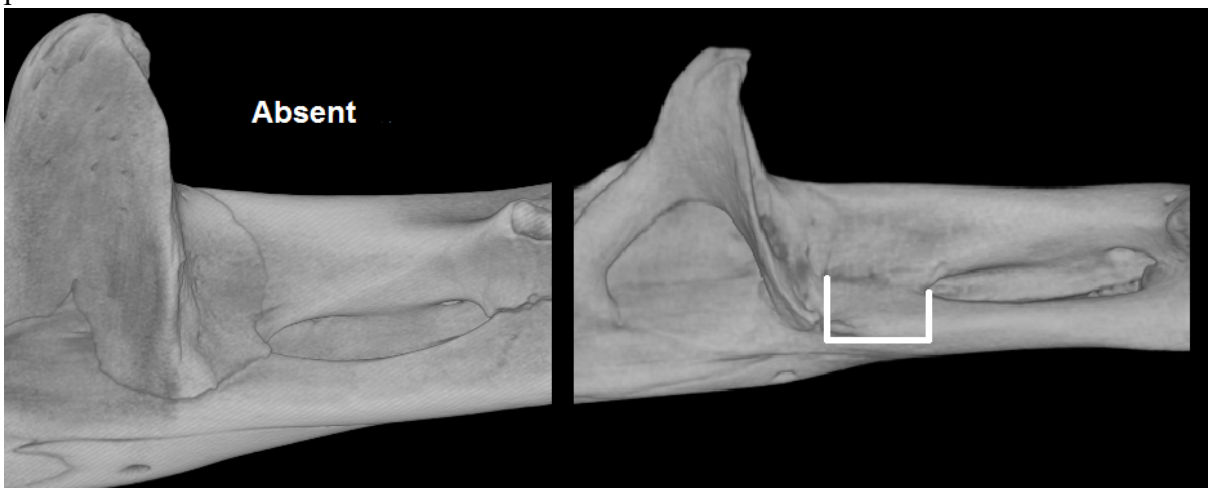

Figure A2.18: The prearticular broadly contact the surangular in medial view unless covered by the posteromedial ramus of the coronoid as shown by *Corucia zebrata* SAMA R35767 in the left image; or is still visible in *Liopholis whitii* SAMA R35688 on the right.

Retroarticular Process and Mandibular Cotyle (Glenoid)

46. Retroarticular process orientation in dorsal view (scored with teeth pointing vertically upwards, and relative to axis from coronoid apex to centre of anterior margin of articular cotyle (below, *Lissolepis luctuosa*): (0) not inflected medially; (1) inflected medially less than 30° (2) inflected medially 30-45° (3) inflected medially more than 45°. (ordered)

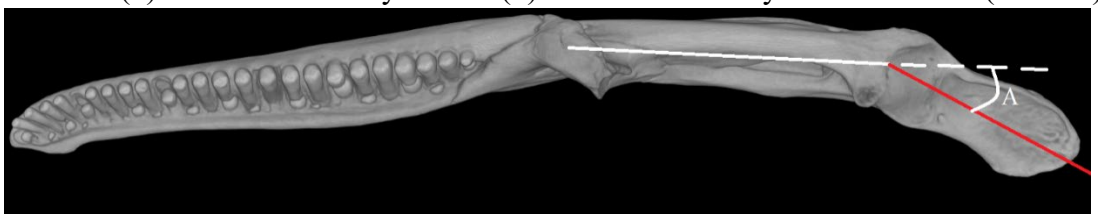

Figure A2.19: To measure the angle of inflection of the retroarticular process, view the mandible in dorsal view perpendicular to the maximum height of the dentary and surangular. Draw a through the centre of the length of the surangular from the coronoid apex through the edge of the mandibular cotyle. The angle (A) is measured from this line to the centre of the posterior edge of the retroarticular fossa, as shown on *Lissolepis luctuosa* WAM R36018.

47. Retroarticular process orientation in lateral view (angle from roughly parallel compound bone dorsal and ventral edges (below, *Liopholis whitii,* <30° inflected ventrally): (0)

inflected dorsally <30°; (1) extends approximately horizontally posteriorly (<10° either dorsally or ventrally); (2) inflected ventrally <30°; (2) inflected ventrally >30°. (ordered)

Figure A2.20: The dorso-ventral orientation of the retroarticular process is measured from medial view when the dentary and surangular maximum height is visible. Near-parallel dorsal and ventral edges of the surangular are the base from which to view the angle of the retroarticular, as shown with *Liopholis whitii* SAMA R35688.

48. Retroarticular process breadth (greatest width) relative to mandibular cotyle (glenoid): (0) narrower; (1) equal width; (2) wider. (ordered)
49. Retroarticular process (RAP) length as ratio of dentary length, measured on midline from posterior edge of cotyle to tip of retroarticular process (*Liopholis whitii*, dorsal view): keep raw measurements.

Figure A2.21: Length of the retroarticular process is measured in the centre of the margin between the retroarticular process and mandibular cotyle to the centre of the posterior edge of the RAP. Figured specimen is *Liopholis whitii* SAMA R35688)

Teeth

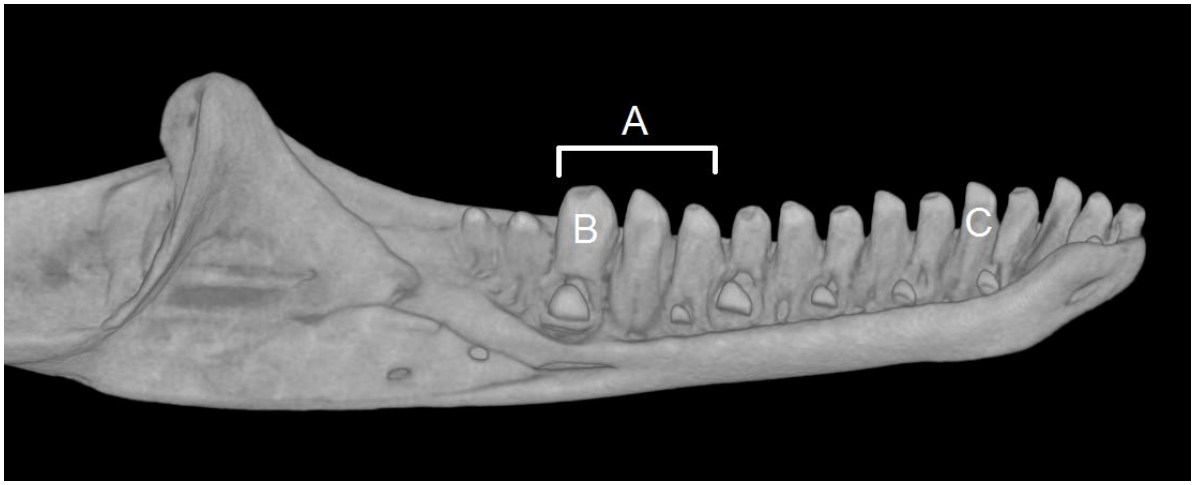

Figure A2.22: *Cyclodomorphus melanops* SAMA R35681 in medial view, showing the following features. A: Zone of enlarged teeth, teeth appearing at least ~25% larger than the modal tooth size; B: Largest tooth; C: 'Typical' tooth, median sized tooth located ¼ along length of tooth row from anteriormost point of dentary.

50. Number of dentary teeth: keep raw value.

51. Length of tooth row: keep raw measurement & scale to dentary length.
52. Number of enlarged teeth (roughly 25% larger than 'typical' tooth): raw value.
53. Zone of enlarged teeth (A), size of zone as % of tooth row length: keep raw values
54. Size of largest enlarged teeth: (NA) no enlarged teeth; (0) greater than 25% larger than 'typical' tooth; (1) 25-50% larger than 'typical tooth'; (2) 50-75% larger; (3) 75-100% larger; (4) >100% larger than 'typical tooth' (ordered).
55. Shape of tooth crown of typical tooth: (0) rounded, A (*Cyclodomorphus gerrardii*); (1) conical, B (*Cyclodomorphus melanops*); (2) mediolaterally compressed, single-ridged, C (*Egernia stokesii*); (3) lanceolate, leaf-shaped, D (*Corucia zebrata*); (4) bicuspid, E (*Lissolepis luctuosa*). Unordered..

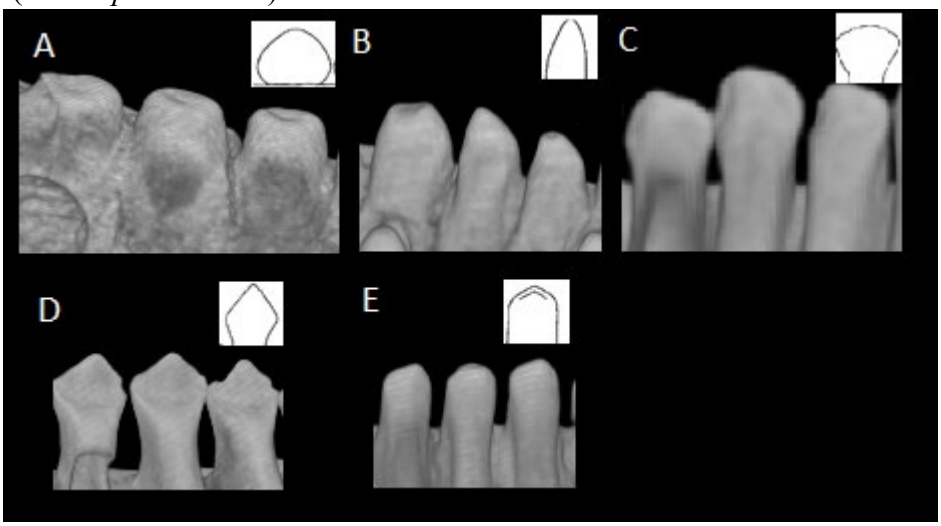

Figure A2.23: Tooth crown shape variation in the Egerniinae. Specimens A–E as are follows: *Cyclodomorphus gerrardii* SAMA R47699, *C. melanops* SAMA R35681, *Egernia stokesii* WAM R28909, *Corucia zebrata* SAMA R35767, and *Lissolepis luctuosa* WAM R36018. Outline images from Kosma (2003)

56. Tooth length from bottom edge of base to tip of crown of typical tooth, as ratio of dentary depth (A, *Liopholis whitii*): keep raw measurement.
57. Height of typical tooth above lateral edge of dentary (B), measured as ratio of total tooth length. This character relates to the position of the teeth relative to the tooth-bearing element (entirely on medial surface or positioned more on apical edge).
58. Diameter of crown (C) of typical tooth, as ratio of tooth row length: keep raw value.
59. Tooth base expanded relative to neck/crown: (0) no expansion; (1) slight expansion (25% increase); (2) great expansion (>25% increase).
60. Dental cementum coverage: (0) minor, present around bases of teeth and immediately between tooth and dentary wall; (1) partial, present as above but with some areas of cementum fulling spaces between teeth, resorption pits semi-circular shapes obvious; (2) heavily cemented, circular resorption pits obvious, bases of teeth obscured and spaces between teeth filled; (3) dental sulcus obliterated, teeth appear acrodont, no tooth bases visible.
61. Tooth crown striae: (0) absent; (1) present, fewer than 20; (2) present, many more than 20.
62. Teeth angled from base of shaft to tip of crown: (0) absent, vertical; (1) slight anterior curve.

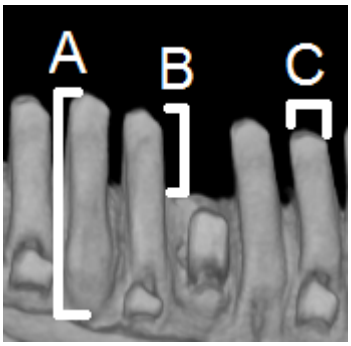

Figure A2.24: Tooth size measurements; A is ehight, B is height about dentary and C is crown width. Figured specimen is *Liopholis whitii* SAMA R35688

Premaxilla

63. Premaxilla body anterior ethmoidal foramina exit via (Lee, 2000; Gauthier et al., 2012): (0) external naris; (1) premaxilla notch; (2) premaxilla body; (3) between premaxilla and maxilla; (4) in maxilla (ordered).

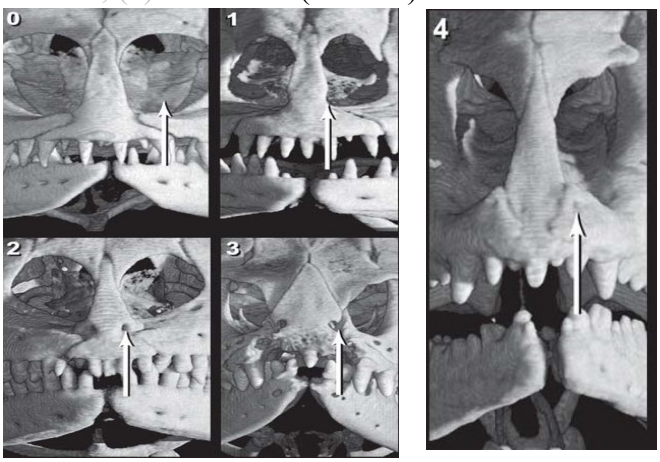

Figure A2.25: Arrows mark the exit location of the ethmoidal foramen. Specimen details are in captions from Gauthier et al. (2012) p80.

64. Premaxilla body ventral ethmoidal foramen (Gauthier et al., 2012): (0) absent; (1) small (barely visible); (2) large (obvious). (ordered)
65. Premaxilla internasal process height (A) as ratio of maxilla length: keep raw measurements.
66. Premaxilla maxillary process length (B) as ratio of height (A): keep raw measurements.
67. Number of left premaxillary teeth: raw value. A modified version of the premaxillary tooth count identified by Greer (1979).
68. Number of right premaxillary teeth: raw value.
69. Posterior angle of nasal process from tooth row, see Figure 2.26 A below: raw measurement.
70. Posterior angle of facial process of premaxilla from suture with opposing premaxilla to lateral suture with maxilla, see B below: raw measurement.

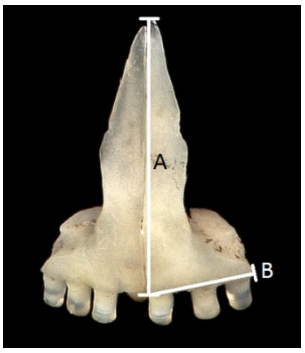

Figure A2.27: Size measurements of the premaxillae. Height is measured from the tip of the nasal process to the anterior ventral edge of the facial process. Width is measured from the ventral corner of the medial edge of the facial process to the lateral edge.

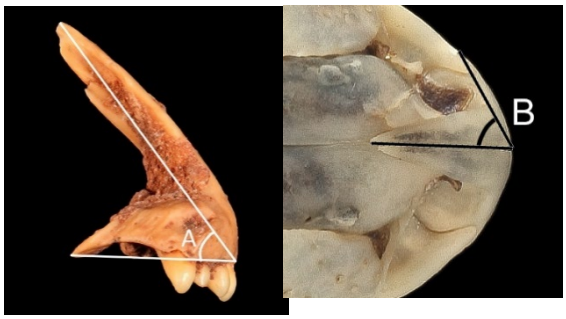

Figure A2.26: Measurements of the angles in the premaxilla. Posterior angle of nasal process taken in lateral view *Tiliqua frangens*, AM F145611. Angle of facial process is measured in dorsal view with teeth pointing in opposite direction to viewpoint, *Egernia napoleonis*, WAM R44673.

Nasals

71. Nasal anterior width (Gauthier et al. 2012): (0) exceeds nasofrontal joint width; (1) is subequal to nasofrontal joint width; (2) less than anterior nasofrontal width. Anterior width is defined as the maximum transverse dimension anywhere along the anterior 10% of nasal. (ordered)

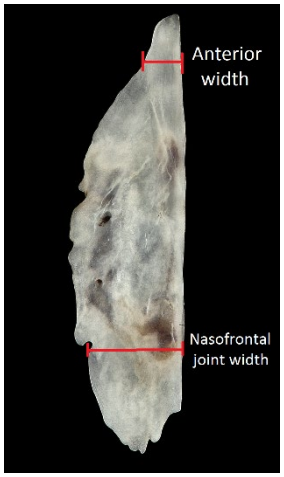

Figure A2.28: Nasal continuous measurements are taken in dorsal view on articulated specimens. Isolated nasal from *Bellatorias frerei* SAMA R21133 pictured.

72. Sutures in facial region: (0) Nasal-prefrontal sutural contact, separating frontal and maxilla; (1) frontal-maxilla contact.
73. Nasals; ventral contact beneath premaxillary internasal process (Gauthier et al., 2012): (0) broad contact below; (1) or not in contact except in posterior 10% of length (near apex).
74. Nasal-maxilla suture in cross section anteriorly (Gauthier et al. 2012): (0) maxilla overlaps nasal at roof of nasal chamber; (1) nasal partly overlaps maxilla dorsally; (2) nasal abuts maxilla; (3) nasal underlaps maxilla to floor of narial chamber. Unordered. States illustrated in Gauthier et al. (2012), p84.

Frontal

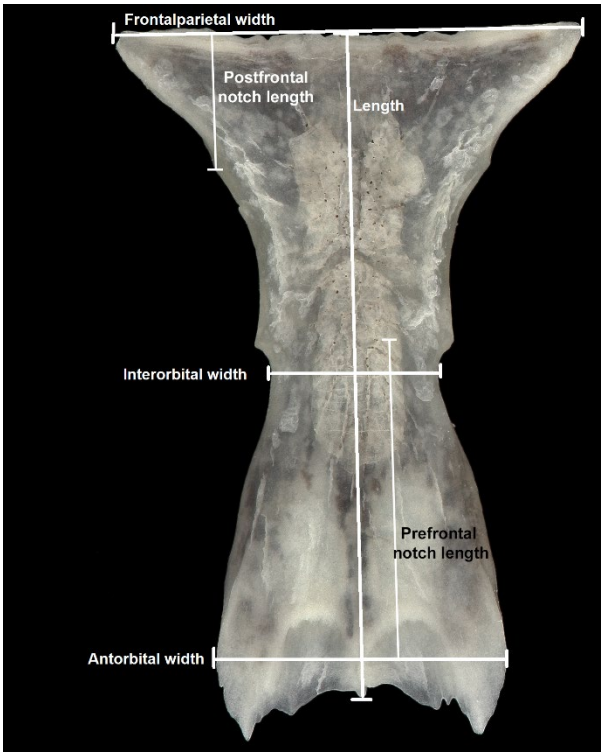

Figure A2.29: Measurement points for the frontal continuous characters. *Bellatorias frerei* SAMA R21133 isolated frontal, dorsal view.

75. Frontal anteroposterior length along midline, as ratio of frontoparietal suture width: keep raw measurements.
76. Frontal, frontoparietal suture width: keep raw measurements.
77. Frontal, interorbital width as ratio of frontoparietal suture width: keep raw measurements.
78. Frontal, width of widest point of the antorbital region, as ratio of frontoparietal width: keep raw measurement.
79. Frontal subolfactory process depth, measured from CT cross sections from the maximum ventral limit of the subolfactory process to the dorsal surface of the frontal (excluding osteoderms), as a ratio of frontoparietal suture width: keep raw measurements.
80. Extent of the prefrontal notch on the frontal, measured along anteroposterior midline from the antorbital greatest width, to posterior of notch as a ratio of total frontal length: keep raw measurements.
81. Extent of the postfrontal notch on the frontal, measured along anteroposterior midline from the frontoparietal suture, to the anterior-most point of the notch as a ratio of total frontal length: keep raw measurements.

Maxilla

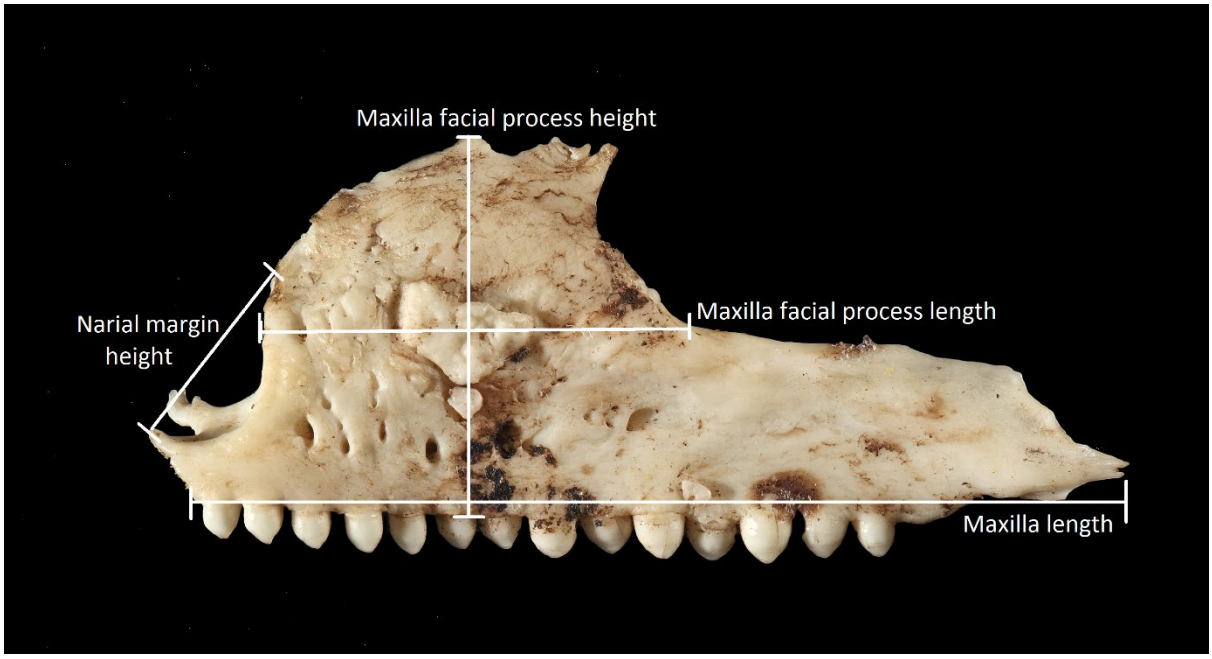

Figure A2.30: Continuous measurements of the maxilla (Char. 82–84) shown on *Tiliqua rugosa* SAMA R27027 in lateral view.

82. Maxilla facial process length/maxilla length (maxilla length measured just above base of tooth row from premaxillary articulation to posterior terminus of the element, maxilla facial process length measured from mid-height of narial margin to edge of jugal articulation) modified from Gauthier et al. (2012): keep raw measurements.
83. Maxilla facial process height (measured from dorsal tip to tooth row), as ratio of maxilla length: keep raw measurements.
84. Height of narial margin, as ratio of maxilla facial process height: keep raw measurements.
85. Shape of maxilla suborbital process tip at jugal articulation (Gauthier et al., 2012): (0) suborbital margin slopes smoothly to tip; (1) with distinct step (see *T. rugosa* above); (2)

with V-shaped notch distally at jugal articulation (*Egernia pilbarensis*, below).

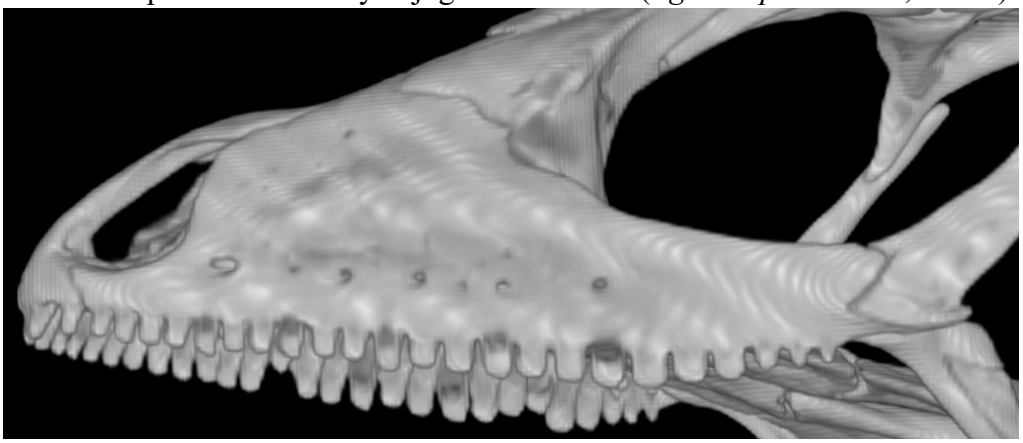

Figure A2.31: The V-shaped notch at jugal articulation shown on *Egernia pilbarensis* WAM R78945 in lateral view.

86. Number of maxillary teeth: keep raw value.
87. Length of tooth row (see figure for character 85 below): keep raw measurement, scaled to maxilla length.
88. Number of enlarged teeth (roughly >25% larger than 'typical' tooth teeth)
89. Size of enlarged teeth: (NA) no enlarged teeth; (0) 25% larger than 'typical' tooth; (1) 26-50% larger than 'typical tooth'; (2) 50-75% larger; (3) 75-100% larger; (4) >100% larger than 'typical tooth' (ordered).
90. Shape of tooth crown of typical tooth (located between 30-50% along tooth row, for images see character 59): (0) rounded, A (*Cyclodomorphus gerrardii*); (1) conical, B (*Cyclodomorphus melanops*); (2) mediolaterally compressed, single-ridged, C (*Egernia stokesii*); (3) lanceolate, leaf-shaped, D (*Corucia zebrata*); (4) bicuspid, E (*Lissolepis luctuosa*).
91. Zone of enlarged teeth (25% larger than 'typical' tooth), size of zone as % of tooth row length: (0) <25%; (1) 25-50%; (2) >50%. (ordered)
92. Width of medial tooth 'platform' at widest point, the palatine process of the maxilla, as ratio of maxilla length (A, below): keep raw measurements.

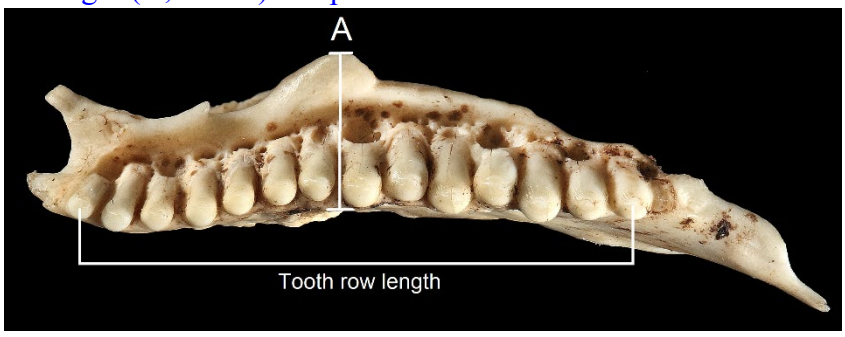

Figure A2.32: Continuous character measurement locations for maxilla tooth row length and width of medial palatine process of the maxilla (A). Figured specimen is *Tiliqua rugosa* SAMA R 27027 in ventral occlusal view.

93. Number of maxillary foramina above tooth row: keep raw value as Left#/Right#, highest value chosen or average if whole number. This character refers to the large foramina running parallel to the tooth row on the lateral face of the maxilla.
94. Maxilla suborbital ramus extends posteriorly, in lateral view with jugals aligned (modified from Lang, 1991): (0) no more than to approximately mid-orbit; (1) to posterior quarter of orbit; (2) to posterior edge of orbit; (3) posterior to orbit (or level of frontoparietal suture, if posterior orbital margin not bordered by bone). (ordered)

Prefrontal

95. Prefrontal orbitonasal margin (Gauthier et al., 2012): (0) slopes ventrolaterally; (1) vertical; (2) slopes ventromedially; (3) extends beneath subolfactory processes of frontal; (4) extends beneath subolfactory processes to near contact with its opposite on midline.

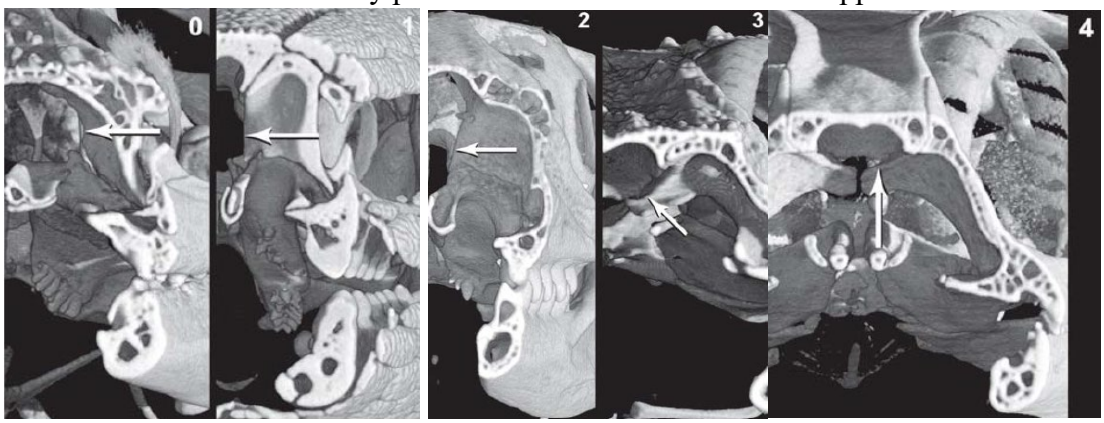

Figure A2.33: Arrows mark the medial extent and shape of the orbitonasal margin of the prefrontal (Char. 95). Images are from Gauthier et al. (2012) p121.

96. Prefrontal posterior extent along orbital margin (Lee et al., 2009b): (0) terminates in anterior half of orbit; (1) extends to midorbit; (2) extends posterior to midorbit. Images from Gauthier *et al*. 2012 (ordered). This trait can be scored from an isolated fossil frontal using the position of the prefrontal notch, in relation to the midpoint of the frontal length and position of the postfrontal notch.
97. Prefrontal shape at orbital margin: (modified from prefrontal boss character in Gauthier, 1984): (0) smooth curve from frontal to facial process of maxilla; (1) laterally-projecting lump in the corner of the orbit when viewed anteriorly or in cross-section.
98. Prefrontal-maxilla contact: (0) prefrontal posteroventromedial corner narrowly (or not) in contact with maxilla lateral to palatine; (1) prefrontal broadly contacts maxilla supradental shelf lateral to palatine (Tchernov et al., 2000; Gauthier et al., 2012); (2) prefrontal has mobile contact with maxilla; (3) rod-like prefrontal arched dorsally, bifid at each end, with mobile joints at maxilla and frontal (prefrontal functionally part of upper jaw).
99. Prefrontal-frontal suture in cross-section (Gauthier et al., 2012): (0) prefrontal arcs gently about anterolateral frontal margin along entire anteroposterior length; (1) prefrontal strongly bifid, clasps frontal posteriorly then spreads dorsally and reduced ventrally anteriorly; (2) frontal clasps prefrontal in V-shaped notch (ordered).

Lacrimal

100. Lacrimal (Estes et al., 1988): (0) present; (1) absent.
101. Lacrimal position and size relative to lacrimal duct (Gauthier et al., 2012): (0) lacrimal with broad exposure laterally, reaching from lateral floor of lacrimal duct up the medial face of the maxilla to contact a lateral process of the prefrontal that roofs the lacrimal duct in cross section; (1) lacrimal arches over the lacrimal duct to replace the prefrontal dorsally, broadly floors the lacrimal duct with a medial process posteriorly passing up the lateral face of the prefrontal; (2) lacrimal reduced to floor of lacrimal duct and lingual surface of maxilla, and barely, if at all, exposed laterally; (3) lacrimal bone reduced ventrally, confined mainly to dorsolateral corner of lacrimal duct.

Jugal

102. Jugal extent anteriorly with respect to tooth row, viewed dorsally (Gauthier et al., 2012): (0) jugal broadly overlaps level of posterior maxillary tooth row; (1) jugal overlaps the most posterior maxillary tooth; (2) jugal just reaches base of, or stops short of, the most posterior maxillary tooth. (ordered)
103. Jugal anterior extent (Gauthier et al., 2012): (0) broadly separated from prefrontal; (1) reaches level of prefrontal.
104. Jugal postorbital ramus width at midpoint along length: (0) <25% of jugal height; (1) ramus 25%-50% jugal height; (2) >50% jugal height. (ordered)
105. Jugal contacts squamosal (Tchernov et al., 2000; Gauthier et al., 2012): (0) absent; (1) present but narrow; (2) broad contact. (ordered)
106. Jugal posterior process (Benton, 1984; Gauthier et al., 1988; Gauthier et al., 2012): (0) complete lower temporal bar; (1) reduced to a discrete bony posterior process; (2) absent. (ordered)
107. Jugal medial ridge on the postorbital ramus (Gauthier et al., 2012): (0) medial ridge weak, jugal lateral to ectopterygoid at base in dorsal view; (1) medial ridge pronounced, base of medial ridge projects behind ectopterygoid base in dorsal view.

Postfrontal

108. Postfrontal supratemporal shelf (Gauthier et al., 1988; Gauthier et al., 2012): (0) absent; (1) present as thin shelf extending over anterodorsal corner of supratemporal fenestra; (2) extending posteriorly further than laterally across upper temporal fenestra; (3) extending both posteriorly and laterally to (nearly) occlude upper temporal fenestra. (ordered)

Parietal

109. Parietal nuchal fossa width (modified from Gauthier et al., 2012): (0) wider that 1/3 of the width of posterior process of parietal in dorsal view; (1) narrower than 1/3 of posterior process of parietal in dorsal view; (2) not visible in dorsal view, overgrown by parietal (nearly) to midline. (ordered)
110. Parietal supraoccipital process near midline (Gauthier et al., 2012): (0) absent; (1) present.
111. Parietal supraoccipital process (Lang, 1991; Gauthier et al., 2012): (0) not bifid; (1) bifid but not clasping supraoccipital crest; (2) bifid clasping supraoccipital crest. (ordered) This is NA in taxa without the process.
112. Parietal foramen (Estes et al., 1988): (0) present; (1) absent.
113. Parietal epipterygoid process (Estes et al., 1988): (0) absent; (1) distinct process but not reaching alar process of prootic; (2) distinct process reaching alar process of prootic. (ordered)

Quadrate

114. Quadrate-pterygoid overlap (Gauthier et al., 2012): (0) extensive; (1) short overlap or small lappet; (2) very narrow overlap or lappet absent; (3) no overlap, ligamentous connection only. (ordered)
115. Quadrate height as ratio of maxilla length: keep raw measurement.
116. Maximum quadrate width (mediolateral): keep raw measurement.
117. Tympanic crest of lateral face of tympanic conch of quadrate: (0) absent; (1) present; (2) thickened, engorged.

118. Medial ridge of quadrate visible from lateral view: (0) present; (1) obscured by curvature of tympanic conch.

Squamosal

119. Temporal ramus shape, in cross-section (Gauthier et al., 2012): (0) circular; (1) depressed (dorsoventrally flattened).
120. Temporal ramus width at widest point: (0) narrow; (1) wide (>15% of length). Keep raw measurements.

Supratemporal

121. Supratemporal in dorsal view (Gauthier et al., 2012): (0) supratemporal at least partly exposed dorsally on lateral side of parietal supratemporal process; (1) slender and hidden completely from view by parietal-squamosal contact dorsally.

Vomer

122. Vomer fusion (Estes et al., 1988): (0) absent; (1) partial; (2) fully fused.
123. Vomer overlaps (dorsally) the palatal shelf of the maxilla behind posterior margin of opening of vomeronasal organ (Gauthier et al., 1988): (0) absent; (1) present.
124. Vomer, transverse flange rises vertically to meet septomaxilla and encloses vomeronasal organ posteriorly (pictured; Gauthier et al., 2012): (0) absent; (1) present.

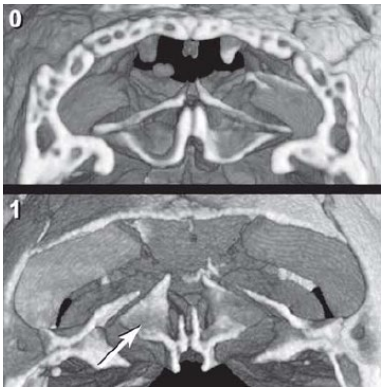

Figure A2.34: Transverse flanges of the vomer (Char. 124) are marked with a white arrow. Images from Gauthier et al. 2012 p161.

Palatines

125. Palatine ventral plates contact (Lee, 1998): (0) separated; (1) anterior contact only; (2) contact extends from anterior to midpoint, or beyond; (3) posterior contact only.
126. Palatine contribution to suborbital fenestra (Gauthier et al., 2012): (0) reduced posteromedially, and pterygoid broadly exposed in suborbital fenestra; (1) palatine extends posteriorly along lateral edge of pterygoid so that pterygoid only narrowly enters suborbital fenestra; (2) palatine fully excludes pterygoid from border of suborbital fenestra. (ordered)
127. Palatine (modified from Gauthier et al., 2012): (0) incipient duplicipalatinate, >20% of circumference open in cross section (1) moderately duplicipalatinate, >10% of circumference in cross section is open (image below, anterior cross section through palatines *Lissolepis coventryi*); (2) fully duplicipalatinate (closed or with <10% of circumference open in cross section). (ordered)
128. Palatine, subchoanal process medial edge shape in ventral view (Gauthier et al., 2012): (0) present

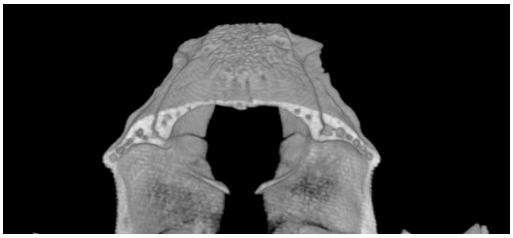

Figure A2.35: Palatine shape in cross section, showing the degree to which the palatine forms a complete duplicipalatinate (tube) structure. Specimen figured is *Lissolepis coventryi* SAMA R35686 in cross section viewed from the anterior.

only on anterior one-third of palatine; (1) roughly arcuate; (2) roughly parasagittal. (ordered)

Pterygoid

129. Pterygoid separation on midline (Estes et al., 1988): (0) pterygoids narrowly separated for most of their length; (1) separation broad posteriorly, narrow anteriorly; (2) broad posteriorly, but not as narrowly separated anteriorly; (3) broad throughout length. Images in Gauthier et al. (2012) p172 (ordered)
130. Pterygoid, palatine ramus clasps, or has extensive contact with, pterygoid ramus of palatine (Wu et al., 1996): (0) absent; (1) present. This character corresponds to the lateral process of the palatine ramus of the pterygoid, images in p173 in Gauthier et al. (2012).
131. Pterygoid teeth (Pregill et al. 1986): (0) present; (1) absent.
132. Pterygoid inter-ramus width (across palatine and ectopterygoid rami) as ratio of total length: keep raw measurements.
133. Pterygoid total length as ratio of maxilla length: keep raw measurements.
134. Pterygoid quadrate ramus in cross section: (0) is arcuate, forming a long 'wing' shape; (1) circular or flat, rod shaped overall, no flanges.
135. Divot in ventral surface of the pterygoid anterior to the epipterygoid notch: (0) absent; (1) present, shallow smooth curve; (2) present, deep with ridges edges.

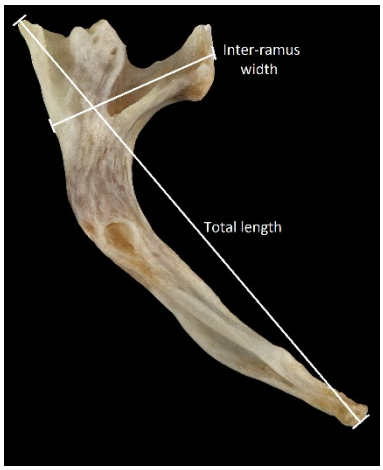

Figure A2.36: Continuous measurement points for the pterygoid total length and inter-ramus width. Specimen figured is *Egernia cunninghami* SAMA R27151 in dorsal view.

Ectopterygoid

136. Ectopterygoid size and restriction of suborbital fenestra (Estes et al. 1988): (0) ectopterygoid relatively slender, fenestra widely open; (1) ectopterygoid enlarged medially, restricting suborbital fenestra; (2) ectopterygoid highly enlarged medially, closing suborbital fenestra. Images in Gauthier et al. (2012) p175 (ordered)

Epipterygoid

137. Epipterygoid, in resting position (Gauthier et al., 2012): (0) located lateral to prootic; (1) located entirely anterior to prootic.

Braincase

138. Calcified or ossified processus ascendens of synotic tectum (Estes et al., 1988): (0) absent; (1) present.
139. Prootic, supratrigeminal process (Estes et al., 1988): (0) absent; (1) weakly developed, not projecting beyond cupola anterior; (2) present as a finger-like projection above trigeminal notch, projecting beyond cupola anterior. (ordered)
140. Crista prootica (Estes et al., 1988): (0) does not extend onto basipterygoid process; (1) extends onto basipterygoid process forming open or closed bony canal.
141. Crista prootica aliform in outline in ventral view, extended butterfly shape (Estes et al., 1988; Gauthier et al., 2012): (0) absent; (1) present but not prominent; (2) prominent, extending far laterally. (ordered)

142. Cultriform process, ossified base (Gauthier et al., 2012): (0) long; (1) short; (2) absent. (ordered)
143. Vidian canal, caudal opening (Estes et al., 1988): (0) within basisphenoid; (1) anterior margin at basisphenoid-prootic suture; (2) entirely within prootic. (ordered)
144. Carotid artery exits at rostral end of vidian canal (Rieppel et al., 2008): (0) at same level (or slightly above) as the base of the cultriform process; (1) below the level of the cultriform process.
145. Supraoccipital crest (Rieppel, 1981): (0) absent; (1) present but does not contact parietal (Estes et al. 1988); (2) present and contacts parietal. (ordered)
146. Occipital condyle (Lee, 1998): (0) posterior surface of condyle straight in ventral view; (1) posterior surface of condyle concave in ventral view.
147. Hypoglossal (XII) modal condition of the foramina relative to vagus (X–XI) foramen on external surface of braincase (Conrad, 2008; Gauthier et al., 2012): (0) all hypoglossal foramina separated from vagus (jugular) foramen; (1) one hypoglossal foramen emerges from the same fossa as the vagus foramen; (2) two hypoglossal foramina emerge from the same fossa as the vagus foramen; (3) all three hypoglossals emerge from the same fossa as the vagus foramen. (ordered)
148. Depth of posterior processes (A below) as ratio of anteroposterior length of the supraoccipital, measured from the anterior face of the processus ascendens to the posterior edge of the supraoccipital mid-way between the paraoccipital processes (B below).

Figure A2.37: Continuous measurement of the posterior processes of the braincase (Char. 148), figured specimen is *Tiliqua rugosa* SAMA 35760.

149. Angle of deflection of the paraoccipital processes, A below (*Tiliqua rugosa*).

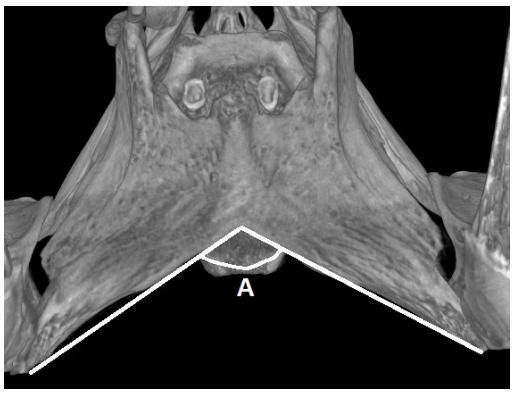

Figure A2.38: The angle between the paraoccipital processes is measured in dorsal view as shown on *Tiliqua rugosa* SAMA R35760.

150. Angle of opening of trigeminal notch, measured between ventral line of cupola anterior and dorsal edge of sphenoid (A below; *Tiliqua rugosa*).

References

Benton, M. J. 1984. The relationships and early evolution of the Diapsida; pp. 575–596 in M. W. J. Ferguson (ed.), The Structure, Development and Evolution of Reptiles. Cambridge University Press, London, United Kingdom.

Conrad, J. L. 2008. Phylogeny and systematics of Squamata (Reptilia) based on morphology. Bulletin of the American Museum of Natural History:1–182.

Estes, R., K. De Queiroz, and J. Gauthier. 1988. Phylogenetic relationships of the lizard families. Stanford Univ Press, Stanford, CA, Stanford, California, 648 pp.

Etheridge, R., and K. de Queiroz. 1988. A phylogeny of Iguanidae; pp. 283–367 in R. Estes and G. Pregill (eds.), Phylogenetic relationships of the lizard families. Stanford University Press, Stanford, California.

Frost, D. R., and R. Etheridge. 1989. A phylogenetic analysis and taxonomy of iguanian lizards (Reptilia: Squamata). Miscellaneous Publication of the University of Kansas Museum of Natural History 81:1–65.

Gauthier, J. 1984. A cladistic analysis of the higher systematic categories of the Diapsida. University of California, Berkley, California, USA.

Gauthier, J., A. G. Kluge, and T. Rowe. 1988. Amniote phylogeny and the importance of fossils. Cladistics 4:105–209.

Gauthier, J. A., M. Kearney, J. A. Maisano, O. Rieppel, and A. D. B. Behlke. 2012. Assembling the Squamate Tree of Life: Perspectives from the Phenotype and the Fossil Record. Bulletin of the Peabody Museum of Natural History 53:3–308.

Greer, A. E. 1979. A phylogenetic subdivision of Australian skinks. Records of the Australian Museum 32:339–371.

Hollenshead, M. G., J. I. Mead, and S. L. Swift. 2011. Late Pleistocene *Egernia* group skinks (Squamata: Scincidae) from Devils Lair, Western Australia. Alcheringa: An Australasian Journal of Palaeontology 35:31–51.

Kosma, R. 2003. The dentitions of recent and fossil scincomorphan lizards (Lacertilia, Squamata) - Systematics, Functional Morphology, Palecology. Department of Geosciences and Geography, University Hannover, Hanover, Germany, 231 pp.

Lang, M. 1991. Generic relationships within Cordyliformes (Reptilia: Squamata). Bulletin de l'Institut Royal des Sciences Naturelles de Belgique. Biologie 61:121–188.

Lee, M. S. Y. 1998. Convergent evolution and character correlation in burrowing reptiles: towards a resolution of squamate relationships. Biological Journal of the Linnean Society 65:369–453.

Lee, M. S. Y. 2000. Soft anatomy, diffuse homoplasy, and the relationships of lizards and snakes. Zoologica scripta 29:101–130.

Lee, M. S. Y., M. N. Hutchinson, T. H. Worthy, M. Archer, A. J. D. Tennyson, J. P. Worthy, and R. P. Scofield. 2009b. Miocene skinks and geckos reveal long-term conservatism of New Zealand's lizard fauna. Biology Letters 5:833–837.

Rieppel, O. 1981. The skull and the jaw adductor musculature in some burrowing scincomorph lizards of the genera *Acontias*, *Typhlosaurus* and *Feylinia*. Journal of Zoology 195:493–528.

Rieppel, O., J. Gauthier, and J. Maisano. 2008. Comparative morphology of the dermal palate in squamate reptiles, with comments on phylogenetic implications. Zoological Journal of the Linnean Society 152:131–152.

Smith, K. T. 2009. Eocene lizards of the clade *Geiseltaliellus* from Messel and Geiseltal, Germany, and the early radiation of Iguanidae (Reptilia: Squamata). Bulletin of the Peabody Museum of Natural History 50:219–306.

Tchernov, E., O. Rieppel, H. Zaher, M. J. Polcyn, and L. L. Jacobs. 2000. A fossil snake with limbs. Science 287:2010–2012.

Thorn, K. M., M. N. Hutchinson, M. Archer, and M. S. Y. Lee. 2019. A new scincid lizard from the Miocene of Northern Australia, and the evolutionary history of social skinks (Scincidae: Egerniinae). Journal of Vertebrate Paleontology 39:e1577873.

Wu, X.-C., D. B. Brinkman, and A. P. Russell. 1996. *Sineoamphisbaena hexatabularis*, an amphisbaenian (Diapsida: Squamata) from the Upper Cretaceous redbeds at Bayan Mandahu (Inner Mongolia, People's Republic of China), and comments on the phylogenetic relationships of the Amphisbaenia. Canadian Journal of Earth Sciences 33:541–577.

Appendix 3: Supplementary Information for Chapter 4

Materials and Methods

Material preparation

Specimens AM F73805, 107904, 58265, 58257 and 143321–143325, were located in the Australian Museum Palaeontology collection (AM), with provenance indicated as 'Wellington Caves, N.S.W.'.

New specimens AM F145608–F145627 were obtained from ongoing excavations at Cathedral Cave led by DAF and GJP. Stratigraphic ages were derived by means of Optically Stimulated Luminescence Dating of sediments. The youngest specimen of confirmed provenance is an isolated osteoderm from Layer 10 (AM F145627). An isolated osteoderm fragment recovered from Layer 7 (AM F145626) is mostly likely the result of crevice-fill (Fusco pers. comm.) and is not a convincing minimum age reference specimen. Dates are not presented in this thesis as they are the results of DAF's thesis. All fossil squamate specimens were initially identified to family level using comparative specimens housed in the South Australian Museum Herpetology Collection (SAMA) and Flinders University Palaeontology Reference Collection (FUR). The only squamates found in this deposit similar to *Tiliqua frangens* in size were a large varanid species (cf. *Varanus varius*) and snakes (*Wonambi* sp. cf. *naracoortensis*, and *Morelia* sp.).

All newly recovered fossil specimens described herein were cleaned of adhering matrix, mechanically using a microjack, or with dilute acetic acid before being consolidated with a solution of Paraloid b72 in acetone. Selected specimens were photographed with a stacking camera set up at either the South Australian Museum or Flinders University Palaeontology. Imaged were stacked using a StackShot set up with Zerene photostacker software. Micro computed tomography (Micro-CT) scans were generated using the Skyscan-1076 at Adelaide Microscopy. Resulting files were reconstructed in NRecon (Bruker), and rendered and viewed in Avizo Light (version 9.0). Due to the size of the material, 17μ resolution was chosen for all specimens. Voxel size was recorded and defined in Avizo to standardise measurements. Scanning Electron Microscopy of the tooth crowns was conducted at Flinders University Microscopy facilities using an Inspect FEI F50 SEM. All digital measurements were recorded in micrometres and converted to millimetres for the description and body size analyses.

Phylogenetic analyses

Taxa sampled for this analyses were 32 extant egerniine species, two mid-Miocene fossil taxa: *Egernia gillespieae* Thorn, Hutchinson, Archer and Lee, 2019 (14.17–15.11 Ma; Thorn et al., 2019), and *Tiliqua pusilla* Shea and Hutchinson, 1992 (14.47–16.86 Ma; Shea and Hutchinson, 1992); and outgroup taxon *Eutropis multifasciata* (as per Gardner et al., 2008; Thorn et al., 2019).

Extant taxa used in this analyses were chosen to ensure broad taxonomic sampling as well as availability of published molecular data.

A character by taxon matrix was constructed by expanding the set of morphological characters in Thorn et al. (2019). Eight new continuous and seven discrete characters were added to capture variation introduced with the addition of the new fossil taxon, focusing on the dentary, frontal and braincase elements. Continuous characters were measured with callipers or from Micro CT scans reconstructed in Avizo Lite (v. 9.0) to the nearest micrometre. All measurements for the continuous characters were log transformed and converted to ratios of total element length to scale for size. New numbered characters 60–62, 69–70, 80–81, 116–118, 134–135, and 148–150 were dovetailed into the existing character set and matrix (see Appendix 2), rather than appended to end, so that when coding taxa the characters are still arranged by element.

The molecular alignment was derived from concatenating loci (T12S 412bp, 16S 681bp, ND4 693bp BDNF 699bp, CMOS 835bp) in Tonini et al. (2016) and B-fibrinogen intron, 1051 alignable bp, from Gardner et al. (2008), and is available in the supplementary information to Thorn et al. (2019).

Maximum Parsimony

The parsimony analyses for the combined discrete morphological and molecular data was performed using TNT v.1.5 (Goloboff and Catalano, 2016). *Eutropis multifasciata* was set as the most distant outgroup in all runs (as in Gardner et al. 2008 and Thorn et al. 2019). The most parsimonious tree for the combined data was found with a heuristic search using 1000 replicates of tree-bisection-reconnection (TBR) with up to 1 000 000 trees held. To assess clade support, 200 partitioned bootstrap replicates (with separate resampling partitions for discrete characters, continuous characters, and each gene locus treated), were performed using TNT, using new search methods (XMULT) with 1000 replicates and 1 000 000 trees held. The MPT and bootstrap trees from TNT were exported as nexus format, and continuous and discrete characters were traced in Mesquite v3.5, (Maddison and Maddison, 2017). An additional analysis was also performed with continuous characters, which were each transformed to span values ranging from 0–2, matching the average number of character states (3) in the discrete morphological data (as per Thorn et al. 2019). The executable files for these analyses are in the digital appendices for this chapter.

Bayesian analyses

The above discrete morphological and DNA data were also analysed using tip-dated Bayesian phylogenetics in BEAST v.1.8 (Drummond et al., 2012). Discrete morphological characters were analysed using the Mk-model with correction for non-sampling of constant

characters (Lewis, 2001; Alekseyenko et al., 2008) which has been well-tested (Wright and Hillis, 2014; O'Reilly et al., 2016). Polymorphic morphological data (e.g. 0&1) could be treated exactly as coded (e.g. 0 or 1 but not 2), not as total uncertainty (0 or 1 or 2). For DNA data, the most appropriate partitioning scheme, substitution matrices, and among-site rate variability model for the molecular loci was identified via PartitionFinder 2 (Lanfear et al., 2016), using BIC with each locus and codon treated as a candidate partition. For dating, the root age was loosely constrained to lie between the most extreme values found across multiple recent studies (see Tonini et al., 2016; Zheng and Wiens, 2016; Thorn et al., 2019), with a normally-distributed prior set to 57.665 ± 2.7 Ma; the age of each fossil was also allowed to vary to reflect stratigraphic uncertainty. No other node age constraints were imposed; the retrieved dates are generated from the phenotypic and stratigraphic information contained in the fossil taxa (tips). The significance of rate variation across lineages (strict versus relaxed clocks), in each of the three character sets, was tested using Bayes Factors. An additional analysis was also performed with continuous characters included; these were analysed using a Brownian motion model bounded between 0 and 2, since all characters were rescaled to span these values (see above). The most appropriate available tree prior in BEAST (birth-death serial sampling) was employed (note: the SABD prior in BEAST2 cannot be implemented with continuous traits).

Each of these two final Bayesian analyses was repeated four times to confirm stationarity, with the post-burnin samples of all four runs combined for statistical analyses and consensus trees in Tracer (v1.6.0 Rambaut et al., 2014). The executable files can be found in SI folder 'Wellington/Bayesian analyses in BEAST' supplied as supplementary information for this thesis.

Body size estimation

The *Tiliqua frangens* adult is known in sufficient detail to reconstruct total head length. In absence of the parietal of this species, the squamosal length contributes to the estimate of total skull length of *T. frangens* of 70 mm, a value supported by total mandible length. Head length of comparative extant *Tiliqua rugosa* was measured as the total length from the anterior tip of the nares to the rear of the interparietal scale.

Head length of *Tiliqua frangens* was calculated by reassembling the adult skull using the adult nasal (AM F145612), frontal (AM F145614) and squamosal (AM F145619). This length is supported by a similar measurement generated with the mandible using the dentary and post-dentary complex (AM F143321).The relationship between head length and body length/weight across extant *Tiliqua rugosa* (the most appropriate living analogue, based on the phylogenetic analyses) was used to infer the body size of the fossil taxon. Body size in extant populations of

Tiliqua rugosa is biogeographically highly variable, with subspecies in Western Australia weighing ~250g but >1kg in eastern Australia (Wilson and Swan, 2017). Comparative measurements of the head length of modern specimens of *Tiliqua rugosa* (digital appendix file '*T. frangens* measurements.xls') show associated variability in size; 210 specimens were measured spanning 29–55 mm in head length. Standardised Major Axis Regressions (SMAR) were performed using the SMATR package v3.4-8, and graphed using ggplot in RStudio (RStudio Team, 2016; Wickham, 2016; Warton et al., 2018) of the log-transformed head length vs body length and head length vs body mass data for *T. rugosa*, and the allometric regressions used to infer body length and body mass for *T. frangens.*

Shape analyses

Dentary length, height, and width; tooth row length; symphysis length and width were measured to the nearest millimetre. Recognisable vertebrae such as the axial, sacral, and first caudal, had measurements taken of the following; centrum length, centrum width, neural spine height, prezygopophyses width, transverse process length, width and depth. Isolated osteoderms were measured from modern reference specimens of *Tiliqua rugosa* and fossil material attributed to *T. frangens*; width (mediolateral), length (anteroposterior) and dorsoventral depth. Shape variation in extant *Tiliqua rugosa* was captured by measuring multiple variables in skeletal specimens from the South Australian Museum (SAMA), Australian Museum in Sydney (AM), Queensland Museum (QM), and Museums Victoria (NMV) collections from across the geographical range of the species using fine-pointed digital callipers. Measurements were read to 0.01 mm then rounded to 0.1 mm. Frontal measurements of extant *Tiliqua rugosa* specimens were sourced from the original description of *T. laticephala* (Čerňanský and Hutchinson, 2013), and new specimens were measured using the same method.

One-way PERMANOVAs were calculated to test for statistical separation of extant and extinct specimens using both the mandibular and vertebral measurements, these and Principal Components Analyses (PCAs) of the same data were conducted in PAST v.3.14 (Hammer et al., 2001). One-way PERMANOVAs were calculated to test for statistical separation of extant and extinct frontal dimensions in PAST v.3.14 (Hammer et al., 2001).

All anatomical terminology follows Evans (2008), Russell and Bauer (2008), and both Kosma (2003) and Richter (1994) for tooth crown features. We describe the material first, and then discuss our reasons for associating these elements in detail immediately afterwards.

Systematic Palaeontology

Order Squamata Oppel, 1811

Infraorder Scincomorpha Camp, 1923

Family Scincidae Gray, 1825

Subfamily Egerniinae, Welch, 1982

Tiliqua Gray, 1825

Tiliqua frangens (Hutchinson and Scanlon, 2009)

'Lacertilian' (Etheridge, 1917: plate 8, figures 6–8), cluster of fused osteoderms.

Tiliqua scincoides; Bartholamai (1977: plate 16, fig. 1), partial left dentary QM F7709, Cement Mills, Gore, Queensland, Pleistocene. Not *Tiliqua scincoides* (White, 1790).

Tiliqua rugosa; Price and Sobbe (2005: p182), osteoderm Figure 8J [QM F44603-44605]. Not *Tiliqua rugosa* Gray, 1825.

Aethesia frangens Hutchinson and Scanlon, 2009: 140, figures 1, 2 – Holotype, anterior half left mandible SAMA P43196 (Hutchinson and Scanlon, 2009).

'Unknown, possibly lizard like animal' (Kear and Hamilton-Bruce, 2011) Figured p135. Cluster of fused osteoderms described in Etheridge (1917). Not Mesozoic.

Tiliqua laticephala Čerňanský and Hutchinson, 2013: 133, figures 2, 3 – Holotype, incomplete frontal AM F135900 (Čerňanský and Hutchinson, 2013).

Referred specimens

From 'Wellington Caves, N.S.W.' exchanged with the Dept. of Mines NSW are AM F73805 (left dentary), F107904 (osteoderm cluster), F58265 (sacrum and braincase), F58257 (sacrum), F143321 (adult mandible), F143322 (young adult mandible), F143323 (left and right peramorphic adult dentaries), F143324 (left and right adult dentaries), and F143325 (left adult dentary). From the Prideaux and Fusco 2016 excavation, Cathedral Cave, Wellington Caves are AM F145608 (right neonate dentary), F145609–10 (two right maxillae), F145611 (right premaxilla), F145612 (right nasal), F145613–4 (young adult and adult frontals), F145615 (right partial pterygoid), F145616 (young adult braincase), F145618 (right quadrate), F145619 (right squamosal), F145620 (left tibia), F145621 (presacral vertebra), F145622 (pygal vertebra), F145623 (osteoderm), F145624 (adult right maxilla), F145626 (isolated osteoderm) and F145627 (cranial osteoderm). QM F41532, an associated skeleton comprising both humeri, both prefrontals, a premaxilla, ectopterygoid, frontal,

and multiple associated osteoderms from Sobbe Site. An unregistered right dentary with 18 loci and 11 preserved teeth from 'Mulloch Heap' held in the Queensland Museum collection. A right dentary fragment with 8 teeth (QM F35777) and a neonate left dentary tooth row with 7 teeth (QM F42173) from Sutton's site, osteoderms QM F44603–5 all from Kings Creek Catchment, Darling Downs southeast Queensland. An isolated frontal (NMV P253558) and numerous broken osteoderms (unregistered) were recovered from Fisherman's Cliff, on Moorna Station in southern New South Wales. See Figure A3.1–Figure A3.13.

Distribution and age of taxon

West of the great dividing range, north of the Murray River, through to the Darling Downs of south-eastern Queensland, eastern Australia. Plio-Pleistocene. Oldest material is the Plio-Pleistocene Holotype for *Aethesia frangens*. Youngest material from the late Pleistocene Fusco excavation of Cathedral Cave, Wellington, New South Wales. See Figure A3.14.

Revised Diagnosis

Very large egerniine skink, adult basicranial (skull) length of 70 mm and (inferred) adult snout-vent length of up to 600 mm, with very stout deep mandible, and thick and extensive body armour. Dentary with Meckel's groove closed and a large splenial notch. Adult dentary with 18 or fewer teeth, peramorphic adult form does not replace last two tooth positions. Dental cementum increases with age, dentition becomes pleuro-acrodont at rear of tooth row. Circular tooth resorption pits present in cancellous dental matrix filling entire dental sulcus in adult. Two rows of mental foramina on dentary. Robust, posteriorly elongate symphysis and bridging chin structure extends approximately 30% the length of the tooth row. Very broad head, as shown by adult frontal width >60% of frontal length (see Figure A3.16), the obtuse angle of the symphysis between the two dentaries, and the angle of the premaxillae facial processes. Osteoderm surfaces have a globular texture, primary dorsal row osteoderms have tall sub-pyramidal projections forming horned ornamentation.

Description

The Mandibles

<u>*Neonate dentary.*</u> AM F145608 is a near complete right dentary, with some breakage of the lateral surface, and lacking the extremities of the surangular and coronoid processes. The ventral surface of the dentary forms a convex arc from the symphysis to the broken edge of the angular process. The lateral face of the dentary is slightly convex, the medial face relatively flat and angled inwards ventrally from the dental sulcus. The dentary is 22.52 mm long, 5.9 mm deep and 3.8 mm wide (50% along tooth row). The symphysis is a reverse '7' shape in medial view (Figure A3.1 and

Figure A3.2), with a large Meckel's foramen preserved in the fold. The symphysis is 2.25 mm wide and lengthened into a long sheet-like medial 'chin', which is approximately 25% the length of the tooth row at 5.33 mm long. This structure is thin, but porous, suggesting future growth in the area. The splenial notch is thin at the anterior end, reaching 50% the length of the dentary, and widening in a V-shape towards the posterior at an angle of roughly 30°. The lateral face of the dentary preserves 12 mental foramina arranged in two rows. The foramina vary in size, but exhibit no clear spatial pattern along the row.

AM F145608 preserves 12 tooth positions and 12 teeth. The third tooth crown is broken. The tooth crowns are cylindrical in occlusal view and come to a symmetrical, conical point at the apex. Numerous striations mark the surface of the crown, radiating from the apex on all sides. There is no clear margin where the enamel ends and the tooth shaft begins, the striations extend less than halfway down the length of the tooth. Tooth bases are expanded and sit inside a porous cement on the dental sulcus. The medial surface of the tooth is exposed, showing pleurodont dentition, dental cementum fills the spaces between teeth and overlies the base of the shaft to approximately 1/3 of the tooth height. Measurements taken of the ninth tooth, median in the row, indicates the size of these teeth; 2.58 mm tall, 1.59 mm wide at the base of the crown, reaching 1.31 mm higher than the dentary wall.

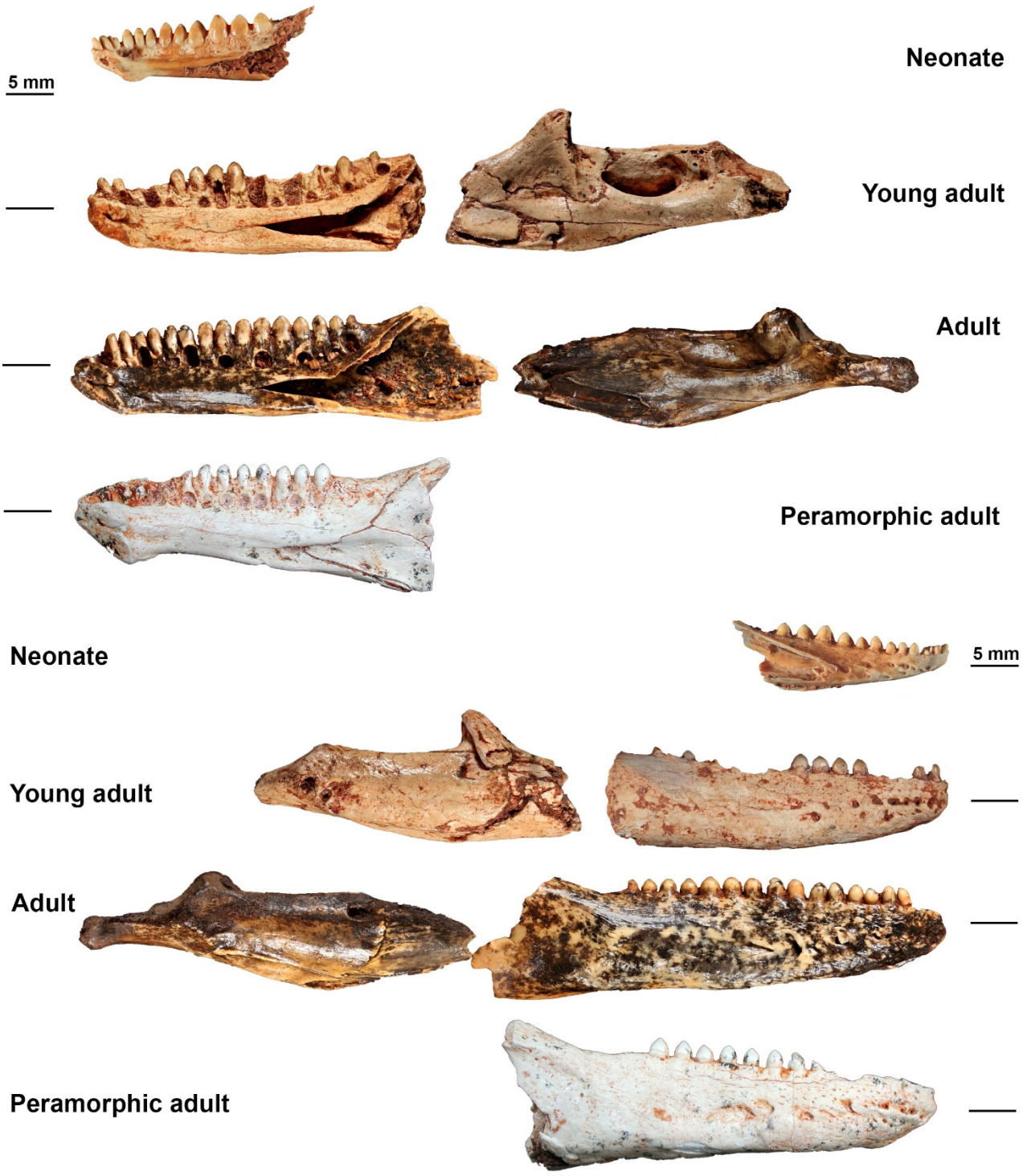

Figure A3.1: Comparative photographs of *Tiliqua frangens* ontogenetic stages. The neonate (AM F145608), young adult (AM F143322), adult (AM F143321) and peramorphic adult (SAM P43196) morphotypes. Images flipped horizontally for ease of comparison, for true left/right orientation see descriptive text.

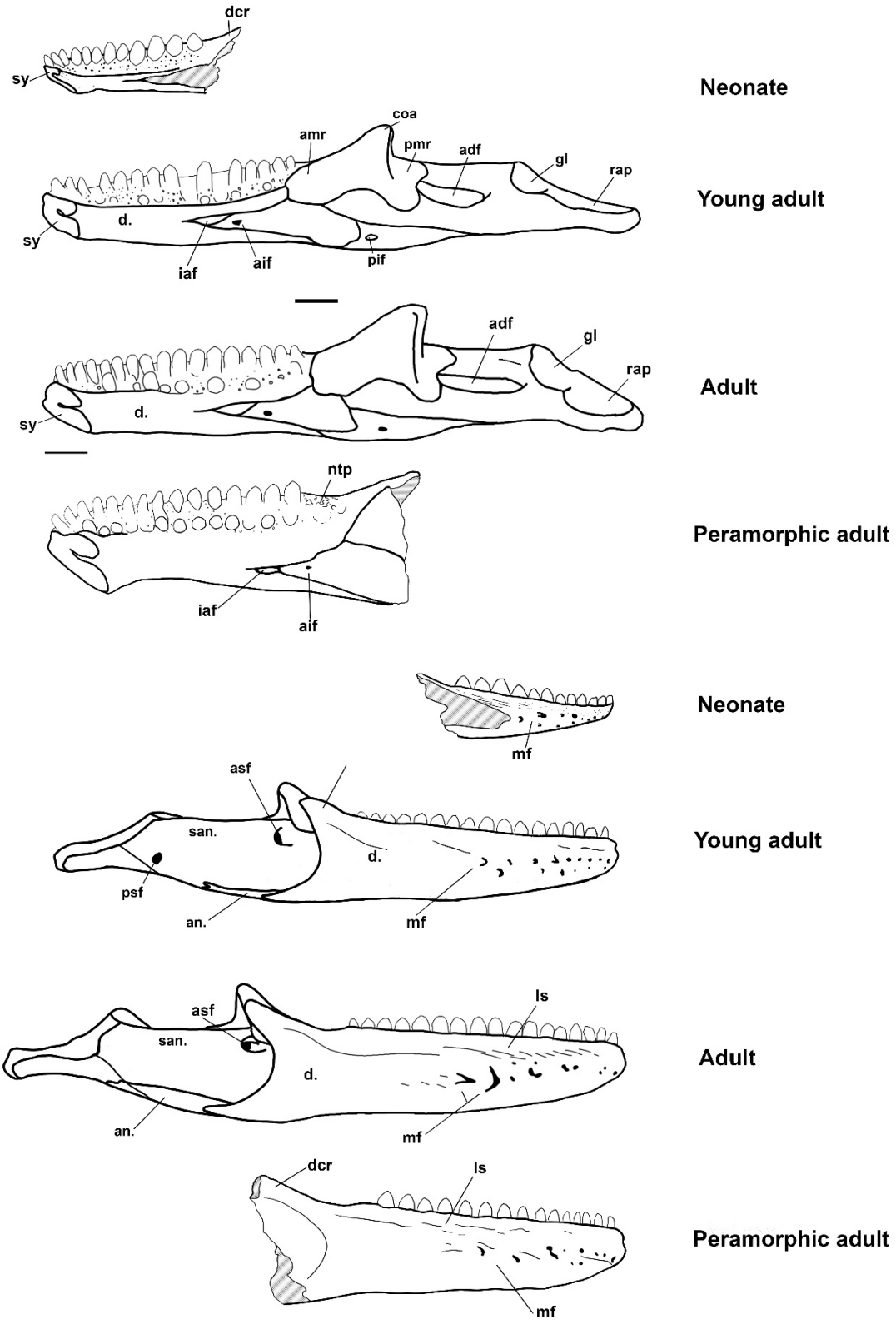

Figure A3.2: Reconstructed ontogenetic morphotypes of *Tiliqua frangens* drawn from the specimens photographed in Fig. S1. adf adductor fossa; aif anterior intermandibularis foramen; an. angular; amr anterior medial ramus of the coronoid; art. articular; asf anterior surangular foramen; co. coronoid; coa coronoid apex; d. dentary; dcr dentary coronoid ramus; ds dental sulcus; gl glenoid; iaf inferior alveolar foramen; ls lateral striations; mf mental foramina; ntp posterior tooth position not replaced; pif posterior intermandibularis foramen; pmr posterior mandibular ramus of coronoid; psf posterior surangular foramina; sp. splenial; and sy symphysis.

Young adult mandible. AM F143322 is a near-complete left mandible, preserving all mandibular elements from the symphysis of the dentary to the glenoid fossa, missing only the retroarticular process. The mandible was fractured post-mortem, the break occurring at the posterior of the dentary, anterior to the coronoid apex and through the midline of the splenial. The break is old, with matrix (before preparation) congealed to the broken faces of the bone and filling all externally visible sutures, the resorption pits below the teeth, the splenial notch covering the anterior of the splenial, all foramina and the adductor fossa.

The symphysial 'chin', still faintly visible in occlusal view (Figure A3.10), extends to 30% the length of the tooth row, bone growth thickening the dentary both laterally and medially in this area, and flattening the ventral margin of the dentary that was convex ventrally in the neonate. The shape of the splenial notch is preserved in this specimen more completely than in the neonate, beginning at 50% the length of the tooth row, widening beneath the 16th tooth, transforming the outline from a straight-sided V-shape (to more Y-shaped). The dental shelf is considerably weaker in profile, visible in the anterior teeth and absent at the end of the tooth row. The young adult dentary when reconstructed is 44.2 mm long, and is 5.6 mm wide and 7.5 mm deep measured 50% along the tooth row. The symphysis is 7.6 mm long and 4.4 wide, with the bone thickening to obscure the 'chin' that was visible in the neonate morphotype. The dental cementum is similar to the neonate matrix of spongy, foramina-pocked bone surrounding the base of the teeth on the dental sulcus. 18 tooth loci and 8 teeth are preserved showing multiple stages of tooth replacement and varying wear. The resorption pits are circular in shape, and appear below roughly every second tooth, and are made obvious by the red matrix fill contrasting with the dental cementum. The lateral surface of the dentary exhibits 16 mental foramina and is marked by a muscular ridge associated with the ventral aponeurosis of *M. adductor mandibulae externus superficialis* (Haas, 1974).

The splenial preserved from the inferior alveolar foramen to the anterior tip has shifted ventrally to sit within the dentary, no longer preserving the shape of the inferior alveolar foramen. When repositioned, it extends anteriorly approximately 50% the length of the dentary tooth row, the posterior extent remains anterior to the coronoid apex, and is a maximum of 4.4 mm high. The inferior alveolar foramen is positioned anterodorsally to the anterior intermandibularis foramen, the shape of the splenial tip is curved ventrally allowing for the foramen opening between the splenial and dentary.

The coronoid ramus ascends at a low angle of 30° from the dentary and reaches a height of 4.5 mm from the surangular. The coronoid apex is rounded, and from the base of the posterior coronoid ramus to the apex is 9.6 mm. No posterolateral ridge, from the coronoid apex to the

posterior ramus observed on the lateral face; the medial ridge is instead considerably thick. The suture between the surangular and articular is not exposed between the anterior and posterior coronoid rami, the area is covered by expansion of bone forming a flat medial surface.

The angular preserves the posterior intermandibularis foramen positioned mid-height, on the medial face of the mandible. The angular extends along the medial face of the mandible from the posterior margin of the splenial and passes to the ventral surface of the mandible posteriorly to the coronoid, terminating directly beneath the posterior surangular foramen.

The surangular is very robust, 5.7 mm at its thickest point, measured roughly 50% along its length. The adductor fossa is 7.8 mm long comparative with the total length of the reconstructed mandible (68 mm) 11.4%. One very large foramen is present immediately behind the coronoid and two anterolateral of the glenoid. The lateral face of the surangular is marked with a thick muscle scar, forming the edge of the attachment of the ventral aponeuroses of *M. adductor mandibulae externus superficialis*.

Adult mandible. Two specimens, a right dentary and left post-dentary complex (AM F143321) represent the adult mandibular morphology of *Tiliqua frangens*.

The dentary preserves a complete symphysis, but is missing the posterior-most tips of the coronoid and surangular processes. The splenial notch shape is slightly altered by missing bone broken off below the dental sulcus posteriorly. The notch begins anteriorly with a small extension of what appears to be Meckel's groove at 50% the length of the tooth row, extending to accommodate the missing splenial and inferior alveolar foramen at 60%. Below the 14th tooth position the notch widens into the Y-shape also exhibited in the young adult morph. The lateral side of the dentary displays 14 mental foramina. The posterior two foramina, positioned beneath the eighth and tenth tooth, are, shaped like two chevrons. Two other pairs of foramina are only separated by a thin margin of bone. Above the mental foramina, below the dental row, a stretch of the lateral face of the bone is marked by elongate furrows in the surface running parallel to one another at an angle of approximately 30°. The posterior end of this phenomenon loses the furrowed pattern and becomes a ridge, curving upward, marking the accommodation of the ventral aponeurosis of *M. adductor mandibular externus* beneath. The ventral surface of the dentary is flattened as a result of lateral expansion of the bone, forming a relatively square corner with the medial face and curving up more gently on the lateral side. Total length from symphysis to what remains of the surangular process is 44.2 mm. The height of the dentary at 50% along the length of the tooth row is 8.3 mm and width 6.5 mm. The symphysis, now filled out to the entire length of the

‘chin’, is 7.8 mm long and 4.2 mm wide in the same reversed ‘7’ shape and preserves the internal angle of articulation with the opposing dentary at 53°, see Figure A3.10.

The dentition in the adult specimens is better preserved than that of AM F143322 (Young Adult) with 15 teeth retained in 18 loci. The two anterior-most teeth are missing, the first broken through the shaft and the second represented by an empty locus. The last tooth locus has been overgrown by tooth cementum and bone and tooth-replacement was no longer possible in this position. The tooth row measures 29.4 mm in length from the first locus to the remaining 17th tooth.

No coronoid was recovered for the adult morphotype.

The post-dentary specimen AM F143321 is complete from the anterior extent of the articular and surangular to the retroarticular process, preserving the continuation of the inferior alveolar canal. The angular remains articulated, preserving the shape of the notch for the dentary on the lateral face. The posterior end of the angular is partly fused with the surface of the surangular, the suture only detectable in micro-CT cross-sections. The posterior intermandibularis foramen is positioned medially. The specimen is more robust than the young adult form, measuring 9 mm tall and 6.4 mm wide at the widest point of the surangular. The adductor fossa is longer, measuring 9.8 mm. The retroarticular process is 8.1 mm long and the same width as the glenoid (9 mm) with a thick ridge tracing the edge of the bone creating a concave dorsal surface.

The overall reconstructed length of the adult mandible is 72 mm from the tip of the symphysis to the retroarticular process.

Peramorphic adult dentary. The peramorphic morphotype was previously described in detail by Hutchinson and Scanlon (2009), when they described *Aethesia frangens*, but it is reiterated briefly here for continuity.

The left dentary is robust with 15 teeth, the first seven being of the typical scincid pleurodont form, then the tooth row becomes pleuro-acrodont with the absence of a dental sulcus posterior of the seventh tooth. Teeth show multiple stages of tooth wear and replacement. Resorption pits are circular and present beneath tooth implantation, inside a solid wall of dental cementum that cannot be differentiated from dentary bone externally or with the aid of Micro-CT cross sections. The lateral face of the dentary has two parallel rows of mental foramina, totalling eight in all. The anterior portion of the splenial remains articulated, preserving the location of the inferior alveolar foramen. No intermandibularis foramen is preserved. The coronoid process of the dentary extends above the height of the largest tooth. The anteromedial ramus of the coronoid is still in articulation with the dentary.

With no surangular or articular bones preserved in association with this specimen or any that are convincingly different to the adult morphotype, a reconstruction of the complete peramorphic adult mandible is not possible. The dentary retains enough characters to associate the specimen with both the young and the adult morphotype.

Synapomorphies of all the *T. frangens* ontogenetic morphotypes are: the lateral striations between the mental foramina and tooth row, a double row of mental foramina also shared with the neonate form, increased symphysis size, angle between the dentaries and increased depth and thickness of the dentary compared to other *Tiliqua*, the flattened ventral surface, and the shape and extent of the splenial notch.

Dentition

The tooth row of *Tiliqua frangens* increases from 12 positions in the neonate dentition to 18 tooth positions in an adult, before decreasing to 15 positions due to loss of the 3 posterior tooth positions in the peramorphic adult form. No evidence of tooth replacement is observed in these posterior loci at this ontogenetic stage. The termination of tooth replacement for the last three tooth positions on the dentary leave the largest tooth at the posterior end of the row. Teeth are pleurodont in the anterior of the adult tooth row, becoming pleuro-acrodont at the posterior due to increased growth of dental cementum covering the bases of teeth and filling out the dental sulcus. Cementum coverage and density increases with age, becoming less pocketed with foramina and nearly indistinguishable from true bone in adulthood. Tooth replacement pits are circular and emerge from directly below the tooth in all adult forms. Tooth replacement stages are scattered along the row with an observed maximum of three empty loci at any one time awaiting tooth replacement. Tooth crowns change in profile and cusp shape with ontogeny, replacement, and wear.

Neonate tooth bases are expanded relative to the crown width, producing a pointed conical unworn tooth with numerus striations radiating from the central cusp (Figure A3.3, A). With wear, the neonate tooth crown apex transforms from a single central cusp to two visible cristae and a shallow *intercristatum* that extends anteroposteriorly across the apex of the tooth.

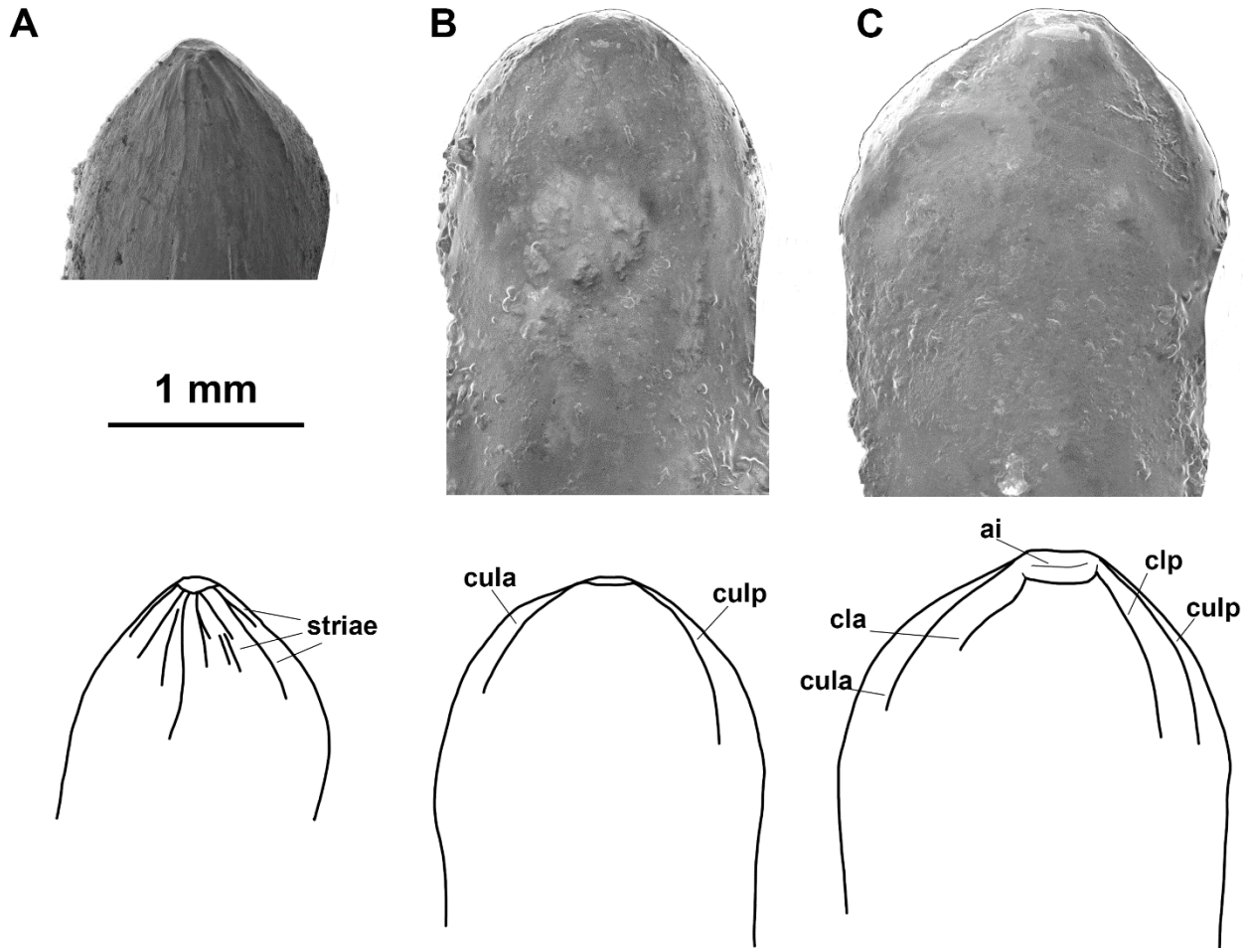

Figure A3.3: The dentary tooth crowns of A, an unworn neonate tooth (AM F145608); B, an unworn adult tooth, 13th in the row; and C, a mildly worn adult tooth from the same individual of *Tiliqua frangens* (AM F143321). Abbreviations: ai, *antrum intercristatum*; cla, *crista lingualis* anterior; clp, *crista lingualis* posterior; cula, *culmen lateralis* anterior; and culp, *culmen lateralis* posterior.

The adult tooth (Figure A3.3, B and C) replaces that of the neonate and is less pointed in profile. The tooth shaft narrows ventrally, and the crown has a round expanded profile, still with a central cusp at the apex, which now extends into prominent posterior and anterior *culmen lateralis* on the lingual face of the tooth. The single cusp is again worn into two visible cristae running anteroposteriorly across the centre of the tooth with a shallow *intercristatum* between them. The widest point of the *intercristatum* is central to the tooth between the *cuspis labialis* and cuspis lingualis, and narrows anteriorly and posteriorly, almost pinching out before meeting the *culmen lateralis*. A slight concave depression marks the lingual face of the crown beneath the worn cusps. The tooth crown expands medially beneath this shallow depression, out to the full width of the tooth shaft. The depression in the lingual face allows the two cristae and *culmen lateralis* to protrude further from surface of the tooth creating a prominent ridge along the tooth row.

Maxilla

Two right maxillae of *Tiliqua frangens* (AM F145609, and AM F145610) were recovered from the recent Cathedral Cave excavation (one from Unit 14, 515-520 cm deep, and one from *ex*

situ sediments The *ex situ* sediment originates from unknown locations within the Wellington Caves and has been spread on top of the *in situ* sediment floor of Cathedral Cave to level it for cave tours (Dawson and Augee, 1997). AM F145609 was recovered by acid preparation and is nearly intact, preserving a full facial process height, premaxilla notch, a near complete tooth row with 12 of 14 teeth preserved, and a large section of the anterior margin of the orbit (Figure A3.4, A).

Total preserved maxilla length is 28.7 mm from the suture anterior to the first tooth to the broken tip of the facial process below the jugal facet on the more complete specimen. The facial process is 17.2 mm tall, and fairly robust at 1.5 mm thick. Viewed anteriorly, the lateral face of the maxilla rises dorsally parallel with the tooth row, a prominent groove marks the lateral surface of the facial process above the maxillary foramina, associated with the termination of the upper lip and the attachment of osteoderms. Anteriorly, the facial process preserves a steep angle with increase in height, the anterior edge of the face shallowly curving inwards to meet the nasal and frontal, indicative of a broad head. Nine maxillary foramina are visible on the lateral face, the anterior-most foramen opening is elongate and directed towards the premaxilla. The facial process bone is also much thicker than any *Tiliqua* specimen in the SAM herpetology collection, >2 mm in its centre. The anterior tip where the maxilla articulates with the premaxilla preserves both the medial premaxillary process and the premaxillary process on the lateral face (see Figure A3.4, A).

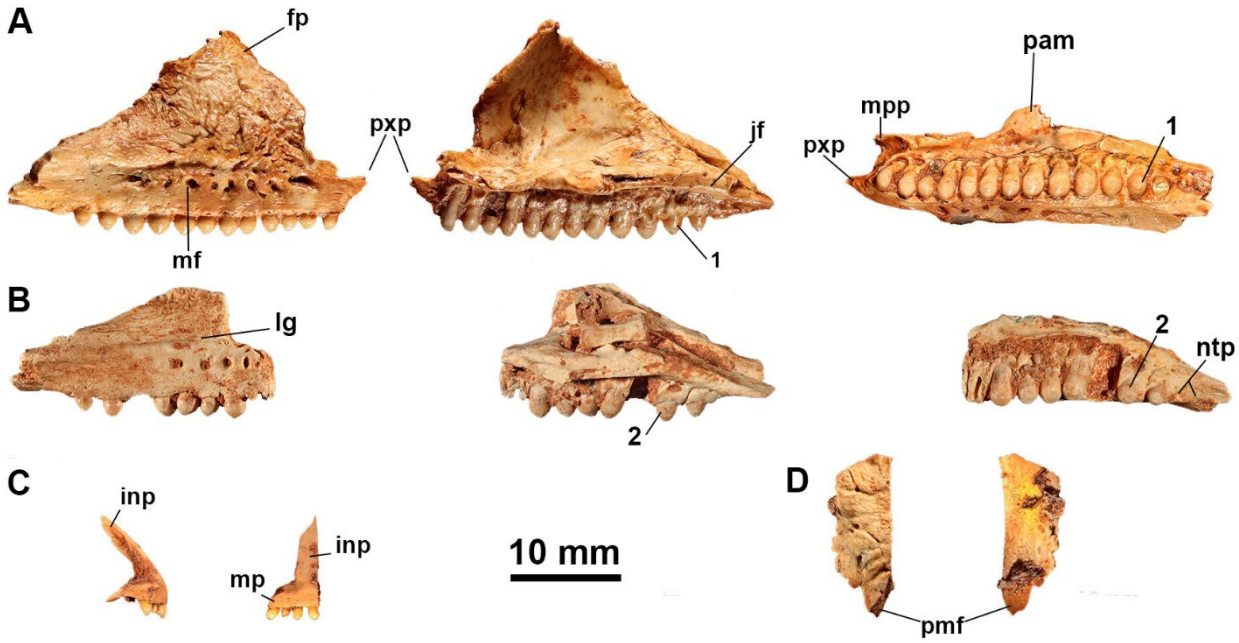

Figure A3.4: The adult maxilla AM F145609 (A), peramorphic adult maxilla F145610 (B), premaxilla AM F145611 (C) and nasal AM F145612 (D) of *Tiliqua frangens*. Note the pronounced thickening of the bone and deep labial groove left after disarticulation of the osteoderms on both maxillae. Abbreviations: fp facial process; inp internasal process; jf jugal facet; lg labial groove; mf mental foramina; mp maxillary process; mpp medial premaxillary process; ntp location of teeth not replaced in peramorphic adult; pam palatine process of the

maxilla; pmf premaxillary facet; pxp premaxillary process. 1 the 11th tooth of the adult maxilla; 2 the 11th tooth of the peramorphic adult maxilla.

In occlusal view the maxilla has a gentle s-bend, laterally convex anteriorly and concave posteriorly, the tooth row following the same line but with a shallower curve. The tooth platform is widest approximately 50% along the length of the tooth row at 8.8 mm. The tooth row is 23 mm long; 14 tooth positions are present, the two most posterior have replacement pits but the dental cementum appears to have overgrown the tooth position, so as in the adult and advanced adult dentary morphs, these teeth loci had ceased regrowing teeth. Of the remaining teeth, multiple stages of tooth replacement are visible, and wear to the crown structure can be best observed on the 10^{th} and 11^{th} teeth (Figure A3.5), matching the dentary row. The median tooth is 1.5 mm wide, and 3.1 mm tall in occlusal view. The widest teeth are the 9^{th} and 10^{th} teeth, both are 1.7 mm in diameter.

In occlusal view, the teeth are almost square with the *crista labialis* running anteroposteriorly across the apex of the tooth in the medial half of the square. The *cuspis labialis* is positioned slightly posteriorly and medially off-centre. The teeth are angled slightly anteriorly (<15°) from the base to the apex of the crown. The tooth row is convex when viewed medially, the widest teeth are longest, leaving the deepest part of the convex curve roughly 60% along the tooth row. In medial view each tooth in this region has a broad base and shaft, narrowing quickly at the crown creating a squat conical profile (Figure A3.5). Beneath the *cuspis lingualis* the medial face of the tooth is slightly concave. The cristae extending to *culmen lateralis* form a prominent ridge along the tooth row. No obvious striae are noted on the medial face of the tooth crown.

AM F145610 from the disturbed sediment is incomplete (Figure A3.4, B), missing portions of the dorsal and posterior facial processes, the posterior end of the maxillary process where it articulates with the jugal, and the anterior of the tooth row and its articulation with the premaxilla. The larger individual, although incomplete, represents a later ontogenetic stage, with more robust bone (2.76 mm facial process thickness), the texture on the lateral face of the facial process is more rugose, dense dental cementum fills more of the space surrounding the teeth, the two most posterior teeth are not replaced, and the scar marking the termination of the upper lip is more pronounced than that of the more complete specimen (AM F145609). This modification of the tooth row, increased surface scarring associated with soft tissue connections and general robustness were all noted in the ontogenetic phases represented by the aforementioned dentaries.

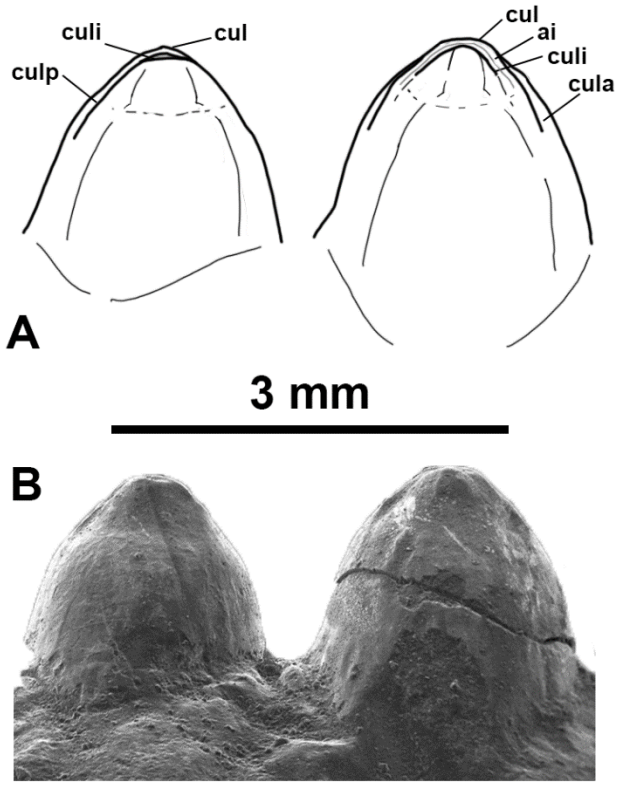

Figure A3.5: Tooth crowns of the 11th (left) and 10th (right) teeth on the adult *Tiliqua frangens* maxilla AM F145609 from medial view. A: Simplified line diagram of major tooth crown features. B: Unaltered SEM image. Abbreviations: ai, *antrum intercristatum*; cul, *cuspis labialis*; cula, *culmen lateralis* anterior, culi, *cuspis lingualis*; and culp, *culmen lateralis* posterior.

Premaxilla

The right premaxilla (AM F145611, Figure A3.4, C) recovered from the disturbed sediment derived from earlier excavations and overlying the 2016-17 Cathedral Cave excavation site is assigned to the young adult morphotype of *Tiliqua frangens*. It is complete including four teeth and has a complete internasal process length. It shows no evidence of fusion to its opposing left side. The third tooth is slightly shorter than its neighbours as it is in the process of being replaced, meaning that this specimen is older than the neonate individual represented by the small dentary (AM F145608). The maxillary process is orientated almost laterally at an angle of <30°, creating a broad, flat, nose shape. This process is 4.6 mm long. The internasal process sweeps back at an angle roughly 45° and is 9.5 mm tall. A notch in the base of the internasal process where it meets the maxillary process is visible anteriorly, marking the position of the ethmoidal foramen. At the dorsal tip of the internasal process a flat surface marks the facet for articulation with the right nasal. Premaxillary teeth are often simple and smaller than most other teeth, excepting the first few on the maxilla. With a tooth height of 2.9 mm and width of 0.9 mm, this premaxilla corresponds well with the anterior teeth on the smaller maxilla of *T. frangens* (AM F145609).

The slender/lightweight frame of this premaxilla in comparison with other neighbouring elements of *T. frangens* indicate that this specimen has not reached a large adult growth phase. The minimal dental cementum present and evidence of some tooth replacement and tooth wear support an estimate of a young adult–adult growth stage.

A single right adult premaxilla was retrieved with the associated partial skeleton of *Tiliqua frangens* (QM F41532) from Sobbe Site of the Darling Downs of Queensland. This adult specimen preserves a single tooth, in the first position in the row of four loci. This tooth crown matches those of the anterior-most teeth on the adult maxilla. The dorsal tip of the internasal process is broken immediately below the location of the facet for articulation with the right nasal. The remaining anterior face of the internasal process is preserved, rising steeply posterodorsally to the nasals at an angle of approximately 80°. Anteriorly, the face preserves four foramina, and is broader ventrally. Laterally the face preserves a shallow curve for the naris before sharply changing angle to rise dorsally to the nasals.

This specimen has peramorphic adult traits, most prominently displayed in its increased mediolateral width, overall bone thickness, heavy tooth wear, increased dental cementum growth and the acute angle of the maxillary process shaping a very blunt nose. The same blunt anterior face shape is reflected in the broad angle preserved in the symphysis of the peramorphic adult dentary.

Nasal

One right nasal (AM F145612, Figure A3.4, D) was recovered from the Cathedral Cave 2016-17 excavation, in unit 14F at a depth of 535-545 cm below datum. A slightly convex plate of bone with an ovular outline shape, longer than wide, the nasal is one of a mirrored pair. The dorsal surface of the nasal is pocketed by numerous foramina and vascular channels, creating an uneven textured surface. A facet is observed anteriorly for the placement of the internasal process of the premaxilla. The ventral face of the nasal is concave, and much smoother than the dorsal face. The nasal measures 14.3 mm long from anterior-posterior and is 5.1 mm wide, parallel sided for most of its length, narrowing to meet the premaxilla anteriorly and frontal posteriorly. The bone is relatively thick across its entire length, 1.6-1.7 mm.

Frontals

Three frontals from the Wellington Caves are attributed to this species. One previously described as *Tiliqua laticephala* (AM F135900, Čerňanský and Hutchinson, 2013), and two from the disturbed sediment in the 2016-17 Cathedral Cave excavations.

The frontal of *Tiliqua frangens* previously described as *Tiliqua laticephala* (Čerňanský and Hutchinson, 2013), is a symmetrical, broad T-shaped bone, with osteoderms fused to the dorsal surface. Anteriorly there are two facets for articulation with the paired nasals. Lateral to these are facets for the posterior processes of the prefrontals. Posteriorly, a notch on each side marks the anterior extent of the post frontal bones.

The smaller frontal (AM F145613) measures 18.8 mm long, 21.4 mm wide posteriorly at the frontoparietal suture, 11.2 mm maximally in ant-orbital region, and is narrowest between the orbits at 10.4 mm. The thickest part of the bone is just posterior to the mid-orbit and is 4 mm deep. From the dorsal surface to the ventral tip of the suborbital projections, the frontal is 6.4 mm deep. The size and bone thickness of this specimen relative to the other two, suggest it came from a young adult. The largest frontal, the other Cathedral Cave specimen, AM F145614, is 22.3 mm long, 24.7 mm wide at the frontoparietal suture, and ant-orbital width of 12.1 mm. The frontal narrows slightly between the orbits to 11.9 mm and has a suborbital depth of 7.9 mm. The bone is significantly thicker, up to 4.8 mm. This specimen is from an older animal, indicated by increased robustness and the greater degree of fusion of the osteoderms to the dorsal surface.

Prefrontal

The left and right paired prefrontals were recorded from the associated skeleton of *Tiliqua frangens* from Sobbe Site (QM F41532). These elements articulate with the frontal from the same specimen and are near complete, both missing the anterior process for articulation with the maxilla. The left prefrontal is also missing the dorsal extremity and anterior corner of the dorsal surface of the element.

The right prefrontal is described in detail as the most complete of the pair. It is a curved plate of bone that extends from the dorsal surface of the anterior part of the medial shelf of the maxilla, to the prefrontal facet of the frontal. It is convex anteriorly, concave posteriorly, and thins medially where it meets the opposing prefrontal with parallel vertical edges (with unknown gap between the isolated elements). Medially the ventral edge of the bone has a flat facet for articulation with the medial shelf of the maxilla. Laterally, the ventral edge of the plate has a similar facet for articulation with the medial side of the facial process of the maxilla. The lateral edge of the bone preserves a broken cross section of a slight prefrontal boss of similar shape to that seen in *Tiliqua rugosa*.

Both prefrontals are near identical to the same elements in *Tiliqua rugosa*, excepting a slight thickening of the bone and dorsoventral lengthening corresponding with increased skull height.

Pterygoid

A single, broken right pterygoid (AM F145615) was found in unit 14F at a depth of 520-535 cm in the Cathedral Cave 2016-17 excavation. It is missing the entire quadrate process and the anterior tip of the palatine ramus. The bone is robust, with a deep concave sulcus on the palatine process directed anteriorly. Two foramina separate this concavity from the epipterygoid notch, each foramen is elongate with exits directed towards the space between the ectopterygoid and palatine processes. A large flat facet on the lateral edge, for articulation with the ectopterygoid is preserved entirely and is 5.5 mm long and 3 mm deep. Length between what remains of the palatine process, and the ectopterygoid process is 9.8 mm. The epipterygoid notch is fairly deep and ovular in shape, 2.8 mm long and 2.1 mm wide.

Braincase

The larger of the two recovered braincases AM F58265 (Figure A3.6), is complete, except for the dorsal tip of the left paroccipital process, a fragment of the right crista prootica and both basipterygoid processes. The younger specimen, AM F145616 is poorly preserved with most projecting extremities missing, and the foramen magnum filled with calcified matrix. The braincase of *Tiliqua frangens* is composed of multiple fused bones described below; the supraoccipital, otoccipital, prootic, basioccipital, and sphenoid.

The supraoccipital is a singular bone, located in the centre of the dorsal surface of the braincase. A prominent, *processus ascendens* of the synotic tectum extends anterodorsally from the centre of the supraoccipital, at an angle of 20°. The nuchal crest is prominent, extending posteriorly at an angle of 90° from the *processus ascendens* and forking slightly before extending ventrally towards the posterior processes. Either side of the nuchal crest is a deep concave trench, anteriorly ending in a fine point on the internal surface of the alar process of the prootic, forming the lateral processes of the supraoccipital.

The otoccipital is fully fused to the supraoccipital and no sutures are visible externally or in cross-section. The paroccipital processes extending posterolaterally at an angle of 120° from one another. The dorsal surface of the processes are flattened for half their length and then become mediolaterally compressed at the posterior. Muscle scarring for the lateral attachment of the *M. adductor mandibulae externus* is preserved on the lateral face of the paraoccipital processes. An articular surface for the quadrate is visible on the ventrolateral face of the posterior process, see Figure A3.6 C.

The alar process of the paired prootics of *Tiliqua frangens* from medial view (Figure A3.6, C) is parallel sided dorsoventrally with curved anterior and posterior edges. This surface is

mediolaterally concave. The anterior-most point sits at the same height as the supraoccipital, beneath the processus ascendens. The trigeminal notch is preserved with an acute angle (measured 47.4° in micro CT) between the prootic and the sphenoid. The supratrigeminal processes are both broken off, not preserving their extent anteriorly beyond the alar process.

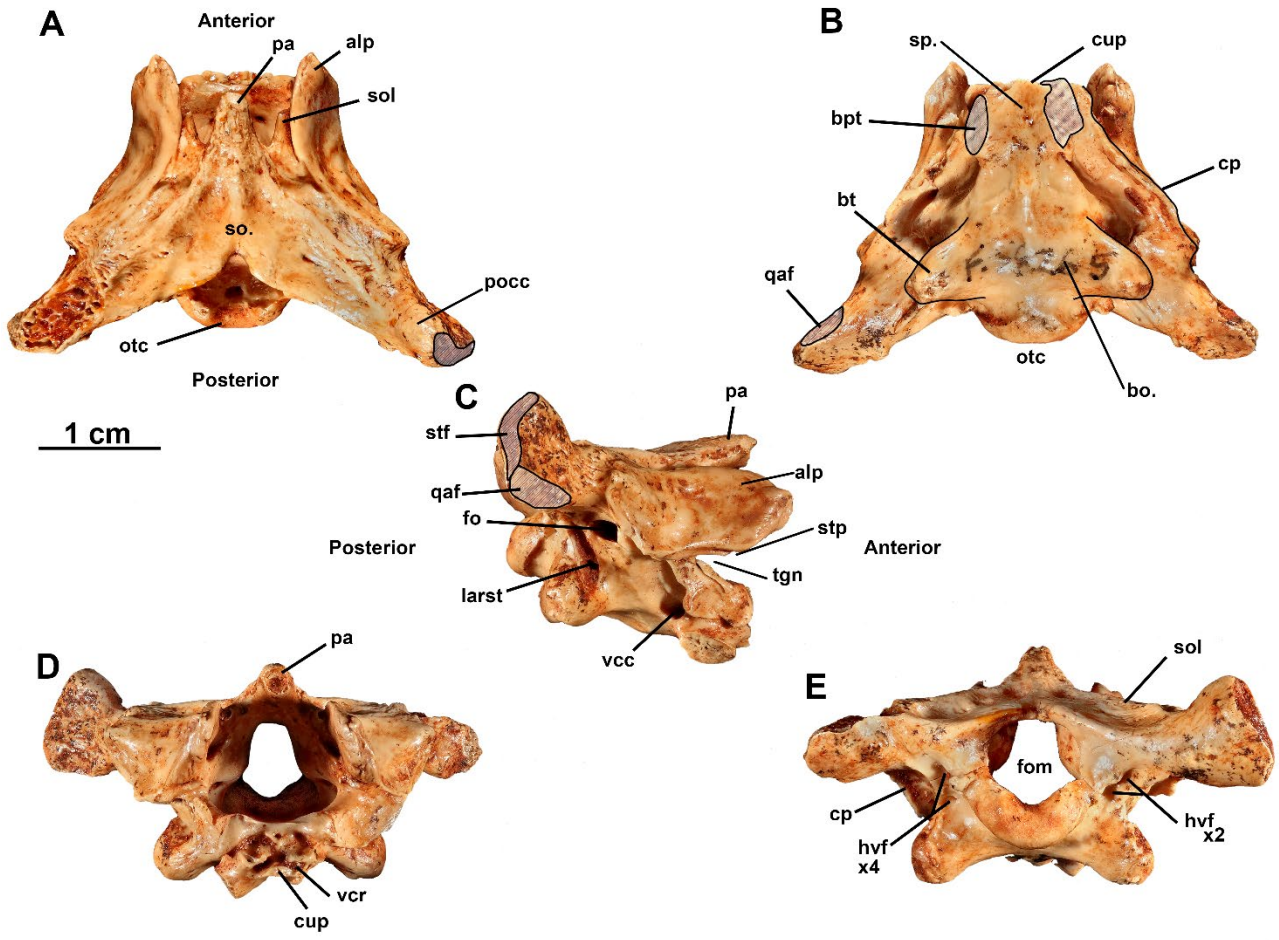

Figure A3.6: Braincase (AM F58265) of *Tiliqua frangens* from dorsal (A); ventral (B); left lateral (C); anterior (D); and posterior (E) views.

Abbreviations: alp alar process of the prootic; bo basioccipital; bpt basipterygoid process; bt basal tubera; cp crista prootica; cup cultriform process; fo fenestra ovalis; fom foramen magnum; hvf hypoglossal and vagus foramina; larst lateral aperture of the recessus scalae tympani; otc occipital condyle; pa processus ascendens of synotic tectum; paf paroccipital articular facet; pocc paroccipital processes; qaf quadrate articular facet; so. supraoccipital; sol supraoccipital lateral process; sp. sphenoid; stf supratemporal facet; stp supratrigeminal process; tgn trigeminal notch; vcc vidian canal of the carotid artery; and vcr vidian canal rostral exit.

The crista prootica project in a prominent aliform (wing-like) shape in ventral view with a well-developed lateral flange. They extend posteriorly up to and connecting to the posterior edge of the prootic. The prootic-opisthotic suture is fully fused. The carotid artery appears to exit the vidian canal just above the cultriform process. The tips of the supratrigeminal processes above the trigeminal notch have broken off, but their size predicts that they would extend beyond the cupola anterior of the alar processes of the prootic.

No suture between the sphenoid and basioccipital is visible externally or in µCT cross-sections in AM F58265. The suture runs mediolaterally between the two bones on the ventral face of the braincase AM F145616, immediately anterior to the basal tubera. The sphenoid narrows anteriorly, widest at the sphenoid-basioccipital suture. The ventral surface between the basipterygoid processes is concave. Both basipterygoid processes are broken off (see Figure A3.6, B). The ventral surface of the basioccipital is lightly concave, extending laterally and posteriorly out to the basal tubera. Posteriorly, the occipital condyle is u-shaped with a concave dorsal surface and is slightly convex posteriorly in ventral view. The crista tuberalis is prominent and descends from the posterior processes to the thick, rounded, basal tubera dividing the vagus foramina from the ovular lateral aperture of *recessus scalae tympani*. There are two hypoglossal/vagus foramina on the right and four on the left side of the foramen magnum.

Total width of the braincase anteriorly between the alar processes is 16.3 mm, the shape extending to 36.5 mm between the two posterior processes. The anterior of the braincase measures 17.2 mm from the ascending process to the basioccipital. Posteriorly, the tallest dimension is between the posterior processes and the basal tubera at 17.9 mm. The length of the posterior processes from the centre of the posterior dorsal surface of the supraoccipital is 19.3 mm. The processes expand dorsoventrally at the tip to 8.8 mm. Viewed ventrally, the length of the braincase from the base of the cultriform process to the occipital condyle is 20.9 mm. The foramen magnum measures 7.2 mm wide by 7.3 mm high.

Squamosal

A complete right squamosal recovered from the Cathedral Cave excavation (AM F145619; Figure A3.7, A–C) at a depth of 550-560 cm, and has a solid arcuate shape measuring 28.1 mm long with a maximum width of 6.1 mm roughly 80% along the length of the bone. The jugal facet on the lateral face, and postfrontal facet on the medial side are preserved. The posterior tip of the bone is a prominent condyle, with a supratemporal facet. Numerous foramina mark the medial anterior, and posterior, dorsal surfaces.

Quadrate

A right quadrate (AM F145618; Figure A3.7, D–G) was recovered from disturbed sediments of Cathedral Cave. It is mostly complete, with the surface of the bone removed from the posterior side of the tympanic conch, exposing the internal trabecular structure, and small chips have broken off the medial ridge. The bone is posteriorly arched, with the tympanic conch open medioposteriorly. The quadrate is mediolaterally broad over the entire length of the bone, slightly narrowing at the two opposing condyles. Most of the curvature in the bone is visible from the

medial view, showing an internally arced medial ridge, while the conch appears almost flat along the anterior face. The quadrate dorsal foramina is an elongate oval shape almost overgrown with thickened bone. The articular facet for the posterior process of the braincase is fairly flat, and a concave surface extends between this facet and the dorsal foramina, accommodating the squamosal.

The tympanic crest is thickened relative to the wall of the tympanic conch, reinforcing the lateral face of the quadrate. Laterally, the tympanic conch extends posteriorly, obscuring the medial ridge entirely from view, creating a broad, flat surface for attachment of *M. adductor mandibulae externus*. Anteriorly the wall of the lower half of the tympanic conch is relatively flat. The dorsal half of the face shows a deep trench, the true depth obscured by breakage of the bone surface extending ventrally from the cephalic condyle.

Maximum quadrate height is 18.4 mm, the widest point of the conch is 12.3 mm and the mandibular-quadrate condyle is 9.2 mm across.

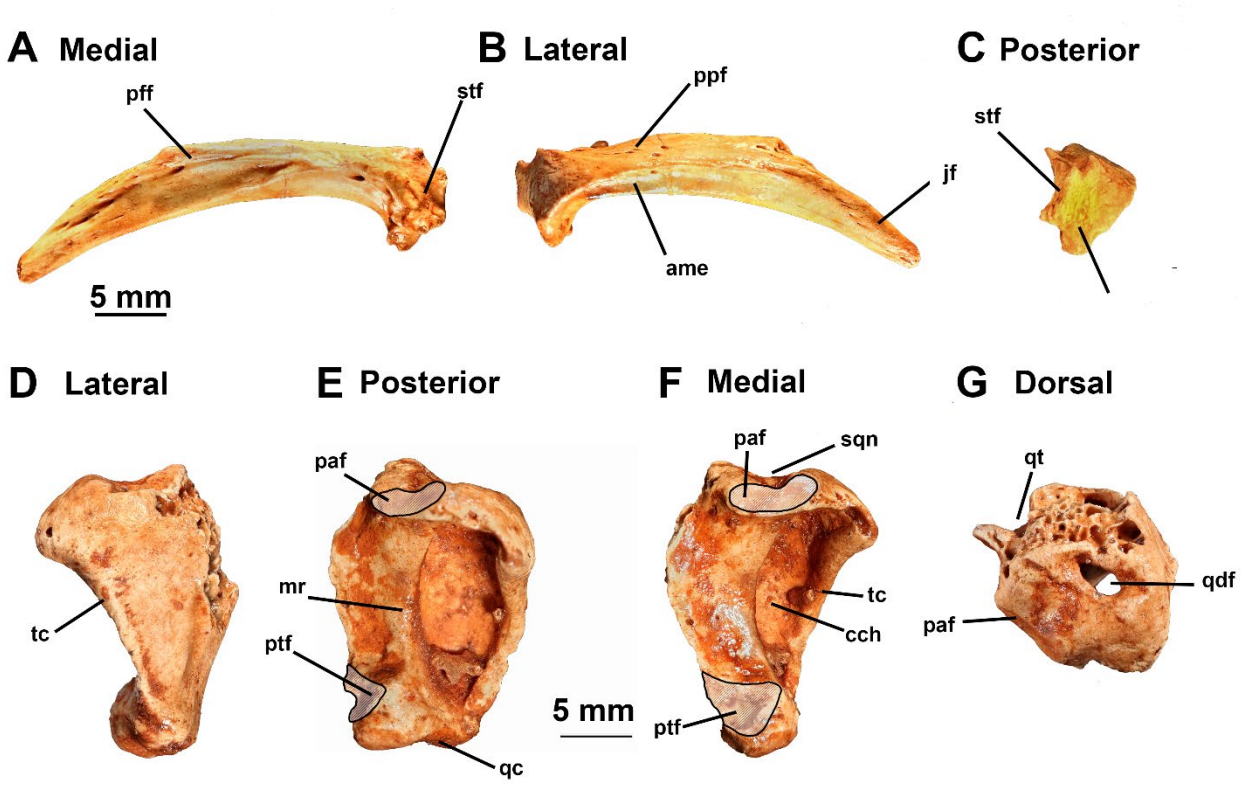

Figure A3.7: Right squamosal (A–C AM F145619) found in the Fusco excavation at a depth of 550-560 cm; and left quadrate (D–G, AM F145618) of *Tiliqua frangens* found in disturbed sediments overlying the same excavation.
Abbreviations: ame attachment area for the mandibular externus muscle, cch tympanic conch, jf jugal facet, mr medial ridge of the quadrate, pff postfrontal facet, ptf pterygoid facet, qc quadrate condyle, qdf quadrate dorsal foramen, qt quadrate trench, sqn squamosal notch, and tc tympanic crest.

Comparisons with other species of *Tiliqua*

Ontogenetic stages were elucidated by examining the mandibular specimens of *Tiliqua frangens* and using direct comparisons with modern specimens of *Tiliqua* from the South Australian Museum. Mandibles were chosen to represent the major ontogenetic stages due to the number of observable discrete and continuous characters of these elements, the various diets and tooth shapes within extant *Tiliqua*, and the increased number of elements recovered from the excavation, likely due to the 'tooth' search image bias of mammal-focused palaeontologists.

Neonate

AM F145608 was identified above as the neonate morphotype due to the entirely unworn tooth crowns, lack of tooth replacement cycles and decreased number of teeth in the row, thin, pitted bone texture, and the staggered tooth crown heights; all features as observed in the neonates from ontogenetic series of other *Tiliqua* species assessed here (*Tiliqua rugosa*, *T. scincoides* and *T. adelaidensis*). The neonate specimen of *Tiliqua frangens* most closely resembles that of *Tiliqua rugosa* (Figure A3.8) with a similar pattern of enlarged teeth at the rear of the tooth row, an unworn conical tooth crown shape, a pronounced thin wing of bone protruding from the base of the symphysis, a relatively deep dentary profile (than other taxa examined) and a splenial notch reaching roughly 50% along the tooth row length.

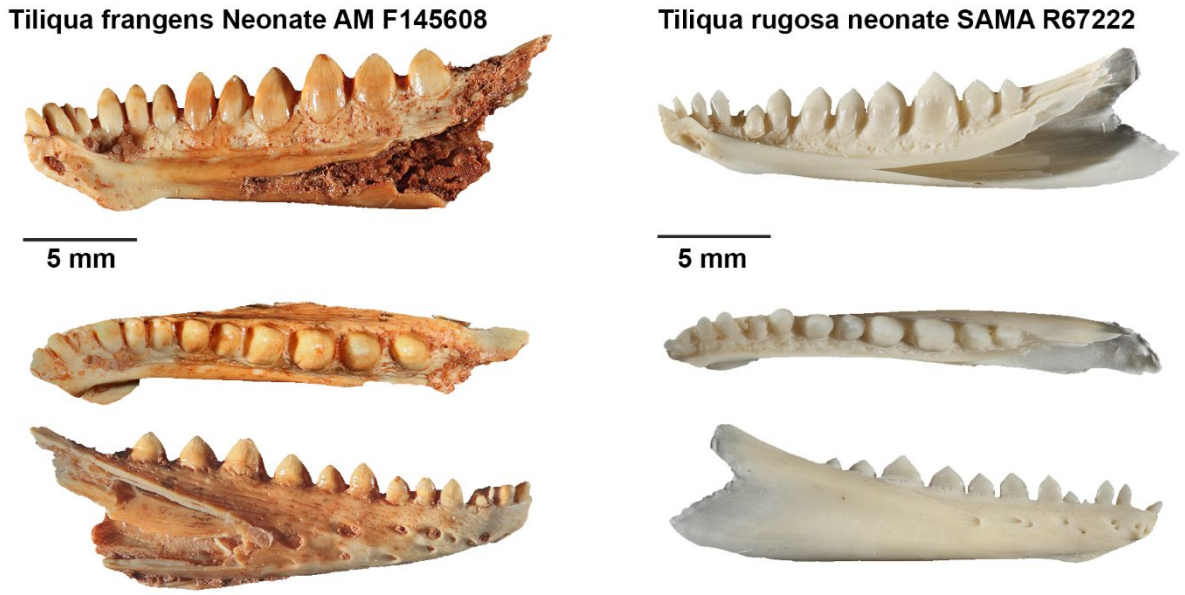

Figure A3.8: Neonate dentary of both *Tiliqua frangens* and *Tiliqua rugosa* demonstrating similarities between symphysis shape, unworn tooth crown morphology and position of splenial notch. Note differences in robustness, number of mental foramina and tooth positioning relative to the dental sulcus.

Tiliqua frangens differs from the neonate of *T. rugosa* in the ratios of dentary depth and width, to overall length; *T. frangens* is 26% and 16%, compared to *T. rugosa* with 14% and 11%. The averages for *Tiliqua* are 15.2% and 11% (Data S1 Measurements.xlsx). The dental cement holding the teeth in position is only on the base of the tooth shafts in *Tiliqua rugosa*, exposing a

deep dental shelf and clear pleurodont dentition. The tooth shafts of *T. frangens* are mostly obscured by the dental cementum, the teeth anchored in place roughly a third of the way up the tooth shaft (observed from Micro-CT cross sections). A dental sulcus is present but less pronounced than in any other species of *Tiliqua.* The shape of the splenial notch varies slightly with *T. rugosa* showing no medioventral support for the splenial, in *T. frangens* the splenial notch is much shallower, with a ventral extension of the dentary beneath it extending to the posterior-most preserved extent of the bone.

Young adult

AM F143322 the young adult mandible of *Tiliqua frangens* still slightly resembles those of other species of *Tiliqua* with the large splenial notch, large conical teeth that are relatively few in number compared to most scincids, and a short coronoid. However, the shape of the coronoid apex is unlike any other *Tiliqua*, it is convex, like other egerniines, and does not retain the concave depression for attachment of the *M. adductor mandibulae externus*. The dentary is much deeper and thicker than all other species. The posterior section of the mandible is more robust in form than all other *Tiliqua*. The surangular is considerably thicker compared to other *Tiliqua* species and lateral ridge of muscle scarring on the surangular is more pronounced. The angle of inflection of the articular is roughly 30° and the retroarticular process slopes <30° ventrally. This is similar to all *Tiliqua* species with the exception of *T. adelaidensis*.

The change in morphology with age matches that seen in *T. rugosa*, with a decrease in the number of mental foramina, increased bone thickness and overlap and partial fusion of the post-dentary bones. The number of teeth and the length of the tooth row has increased with dentary length, in *Tiliqua rugosa* starting with 12 teeth and increasing to 18; *T. frangens* has done the same as more room is made available.

New apomorphies from this ontogenetic stage relate to the continuous characters based on ratios of dentary height and width compared to length of the jaw: the dentary of *Tiliqua frangens* is much thicker and deeper than those of other egerniine species. Although not yet fully grown-over, the dental sulcus is beginning to disappear and growth of the dental cementum is infilling the spaces between teeth.

Adult

The right dentary and left post-dentary (both AM F143321) representing the adult morphotype of *T. frangens* transitions in a similar way to *Tiliqua rugosa* with the step from young adult to full adult. The teeth show multiple stages of tooth wear and replacement and the posterior tip of the angular is difficult to trace due to partial fusion with the articular. The number of teeth has

stopped increasing, as the length of the dentary and tooth row has not expanded enough to allow for more tooth positions. Each of these ontogenetic changes are exemplified in observed specimens of extant *Tiliqua scincoides* (SAMA R27036) and *T. rugosa* (SAMA R27027 and FUR055) adults.

Peramorphic adult

The peramorphic morphotype SAM P43196, the holotype of *Tiliqua frangens*, shares many features with the adult AM F143321, but without the earlier ontogenetic stages was unrecognised as *Tiliqua* by Hutchinson and Scanlon (2009). The wide angle between the two dentaries (see Figure A3.10) is made obvious by the increased bony growth along the symphysial ridge, the angle >50° is well beyond modern *Tiliqua* species (max 46° in *T. gigas* and *T. multifasciata*). The increased number and size of mental foramina is the result of the double row noted in all other stages, now beginning to fuse and grow over. The heavily textured lateral face of the dentary resulted from an increase in bone growth around muscle attachment sites possibly related to bite force stresses. The dentary depth, width and length increasing while tooth count does not, is typical of adult egerniines. The tooth count dropping as bony growth at the rear of the row has enveloped the posterior two teeth loci is an apomorphy of this species. The dental cementum has obliterated the dental sulcus at the rear of the tooth row, the last few remaining teeth appearing pleuro-acrodont, sitting on the top of the dentary due to the cementum billowing out on the medial side and increased bone growth on the lateral side.

Despite numerous apomorphies, the peramorphic morphotype still shares some character states with *Tiliqua* that have not been masked by age and growth. Meckel's groove is still closed, ending posteriorly in an enlarged splenial notch; the tooth crowns are fairly conical with the apex marked with a similar single crest as *Tiliqua rugosa* and *T. nigrolutea*; the coronoid ramus of the dentary still rises taller than the posterior tooth to cover most of the lateral face of the coronoid; and the coronoid process is fairly short, while being thick.

The shape of the tympanic conch of the quadrate of *Tiliqua frangens* differs from that of *Tiliqua rugosa*, the lateral face curving around to entirely obscure view of the medial ridge. This surface represents the attachment site for the *M. adductor mandibulae externus*. The increased thickness of the tympanic crest also suggests further reinforcement of the bone to deal with increased size and strength of this muscle. Relative height compared to maxilla length could not be determined due to breakage of the maxilla, but proportionally the bone is not more elongate in shape or considerably wider but instead the bone is more robust and measures considerably thicker. The relative width of the quadrate across the conch at 71.4% quadrate height, is considerably higher than any other *Tiliqua* (average 51.7%). The closest comparisons are *Corucia* with 67.2%, *Egernia*

epsisolus (76.5%) and *Liopholis kintorei* (66.2%). Each of these species have different habitat specialisations; *Corucia zebrata* an arboreal herbivore, *E. epsisolus* a rocky-crevice dwelling insectivore, and *L. inornata* nocturnal, burrowing, insectivore; so, the similar quadrate dimensions cannot be linked to any functional purpose.

The squamosal with the extent of the protruding ridges and muscle scars, exaggeration of the condyle shapes, and numerous foramina pocketing the surface is testament to the increased size, robustness and strength of the skull of *Tiliqua frangens* compared to *T. rugosa*.

Dentition

Scincid dentition is typically pleurodont, with resorption pits and replacement teeth positioned directly beneath the old tooth. Variation in the number of teeth in a tooth row, the size of the teeth, the shape of the base, shaft, and crown of the tooth and the details of cusp lengthening/shortening/loss are all factors that vary between species of Egerniinae. The clade inclusive of *Tiliqua* and *Cyclodomorphus* is united by several characters of their dentition, centred on the presence of one or more enlarged teeth at the rear of the tooth row. The number of teeth in the dentary tooth row varies considerably in the group, from 10–15 in *Cyclodomorphus*, 14 in *Tiliqua pusilla* and 12–19 in extant *Tiliqua*. This is less than the variation in *Egernia,* a sister clade with 20–29 dentary teeth. A reduced number of teeth in the dentary first occurs in *Tiliqua pusilla* Shea and Hutchinson, 1992 from the middle Miocene of Riversleigh, Queensland (Shea and Hutchinson, 1992). The tooth crowns in this dentition also sharing a flattened, round apex, highly modified from other egerniine shapes.

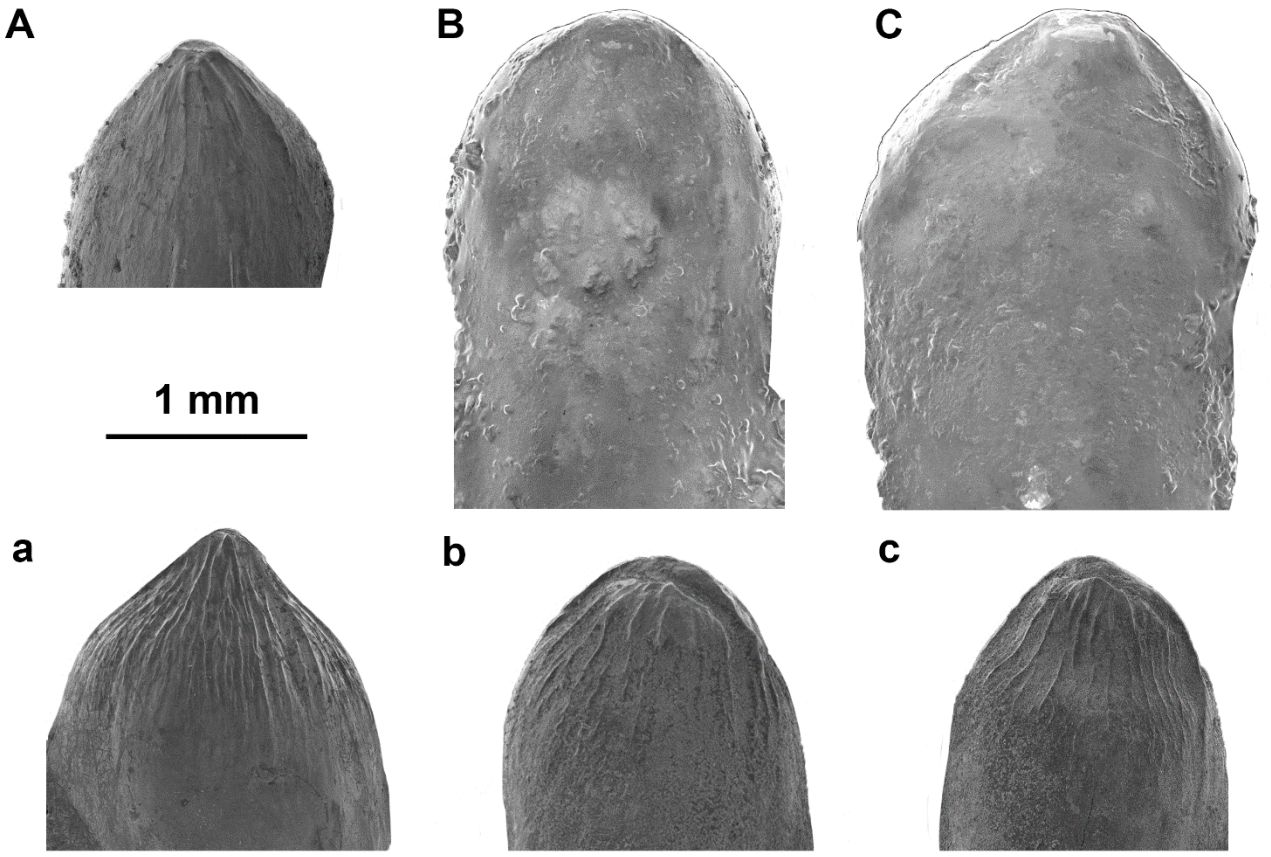

Figure A3.9: Tooth crowns of the fossil *Tiliqua frangens*, neonate (A) and adult (less worn B and largest tooth C), and *Tiliqua rugosa* neonate (a), adult (less worn b, and large worn tooth c). Striations are apparent on the neonates of both species, but absent in the adult *T. frangens*. Adult tooth crowns of both species have prominent lateral cristae extending into the *culmen laterales*.

The typical scincid condition is a bicuspid tooth crown with pointed medial and lateral cusps separated by an intercristatum (see Kosma, 2003). The dentition of *Egernia*, see Thorn et al. (2019), is atypical; all species have lateral compression of the tooth shaft and lengthened anterior and posterior cristae to produce an almost triangular crown in lateral profile. Comparison of tooth crowns with extant *Tiliqua rugosa* with those of *Tiliqua frangens* has highlighted further differences between ontogenetic stages and species (Figure A3.9).

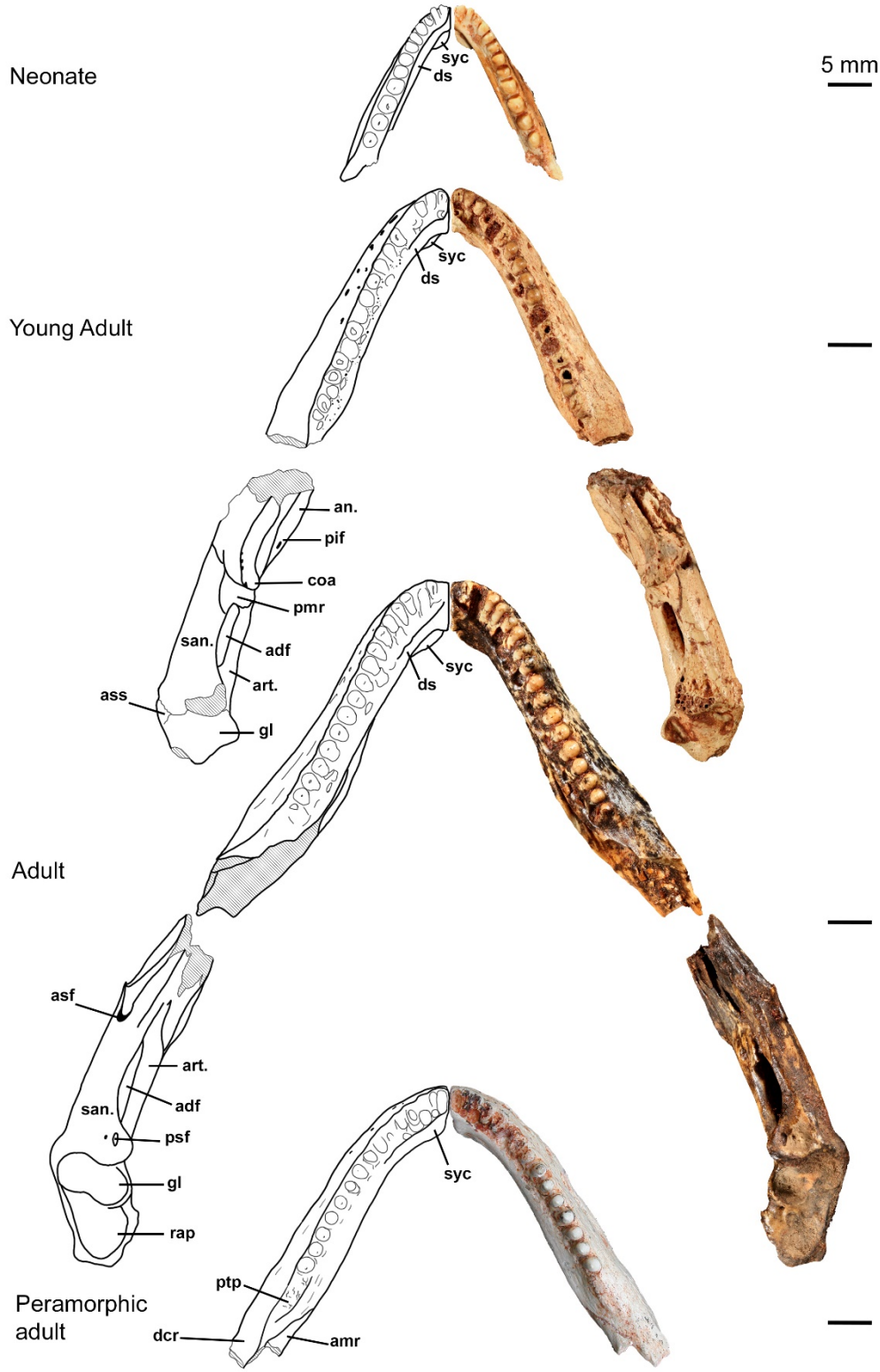

Figure A3.10: Occlusal view of *Tiliqua frangens* neonate, young adult, adult, and peramorphic adult (*Aethesia* holotype SAMA P43196) morphs. Dentary and post-dentary elements are not articulated, so total length is not an accurate portrayal, see Figure A3.2. Abbreviations: adf adductor fossa amr anterior medial ramus of the coronoid an. angular art. articular asf anterior surangular foramen ass articular-surangular suture coa coronoid apex dcr dentary coronoid ramus ds dental sulcus gl glenoid pmr posterior mandibular ramus of coronoid psf posterior surangular foramina ptp posterior tooth position rap retroarticular process syc symphysial chin.

Ontogenetic changes in dentition were noted in both the extant species and in *Tiliqua frangens* from neonate, through young adults and to the peramorphic condition (Figure A3.10). The juvenile dentition of species of *Tiliqua* and *Cyclodomorphus* is sometimes characterised by one enlarged tooth at the rear of the tooth row. This tooth is replaced by 3-4 teeth in adult specimens of the same species, as observed in *Tiliqua scincoides* (FUR071, and FUR076 juveniles and FUR130 an adult). Other species of *Tiliqua*, such as *T. rugosa* maintain similar tooth crown shapes and relative sizes from juvenile to adulthood, but add more teeth to the tooth row as the dentary lengthens with the increase in overall body size. Figure A3.9 illustrates the similar ontogenetic changes in crown shape for both *Tiliqua rugosa* and *T. frangens*; both species with adult tooth crowns that are wider, rounder and develop stronger lateral cristae and *culmen laterales* than the neonate form. The adult tooth has a wider crown than shaft in both *Tiliqua rugosa* and *T. frangens* and the occlusal surface of the tooth is rounder than the conical neonate crowns. Adult tooth wear appears similar in both taxa, the medial face of the tooth developing a shallow concavity beneath the *crista lingualis*, between the two *culmen laterales*. This depression in the medial face of the crowns accentuates the projection of both the medial and lateral cristae from the rounded surface of the crowns, creating a ridge along the tooth rows.

The Postcranial skeleton

Humerus

A left and right humerus from the partial individual skeleton recovered from Sobbe Site on the Darling Downs of south-eastern Queensland (QMF41532). The right humerus is cemented in a concretion of osteoderms matching those described above and those fused to the adult maxilla and frontals of *Tiliqua frangens*.

Both humeri are unbroken, and lacking proximal and distal epiphyses. Both bones being mirror images of one another, only the left is described herein. Total length of the bone is 30 mm, expanding in width at the proximal end to 14 mm, and is 13.3 mm distally. The minimum circumference of the shaft is located approximately mid-length from the proximal end and is 4 mm in diameter. The proximal end of the humerus widens mediolaterally from the shaft preserving the central, ventral concavity of the bicipital fossa, bounded on the right by the deltopectoral crest. The deltopectoral crest extends laterally from the proximal-distal length of the shaft at an angle of approximately 40°. It does not extend beyond the length of the humeral crest on the opposing side of the bicipital fossa which is slightly longer and projects out from the shaft at a greater angle of approximately 50°. The surface for the attachment of the humeral condyle is preserved, indicating this element is positioned directly in line with the centre of the shaft. In proximal view the bone is thicker in the location of the humeral condyle and the medial tuberosity. Between the humeral

condyle and lateral tuberosity the bone thins. The angle between these two elements is steep in dorsal and ventral view, approximately 70° away from the proximal-distal line of the shaft.

The distal end of the humerus preserves the ectepicondylar foramen, but no ectepicondyle crest or projection is evident, the bone expanding in width in a straight line from the shaft at an angle of ~30° away from the centre line. No visible entepicondyle is visible. In anterior view the space between the radioulnar fossa is triangular with straight sides forking at an angle of ~60°.

The rotation offset of the distal and proximal articulations is similar to that of *Tiliqua rugosa* and *T. scincoides* at approximately 45°. Overall length of the bone is not considerably longer than those of extant *Tiliqua* species but the greater expansion in the width of the bone at both proximal and distal ends and the diameter of the shaft suggest support for increased weight bearing on the limbs, without increased stride associated with greater limb length. The forelimb is the greater weight bearing limb (0.5 full body weight) in belly-dragging blue-tongued lizards (Nyakatura et al., 2014). Therefore, the humerus dimensions relate to body mass and locomotion. *Tiliqua frangens* was a heavy, belly-dragging lizard. Evidence for this method of locomotion is found in the relative mid-shaft width to total bone length of 13.3% (index of robustness, Lécuru, 1969; Russell and Bauer, 2008), and the width of the proximal and distal extremities of the diaphysis compared to total length (max 46.7%).

Tibia

A left adult tibia (AM F145620; Figure A3.11) was recovered from the disturbed sediment from Cathedral Cave. It is complete, with minimal abrasion to the proximal articulation surface. The bone is considerably broader in comparison to *T. rugosa* at the proximal end. The proximal articulation is asymmetrical, ovular, and wider anteroposteriorly in medial view. Beneath this face the shaft narrows slightly, and is compressed dorsoventrally, but not anteroposteriorly until further distally. The cnemial crest is pronounced (Figure A3.11) and sits roughly half-way down the length of the bone, indicating a lower-geared muscle attachment, for increased strength over speed in locomotion. The groove between the medial and lateral malleolus is very pronounced. The tibia is 23.2 mm tall, with a minimum shaft circumference of 4.2 mm, and widening on either end. The distal profile is 6.8 mm at the widest point and 6.6 mm perpendicular to that point. The proximal width is 11.2 mm measured parallel with the malleolar groove, and 8.4 mm wide perpendicular to that measurement.

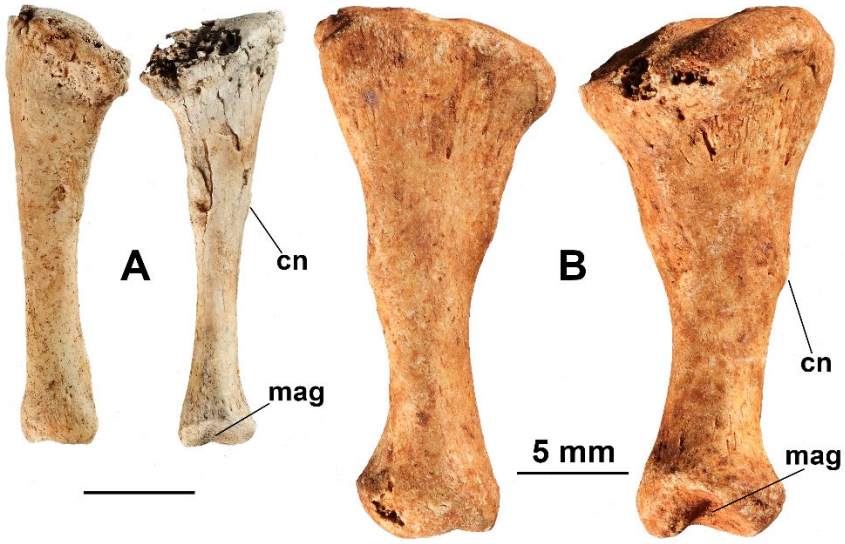

Figure A3.11: Left tibiae in dorsal (left) and ventral (right) views. A, *Tiliqua rugosa* (SAMA R67609); B, *Tiliqua frangens* (AM F145620). Abbreviations: cn cnemial crest, and mag malleolus groove.

The shape is similar to that of *Tiliqua rugosa*, with extreme proportions. The tibia of *Tiliqua frangens* is only 20% longer than *T. rugosa,* but 100% wider. The cnemial crest—the attachment site for the *M. quadriceps*—is more pronounced in *T. frangens*, with lower gearing for increased weight-bearing strength rather than increased speed. The groove between the medial and lateral malleolus is deep in *Tiliqua frangens*, indicating a more reduced lateral movement of the pes than in *T. rugosa*. The tibia is the primary load-bearing bone in the hind limb (Russell and Bauer, 2008). Differences in the proportions of the distal hind limb paired with the lower placement of the cnemial crest and deep malleolus groove of *Tiliqua frangens* indicate a heavier individual body mass comparative to *T. rugosa*, with strong limbs for slower, shorter-stride locomotion with minimal use of the hind feet.

Vertebrae

All vertebrae are procoelous as typical of scincid lizards. Two axis vertebrae have been recovered, AM F58265 and AM F121157. Measurements taken of the larger AM F58265 (Figure A3.12:1a–d) suggest this is an adult specimen. Anteriorly the articular surface measures 8.5 mm wide x 7.1 mm tall. The anterior face of the articulation with the atlas vertebra is concave dorsoventrally and convex mediolaterally, creating a saddle shape. The dorsal margin of the saddle, marking the odontoid process, projects forward into the arch of the atlas vertebra. The bone is generally robust, highlighted by the width of the lateral walls of the neural canal of 2.7 mm. The neural spine, rises posterodorsally 10.6 mm from the top of the neural arch, the anterior face is broken not preserving the true angle. The neural spine widens posteriorly to be 6.5 mm dorsally with parallel sides running ventrally almost to the neural arch, before widening to meet the postzygapophyses which spread out to a width of 12.3 mm. Viewed anteriorly, the intercentrum beneath the centrum is thickly built,

expanding laterally at the base, a small puncture is observed laterally in the thinnest part of the bone roughly in the centre. The intercentrum extends from beneath the articular facet for the atlas vertebra to posterior of the condyle on the centrum. The distal end of the intercentrum is rounded and thickened relative to the rest of this feature.

The axis vertebra of *Tiliqua frangens* is considerably more robust than that of *Tiliqua rugosa*, with thicker bone, a neural spine proportionally twice as broad, and an expanded base on the intercentrum. The dorsal tip of the neural spine of the axis vertebrae of *Tiliqua rugosa* widens posteriorly to 46% of its height, while in *T. frangens* it broadens to 62%. Comparative measurements of the neural canal maximum width, to the thickness of the wall of the neural canal best demonstrates this difference, with *T. frangens* bone 57.8% and *T. rugosa* 29.4% as wide as the neural canal. The shape of the intracentrum is similar between the two taxa, excepting the base and the distal tip. The intracentrum in *Tiliqua rugosa* remains thin, not thickening ventrally like that of *T. frangens*. The distal tip on the intracentrum of *T. frangens* is bulbous and rounded in lateral view while the same feature on *T. rugosa* is squared and thin.

Numerous presacral vertebrae were found in the collections of the AM and recovered from the new excavation of Cathedral Cave. Of these, AM F145621 was chosen as a representative specimen (shown in Figure A3.12:2a–d), with centrum 5.61 mm in diameter, similar to the larger axis vertebra and corresponding to an adult individual.

The sacrum comprises two vertebrae fused at the centrum and lateral extremities of the transverse processes. Four examples of this bone were identified from the new excavation and the existing collections of the Australian Museum. One large, complete sacrum was recovered from Sutton's Site on the Darling Downs. The centrum of the sacrum preserves a circular, cotyle anteriorly and condyle posteriorly with minimal dorsoventral compression distinguishing them from the highly compressed articulations on varanid vertebrae. Posteriorly, the condyle is slightly narrower than the centrum anterior to it, creating a very shallow lip of bone on the ventral surface. The transverse processes on the anterior vertebra are almost square in cross section, but rounded ventrally and extend laterally, angled posteriorly to meet the adjacent process on the posterior sacral vertebra. The processes widen distally and dorsoventrally to fuse with the transverse processes of the posterior sacral vertebra creating a posteriorly open 'C' shape in lateral view when fused, the posterior vertebra's transverse process forming a third of the 'C' at the base. The transverse process of the posterior vertebra is dorsoventrally compressed and anteroposteriorly curved in order to meet with the anterior transverse process. The ventral and anterior faces of this process preserve elongate furrows between supporting struts of bone connected to the centrum. In anterior view, the transverse

processes curve ventrally from the level of the centrum. The prezygapophyses of the sacrum are angled dorsally from the centrum at approximately 30° and preserve deep furrows medially on the dorsal surface where it meets the neural arch, and is then flattened to an ovular shape to support the articulation of the preceding vertebra's postzygapophyses. The neural spine on the dorsal surface of the vertebra begins immediately above the anterior edge of the neural arch and widens posteriorly. The dorsal tip of the neural spine was not preserved on any sacra.

The largest of the sacra based on centrum length and width, AM F58265, is missing the left transverse processes; the right extends 19.6 mm from the centre of the centrum to the articulation with the ilium. The centrum diameter is similar to the aforementioned vertebrae groups. Two specimens, parts a and b of AM F58257 are similar in size, with centrum widths of 7 and 7.2 mm and transverse process lengths of 22.8 and 19.9 mm (healed fracture) respectively. See the supplementary information for the remaining measurements and Figure A3.18 for their relative sizes in the morphospace.

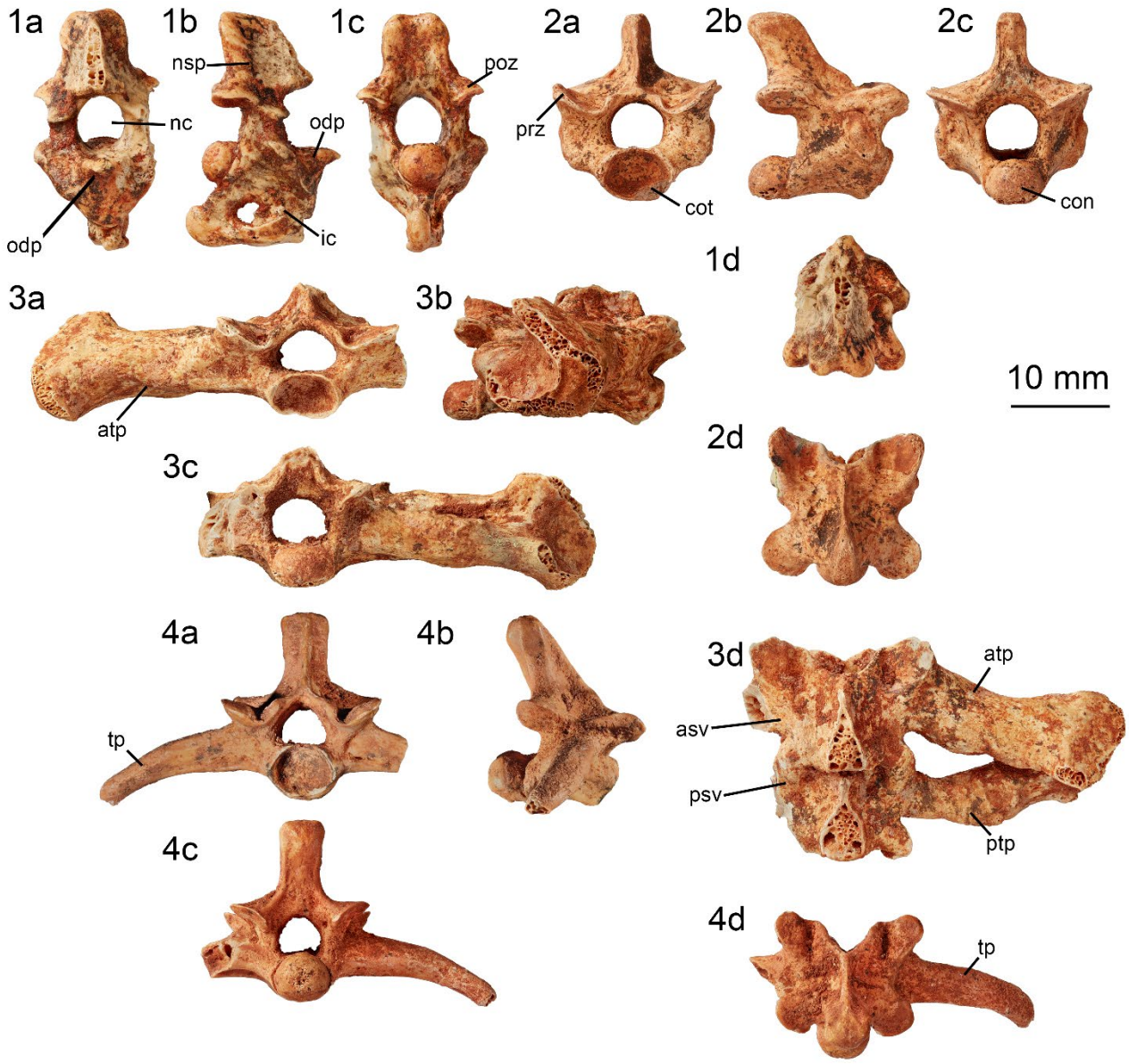

Figure A3.12: Anterior (a), lateral (b), posterior (c) and dorsal (d) views of the axial (1, AM F58265), presacral (2, AMS F145621), sacral (3, AM F58257) and pygal (4, AM F145622) vertebrae of *Tiliqua frangens*. Abbreviations: asv, anterior sacral vertebra; atp, anterior transverse process con, condyle; cot, cotyle; ic, intracentrum; nc, neural canal; nsp, neural spine; odp, odontoid process; poz, postzygapophysis; prz, prezygapophysis; psv, posterior sacral vertebrae; ptp, posterior transverse process; and tp, transverse process.

The pathology of broken sacral vertebrae transverse processes found on AM F58257 (Figure A3.12:3a–d) was found to be a common occurrence in *Tiliqua* across the herpetology skeletal reference collection of the South Australian Museum and noted in FU055. The 'healed fracture' pathological appearance may be a result of a growth deformity or common injury. Proportions and overall size of the vertebrae were compared with the use of a Principal Components Analysis (PCA).

A single pygal vertebra (Figure A3.12:4a–d) was recovered from the disturbed sediments overlying the main Cathedral Cave excavation (AM F145622). This specimen is preserved almost entirely, missing only the right transverse process. The centrum and condyle/cotyle are the same

shape as the sacral vertebrae and similar in size. A long lateral transverse process extends from the centrum on each side of the vertebra, narrowing distally. The length and shape of the transverse process positions the vertebra posterior of the thoracic region of the vertebral column. No ventral processes are observed on the centrum for articulation with a chevron to form the haemal arch as noted on the anterior-most caudal vertebrae in scincids. This vertebra can then be limited in its position to the 1st–3rd pygal vertebrae for comparisons with other *Tiliqua*.

Osteoderms

Osteoderms of *Tiliqua frangens* are typified by their raised, globular texture on the dorsal surface and the presence of large subpyramidal projections on the osteoderms from the central dorsal rows. These projections decrease in size and change orientation based on the lateral positioning of the osteoderm on the body.

The dorsal surface is covered in a small shiny, globular structures with apparent trenched lines running along the dorsal surface to the edge of the bone, possibly accommodating vascular channels for the skin. The margin that marks the area of the osteoderm overlapped by the proceeding osteoderm in the row has a smooth dorsal surface. The ventral surface accommodates the preceding osteoderms to occlude in a brick-like pattern, either side of the centre.

Figure A3.13: Central row dorsal osteoderm of *Tiliqua frangens* (AM F145623) and of a large adult *Tiliqua rugosa* (SAMA R67609). From left to right the dorsal, lateral, posterior and ventral views shown.

The dorsal subpyramidal projection has a broad base and terminates in an extended ridge, or a rounded apex, rather than a sharp point. The ventral surface of the osteoderm has a depression under the projection, but the projection itself is not hollow.

A large osteoderm collected from Cathedral Cave AM F145623 (Layer 13F 510-515 cm) measures 29.7 mm wide, 23.1 mm long, with a projection reaching 8 mm high. The external outline of the larger ornamented osteoderms matches those of the central dorsal rows on *Tiliqua rugosa*.

The best preserved osteoderm, pictured in Figure A3.13, resembles the shape of the central dorsal row form in *Tiliqua rugosa*, but is considerably larger in all dimensions.

Numerous complete osteoderms and fragments were collected from the Cathedral Cave excavation, but no detailed histological details have been noted. The surface texture and overall thickness remain the distinguishing factors separating the osteoderms of *Tiliqua frangens* from the only other compound osteoderms found in Australian lizards, belonging to *T. rugosa*. *Tiliqua frangens* has a more rugose, raised globular texture, and *T. rugosa* appears more uniform with a pitted surface. Osteoderms are considerably thicker in all specimens of *T. frangens*. This increased bone growth would have amplified the overall weight of the animal considerably.

Association of the material

All material referred to in the following description has been assigned to a single species, *Tiliqua frangens*, rather than the two species *Aethesia frangens* and *Tiliqua laticephala*. This decision was based on the observation that across the sites where both putative taxa potentially occur, there is only evidence of one giant egerniine species: i.e., each element (e.g., mandible) comes in only a single morphotype, and all elements show unusual features (e.g., large adult size, heavy ossification, double row of mental foramina) that suggest they come from a single distinctive taxon, and all articulate sensibly with each other (see below). All cranial and postcranial material recovered for this animal is noticeably more robust and generally heavier than any modern *Tiliqua* species. Notably, even the neonate material, despite its small size, is more robust than neonate material from other living egerniines, and can be linked to the adult material through ontogenetic intermediates. This egerniine is not similar in shape nor shares any characters with the similar-sized varanid species recovered from the same site. The postcranial material was compared with multiple varanid taxa and still retains a more scincid-like morphology; the vertebrae with round centra, and humeri with a deltopectoral crest almost parallel to the humeral condyle. No other *Tiliqua* material was found in the Cathedral Cave excavations, the next largest scincid species represented are presently referred to as *Egernia* cf. *E. cunninghami* and *E.* cf. *E. rugosa,* the adult material of which is considerably smaller and less robust than the referred material here described, and lacks any character states that are unique to *Tiliqua*. Furthermore, several pairs of articulable conjoining cranial elements link the isolated holotype elements of *Aethesia* and *Tiliqua laticephala*. Although the holotypes of the *A. frangens* (mandible) and *T. laticephala* (frontal) are non-overlapping, they occur in association with other elements, which allow comparisons. The mandibles that are found with frontals that can be matched to the *T. laticephala* holotype cannot be clearly distinguished from the holotype of *A. frangens*; similarly, the frontals found in association with *A. frangens*

peramorphic morphotypes cannot be clearly distinguished from the holotype frontal of *T. laticephala.*

The variation observed in these assemblages is consistent with ontogenetic variation observed in living egerniines (see below). Thus, the most conservative and parsimonious interpretation is that all material pertains to a single taxon, with neonates, juveniles, young and old adults being present.

The frontal AM F135900 described as *Tiliqua laticephala* by Čerňanský and Hutchinson (2013), and two new specimens (AM F145613 and F145614) confirm the association of the large osteoderms with this taxon. The frontals have some osteoderms fused onto their dorsal surface, which share the globular texture and extraordinary thickness seen in the isolated horned osteoderms. These frontals articulate well with the nasal (AM F145612), which also has similar bone texture and thickness.

The maxillae are united with the frontal specimens by means of a fused osteoderm on the lateral side of the facial process on AM F145609. The mandibles are associated with the maxillae by their concordant tooth row length, dentition patterns, and matching tooth crowns. The anterior teeth on the maxilla match those on the premaxilla, and the anterior suture and facial process height on the maxilla match the corresponding angle with the internasal height of the premaxilla and nasal length and so we can estimate the premaxilla has reached a similar point along the growth trajectory. The quadrate, squamosal and braincase all share clean facets for articulation with one another, the adult forms of each can be articulated without unnatural twisting or reshaping. The complete mandible of the adult morphs moreover fit to the reconstructed caudal parts of the skull by their concordant length and shared angle of inflection of the tooth rows.

The holotype dentary for *Aethesia frangens* was not allocated to the genus *Tiliqua* by Hutchinson and Scanlon (2009) because of its isodont dentition (*Tiliqua* species being heterodont); the absence of a dental sulcus; the convex rather than concave scarring of the adductor muscle on the lateral face of the posterior region of the dentary; and the exaggerated size and angle of deflection of the symphysis. However, the recovery of neonate AM F145608 through to adult AM F143321 provides an ontogenetic context to the *Aethesia* holotype, highlighting the peramorphic extremes it has reached from a more typical *Tiliqua* starting point. The apomorphic character of the obliterated dental sulcus in *Aethesia* is found to be a peramorphic trait, caused by the gradual build-up and ossification of dental cementum. The seemingly extreme dimensions of the dentary of *Aethesia* in width and height are also allometric, increasing with size and presumed age. The positioning of the largest tooth at the back of the row is not a constant apomorphic trait, but a result

of the loss of regeneration of the last two tooth positions during growth. Using these features, and their ontogenetic pathway, the holotype of *Aethesia* and specimens sharing the same apomorphic character states are considered to be representative of the peramorphic morphotype of *Tiliqua frangens*.

The postcranial elements from Cathedral Cave are referred to *Tiliqua frangens* as there are no other species of *Tiliqua* represented during the Pleistocene at this site. Comparisons made between all of these elements and all extant *Tiliqua* demonstrate multiple distinguishing features, most related to robustness and a shape reflective of increased load-bearing ability. Identification of some postcranial elements were confirmed using the association partial skeleton (QM F41532) from Sobbe Site.

Results

Distribution

Tiliqua frangens was widely distributed across eastern Australia, in regions not concurrently occupied by *T. rugosa.* Extensive searches of museum collections covering material from all latitudes of eastern Australia were conducted, and all sites containing material that can be confidently attributed to *Tiliqua frangens* are mapped in Figure A3.14. No Pleistocene sites south of the Murray River were found to contain *T. frangens*. The geographically closest material of a large extinct fossil skink that could be referred to this species was from Fisherman's Cliff on Moorna Station (Figure A3.14) on the northern side of the Murray River in NSW (frontal bone NMV P253558). The associated mammalian fauna and magnetic polarity of the stratigraphy at Moorna station suggest an early Pleistocene accumulation for this material (Whitelaw, 1991). Numerous specimens of *Tiliqua frangens* were located in the Quaternary Wellington Caves deposits: the two named holotype specimens and those described in this chapter. The northern-most specimen of *Tiliqua frangens* is QM F7709 from the Pleistocene site of Cement Mills, Gore, Queensland. First identified as '*Tiliqua scincoides*' (Bartholomai, 1977), the morphology of this half-dentary matches the peramorphic *T. frangens* morphotype with dental cementum obliterating the sulcus, identical tooth crown shape and a very deep dentary bone. South-eastern Queensland preserves an associated skeleton from Sobbe Site (humeri and skull fragments); and isolated osteoderms, an unregistered right dentary with 18 loci and 11 preserved teeth (from 'Mulloch Heap'), a right dentary fragment with 8 teeth (QM F35777) and a neonate left dentary tooth row with 7 teeth (QM F42173) from Sutton's site. The isolated osteoderms from Kings Creek Catchment site (QML1396) QM F44603–F44605 were first noted in Figure 8 of Price and Sobbe (Price and Sobbe, 2005). Originally identified as *Tiliqua rugosa*, the three specimens have now been confirmed with the aid of

comparative material from Wellington Caves as the thickened, globular-textured osteoderms of *T. frangens*.

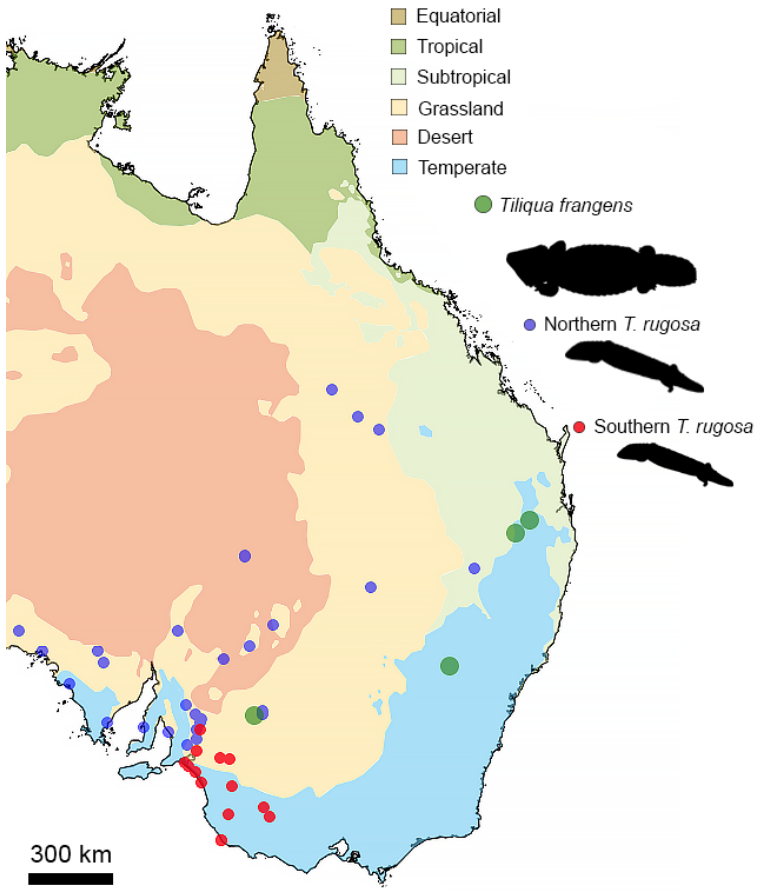

Figure A3.14: Map showing the current distribution of the two populations of *Tiliqua rugosa* in eastern Australia (*T. rugosa* data from (Ansari et al., 2019)); and the Pleistocene localities of *Tiliqua frangens*. Present climate zones as per the Köppen classification system, using data collected by the Australian Bureau of Meteorology (Australian Bureau of Meteorology, 2006). Map generated using the spatial portal provided by the Atlas of Living Australia (Atlas of Living Australia, 2019).

Body size and shape variation

Head length of living individuals of *Tiliqua rugosa* correlate (with some minor sexual dimorphism) with snout-vent length (Bull and Pamula, 1996), and with body mass. A major axis regression of the log-transformed head length (mm) and snout-vent (mm) of extant *T. rugosa* specimens (Figure A3.15) produced the relationship: Snout-Vent Length = 1.274 (Head Length) + 0.697 (see Data S1. Measurements.xlsx). Calculated from a skull length of 70 mm the inferred total snout-vent length of *T. frangens* is ~594 mm. A major axis regression of the log-transformed head length (mm) and body mass (grams) of extant *T. rugosa* specimens (Figure A3.15) produced the relationship: Body Mass = 2.767 x (Head Length) + 1.0395. When the reconstructed head length figure for *T. frangens* is inserted into the body mass equation for its *T. rugosa* its sister taxon, the total body mass of *T. frangens* is ~2387 grams (see calculation in Data S1. Measurements.xlsx).

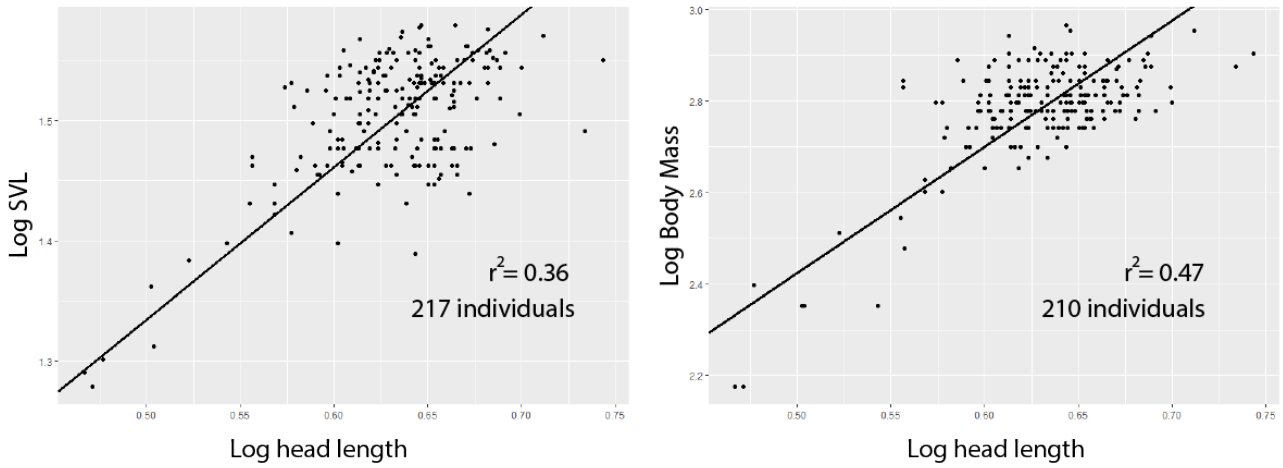

Figure A3.15: Standardised major axis regressions between logged head length (mm) and logged snout-vent length (SVL; mm), and logged body mass (g) in extant *Tiliqua rugosa*.

Previously, plots of the frontal antorbital-width vs length clearly separated *Tiliqua rugosa* and *T. frangens* (Čerňanský and Hutchinson, 2013). With four newly added frontal specimens, the major axis regression (MAR) lines show two separate growth trajectories (Figure A3.16), one animal considerably wider than the other. The slopes are significantly different, the ratios of antorbital width to total frontal length for each species, when subject to a Student's *t* test produced a very significant probability that the means are unequal ($p<<0.01$; see Data S1. Measurements.xlsx). A Permutation test of the logged frontal length and antorbital width also resulted in a minimal probability that the two groups are similar ($P<0.01$).

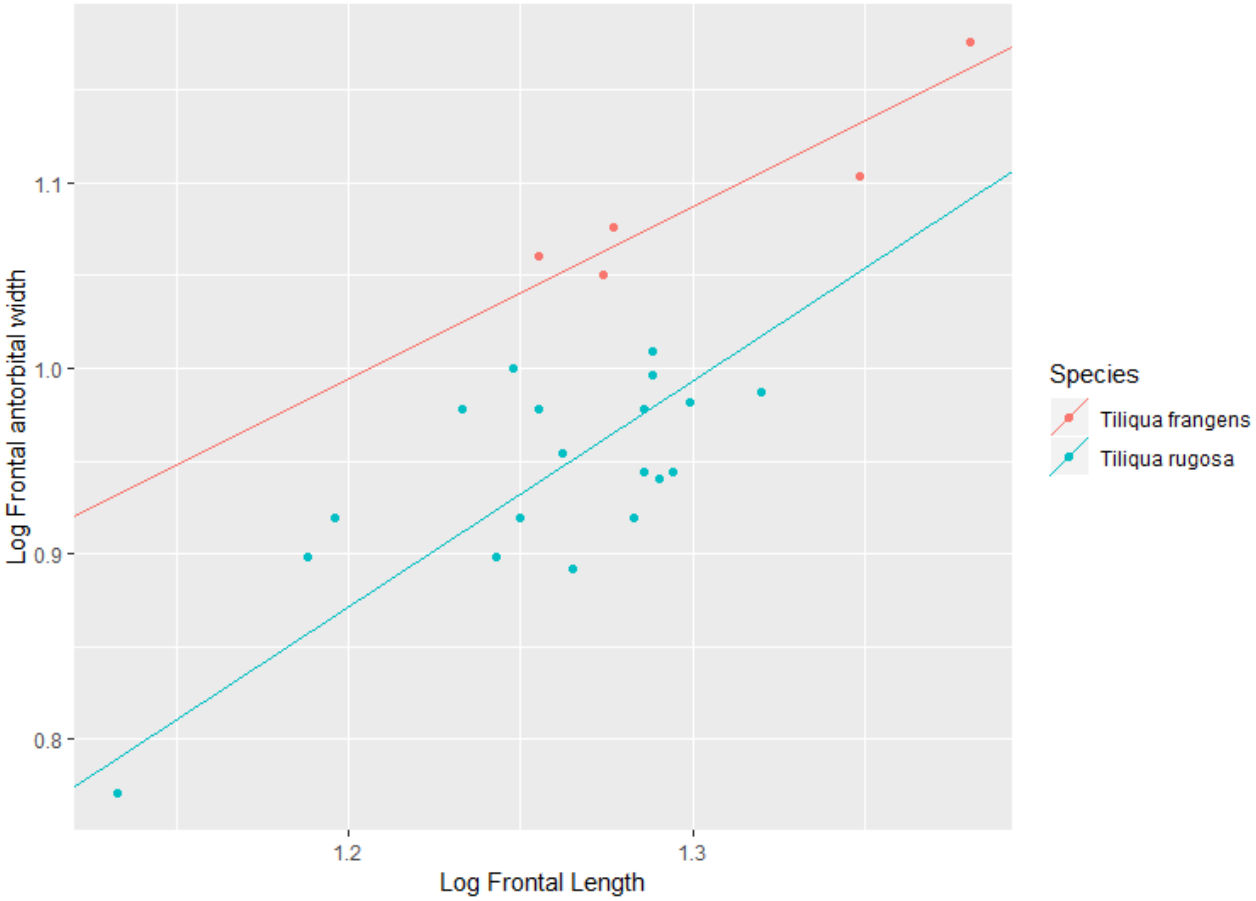

Figure A3.16: Frontal antorbital width and total anteroposterior length of *Tiliqua frangens* (red dots and SMA regression line above) and *Tiliqua rugosa* (blue dots and SMA regression line below) measured in millimeters and log transformed. Data for *T. rugosa* sourced from Čerňanský and Hutchinson (2013).

Clear shape separation is not attainable with every element; a Principal Components Analysis (PCA) comparing the dentaries produce slightly overlapping convex hulls for the two species (Figure A3.17). Component 2 is weighted heavily by tooth row length (loading of 0.759), *Tiliqua rugosa* forming a tighter cluster below the majority of *T. frangens* data points. Tooth row length (TRL) is a better indicator of true dentary length as the angular process of the dentary is often broken, reducing the overall dentary length measurement on many fossil specimens. Simple measurements do demonstrate some separation between the adult specimens, *Tiliqua frangens* have on average a wider (28% of TRL) and deeper (21% TRL) dentary profile in relation to tooth row length, than *Tiliqua rugosa* (24%, 18% TRL).

A PERMANOVA showed no significant statistical difference between the *Tiliqua rugosa* and *T. frangens* dentary measurements shown in the above PCA (p=0.1202), more resolution might be possible with the aid of geometric morphometrics or by examining the weight-bearing skeletal elements.

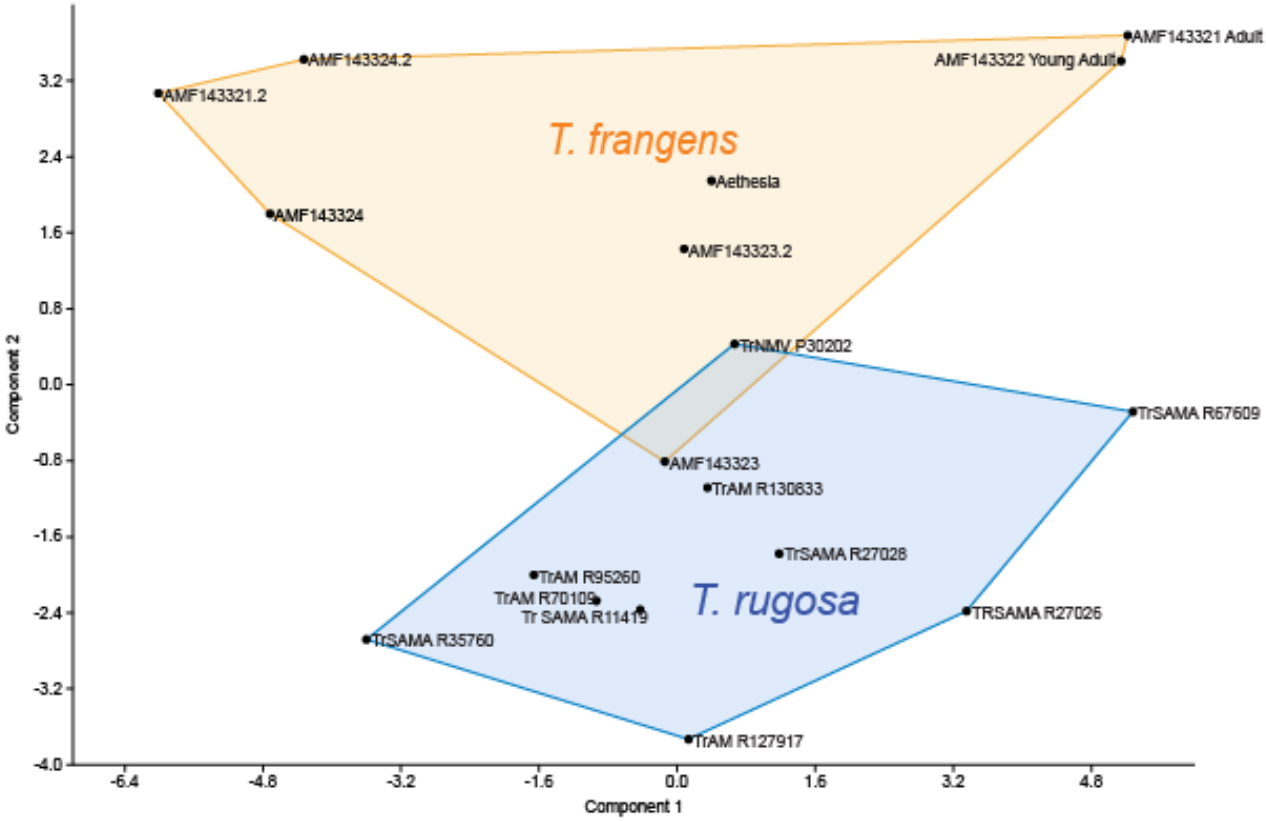

Figure A3.17: Principal Components Analysis of the mandibular elements of extant *Tiliqua rugosa* and fossil *Tiliqua frangens*, excluding the neonate specimen. Measurements taken were dentary length, height and width, tooth row length, and symphysis length and width. Component 1 and 2, representing 55.98% and 30.52% of the variation in the data respectively. The loading on component 1 is 0.995 dentary length, component 2 is primarily related to tooth row length (0.759).

A PCA of the measurements of the vertebrae of the two species produced a clear separation in Figure A3.17: *Tiliqua frangens* overlies the *T. rugosa* convex hull with similar proportions in the axial, post-sacral and sacral vertebrae compared to *T. frangens*. Component one represents 76% of the variation in the data, and appears to be driven by changes in width of the vertebral column. Transverse process length is related to width of the body and the vector is directly relational to the largest divide between the two species, highlighting a disparity in body shape. *Tiliqua frangens* vertebrae are built to carry more weight and support a wider body than *T. rugosa*.

A one-way PERMANOVA was calculated to test for the variation between the above species using the vertebrae measurements (data in SI). Significant differences were noted between the two species ($P<0.01$), confirming the separation noted in Figure A3.18.

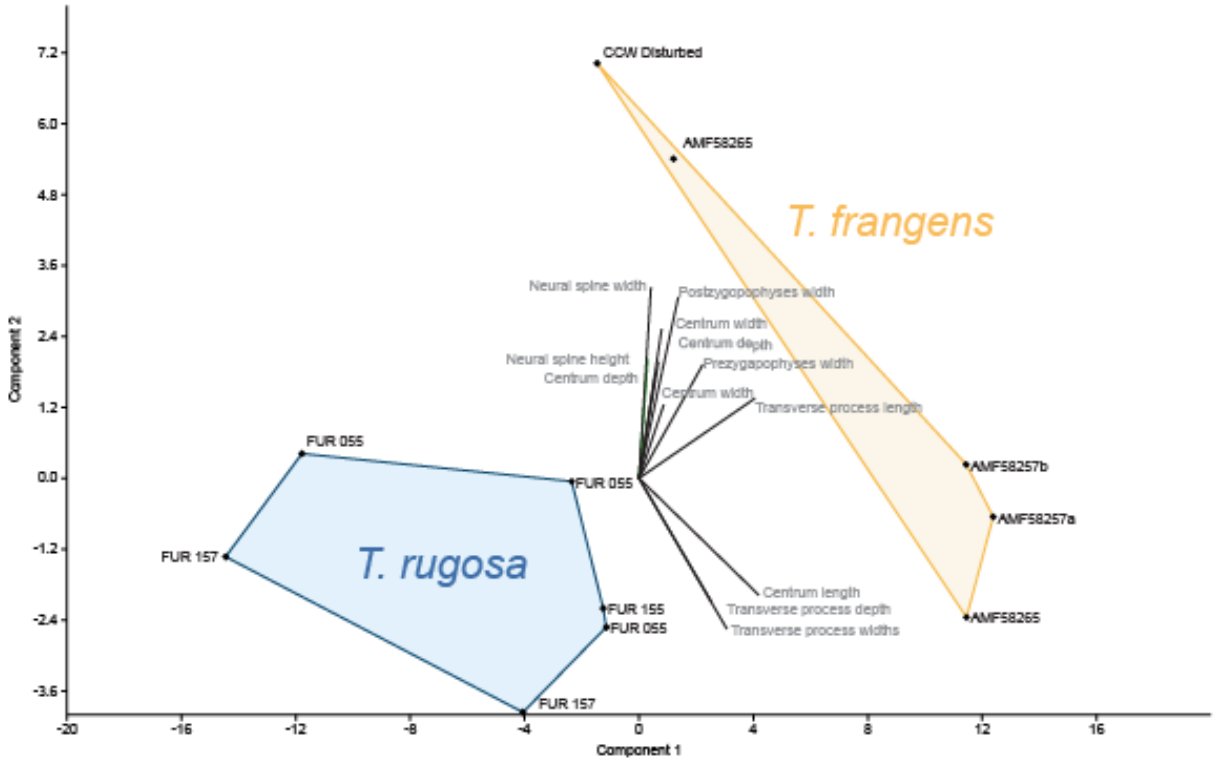

Figure A3.18: Result of the principal components analysis of measurements taken of *Tiliqua rugosa* and *Tiliqua frangens* vertebrae. The two species are clearly separated, the primary components account for 78.7% and 11.27% of the variance in the data respectively.

Parsimony

The analysis using all (continuous, discrete and molecular) data with young and peramorphic adult *T. frangens* coded separately (Figure A3.19, A), resulted in both morphotypes of *T. frangens* as sister taxa to the Solomon Islands' monkey-tailed skink *Corucia zebrata*. A single most parsimonious tree with a length of 4742.561 steps, hit 39 times out of 1000. The resulting consistency index (CI) = 0.403 and retention index (RI) = 0.422. This topology was unexpected and biogeographically extremely discordant, spurring the subsequent three investigations. To test for the effects of ontogeny on the position of the two morphotypes in the tree, separate analyses were run with the combined continuous and discrete data but with the two morphotypes combined into a single taxon, or only including one ontogenetic morphotype and excluding the other.

The topology from the analysis which only included the young adult morphotype paired it with *Corucia zebrata* (Figure A3.19, B). The best score of 4727.261 was found in 45 out of 1000 runs. CI=0.404, RI=0.425. The rest of the topology remained unchanged from the first run that produced Figure A3.19, A. When the analysis was repeated but with only the peramorphic adult, it emerged as nested within a paraphyletic *Tiliqua+Cyclodomorphus* clade, see Figure A3.19, C. This tree is 4725.698 steps in length and was found in 44/1000 runs with a CI=0.404 and RI=0.425. The

paraphyly of *Tiliqua+Cyclodomorphus* is present in all of the resulting MP topologies, it is not a result of the movement of *Tiliqua frangens* into this clade. The peramorphic adult branches before all *Tiliqua* and *Cyclodomorphus gerrardii*, to the exclusion of the small clade of *Tiliqua adelaidensis+T. rugosa*.

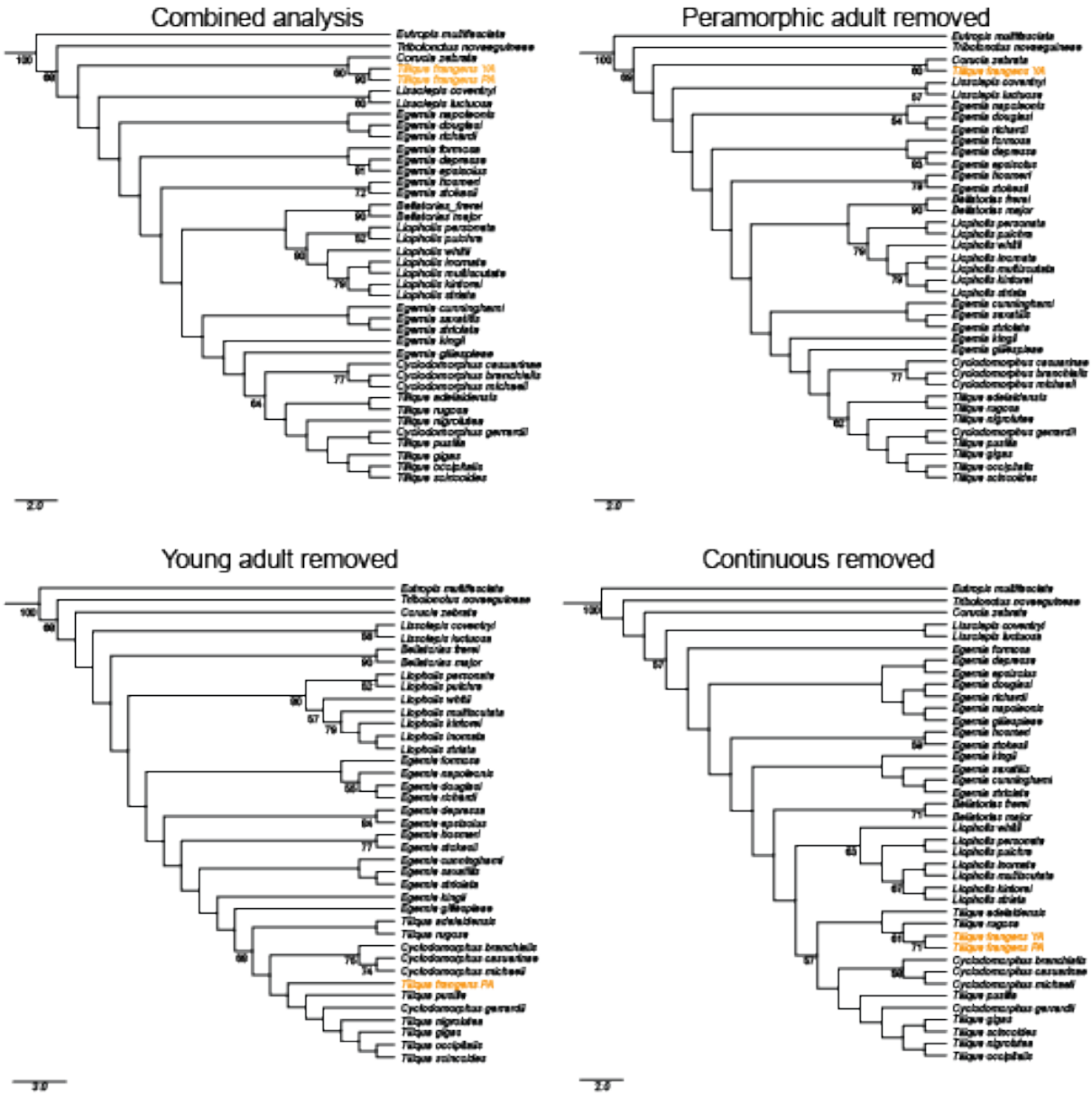

Figure A3.19: Results of four maximum parsimony analyses conducted in TNT. A, Combined analysis is inclusive of all morphological and molecular data and both fossils; B, Peramorphic adult fossil removed from data set; C, Young adult removed; and D, a result inclusive of both morphotypes but no continuous data, which generated six trees due to movement within *Egernia*, tree 1 is shown.

The analysis conducted with a composite taxon, where both the young adult and peramorphic adult morphotypes were combined into a polymorphic coded unit produced a different topology again. Most similar to analysis where the two taxon units were both included and the analysis with just the young adult, this topology was retrieved 54 times out of 1000, with a score of 4734.549 (CI=0.404; RI=0.420). The higher score and retrieval rate most likely due there being less

missing data as both morphotypes have different elements not recovered for the other ontogenetic stage (i.e. a more complete braincase for the peramorphic adult, and a complete coronoid only present for the young adult mandible). The polymorphic taxon appeared as sister to *Corucia zebrata*, with a weak bootstrap support of 46.

In order to test the effect of convergence on cranial shape, another MP analysis (Figure A3.19, D) was run without the continuous matrix. This analysis resulted in six equally most parsimonious trees, each with 4293 steps, hit 308 times in 1000 runs (CI=0.422; RI=0.416). All topological differences between these six trees are confined to the unresolved grade "*Egernia"*, not within the focus of this investigation. Within *Tiliqua*, both *T. frangens* morphotypes are now recovered as sister taxa to the extant *Tiliqua rugosa*. The remaining *Tiliqua* and *Cyclodomorphus* species are in the same positions within the paraphyletic clade as the previous analysis with the young adult morphotype removed (Figure A3.19, C).

The topology of the MP analyses when continuous data were removed changed the positioning of the two other fossil taxa, previously described in Thorn et al. (2019). *Egernia gillespieae* was placed basal to the *Tiliqua+Cyclodomorphus* lineage in the first analysis (Figure A3.19 , A, the total evidence analysis inclusive of continuous data), while the analysis without continuous data (D) caused numerous shifts in the grade *Egernia* and prevented the analysis from producing a single most parsimonious tree. *Tiliqua pusilla* only shifted a small distance across the tree with the removal of continuous characters, from above the major *Tiliqua-Cyclodomorphus* divide to being nested in the middle of the two grades.

Bayesian

In an attempt to test the effects of ontogeny on the resulting phylogeny, brought to our attention by the discordant results from Maximum Parsimony, three morphotypes of *Tiliqua frangens*, the young adult, peramorphic adult, and a composite taxon incorporating both were analyzed using Bayesian methods. Adult specimens of extant taxa were coded, to test if the morphotypes would still end up in a similar position. If ontogeny does recapitulate phylogeny as Haeckel predicted, then an immature fossil should appear basal to egerniines and the adult with a number of apomorphies will appear more nested. The topological placement of *Tiliqua frangens* ontogenetic morphotypes did not concur with this idea. The discordance of the positioning of *Tiliqua frangens* between the varying analyses that include/exclude continuous data, or that were run with the 'Young Adult' or 'Peramorphic' morphotypes separately, highlight the effect of shape variation and ontogeny (Figure A3.20). The extreme deepening and shortening of the skull of *Tiliqua* frangens has created a skull shape convergent on the Solomon Islands' *Corucia zebrata*,

despite numerous discrete characters separating them. This demonstrates the need to be more wary of the effect convergence of shape, when not kept in check with the presence/absence of evolutionarily more-conservative discrete traits.

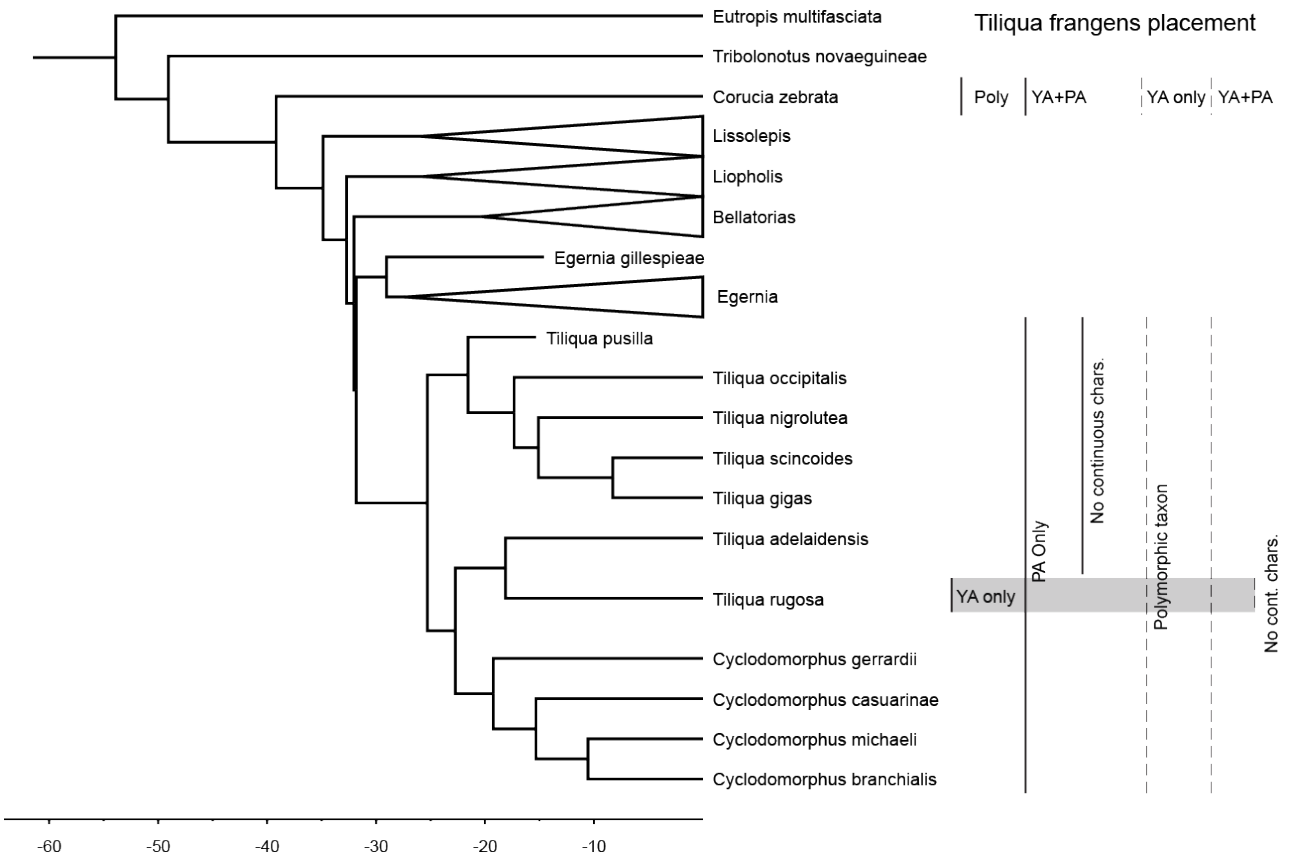

Figure A3.20: Resulting placement of *Tiliqua frangens* from five separate maximum parsimony analyses in TNT, represented by dashed lines (Goloboff and Catalano, 2016). Bayesian analysis results are represented with solid lines, these were conducted in BEAST (Drummond et al., 2012). PA=Peramorphic adult morphotype only; YA= Young adult morphotype only; YA+PA= both morphotypes run in the single analysis; Poly=Polymorphic taxon of combined characters from both morphotypes. The shaded area represents the placement most often resolved.

No clear consensus with biogeographically possible topology was produced by any analysis inclusive of continuous characters. The placement of *T. frangens* with *Corucia* is extremely unlikely. The phylogeny produced with the omission of continuous data depicted in Figure 3.1 is more concurrent with previous analyses (Gardner et al., 2008; Skinner et al., 2011; Thorn et al., 2019) in which *Corucia zebrata* is separated from all Australian egerniines with a PP of 1.0. The age and separation of *Corucia* from Australian egerniines as early as 26 MYA is supported by biogeographical evidence and a detailed intraspecific molecular phylogeny of *Corucia zebrata* (Hagen et al., 2012). Within the *Tiliqua*+*Cyclodomorphus* (*T*+*C*) clade, the most realistic result was that *T. frangens* is a sister taxon to *Tiliqua rugosa*. Other outcomes included *T. frangens* placed just outside *Tiliqua* or the *T*+*C* clade.

Potential convergence on head shape similar to that of *Corucia* is driven by increased head height and width in the young adult, adult and peramorphic morphotypes of *Tiliqua frangens*. The peramorphic dentary of *Tiliqua frangens*, previously described as *Aethesia frangens,* was understandably attributed to a new genus, as it has so little in common with any extant *Tiliqua*, having lost the dental sulcus, changed the shape of the dentary entirely by means of lateral expansion, and the symphysis suggesting a much wider jaw angle. Only with the collection of sequential ontogenetic growth phases of the dentary and other cranial elements, were we able to justify its reallocation to *Tiliqua*. Characters supporting the allocation of *T. frangens* to *Tiliqua* include an increased relative splenial height (char. 25), which is not as tall in *Cyclodomorphus*; a decreased number of dentary teeth (char. 51) and increased number of enlarged teeth (char. 53); and a reduced number of premaxillary teeth (7–8 total; chars. 69–70) compared to *Egernia* spp. Shared characters between *Tiliqua rugosa*, and *T. frangens* are detailed in the description, but notable synapomorphies of the two taxa include an increased symphysis width and length relative to dentary length (chars. 5–6); increased frontoparietal width relative to frontal length (char. 78); and thickened squamosals (char. 122). The *T. rugosa*+ *T. adelaidensis*+ *T. frangens* clade share shorter retroarticular processes relative to dentary length, than all other egerniines. *Tiliqua rugosa* and *T. frangens* have increasingly wider retroarticular processes, *T. frangens* balancing a shortening of the skull with increased surface area by widening this feature.

Discussion

Phylogeny

Tiliqua frangens is most closely related to the living armour-plated Shingleback skink, *Tiliqua rugosa* (Figure 3.1). Measurements reflecting frontal and mandibular convergence on tall, wide skulls for herbivory (i.e. those shared by *Corucia zebrata*) interfere with any phylogenetic signal in the continuous characters. The exclusion of continuous characters produce stronger posterior probabilities for the topological placement of this taxon, positioning *T. frangens* in a clade that is biogeographically sensible. Traits supporting the relationship with *T. rugosa* include an increased symphysis width and length relative to dentary length (chars. 5–6); increased frontoparietal width relative to frontal length (char. 78); the prearticular and surangular contact anterior of the adductor fossa is obscured by the coronoid (char. 45); and (at least as neonates) both species share paired rows of mental foramina (char. 15). The *T. rugosa*+ *T. adelaidensis*+ *T. frangens* clade share a conical tooth crown shape (char. 55) and shorter retroarticular processes relative to dentary length (char. 49), than all other egerniines. *Tiliqua rugosa* and *T. frangens* have increasingly wider retroarticular processes, *T. frangens* balancing a shortening of the skull with increased surface area by widening this feature. Both *T. rugosa* and *T. frangens* are large, armoured

skinks: however, *T. frangens* takes these trends to the extreme, and is the largest and most bizarre skink to have ever existed. This extends to dentition: unique dental traits not found in any other skinks include pleuro-acrodont dentition in adults and a halt in tooth replacement for the last two teeth in each row in peramorphic adults.

The post-crania of *T. frangens* also share other parallels with modern *Tiliqua*, the compound osteoderms have fused to create a hard dermal skeleton. The vertebrae share the same shape, albeit transposed by increased size they are more robust in *Tiliqua frangens* than *T. rugosa*. The tibiae and humeri are alike in shape to other *Tiliqua*, more so than other Australian squamates. The change in proportions are most likely due to supporting an increased weight in comparison to other egerniines. These changes in limb proportion and shape are more likely due to function rather than phylogeny, a pattern observable in many other squamates (Russell and Bauer, 2008).

The topological uncertainty of *Tiliqua frangens* has decreased the posterior probabilities of all of the nodes in the *T+C* clade, but some similar relationships are resolved in all analyses. *Tiliqua adelaidensis* and *T. rugosa* are sister taxa in all trees, the remaining *Tiliqua*, *T. nigrolutea*, *T. occipitalis*, *T. scincoides* and *T. gigas* forming a clade. *Cyclodomorphus michaeli*, *C. branchialis* and *C. casuarinae* consistently form a clade, but *C. gerrardii* floats between *Tiliqua* and *Cyclodomorphus*. Phylogenetic positioning of relatively young calibration point fossils needs to be more precise and well supported in order to produce relatively low confidence intervals for divergence dates (Lee et al., 2009a). This uncertainty in the monophyly of *Tiliqua* leaves plenty of space for future research. The phylogeny of *Tiliqua* and *Cyclodomorphus* warrants a complete reworking, inclusive of the molecular data for currently missing taxon *Tiliqua multifasciata*, *Cyclodomorphus celatus*, *C. maximus*, *C. melanops*, *C praealtus* and *C. venustus*; and the morphological data for Pliocene fossil taxon *Tiliqua wilkinsonorum* Hutchinson and Mackness, 2002.

Morphological extremes

With an inferred weight in excess of 2kgs, *Tiliqua frangens* is by far heaviest known scincid ever (see histogram in Figure 3.1). The egerniines *Bellatorias major* (land mullet: 670 g) and *Corucia zebrata* (Prehensile-tailed skink: 1 kg) are the two largest living skinks (Klingenböck et al., 2000; Meiri, 2010; Hagen et al., 2012). The Australian Quaternary record preserves two other extinct egerniine giants, *Tiliqua wilkinsonorum* Hutchinson and Mackness, 2002 from Chinchilla, and a *Tiliqua* sp. mentioned from the Mt Etna collection (Hocknull, 2005). Both of these Queensland species, described from isolated dentaries, occur further north than any record of *T. frangens* and have unique dentitions. No estimates of the total length or weight could be made from

isolated dentaries for comparison with *T. frangens*. *Tiliqua wilkinsonorum* has a longer, but less robust dentary than *Tiliqua rugosa* or *T. scincoides*.

Among skinks, *Bellatorias major* (300 mm; Wilson and Swan, 2017), *Corucia zebrata* (350 mm; Gardner et al., 2008), and *Acontias plumbeus* (490 mm; Greer, 2001) have snout-vent lengths approaching *T. frangens*, but they are elongate animals with lesser comparative masses, as discussed above. The extinct *Leiolopisma mauritiana* (Gunther, 1877), from the Quaternary of Mauritius attains an impressive SVL (340 mm; Austin and Arnold, 2006), but is similarly likely to be much lighter than *Tiliqua frangens*. Evidence for the great disparity in bulk is in the comparison of their tibiae and vertebrae. Most *Tiliqua* species have shortened limbs; *T. frangens* is no exception and the recovered tibia is shorter than *L. mauritiana* (23 mm to 28 mm), but the proximal width is greater than the island giant, i.e. 11.2 mm (49%) to the 10 mm (36%) recorded for *L. mauritiana* (Hoffstetter, 1949). *Tiliqua frangens* vertebrae are also built to carry more weight, possessing broader and deeper centra than *L. mauritiana*.

Even the largest and oldest *Tiliqua rugosa* individuals do not approach the shape and size of the peramorphic *T. frangens*. The early life stages represented by the neonate dentaries are similar, but with age *T. frangens* acquires a number of automorphic features through disproportionate bone growth. The numerous generalised features shared by the neonates include: a double row of mental foramina, a thin extension of the dentary bone anteriorly forming a chin, alternating tooth heights, the same conical tooth shape with radiating unworn striae from a central cusp (Figure A3.8); and a similar overall shape excepting that the *T. frangens* dentary is considerably deeper in profile. *Tiliqua frangens* is defined by the addition of new autapomorphies at each life stage from the neonate AM F145608, young adult AM F143322, adult AM F143321; but without this ontogenetic progression, the peramorphic holotype SAMA P43196 was previously not recognised as *Tiliqua* (Hutchinson and Scanlon, 2009). The increased number and size of mental foramina in adults is the result of the double row noted in earlier life stages, obscured by excessive bone growth in the peramorphic adult. The wide angle between the two dentaries is exacerbated by increased bony growth along the symphysial ridge, the angle between the left and right jaws at >50° is well beyond modern *Tiliqua* (max 46° in *T. gigas* and *T. multifasciata*). The heavily textured lateral face of the dentary resulted from an increase in bone growth around muscle attachment sites, possibly to withstand bite force stresses. The increase in dentary depth, width and length while tooth count remains constant, is typical of adult egerniines. A tooth count that decreases in the largest adults, as bony growth at the rear of the row envelopes the posterior most two tooth positions is an apomorphy of *T. frangens*. The last few remaining teeth become pleuro-acrodont with infilling of the dental sulcus with cementum medially, and immense bone growth on the lateral side.

Tiliqua frangens greatly extends the 'land tortoise' niche theory proposed for *T. rugosa* (Milewski, 1981). The increased body mass and heavy spiky armour on *T. frangens* demonstrates a peramorphic extreme over its closest (and already peramorphic) relative, *T. rugosa*. A heavy but flexible carapace covers the animal dorsally, laterally and ventrally, the short stocky limbs are geared for power over speed, and gigantic body size (for a skink) allows efficient processing of herbivorous matter. Armour plating has been hypothesised to be an adaptation to aridity in other scincomorphs (Broeckhoven et al., 2018); but without detailed palaeoclimate information for the sites preserving *T. frangens* this relationship cannot be confirmed here. Solid ossified dorsal spines are not present on any other Australian squamates. The spiny tails of *Egernia* project posteriorly and are localised to the tail region; the osteoderms within the spiny scales are not single but composed of multiple narrow plates. Australian agamid lizards have soft spines (without osteoderms) running in a dorsal row or as lateral lines. One suggestion (A. Palci pers. comm.), is that solid spines would have made it less comfortable for predators to constrict *T. frangens*. *Wonambi naracoortensis* and a *Morelia* sp. are found in the same deposits as *T. frangens*; spines would also make swallowing this large lizard more difficult for *Wonambi* as it had a smaller gape than modern constrictors (Palci et al., 2018).

The increase in body size, and taller skull with a shorter snout may correlate with an herbivorous diet, tough plant matter requiring a stronger bite force (Metzger and Herrel, 2005). The deep jaw and tall skull profile of *Tiliqua frangens* is similar to those observed in herbivorous skinks such as *Corucia zebrata,* and iguanians like the Indian spiny-tailed lizard *Uromastyx hardwickii,* and the marine iguana *Amblyrhynchus cristatus*. A deeper mandible profile paired with shorter dentary length allocates force over a shorter lever, generating a stronger bite at the anterior of the dentary in herbivorous lizards and land tortoises (King, 1996). The comparative depth of the anterior tip of the mandible to other egerniines, and the increased surface area of the symphysis due to the posterior elongation of the 'chin', also suggests this increase in force. Although the feeding mechanics of *Tiliqua rugosa* are well documented (Wineski and Gans, 1984), no study has examined the role of tooth crown shape in relation to diet in extant egerniines. A common trait associated with a durophagous diet, present in many *Tiliqua* and *Cyclodomorphus* species, are blunt posterior teeth, suggesting a crushing rather than cutting action (Gans et al., 1985). *Tiliqua frangens'* teeth retain a fairly blunt profile with a single ridge, similar to *T. rugosa*, providing a single pressure point to puncture the surface of a hard object rather than crush it with brute force. *Tiliqua rugosa* are predominantly herbivorous, seasonally relying on small flowers for 88.2–93.7% of their adult diet (Brown, 1991).

Distribution and ecology

Fossil fragments identifiable as *Tiliqua frangens* are localised to the western side of the Great Dividing Range, north of the Murray River, and to as far north as the Darling Downs area in southern Queensland. These sites are not restricted to a particular extant Köppen climatic zone (Stern and Hoedt, 2000), instead spread over current grassland, temperate and subtropical regions (Figure A3.14). Shifting climatic areas in the late Pleistocene may provide a better indicator of *T. frangens* preferred habitat, possibly analogous to the northern population of *T. rugosa* which prefers a mosaic of open understorey vegetation (usually composed of bluebush/saltbush (Norval and Gardner, 2019)). Land tortoises, a potential analogue of *T. frangens,* are absent from Australia today, and the relict forms present in the Pleistocene (meiolaniids) were not only far larger but only found in the northern half of Pleistocene Australia, predominantly north of the range of *T. frangens*. Thus, *T. frangens* would have had little or no competition from true tortoises.

Table A3: Biology of skinks highlighting the affinities of *Tiliqua rugosa* and *Tiliqua frangens* shared with terrestrial tortoises.

Trait	Plesiomorphic skink	*Tiliqua rugosa*	*Tiliqua frangens*	Tortoise (terrestrial)
Skull shape	Longer, narrow, and shallow (Paluh and Bauer, 2017)	Long, wide, and shallow	Long, wide, and deep	Long, wide, and deep
Armour plating	Thin osteoderms (Paluh and Bauer, 2017)	Large osteoderms	Large, thick osteoderms with spikes	Solid carapace (Woodbury, 1948)
Digit reduction	M: 2-3-4-5-3 P: 2-3-4-5-4 (Greer, 1989)	M: 2-3-4-4-3 P: 2-3-4-4-3 (Greer, 1989)	?	M: 2-2-2-2-2 P: 2-2-2-2-0 (Hall, 2007)
Hind limb flexibility		Some ankle rotation (pers. obs.)	Minimal/no ankle rotation	Graviportal
Locomotion	Fast 7.2km/h (Watson and Formanowicz, 2012)	Slow 2.7km/h (John-Alder et al., 1986)	Slow	Slow 2–4km/h (Woodbury, 1948)
Foraging behaviour & habitat preference	Wide or local foraging, with cover and use of retreats (Taylor, 1986)	Wide-scale, in the open (Norval and Gardner, 2019)	?, open habitat	Wide-scale, in the open (Lagarde et al., 2003)
Foraging time per day	>78% of the day (Taylor, 1986)	<12 mins (Dubas and Bull, 1991; Norval and Gardner, 2019)	?	<15 mins (Lagarde et al., 2003)
Diet	Insectivore or Omnivore (Greer, 1989)	Herbivore (Brown, 1991)	?	Herbivore (Lagarde et al., 2003)
Metabolism	Medium to fast (John-Alder et al., 1986; Wu et al., 2015)	Slow (John-Alder et al., 1986)	?	Slow (Lagarde et al., 2003)
Time from birth to maturity & longevity	0.75–2yrs (Greer, 1989)	3–4yrs >50yrs (Norval and Gardner, 2019)	? Most likely long (peramorphy)	12–20yrs >30yrs (Germano, 1994)

In none of the recorded fossil sites do *T. frangens* and *T. rugosa* occur concurrently, despite modern populations of *T. rugosa* existing in these areas today (see Figure A3.14). Fossil calibrated molecular phylogeography of extant *T. rugosa* populations estimate a fast geographic expansion of the northern population sometime during the Pleistocene (Ansari et al., 2019). The largest recorded specimens of *T. rugosa* are localised to north-eastern extremities of their extant distribution (Ansari

et al., 2019). The range expansion, rapid diversification and body size increase for this population may be correlated with the extinction of *T. frangens* leaving an open niche to fill in this area.

The incredible size, peramorphy, unusual shape and robust armour plating of *Tiliqua frangens* is unlike any lizard in the world, greatly expanding the diversity of skinks, and squamate reptiles as a whole. This bizarre Pleistocene skink also highlights that, just like mammals and birds, Australia's reptile fauna exhibited a much greater diversity of forms before human colonisation. This identifies a major gap in our understanding of Quaternary Australian herpetofaunal diversity: squamate reptiles are this continent's most speciose terrestrial vertebrates, but our knowledge of their pre-human diversity lags substantially behind that of mammals and birds.

References

Alekseyenko, A. V., C. J. Lee, and M. A. Suchard. 2008. Wagner and Dollo: a stochastic duet by composing two parsimonious solos. Systematic biology 57:772–784.

Ansari, M. H., S. J. Cooper, M. P. Schwarz, M. Ebrahimi, G. Dolman, L. Reinberger, K. M. Saint, S. C. Donnellan, C. M. Bull, and M. G. Gardner. 2019. Plio-Pleistocene diversification and biogeographic barriers in southern Australia reflected in the phylogeography of a widespread and common lizard species. Molecular Phylogenetics and Evolution 133:107–119.

Atlas of Living Australia. 2019. Mapping and Analyses Spatial Portal;Commonwealth Scientific and Industrial Research Organisation.

Austin, J. J., and E. N. Arnold. 2006. Using ancient and recent DNA to explore relationships of extinct and endangered *Leiolopisma* skinks (Reptilia: Scincidae) in the Mascarene islands. Molecular Phylogenetics and Evolution 39:503–511.

Australian Bureau of Meteorology. 2006. Koeppen climate classification (base climate related classification datasets) Commonwealth of Australia ed Atlas of Living Australia, Victoria, Australia.

Bartholomai, A. 1977. The fossil vertebrate fauna from Pleistocene deposits at Cement Mills, Gore, Queensland. Memoirs of the Queensland Museum 18:41–51.

Broeckhoven, C., C. De Kock, and C. Hui. 2018. Sexual dimorphism in the dermal armour of cordyline lizards (Squamata: Cordylinae). Biological Journal of the Linnean Society 125:30–36.

Brown, G. 1991. Ecological feeding analysis of south-eastern Australian scincids (Reptilia, Lacertilia). Australian Journal of Zoology 39:9–29.

Bull, C. M., and Y. Pamula. 1996. Sexually dimorphic head sizes and reproductive success in the sleepy lizard *Tiliqua rugosa*. Journal of Zoology 240:511–521.

Camp, C. L. 1923. Classification of lizards. Bulletin of the American Museum of Natural History 48:289–481.

Čerňanský, A., and M. N. Hutchinson. 2013. A new large fossil species of *Tiliqua* (Squamata: Scincidae) from the Pliocene of the Wellington Caves (New South Wales, Australia). Alcheringa: An Australasian Journal of Palaeontology 37:131–136.

Dawson, L., and M. Augee. 1997. The late Quaternary sediments and fossil vertebrate fauna from Cathedral Cave, Wellington Caves, New South Wales. Proceedings-Linnean Society of New South Wales 117:51–78.

Drummond, A. J., M. A. Suchard, D. Xie, and A. Rambaut. 2012. Bayesian phylogenetics with BEAUti and the BEAST 1.7. Molecular biology and evolution 29:1969–1973.

Dubas, G., and C. Bull. 1991. Diet choice and food availability in the omnivorous lizard, *Trachydosaurus rugosus*. Wildlife Research 18:147–155.

Etheridge, R. J. 1917. *Megalania prisca*, Owen and *Notiosaurus dentatus*, Owen; lacertilian dermal armour; opalised remains from Lightening Ridge. Proceedings of the Royal Society of Victoria 29:127–133.

Gans, C., F. De Vree, and D. Carrier. 1985. Usage pattern of the complex masticatory muscles in the Shingleback lizard, *Trachydosaurus rugosus*: a model for muscle placement. The American Journal of Anatomy 173:219–240.

Gardner, M. G., A. F. Hugall, S. C. Donnellan, M. N. Hutchinson, and R. Foster. 2008. Molecular systematics of social skinks: phylogeny and taxonomy of the *Egernia* group (Reptilia: Scincidae). Zoological Journal of the Linnean Society 154:781–794.

Germano, D. J. 1994. Growth and age at maturity of North American tortoises in relation to regional climates. Canadian Journal of Zoology 72:918–931.

Goloboff, P. A., and S. A. Catalano. 2016. TNT version 1.5, including a full implementation of phylogenetic morphometrics. Cladistics 32:221–238.

Gray, J. E. 1825. A synopsis of the genera of reptiles and Amphibia, with a description of some new species. Annals of Philosophy 10:193–217.

Greer, A. E. 1989. The biology and evolution of Australian lizards. Surrey Beatty & Sons, Chipping Norton, NSW, 264 pp.
Greer, A. E. 2001. Distribution of maximum snout-vent length among species of scincid lizards. Journal of Herpetology 35:383–395.
Gunther, A. 1877. Notice on two large extinct lizards, formerly inhabiting the Mascarence Islands. Journal of the Linnean Society of Zoology 13:323–327.
Haas, G. 1974. Muscles of the jaws and associated structures in the Rhynchocephalia and Squamata; pp. 285–490 in C. Gans (ed.), Biology of the Reptilia. Academic Press, London and New York.
Hagen, I. J., S. C. Donnellan, and C. M. Bull. 2012. Phylogeography of the prehensile-tailed skink *Corucia zebrata* on the Solomon Archipelago. Ecology and evolution 2:1220–1234.
Hall, B. K. 2007. Fins Into Limbs: Evolution, Development, and Transformation. University of Chicago Press, Chicago, Illinois, 433 pp.
Hammer, Ø., D. A. T. Harper, and P. D. Ryans. 2001. PAST: Paleontological statistics software package for education and data analysis. Paleontologia Electronica 4:9.
Hocknull, S. A. 2005. Ecological succession during the late Cainozoic of central eastern Queensland: extinction of a diverse rainforest community. Memoirs of the Queensland Museum 51:39–122.
Hoffstetter, R. 1949. Les reptiles subfossils de L'ile Maurice: 1. Les Scincidae. Annales de Paleontologie 35:43–72.
Hutchinson, M. N., and B. S. Mackness. 2002. Fossil lizards from the Pliocene Chinchilla Local Fauna, Queensland. Records of the South Australian Museum 35:169–184.
Hutchinson, M. N., and J. D. Scanlon. 2009. New and unusual Plio-Pleistocene lizard (Reptilia: Scincidae) from Wellington Caves, New South Wales, Australia. Journal of Herpetology 43:139–147.
John-Alder, H. B., T. G. Jr., and A. F. Bennett. 1986. Locomotory capacities, oxygen consumption, and the cost of locomotion of the shingle-back lizard (*Trachydosaurus rugosus*). Physiologial Zoology 59:523–531.
Kear, B. P., and R. J. Hamilton-Bruce. 2011. Dinosaurs in Australia: Mesozoic life from the southern continent. CSIRO Publishing, Australia.
King, G. 1996. Reptiles and herbivory. Chapman & Hall, London, UK, 160 pp.
Klingenböck, A., K. Osterwalder, and R. Shine. 2000. Habitat use and thermal biology of the “Land mullet” *Egernia major*, a large Scincid lizard from remnant rain forest in southeastern Australia. Copeia 2000:931–939.
Lagarde, F., X. Bonnet, J. Corbin, B. Henen, K. Nagy, B. Mardonov, and G. Naulleau. 2003. Foraging behaviour and diet of an ecotothermic herbivore: *Testudo horsfieldi*. Ecography 26:236–242.
Lanfear, R., P. B. Frandsen, A. M. Wright, T. Senfeld, and B. Calcott. 2016. PartitionFinder 2: new methods for selecting partitioned models of evolution for molecular and morphological phylogenetic analyses. Molecular biology and evolution 34:772–773.
Lécuru, S. 1969: Étude morphologique de l’humérus des lacertiliens. Annales des Sciences Naturelles, Zoologie (12), 1969.
Lee, M. S. Y., P. M. Oliver, and M. N. Hutchinson. 2009a. Phylogenetic uncertainty and molecular clock calibrations: A case study of legless lizards (Pygopodidae, Gekkota). Molecular Phylogenetics and Evolution 50:661–666.
Lewis, P. O. 2001. A likelihood approach to estimating phylogeny from discrete morphological character data. Systematic biology 50:913–925.
Maddison, W., and D. Maddison. 2017. Mesquite: a modular system for evolutionary analysis. Version 3.2.
Meiri, S. 2010. Length–weight allometries in lizards. Journal of Zoology 281:218–226.

Metzger, K. A., and A. Herrel. 2005. Correlations between lizard cranial shape and diet: a quantitative, phylogenetically informed analysis. Biological Journal of the Linnean Society 86:433–466.
Milewski, A. V. 1981. A comparison of reptile communities in relation to soil fertility in the mediterranean and adjacent arid parts of Australia and Southern Africa. Journal of Biogeography 8:493–503.
Norval, G., and M. G. Gardner. 2019. The natural history of the sleepy lizard, *Tiliqua rugosa* (Gray, 1825) – Insight from chance observations and long-term research on a common Australian skink species. Austral Ecology:doi:10.1111/aec.12715.
Nyakatura, J. A., E. Andrada, S. Curth, and M. S. Fischer. 2014. Bridging "Romer's Gap": limb mechanics of an extant belly-dragging lizard inform debate on tetrapod locomotion during the early carboniferous. Evolutionary Biology 41:175–190.
O'Reilly, J. E., M. N. Puttick, L. Parry, A. R. Tanner, J. E. Tarver, J. Fleming, D. Pisani, and P. C. Donoghue. 2016. Bayesian methods outperform parsimony but at the expense of precision in the estimation of phylogeny from discrete morphological data. Biology Letters 12:20160081.
Oppel, M. 1811. Die Ordnungen, Familien und Gattungen der Reptilien, als Prodrom einer Naturgeschichte derselben. Joseph Lindauer, München, 86 pp.
Palci, A., M. N. Hutchinson, M. W. Caldwell, J. D. Scanlon, and M. S. Lee. 2018. Palaeoecological inferences for the fossil Australian snakes *Yurlunggur* and *Wonambi* (Serpentes, Madtsoiidae). Royal Society open science 5:172012.
Paluh, D. J., and A. M. Bauer. 2017. Comparative skull anatomy of terrestrial and crevice-dwelling *Trachylepis* skinks (Squamata: Scincidae) with a survey of resources in scincid cranial osteology. PLoS ONE 12:e0184414.
Price, G. J., and I. H. Sobbe. 2005. Pleistocene palaeoecology and environmental change on the Darling Downs, southeastern Queensland, Australia. Memoirs of the Queensland Museum 51:171–201.
Rambaut, A., A. Drummond, and M. Suchard. 2014. Tracer v1. 6
RStudio Team. 2016. RStudio: Integrated development for R. RStudio Inc., Boston, USA.
Russell, A. P., and A. M. Bauer. 2008. The appendicular locomotor apparatus of *Sphenodon* and normal-limbed squamates; pp. in C. Gans, A. S. Gaunt, and K. Adler (eds.), The skull and appendicular locomotor apparatus of Lepidosauria. Society for the Study of Amphibians and Reptiles, Ithaca, New York, USA.
Shea, G. M., and M. N. Hutchinson. 1992. A new species of lizard (*Tiliqua*) from the Miocene of Riversleigh, Queensland. Memoirs of the Queensland Museum 32:303–310.
Skinner, A., A. F. Hugall, and M. N. Hutchinson. 2011. Lygosomine phylogeny and the origins of Australian scincid lizards. Journal of Biogeography 38:1044–1058.
Stern, H., and G. d. Hoedt. 2000. Objective classification of Australian climates. Australian Meteorological Magazine 49:87–96.
Taylor, J. A. 1986. Food and foraging behaviour of the lizard, *Ctenotus taeniolatus*. Australian Jorunal of Ecology 11:49–54.
Thorn, K. M., M. N. Hutchinson, M. Archer, and M. S. Y. Lee. 2019. A new scincid lizard from the Miocene of Northern Australia, and the evolutionary history of social skinks (Scincidae: Egerniinae). Journal of Vertebrate Paleontology 39:e1577873.
Tonini, J. F. R., K. H. Beard, R. B. Ferreira, W. Jetz, and R. A. Pyron. 2016. Fully-sampled phylogenies of squamates reveal evolutionary patterns in threat status. Biological Conservation 204, Part A:23–31.
Warton, D., R. Duursma, D. Falster, and S. Taskinen. 2018. (Standardised) Major axis estimation and testing routines. 3.4-8, Randwick, Australia.
Watson, C. M., and D. R. Formanowicz. 2012. A comparison of maximum sprint speed among the five-lined skinks (*Plestiodon*) of the southeastern United States at ecologically relevant temperatures. Herpetological Conservation and Biology 7:75–82.

Welch, K. 1982. Herpetology of the Old World II. Preliminary comments on the classification of skinks (Family Scincidae) with specific reference to those genera found in Africa, Europe, and southwest Asia. Herptile 7:25–27.
White, J. 1790. Journal of a voyage to New South Wales, with sixty-five plates of non descript animals, birds, lizards, serpents, curious cones of trees and other natural productions. Debrett, London, 229 pp.
Whitelaw, M. J. 1991. Magnetic polarity stratigraphy of the Fisherman's Cliff and Bone Gulch vertebrate fossil faunas from the Murray Basin, New South Wales, Australia. Earth and Planetary Science Letters 104:417–423.
Wickham, H. 2016. ggplot2: Elegant graphics for data analysis. Springer-Verlag, New York.
Wilson, S., and G. Swan. 2017. A complete guide to the Reptiles of Australia. 5th Edition. Reed New Holland Publishers, Sydney, Australia, 647 pp.
Wineski, L. E., and C. Gans. 1984. Morphological basis of the feeding mechanics in the shingle-back lizard *Trachydosaurus rugosus* (Scincidae, Reptilia). Journal of Morphology 181:271–295.
Woodbury, A. M. 1948. Studies of the desert tortoise, *Gopherus agassizii*. Ecological Monographs 18:145–200.
Wright, A. M., and D. M. Hillis. 2014. Bayesian analysis using a simple likelihood model outperforms parsimony for estimation of phylogeny from discrete morphological data. PLoS ONE 9:e109210.
Wu, N., L. A. Alton, C. J. Clemente, M. R. Kearney, and C. R. White. 2015. Morphology and burrowing energetics of semi-fossorial skinks (*Liopholis* spp.). Journal of Experimental Biology 218:2416–2426.
Zheng, Y., and J. J. Wiens. 2016. Combining phylogenomic and supermatrix approaches, and a time-calibrated phylogeny for squamate reptiles (lizards and snakes) based on 52 genes and 4162 species. Molecular Phylogenetics and Evolution 94, Part B:537–547.

Appendix 4: List of Namba Formation Specimens

Table A4: List of the squamate specimens referred to in Chapter 5, recovered from Billeroo Creek Fish Lens at Site BC2, or Lake Pinpa Fish Lens at sites LP6 and LP12. All specimens deposited in the SAMA on the 24th October 2019.

Element	Taphonomic Remarks	Notes	Temp. No.	Identification
Maxilla (right)	Fragment	2 teeth, 6 loci, worn, peg-like bicuspid crowns, no tooth crown expansion, large maxillary foramina.	BCF2.1	
Dentary (left)	Fragment	w/ coronoid process, broken below dental sulcus, 4 teeth remain from 7 loci, typical bicuspid teeth, one unworn.	BCF2.2	
Dentary (side)	Heavily weathered	7 tooth loci, 2 broken teeth remain, worn, bicuspid.	BCF2.3	
Dentary (Left)	Mid fragment	12 loci, 6 teeth remain. Some crowns unworn, no crown expansion from shaft. Broken below splenial notch, 1 large and 2 small mental foramina	BCF2.4	
Dentary (Left)	Near complete.	Missing posterior half of angular process, larger teeth than *Lissolepis coventryi*, length approx. the same. Splenial notch 60% length of dentary.	BCF2.5	Paratype
Maxilla (Left)	Posterior fragment	Ten tooth loci, with seven remaining teeth. Jugal articulation not bifid, posterior-most maxillary foramina is the largest.	BCF2.6	
Dentary (Left)	Posterior fragment	10 tooth loci, 5 teeth. Typical bicuspid tooth crowns, broken beneath dental sulcus, no evidence of IAF position.	BCF2.7	
Dentary (Right)	Near complete.	Missing coronoid & surangular processes. Complete symphysis, splenial notch approx. 60% of dentary length. 26 tooth loci, 14 teeth. Varying tooth wear, prominent deep tooth sulcus, 7 mental foramina, bicuspid tooth crowns.	BCF2.8	Holotype
Maxilla (right)	Anterior broken off	16 tooth loci, 9 teeth. Bifid jugal articulation, typical bicuspid tooth crowns, 7 maxillary foramina.	BCF2.9	Ref Sp.
Dentary (Left)	Anterior fragment	No Meckel's groove, symphysis missing (broken), One remaining tooth, bicuspid, narrow and tall.	BCF2.10	
Dentary (Left)	Anterior fragment	Symphysis broken off, 9 loci, 5 teeth, prominent dental sulcus	BCF2.11	
Dentary (Left)	Anterior fragment	Most of symphysis broken off, 12 loci, 7 teeth, narrow teeth with bicuspid crowns, prominent dental shelf.	BCF2.12	
Maxilla (unknown)	Broken mid-section	4 teeth, different stages of wear	BCF2.13	
Maxilla (Left)	Posterior fragment	Bifid, jugal articulation, 9 loci with 5 complete and one broken tooth, 3 maxillary foramina, posterior-most foramen not enlarged	BCF2.14	
Maxilla (Left)	Posterior fragment	Bifid jugal articulation complete, 9 loci, 5 teeth, varying wear on teeth, second to last maxillary foramina the largest	BCF2.15	
Maxilla (right)	Posterior fragment	Bifid jugal articulation, 4 loci, 2 teeth, worn crowns	BCF2.16	
Dentary (Left)	Shard, golden yellow colour	5 loci, two teeth, both worn.	BCF2.17	
Pterygoid (left)	Broken midway along shaft, missing tip of palatine process	Pronounced dip in the ventral surface of the pterygoid head	BCF2.18	Ref Sp.
Dentary (Right)	Posterior fragment	Broken beneath dental sulcus, 4 loci, 2 teeth, one slightly less worn, no coronoid process	BCF2.19	
Pre-sacral vertebra	Complete		BCF2.20	Ref Sp.
Vertebra	Fragment	Possibly turtle, very fragmentary	BCF2.21	Turtle
Vertebrae (2 of)	Fragments	Procoelous (A & B), A: 4mm long, centum approx. 1mm wide, all else is broken off. B: 2.8mm long, 1.8mm tall, centrum >1mm wide, neural spine broken off, both look like caudals.	BCF2.22	
Vertebra (centrum only)	Fragment	Procoelous centrum, everything else broken off, some synapophysis present but broken, 2.7mm long, 3mm wide, centrum is 0.8mm wide.	BCF2.23	
Vertebra	Incomplete	Procoelous pre-sacral vertebra with extended transverse process on right side (left broken), 3.4mm long, centrum is 1mm wide, skink-like lip around centrum, fairly rounded shape, neural spine broken off, right prezygapophysis remains.	BCF2.24	
Dentary (Right)	Pathological specimen	15 tooth loci preserved, 8 complete teeth. Missing anterior and posterior portions inc. coronoid process. Splenial fused to dentary.	BCF2.25	
Dentary (Left)	Posterior section missing.	Preserved 19-20 tooth loci, 12 complete teeth. Anterior completely preserved inc. symphysis.	BCF2.26	
Dentary (Right)	Anterior fragment	3 of 8 teeth preserved. Entire symphysis preserved	BCF2.27	
Premaxilla	Fragment	Nasal process broken off, 3 teeth preserved	BCF2.28	
Tooth row fragment	Fragment	2 teeth preserved	BCF2.29	
Dentary (Left)	Fragment	4 teeth preserved across 8 loci. Posterior portion, no symphysis or splenial notch present	BCF2.30	

Tooth row fragment	Fragment	1 tooth preserved on 5mm long sulcus	BCF2.31	
Vertebra	Fragment	Centrum only remaining	BCF2.32	
Vertebra	Incomplete	Pygal vert. Missing neural spine	BCF2.33	
Vertebra	Incomplete	Transverse processes and prezygopophyses visible	BCF2.34	
Maxilla (Right)	Posterior fragment	4 teeth preserved beneath suborbital process (incomplete)	BCF2.35	
Maxilla (Left)	Anterior portion	4 teeth from 6-7 loci preserved. Very small, possibly gecko	BCF2.36	Gekkota
Maxilla (unknown)	Fragment	3 teeth on small bone fragment, some foramina visible	BCF2.37	Gekkota
Maxilla (Left)	Posterior portion	2 teeth preserved, 5 loci. Suborbital process present but not complete posteriorly. Facial process broken	BCF2.38	Gekkota
Maxilla (unknown)	Mid fragment	2 teeth preserved, five loci.	BCF2.39	
Maxilla (right)	Posterior fragment	4 teeth	BCF2.40	Gekkota
Maxilla (unknown)	Mid-fragment	4 teeth	BCF2.41	Gekkota
Vertebrae (6 of)	Various		BCF2.42	
Vertebra	Complete		BCF2.43	Gekkota
Limb fragment			BCF2.44	
Maxilla fragment (left)	Fragment	No teeth preserved	BCF2.45	
4x limb fragments	Fragments	Proximal femur preserved with short extension of shaft	BCF2.46	Ref Sp.
Maxilla frag (right)	Fragment	Anterior fragment	BCF2.47	Ref Sp.
Premaxilla (left) and compound bone (right)			BCF2.48	Ref Sp.
Compound bone (right)	Incomplete	retroarticular process broken off	LP6.1	Ref Sp.
Partial humerus	Fragment		LP12.1	
Maxilla (Right, posterior half)	Fragment		LP12.2	
Maxilla frag (left)	Fragment	2 teeth preserved	BCF2.49	
Vertebrae x3	Various		BCF2.50	
Dentary (left anterior frag.)	Fragment		BCF2.51	
Maxilla frag (post. Right)			BCF2.52	
Dentary (right)	Fragment	1 tooth present	BCF2.53	
Maxilla frag (right)	Fragment	5 teeth, 3 alveoli	BCF2.54	
Maxilla (frag)	Fragment	2 teeth preserved	BCF2.55	
Vertebra			BCF2.56	
Tibia & other assorted	Various	Appendicular elements, some digestion damage	BCF2.57	
Trunk vertebra	Complete		BCF2.58	
Assorted	Various	Assorted dentaries (left and right fragments), limb shafts.	BCF2.59	
Limb/tarsal/carpal bone?	Fragments		BCF2.60	
Proximal femur	Fragment		BCF2.61	

Appendix 5: Scincidae in the Australian fossil record

Table A5: List of sites that contain fossil Egerniinae, or that may possibly contain unidentified scincid material. Data from either published sources or personal observation of material within museum collections.

Eocene	Oligocene	Miocene	Pliocene	Late Pleistocene	Holocene	State	*Lissolepis*	*Liophoilis*	*Bellatorias*	*Egernia*	*Tiliqua*	*Cyclodomorphus*	*Proegernia*	Scincidae indet.	Lacertilia indet.	Reference
Murgon						Qld									x	
Rundle Fm						Qld								x	x	(Hocknull, 2000)
		Namba Fm				SA							x			Chapter 4
		Etadunna Fm				SA							x			(Martin et al., 2004) Chapter 4
		Riversleigh				Qld			x	x	x	x				(Hutchinson, 1992), Chapter 2
				Wellington		NSW		x		x	x					See Chapter 3
			Chinchilla			Qld					x					(Hutchinson and Mackness, 2002)
			Bluff Downs			Qld				x				x		(Mackness and Hutchinson, 2000)
			Curramulka Caves			SA					x					(Pledge, 1992)
				Moorna Stn		NSW		?		x	x					Pers obs.
				Kings Creek DD		Qld					x	x				(Price and Sobbe, 2005)?
				Hodgsons Creek DD		Qld									x	(Molnar and Kurz, 1997)
				Mt Etna		Qld				x	x	x				(Hocknull, 2005)
				Cement Mills, Gore		Qld					x					(Bartholomai, 1977)
				Naracoorte		SA		x			x					(Reed and Bourne, 2000; Reed and Bourne, 2009)
				Eurinilla Fm		SA				x	x					NMV P254617
				Nullarbor		WA		?		x	x					(Prideaux et al.,

Late Pleistocene	Holocene	State	*Lissolepis*	*Liopholis*	*Bellatorias*	*Egernia*	*Tiliqua*	*Cyclodomorphus*	*Proegernia*	Scincidae indet.	Lacertilia indet.	Reference
	Lake Victoria	NSW					x					NMV collection
Lake Mungo & Mulurulu		NSW					x				x	(Hope, 1978)
	Lake Tandau	NSW					x			x	x	(Balme, 1995)
Cuddie Springs		NSW								x		(Dodson et al., 1993)
Chillagoe, Tea Tree Cave		Qld					x*					(Molnar, 1982)
	Texas Cave	Qld									x	(Archer, 1978)
	Kangaroo Island	SA		x			x					(Hope et al., 1977)
Hookina Creek		SA					x					FU collection
	Burra Creek	SA					x				x	(Williams, 1980)
	Dempsey's Lake	SA					x					(Williams, 1980)
	Devon Downs	SA					x					(Williams, 1980)
Salt Creek		SA									x	(Williams, 1980)
	Forth River Valley	Tas									x	(Cosgrove, 1995)
	McEacherns Cave	Vic		x		x	x					NMV collection
	Devils Lair	WA	x	x		x	x					(Hollenshead et al., 2011)
Koala Cave Yanchep		WA									x	(Archer, 1972)
	Tunnel Cave	WA								x		(Dortch and Wright, 2010)
…	Molong Cave	NSW				x						AM collection
	Nettle Cave, Jenolan	NSW		x		x				x*		(Morris et al., 1997)
	Death Trap Cave	NSW					x					(Price et al., 2019)
	Uluru National Park	NT									x	(Baynes and Baird, 1992)
	Katherine Area	NT										(Marianelli, 1995)
	Venus Bay	SA								x		McDowell Thesis (Hons)
	Mairs Cave	SA									x	(Williams, 1980)
	Fern Cave, Vic	Vic		x			x					NMV collection
	Amphitheatre Cave	Vic					x					NMV collection
	Orchestra Shell Cave Wanneroo	WA									x	(Archer, 1974)
	Witchcliff Rock Shelter	WA								x		(Dortch and Wright, 2010)
	Rainbow Cave, WA	WA								x		(Dortch and Wright, 2010)
	Bremer Bay	WA									x	(Butler and Merrilees, 1971)
	Cape Range Caves	WA									x	(Kendrick and Porter, 1973)

References

Archer, M. 1972. *Phascolarctos* (Marsupialia, Vombatoidea) and an associated fossil fauna from Koala Cave near Yanchep, Western Australia. Helictite 10:49–59.

Archer, M. 1974. Excavations in the Orchestra Shell Cave, Wanneroo, Western Australia: Part III. Fossil vertebrate remains. Archaeology & Physical Anthropology in Oceania 9:156–162.

Archer, M. 1978. Quaternary vertebrate faunas from the Texas Caves of southeastern Queensland. Memoirs of the Queensland Museum 19:61–109.

Balme, J. 1995. 30,000 years of fishery in western New South Wales. Archaeology in Oceania 30:1–21.

Bartholomai, A. 1977. The fossil vertebrate fauna from Pleistocene deposits at Cement Mills, Gore, Queensland. Memoirs of the Queensland Museum 18:41–51.

Baynes, A., and R. Baird. 1992. The original mammal fauna and some information on the original bird fauna of Uluru National Park, Northern Territory. The Rangeland Journal 14:92–106.

Butler, W. H., and D. Merrilees. 1971. Remains of *Potorous platyops* (Marsupialia, Macropodidae) and other mammals from Bremer Bay, Western Australia. Journal of The Royal Society of Western Australia 54:53–58.

Cosgrove, R. 1995. Late Pleistocene behavioural variation and time trends: the case from Tasmania. Archaeology in Oceania 30:83–104.

Dodson, J., R. Fullagar, J. Furby, R. Jones, and I. Prosser. 1993. Humans and megafauna in a late Pleistocene environment from Cuddie Springs, north western New South Wales. Archaeology in Oceania 28:94–99.

Dortch, J., and R. Wright. 2010. Identifying palaeo-environments and changes in Aboriginal subsistence from dual-patterned faunal assemblages, south-western Australia. Journal of Archaeological Science 37:1053–1064.

Hocknull, S. A. 2000. Remains of an Eocene skink from Queensland. Alcheringa: An Australasian Journal of Palaeontology 24:63–64.

Hocknull, S. A. 2005. Ecological succession during the late Cainozoic of central eastern Queensland: extinction of a diverse rainforest community. Memoirs of the Queensland Museum 51:39–122.

Hollenshead, M. G., J. I. Mead, and S. L. Swift. 2011. Late Pleistocene *Egernia* group skinks (Squamata: Scincidae) from Devils Lair, Western Australia. Alcheringa: An Australasian Journal of Palaeontology 35:31–51.

Hope, J. H. 1978. Pleistocene mammal extinctions: the problem of Mungo and Menindee, New South Wales. Alcheringa: An Australasian Journal of Palaeontology 2:65–82.

Hope, J. H., R. J. Lampert, E. Edmondson, M. J. Smith, and G. F. Van Tets. 1977. Late Pleistocene faunal remains from Seton Rock Shelter, Kangaroo Island, South Australia. Journal of Biogeography:363–385.

Hutchinson, M. N. 1992. Origins of the Australian scincid lizards: a preliminary report on the skinks of Riversleigh. The Beagle, Records of the Northern Territory Museum of Arts and Sciences 9:61–70.

Hutchinson, M. N., and B. S. Mackness. 2002. Fossil lizards from the Pliocene Chinchilla Local Fauna, Queensland. Records of the South Australian Museum 35:169–184.

Kendrick, G. W., and J. K. Porter. 1973. Remains of a thylacine (Marsupialia: Dasyuroidea) and other fauna from Caves in the Cape Range, Western Australia. Journal of The Royal Society of Western Australia 56:116–122.

Mackness, B. S., and M. N. Hutchinson. 2000. Fossil lizards from the Early Pliocene Bluff Downs Local Fauna. Transactions of the Royal Society of South Australia 124:17–30.

Marianelli, P. C. 1995. Palaeoenvironmental study of Quaternary fossiliferous fissure fills of the Katherine Area, N. T., Faculty of Science and Engineering, Flinders University.

Martin, J. E., M. N. Hutchinson, R. Meredith, J. A. Case, and N. S. Pledge. 2004. The oldest genus of scincid lizard (Squamata) from the Tertiary Etadunna Formation of South Australia. Journal of Herpetology 38:180–187.

Molnar, R. E. 1982. A catalogue of fossil amphibians and reptiles in Queensland. Memoirs of the Queensland Museum 20:613–633.
Molnar, R. E., and C. Kurz. 1997. The distribution of Pleistocene vertebrates on the eastern Darling Downs, based on the Queensland Museum collections. Proceedings of the Linnean Society of New South Wales 117:107–129.
Morris, D. A., M. Augee, D. Gillieson, and J. Head. 1997. Analysis of a late Quaternary deposit and small mammal fauna from Nettle Cave, Jenolan, New South Wales. Proceedings of the Linnean Society of New South Wales 117.
Pledge, N. S. 1992. The Curramulka local fauna: a new late Tertiary fossil assemblage from Yorke Peninsula, South Australia. The Beagle, Records of the Northern Territory Museum of Arts and Sciences 9:115–142.
Price, G. J., and I. H. Sobbe. 2005. Pleistocene palaeoecology and environmental change on the Darling Downs, southeastern Queensland, Australia. Memoirs of the Queensland Museum 51:171–201.
Price, G. J., J. Louys, G. K. Smith, and J. Cramb. 2019. Shifting faunal baselines through the Quaternary revealed by cave fossils of eastern Australia. PeerJ 6:e6099.
Prideaux, G. J., J. A. Long, L. K. Ayliffe, J. C. Hellstrom, B. Pillans, W. E. Boles, M. N. Hutchinson, R. G. Roberts, M. L. Cupper, L. J. Arnold, P. D. Devine, and N. M. Warburton. 2007. An arid-adapted middle Pleistocene vertebrate fauna from south-central Australia. Nature 445:422–425.
Reed, E. H., and S. J. Bourne. 2000. Pleistocene fossil vertebrate sites of the South East region of South Australia. Transactions of the Royal Society of South Australia 124:61–90.
Reed, E. H., and S. J. Bourne. 2009. Pleistocene fossil vertebrate sites of the South East region of South Australia II. Transactions of the Royal Society of South Australia 133:30–40.
Williams, D. L. G. 1980. Catalogue of Pleistocene vertebrate fossils and sites in South Australia. Transactions of the Royal Society of South Australia 104:101–115.